The inhibition of ABC transporters in cancer multidrug resistance by heterocyclic cyclohexanone analogues of curcumin

Jezrael Lafuente Revalde

A thesis submitted in fulfilment of the requirements for the Degree of Doctor of Philosophy in Pharmacology and Clinical Pharmacology, The University of Auckland, 2014

Abstract

Twenty-four heterocyclic cyclohexanone analogues of curcumin were investigated for inhibitory effects against the major ATP-binding cassette (ABC) transporters involved in cancer multidrug resistance (MDR). The main purpose was to identify superior inhibitors compared to the chemically and metabolically unstable parent compound, curcumin. As some of these analogues have been reported to show potent anticancer activity, the identification of 'dual-role' chemosensitisers with both MDR-reversal and anticancer activity was an exciting possibility. Flow cytometry screening demonstrated that the cyclohexanone analogues inhibited the four ABC transporters (P-gp, BCRP, MRP1 and MRP5) investigated in this study. At 20 μM, two analogues (C10 and RL92) completely inhibited P-gp; four (A12, A13, B11 and RL92) completely inhibited BCRP; and two (A13 and RL92) inhibited both MRP1 and MRP5. These analogues were more potent than, or equally potent to, curcumin, and two, A13 and RL92, were able to inhibit multiple transporters. Cell proliferation assays confirmed that the P-gp and BCRP inhibitors reversed ABC transporter-mediated drug resistance in transporter-overexpressing cell lines, although issues with cytotoxicity prevented resistance reversal effects to be thoroughly examined for MRP1 and MRP5 inhibitors. Evidence from these assays indicates that the analogues were not substrates of the transporters that they inhibited. From both the flow cytometry and resistance reversal assays, it was evident that the analogues were most promising as BCRP inhibitors, and thus, further studies focused on BCRP. Using cell-free membrane vesicles, A12, A13, B11, RL92 were found to potently (sub-μM IC_{50}) and directly inhibit BCRP in a non-substrate-specific manner, and without requiring bioactivation. These analogues did not appear to alter cellular BCRP protein expression although A13 and RL92 rapidly decreased cell-surface expression of the transporter, but only at high concentrations (20 μM).

From these results, it is evident that the cyclohexanone analogues can be considered as alternatives to curcumin as ABC transporter inhibitors. These analogues are particularly promising as inhibitors of BCRP, due to their potent, non-cell-line or substrate-specific inhibition of this transporter. The demonstration of potent and broad ABC transporter inhibition by some analogues such as A13 was particularly encouraging as this compound was reported to have anticancer activity superior to curcumin in a number of different cancer cell lines. Thus A13 should be further

investigated as a dual-role chemosensitiser. Useful structure-activity inhibitory data was also gained from this study which, when considered along with cytotoxicity-screening data, enables the proposal of a new cyclohexanone compound, F14, with hopefully superior ABC transporter inhibition and cytotoxic activity than A13.

Acknowledgements

First, I wish to thank my two supervisors, Asoc Prof James Paxton and Dr Yan Li. For their guidance and support during my honours year, and the four years of my doctoral study. James helped me complete travel grants, annual reviews, scholarship applications and a 290-page doctoral thesis. I will always be grateful for his patience, and his trust in letting me try new things in the lab, and staying cheerful in meetings even when I presented page after page of failed results. These were always met with words of encouragement, which helped me persevere and stay motivated. I wish to thank Dr Li, who, five long years ago, showed me how to grow cells in a flask. He taught me many of the research techniques that I've applied in my doctoral study, and was always available to help me troubleshoot failed experiments. On many occasions, his advice was key to solving issues that stalled the progress of this research.

I wish to thank Dr Rhonda Rosengren of the University of Otago, for providing the cyclohexanone analogues, and for her help in proofreading my research manuscript. Thank you to Dr Lesley Larsen and Dr Bill Hawkins who synthesised the analogues and made sure I always had more than enough for my experiments. I thank my friend and colleague, Dr Kee Tan, for providing the membrane vesicles, for his advice on research techniques, and for his company at international conferences. I thank Stephen Edgar, for patiently teaching me flow cytometry and always being ready to assist whenever problems arose. Also, I am grateful to Prof Piet Borst of the Netherlands Cancer Institute for providing the ABC transporter-transfected cell lines without which this research would not have been possible. I thank the the University of Auckland doctoral scholarship and Genesis Oncology trust for financial support through my doctoral studies. I would like to thank staff and fellow postgraduate students of the University of Auckland, Malcolm, Nuala, Johnson, Mark, Kavita, Nancy, Ray, Joyce, Virginia, JP, Sandy, Benedict, Prashi, Fang, Kathryn, Lulu, Brandi, Brent, Keri and Mike for advice, encouragement, support and especially pubnights.

Lastly I wish to acknowledge the support of friends and family, who were always there when I needed them. I thank my partner, Elaine, who has helped to me get through some of the hardest parts of writing this thesis.

Table of contents

List of figures

List of tables

List of equations

Equation 2-1 p88

$$Y = \left(\frac{SF - BF}{MF - BF}\right) \times 100\%$$

Equation 2-2 p88

$$Y = \left(\frac{A - C}{B - C}\right) \times 100\%$$

Equation 2-3 p90

$$Y = \frac{100}{\{1 + 10\text{^}[(\text{LogIC50} - X) * \text{Hill Slope}]\}}$$

Equation 5-1 p186

$$\frac{\text{Total protein density (treated sample)}}{\text{Total protein density (control)}} = \text{Adjustment factor}$$

Equation 5-2 p186

$$\left[\left(\frac{\text{BCRP BD (treated sample)}}{\text{Adjustment factor}}\right) \div \text{BCRP BD (control)}\right] \times 100 = \%\ \text{BCRP expression of control}$$

Equation 6-1 p206

$$\left[\frac{\text{MFI (Test sample)} - \text{MFI (Isotype control)}}{\text{MFI (DMSO control)} - \text{MFI (Isotype control)}}\right] \times 100 = \text{MFI as \% of DMSO control}$$

Abbreviations

[^{14}C]EASG	Carbon-14 labelled glutathione conjugate of ethacrynic acid
5-FU	5-fluorouracil
ABC	ATP-binding cassette
AhR	Aryl hydrocarbon receptor
Akt	Ak thymoma also known as protein kinase B
AML	Acute myeloid leukemia
ANOVA	Analysis-of-variance
APC	Allophycocyanin
ATP	Adenosine triphosphate
AUC	Area-under-the-curve
BBB	Blood brain barrier
BCECF-AM	2,7-bis-(2-carboxyethyl)-5-(and-6)-carboxyfluorescein
	acetoxymethyl ester
BCRP	Breast cancer resistance protein
BRCA1	Breast cancer 1, early onset
cAMP	Cyclic adenosine monophosphate
CFDA	Carboxyfluorescein diacetate
CFTR	Cystic fibrosis transmembrane conductance regulator
cGMP	Cyclic guanosine monophosphate
C_{max}	Maximum plasma concentration
CPM	Counts per minute
CR	Complete remission
CSC	Cancer stem cells
DDI	Drug-drug interaction
DMEM	Dulbecco's modified eagle's medium
DMSO	Dimethyl sulfoxide
E3S	Estrone-3-sulfate
EGCG	Epigallo-catechin galleate

EGFR	Epidermal growth factor receptor
ER	Estrogen receptor
FBS	Fetal bovine serum
FDA	Food and drug administration
FITC	Fluorescein isothiocyanate
FTC	Fumitremorgin C
GRAS	Generally recognised as safe
GSH	Glutathione
GSSG	Glutathione disulfide
HEK	Human embryonic kidney
HER2	Human epidermal growth factor 2 receptor
HHC	Hexahydrocurcumin
HIF	Hypoxia inducible-factor
HIV	Human immunodeficiency virus
i.p.	Intraperitoneal
i.v.	Intravenous
IAAP	Iodoarylazidoprazosin
JNK	c-Jun N-terminal kinases
KO	Knockout
LTC_4	Leukotriene C_4
MAC	Monocarbonyl analogue of curcumin
MDCK	Madin-Darby canine kidney cells
MDR	Multidrug resistance
MFI	Mean fluorescence intensity
miRNA	MicroRNA
MRP1	Multidrug resistance-associated protein 1
MRP5	Multidrug resistance-associated protein 5
MTT	3-(4,5-dimethylthiazol-2-yl)-2,5-diphenyltetrazolium bromide
MTX	Methotrexate

NBD	Nucleotide binding domain
NF-κb	Nuclear factor kappa-light-chain-enhancer of activated B cells
NMP	N-methylpiperidone
NMR	Nuclear magnetic resonance
NPPB	5-nitro-2-(3-phenylpropylamino)benzoate
OS	Overall survival
PBS	Phosphate-buffered saline
PE	Phycoerythrin
Pen-strep	Penicillin-streptomycin
PFS	Progression-free survival
P-gp	P-glycoprotein
PI	Propidium Iodide
PI3K	Phosphoinositide 3-kinase
PI3K/AKT	Phosphoinositide 3-kinase/Akt
Pim-1	Proto-oncogene serine/threonine-protein kinase 1
PPAR-γ	Peroxisome proliferator-activated receptor gamma
PRM	Phenyl ring methoxy
PSH	Para-substituted hydroxyl
PXR	Pregnane X receptor
QSAR	Quantitative structure-activity relationship
RT-PCR	Reverse transcription polymerase chain reaction
SSZ	Sulfasalazine
TGF-β	Transforming growth factor-beta
THC	Tetrahydrocurcumin
TKI	Tyrosine kinase inhibitor
TM	Transmembrane
TNBC	Triple-negative breast cancer
TMD	Transmembrane domain
VEGF	Vascular endothelial growth factor

XBP-1	X-box binding protein-1

1. General Introduction

1.1 Cancer multidrug resistance

Resistance to chemotherapy is one of the most important obstacles towards the successful treatment of cancer. The development of resistance is common and often expected. Resistance is one of the main reasons for the relative ineffectiveness of cancer chemotherapy, especially against late-stage, metastatic disease in which it is the main or only therapeutic option. This is reflected in the poor 5-year survival rates of late-stage patients of some of the most common cancers such as lung, breast and colorectal cancer. In the US, only 4% of patients diagnosed with stage IV non-small cell lung cancer are expected to be alive in 5 years (Cetin et al., 2011). In metastatic breast and colorectal cancer; the 5-year survival rates are 24% and 13% respectively (Howlander et al., 2013). Due to the high resistance rate, chemotherapy in late-stage disease is often administered with palliative rather than curative intent (Gennari et al., 2011; Simmonds, 2000).

Addressing the issue of resistance in cancer is complicated. Often, resistance of the tumour to one drug or drug combination can cause resistance to other compounds with unrelated structure or mechanism of action (Baguley, 2010; Biedler and Riehm, 1970). This is termed multidrug resistance (MDR) and is a major issue as simply switching to a different anticancer agent may not lead to an improvement in response. This is especially problematic as approved treatment options for a number of cancers are very limited (Tokh et al., 2012).

MDR to chemotherapy is either present at the very start of treatment (intrinsic resistance) or may develop after successive rounds of chemotherapy (acquired resistance) (Baguley, 2010; Gottesman et al., 2002). The latter is often the result of initial chemotherapy eliminating only drug-sensitive cells, leaving a resistant subpopulation to repopulate the tumour. Patients can therefore become clear of any detectable signs of disease, only for it to recur in an aggressive and more resistant form, months or years later (Aguirre-Ghiso, 2007). There is no single cause or mechanism of MDR. In the clinical setting, multiple factors may account for the observed MDR and could involve both resistance mechanisms from the tumour itself or factors such as the tumour microenvironment and host immune response (Baguley, 2010; Trédan et al., 2007).

Current identified mechanisms for MDR include reduced drug uptake by the cancer cells, increased drug efflux, resistance to chemotherapy-induced apoptosis, increased DNA repair, increased intracellular metabolism or the decreased bioactivation of a pro-drug (Baguley, 2010; Gillet and Gottesman, 2010; Lage, 2008). Contributions of the tumour microenvironment include difficulties of drugs to penetrate solid tumours due to disorganised vasculature and increased tissue hydrostatic pressure (a result of the lack of lymphatic vessels) (Minchinton and Tannock, 2006). Basic drugs (e.g., mitoxantrone and doxorubicin) tend to ionize because of the acidic pH of the microenvironment, limiting their diffusion through tumour tissue (Gillet and Gottesman, 2010; Lage, 2008). The disorganised vasculature also leads to hypoxic regions within the tumour where cells are quiescent or cycle slowly. These become insensitive to anticancer drugs which often target rapidly dividing cells (Dean, 2009; Trédan et al., 2007).

Of these mechanisms, the most well studied and the first to be characterised is the efflux of anticancer drugs by ATP-binding cassette (ABC) transporters. This was observed in 1976 with the discovery of the ABC transporter, P-glycoprotein (Juliano and Ling, 1976).

1.2 ABC transporters

ATP-binding cassette or ABC transporters are a family of 49 membrane proteins in humans that utilise the energy from ATP hydrolysis to transport substrates against a concentration gradient (Biemans-Oldehinkel et al., 2006). These transporters are evolutionarily conserved and are present both in plants and prokaryotes (Vasiliou et al., 2009). In humans, ABC transporters are divided into 7 sub-families, designated ABCA to ABCG. Members include cholesterol and lipid transporters (ABCA1), ion channels (ABCC7 or the cystic fibrosis transmembrane conductance regulator, CFTR), drug efflux pumps (ABCB1 or P-glycoprotein) and bile salt exporters (ABCB11) (Vasiliou et al., 2009). The family is grouped phylogenetically based on their sequence similarity at the site where adenosine triphosphate (ATP) is bound, also called the nucleotide-binding domain (NBD) (Figure 1-1) (Dean and Annilo, 2005; Vasiliou et al., 2009). All members carry a unique leucine-serine-glycine-glycine-glutamine (LSGGQ) motif in the NBD, and this is highly conserved within the family (Linton, 2007). ABC transporters with an efflux function also have a transmembrane domain (TMD), composed of hydrophobic α-helices which span the lipid bilayer (Biemans-Oldehinkel et al., 2006). These TMDs are the sites of substrate binding and, unlike the NDBs, these structures vary within and between the sub-families (Sharom, 2008). This accounts for differences in substrate recognition between transporters. A linker region is present which connects the NBDs with the TMDs and allows the coupling of ATP hydrolysis with substrate transport (Linton, 2007; Sharom, 2008). It should be noted that not all members of the family contain a TMD. As an example, ABCE and ABCF subfamilies only have NBDs and do not have a transport function (Vasiliou et al., 2009). A functional ABC transporter requires at least two TMDs and two NBDs as seen with P-glycoprotein (ABCB1) (Figure 1-1) (Biemans-Oldehinkel et al., 2006). Other members such as proteins of the ABCG sub-family (e.g., ABCG2 or breast cancer resistance protein) only contain a single NBD and TMD and consequently are called 'half-transporters' (Woodward et al., 2011). Dimerisation is essential for them to be fully functional.

Currently, only 15 of the 49 transporters have been implicated in cancer resistance (Gillet et al., 2007; Sharom, 2008). The most important of these are members of the ABCB, ABCC and ABCG sub-families. Specifically, ABCB1 or P-glycoprotein (P-gp), ABCC1 or multidrug resistance-associated protein (MRP1) and ABCG2 or breast cancer resistance protein (BCRP) (Figure 1-1), are considered of most relevance in cancer MDR (Gillet et al., 2007; Szakács et al., 2006). These

are frequently expressed or upregulated in tumour tissue and also have the broadest range of anticancer drug substrates (Szakács et al., 2008a). In addition, these are the transporters most commonly found in pharmacological barriers and excretory organs such as the gut, blood brain barrier (BBB), placenta, kidneys and liver (Huls et al., 2009; Szakács et al., 2008a). Hence, they can affect both drug transport in tumour cells and the pharmacokinetics and *in vivo* disposition of substrate drugs. Further discussion in this chapter will therefore focus on these transporters. In addition, the ABCC5 or multidrug resistance-associated protein 5 (MRP5) protein will be included due to its association with pancreatic cancer, currently the hardest cancer to cure with chemotherapy (Hagmann et al., 2010a; Li et al., 2011).

The following sections will give a general overview of each transporter, its structure, function, physiological role and known drug substrates and modulators. Their contribution to MDR in cancer will then be discussed followed by a summary of efforts to inhibit their activity in the clinic.

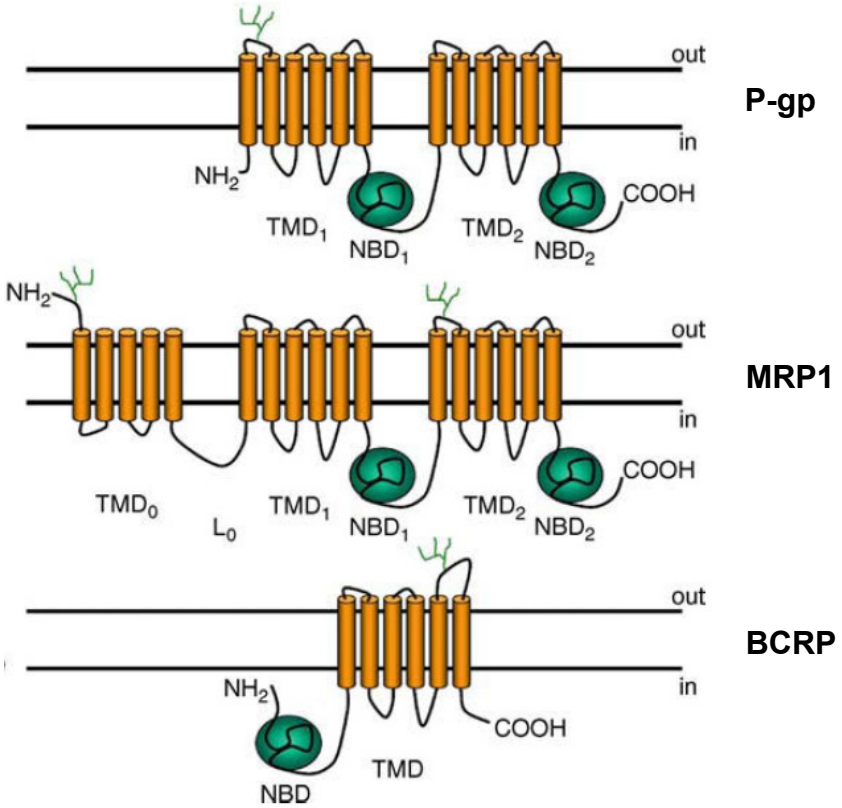

Figure 1-1. The membrane topology of P-glycoprotein (P-gp), multidrug resistance-associated protein (MRP1) and breast cancer resistance protein (BCRP). TMD, transmembrane domain; NBD, nucleotide binding domain; L_0, linker chain between TMD0 and TMD1 of MRP1. Figure used with permission from Szakács et al., 2008b (Appendix V).

1.2.1 P-Glycoprotein

1.2.1.1 Structure

P-gp is 170 kDa in size, with 1280 residues in a single polypeptide (Sharom, 2008; Zhou, 2008b). The protein can be split into two homologous halves, each half composed of one TMD with 6 trans-membrane (TM) α-helices and one cytoplasmic NBD linked by a cytoplasmic 60 amino acid linker chain (Figure 1-1). The topology of the protein is N-TMD1-NBD1-TMD2-NBD2-C and the presence of two TMDs and NBDs make it a 'full-transporter' (see Section 1.2) which means that it does not require dimerization to be functional. P-gp is N-glycosylated at three asparagine residues in the first extracellular loop (Li et al., 2010a; Zhou, 2008b). Glycosylation is not essential for transport activity, but may play a role in the correct trafficking of the protein to the plasma membrane (Li et al., 2010a). The role of phosphorylation on transport activity remains unclear as a P-gp mutant lacking all phosphorylation sites exhibited normal function (Li et al., 2010a).

A high-resolution x-ray crystal structure of human P-gp is not available but considerable insight has been gained from homology modeling and availability of crystallography data from bacterial, *C. elegans* and mouse P-gp (Aller et al., 2009; Jin et al., 2012; Li et al., 2013). These studies show a very large internal cavity, 6000 $Å^3$ within the lipid bilayer formed by the TM helices (Li et al., 2013; Sharom, 2011). This substrate binding site is lined with hydrophobic and aromatic residues which may explain the lipophilicity of P-gp substrates (Aller et al., 2009). The lower half of this cavity, closest to the cytoplasm, has negatively charged residues such as glutamate which could account for binding of positively charged hydrophobic compounds. The binding pocket is large enough to accommodate multiple drugs simultaneously in different regions of the cavity. This was demonstrated by the co-crystallisation of mouse P-gp with two molecules of the inhibitor Q-Z59, bound to an upper and lower site of the pocket (Li et al., 2013). The presence of multiple drug binding sites was predicted from previous transport competition studies. Shapiro and Ling (1997) have previously proposed two distinct substrate binding-sites called the H- and R- site. This was based on observations that the substrates rhodamine-123 and Hoechst-33342 did not interfere with each other's transport.

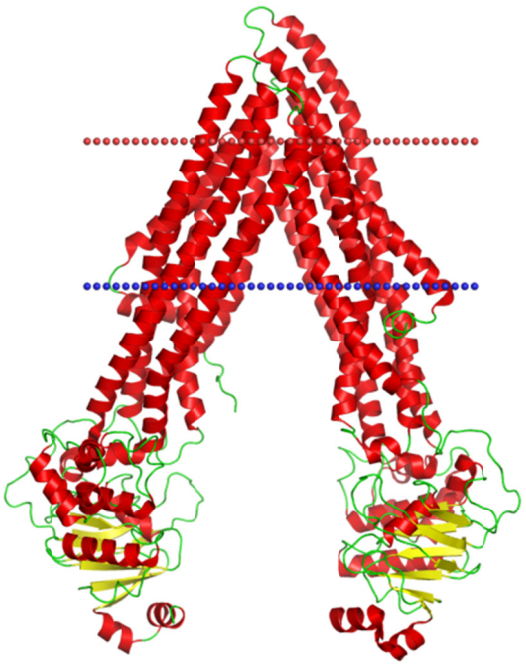

Figure 1-2. Homology model of P-gp in the inward-facing or open conformation. Sourced from Orientation of Proteins in Membranes (OPM) database (http://opm.phar.umich.edu/).

1.2.1.2 Transport mechanism

P-gp is either in an inward- or outward-facing conformation. In the inward-facing or open conformation the two TMDs form an inverse V with the helices intertwined at the outer bilayer leaflet side and open towards the cytoplasm (Figure 1-2) (Aller et al., 2009). The opposite is observed in the outward-facing conformation. Substrate binding occurs in the inward facing conformation where the binding site is directly accessible from the inner bilayer leaflet (Aller et al., 2009; Li et al., 2013). This agrees with observations that membrane partitioning is a necessary first step for substrates and inhibitors which are then able to move from the inner leaflet to the binding pocket (Seelig and Gatlik-Landwojtowicz, 2005). This also explains the propensity for these compounds to be lipid-soluble. Bilayer transport leads to the 'hydrophobic vacuum-cleaner' model which suggests direct interception of substrates at the membrane before entry into the cytoplasm (Sharom, 2011). The exact mechanism of the transport cycle is yet to be fully clarified. In the 'ATP-switch' model (Figure 1-3), the binding pocket is at a high affinity state for substrates in the inward facing (or open dimer) conformation (Higgins and Linton, 2004; Linton, 2007). Substrate binding causes a conformational change in the TMDs that is transmitted to the NBDs. The affinity of the

NBDs for ATP is increased. Two ATP molecules then bind to the two NBDs. This causes a change of the transporter from the inward conformation to the outward conformation (closed dimer). The outward conformation has low-affinity for the substrate, causing its release either to the outer leaflet of the bilayer or to the extracellular space (Linton, 2007; Ward et al., 2013). Hydrolysis of ATP and the release of ADP and inorganic phosphate then resets the transporter back to the high affinity inward conformation. The exact order and mechanism of ATP binding and hydrolysis and coupling with conformational changes at the TMD, remain the subject of debate.

The transport mechanism of P-gp is highly conserved across ABC efflux transporters (Higgins and Linton, 2004). With a few minor differences, the transport cycles of BCRP, MRP1 and MRP5 all proceed through similar steps.

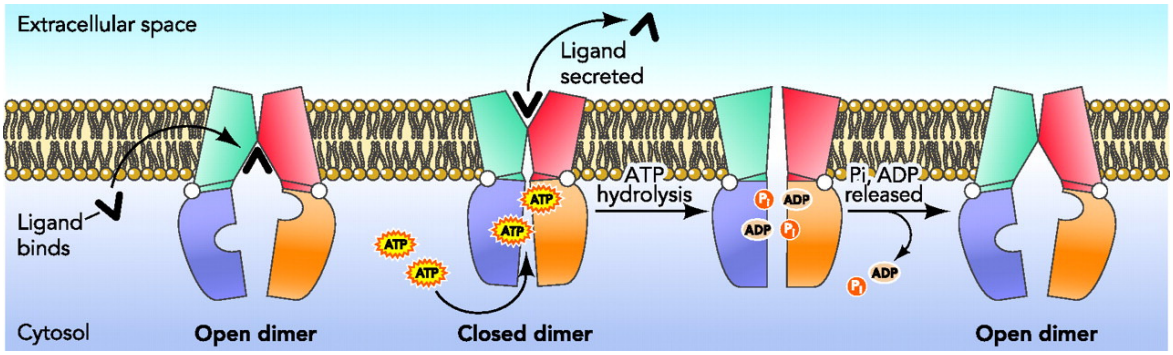

Figure 1-3. The ATP-switch model of P-gp transport. See Section 1.2.1.2 for an explanation of the transport cycle. Source from Linton, 2007 (see Appendix V for permissions).

1.2.1.3 Tissue distribution and function

P-gp knock-out (KO) mice are viable and fertile in a controlled lab environment (Schinkel et al., 1994, 1997). Suggesting that P-gp does not have an essential physiological function. Interestingly, upon exposure to xenobiotic drugs, P-gp KO mice suffer greater toxicity and enhanced pharmacological effects compared to wild-type mice (Chen et al., 2003). Altered pharmacokinetics such as increased oral absorption, decreased clearance and increased accumulation into previously inaccessible compartments were observed. In one example, KO and wild-type mice were treated with the anthelmintic and P-gp substrate, ivermectin, for mite infection (Schinkel et al., 1994). Almost all KO mice died within a day after treatment while wild-type mice were unaffected. It was later found that P-gp KO mice had 20-fold higher brain concentrations of ivermectin than wild-type mice, consistent with the absence of P-gp at the BBB (Schinkel et al., 1994).

These results and fact that high expression of P-gp is found in pharmacological barriers and excretory organs led to the conclusion that P-gp limits exposure of the body to foreign substances (Schinkel et al., 1994). In the intestines, P-gp is found in the apical membrane of enterocytes and is present throughout the entire gut (Cascorbi, 2011). It pumps substrate drugs into the gut lumen thereby limiting drug entry and contributing to intestinal drug excretion (Cascorbi, 2011; Huls et al., 2009). This in turn reduces the bioavailability of substrates, though high drug concentrations in the gut may saturate transporter activity. P-gp is expressed on the luminal side of endothelial cells forming the BBB and is the main efflux pump responsible for limiting drug access to the brain (Huls et al., 2009; Szakács et al., 2008a). This can be a major problem in central nervous system (CNS) diseases such as epilepsy and brain metastasis because P-gp limits the penetration of therapeutic agents (Agarwal et al., 2011; Zhang et al., 2012). P-gp is expressed at the canalicular membrane of hepatocytes and the luminal side of renal proximal tubule cells of the kidney where it contributes to drug clearance through active excretion of drugs into the bile and urine (Huls et al., 2009; Cascorbi, 2011). P-gp expression in the placenta protects exposure of the fetus to drugs in the maternal circulation (Hutson et al., 2010). Other tissues that express P-gp include the endothelial cells that make up the blood-testis-barrier and the bronchial and bronchiolar epithelium of the lung (Leslie et al., 2005). In summary, P-gp can influence the absorption, distribution and clearance of its substrates. It is therefore unsurprising that pharmacokinetic interactions have been observed in

the clinic between substrate drugs and modulators (Glaeser, 2011; Hirata et al., 2005; Mertz et al., 2009). Currently, the US Food and Drug Administration (FDA) has made it a requirement for new candidate drugs to undergo screening for P-gp efflux or modulation in an attempt to limit drug-drug interactions (DDIs) (Giacomini et al., 2013; Huang et al., 2010).

P-gp is also expressed in hematopoietic progenitor cells in the bone marrow suggesting a role in protecting this sensitive cell population from toxins (Dean, 2009; Huls et al., 2009). High expression was also seen in immune cells. P-gp inhibition impaired migration of antigen-presenting dendritic cells, reduced the cytolytic activity of natural killer and CD8+ T-cells and decreased cytokine secretion from activated lymphocytes (Mizutani et al., 2008). Hence, P-gp may potentially play a role in the host immune response. Finally, P-gp expression has been implicated in apoptosis resistance. P-gp can efflux platelet-activating factor which binds to receptors that upregulate anti-apoptotic proteins (Fletcher et al., 2010). It also decreases the production of the pro-apoptotic sphingolipid, ceramide, by limiting the availability of its precursor, sphingomyelin (Fletcher et al., 2010; Mizutani et al., 2008).

1.2.1.4 Substrates and inhibitors

Substrates

P-gp currently has the largest number of identified substrates and modulators of all the ABC transporters. It includes therapeutic drugs, environmental chemicals and endogenous compounds (Table 1-1) (Zhou, 2008b). It is considered the most important active efflux transporter in pharmacotherapy (Sharom, 2011; Zhou, 2008b). Substrates of P-gp are structurally diverse with no readily identifiable pharmacophore. Structure-activity relationship studies still cannot distinguish between substrates and non-substrates with a high degree of confidence (Chen et al., 2012). Substrates are mostly lipophilic, contain hydrophobic groups and hydrogen bond acceptors; and can be positively charged at physiological pH (Chen et al., 2012; Seelig and Gatlik-Landwojtowicz, 2005). P-gp does not seem to transport anionic compounds (Borst and Elferink, 2002). As discussed in Section 1.2.1.1 and 1.2.1.2, the binding pocket is lined with hydrophobic and negatively charged residues, explaining the apparent substrate selectivity. Hydrogen bond donors at the binding site may account for the requirement of hydrogen acceptor groups (Aller et al., 2009;

Seelig, 1998). Also, the requirement for high lipophilicity is necessary in order for substrates to partition into the membrane and reach the binding pocket (Seelig, 1998).

P-gp has substantial substrate overlap with other ABC transporters like MRP1 and BCRP (Zhou, 2008b). These may compensate for the inhibition of P-gp activity. For example, KO mice for P-gp or BCRP alone caused 4- and a 2-fold increases in brain/plasma ratio of lapatinib compared to wild-type mice (Agarwal et al., 2011). This increased to 43-fold in P-gp/BCRP double KO mice (Agarwal et al., 2011).

With the exception of the platin drugs, P-gp can efflux compounds from every major class of anticancer drug. These include the taxanes, anthracyclines, plant alkaloids like topotecan and vinblastine, and kinase inhibitors like erlotinib and imatinib (Table 1-1) (Glaeser, 2011; Szakács et al., 2008a; Zhou, 2008b). Non-anticancer drug substrates include antiretroviral agents, antibiotics, antimalarials, cardiac drugs like digoxin, calcium-channel blockers, anticonvulsants, antihypertensives, immunosuppressants, steroid hormones and neuroleptics (Table 1-1) (Cascorbi, 2011; Glaeser, 2011; Zhou, 2008b). P-gp is therefore implicated in the treatment of disorders and diseases such as epilepsy, depression, cardiovascular disease and human immunodeficiency virus (HIV) infections. It is also known to efflux a number of fluorescent dyes, such as rhodamine-123 and Hoechst-33342; which are widely used in determining P-gp efflux activity in *in vitro* studies (Zhou, 2008b). Transport of ^{99m}Tc-sestamibi by P-gp, a drug used in cardiac imaging, has led to its use in the *in vivo* imaging of P-gp efflux (Kelly et al., 2011).

Endogenous substrates (mentioned in Section 1.2.1.3) include the platelet-activating factor, cytokines and sphingomyelin (Mizutani et al., 2008). P-gp is also known to efflux steroids, such as cortisol, corticosterone, aldosterone and may be involved in secretion of these hormones due to its expression in the adrenal glands (Bello-Reuss et al., 2000). P-gp has been implicated in the secretion of somatostatin and substance P, hormones involved in gastrointestinal and digestive functions (Uchiyama-Kokubu et al., 2004). Recent evidence suggests a role in the efflux of the amyloid-β peptide from the brain (van Assema et al., 2012; Ohtsuki et al., 2010). A decrease in P-gp function was observed in Alzheimer's patients, hinting at a possible role of the transporter in the pathogenesis of this disease (van Assema et al., 2012).

Table 1-1. Selected P-gp substrates

Anticancer agents	*Fluorescent dyes*
Actinomycin D	Rhodamine 123
Dasatinib	Hoechst-33342
Daunorubicin	Calcein-acetoxymethylester
Docetaxel	(AM)
Doxorubicin	Fluoro-2
Docetaxel	Fura-2
Epirubicin	
Etoposide	*Steroids*
Erlotinib	Dexamethasone
Gefitnib	Methylprednisolone
Imatinib	
Irinotecan	*Immunosuppressants*
Mitomycin C	Cyclosporine A
Mitoxantrone	Sirolimus
Paclitaxel	Tacrolimus
Teniposide	
Topotecan	*Flavonoids*
Vincristine	Quercetin
Vinblastine	Naringenin
Ixabepilone	Biochanin A
Olaparib	Kaempferol
Antiarrhythmics	*Antibiotics and antifungals*
Amiodarone	Erythromycin
Digoxin	Itraconazole
Quinidine	Ketoconazole
Verapamil	Cefoperazone
	Tetracycline
HIV agents	
Amprenavir	*Antimalarials*
Indinavir	Chloroquine
Nelfinavir	Quinine
Ritonavir	
Saquinavir	*Steroid Hormones*
Lopinavir	Aldosterone
	Dexamethasone
Anticonvulsants	
Phenobarbital	*Neuroleptics*
Phenytoin	Chlorpromazine
Carbamazepine	Phenothiazine
Lamotrigine	
Primidone	

Compiled from Cascorbi, 2011; Li and Paxton, 2013; Sharom, 2011; Zhou, 2008b.

Inhibitors

Inhibitors of P-gp include current therapeutic drugs, phytochemicals and other natural compounds, lipids, surfactants and peptides (Palmeira et al., 2012a; Zhou, 2008b). One of the earliest to be identified was the calcium channel blocker, verapamil, in 1981 (Tsuruo et al., 1981). Since then, other approved drugs such as the immunosuppressant cyclosporine A; the antimalarial quinine; anesthetic agents (e.g., propofol); antiretrovirals like ritonavir; antibiotics and antifungals like erythromycin and ketoconazole have all been shown to inhibit transport (Palmeira et al., 2012a; Zhou, 2008b). Approved drugs were the first to be combined with chemotherapeutic agents in the clinical setting to reverse MDR. Currently, three generations of P-gp inhibitors have proceeded to clinical trials. These inhibitors and their use in attemptng to block P-gp in the clinic will be discussed further in Section 1.2.5.

Inhibition of P-gp transport can be via direct competition at the substrate binding site (e.g., cyclosporine A, verapamil), inhibition of ATP binding at the NBD, or inhibition by binding to a negative allosteric site of P-gp. Some flavonoids were thought to inhibit the ATPase activity of P-gp by binding to the NBD (Li and Paxton, 2013). Negative allosteric modulation was observed with the thioxanthene derivative cis-(Z)-flupentixol which inhibits transport by preventing substrate translocation and dissociation (Maki et al., 2003). Aside from direct interaction with the P-gp transporter, membrane composition and fluidity may influence transport activity. Inhibition by non-ionic surfactants, such as Tween-20, Triton X-100 and Pluronic P85, is thought to be partially mediated by fluidisation of the membrane which in turn can decrease the ATPase activity of P-gp (Batrakova et al., 2001; Ferté, 2000). Anaesthetics such as chloroform and propofol reverse P-gp mediated resistance without affecting its function by increasing the movement of substrate between the outer and inner leaflet of the bilayer (Palmeira et al., 2012a). This increased transmembrane movement can overwhelm P-gp flippase activity leading to a loss of net transport and reversal of P-gp mediated MDR (Palmeira et al., 2012a).

Inhibition of P-gp is a complex process due to the presence of multiple drug binding sites. For example, in the three-binding site model which includes two distinct H- and R- transport sites and an allosteric P-site, competitive inhibitors of the H-site may have little effect on substrates preferentially binding to the R-site (Shapiro et al., 1999). A range of substrate drugs in inhibitor

screening should be used so as not to identify compounds that only inhibit the transport of a small subset of substrates. Compounds may also display concentration-dependent effects on P-gp activity. (Shapiro and Ling, 1997) For example, at a low concentration, daunorubicin binds to the R-site and stimulates the export of Hoechst-33342 but, as concentration increases, it starts to bind to the H-site and competitively inhibits Hoechst transport. This may have clinical implications as identified inhibitors *in vitro* may be present in the target tissue at low concentrations, where they can enhance efflux of compounds rather than cause inhibition. The multiple binding sites also further complicate the determination of the mechanism of transport inhibition. For example, verapamil is considered a non-competitive inhibitor at low daunorubicin concentrations but a competitive inhibitor at high substrate concentrations (Spoelstra et al., 1994).

1.2.2 Breast cancer resistance protein

1.2.2.1 Structure

BCRP is a 655-amino acid protein with a molecular weight of 72 kDa (Ni et al., 2010a). Unlike P-gp, it is a half transporter and has only one NBD and one TMD (Figure 1-1) arranged in an N-NBD1-TMD1-C topology which is the reverse of P-gp (i.e., TMD1 of P-gp is N-terminal). The TMD is composed of 6 trans-membrane (TM) α-helices TM1-TM6, with the extracellular loop between TM5 and TM6 being glycosylated (Nakanishi and Ross, 2012; Ni et al., 2010a). Full transport activity was observed upon expression of human BCRP in insect cells (Glavinas et al., 2007). Since these cells do not glycosylate the transporter, it is unlikely that glycosylation plays a role in BCRP function.

BCRP is non-functional as a monomer, requiring at least two TMDs to form the central translocation pathway. Also, the NBDs are required to dimerise to be catalytically active. Western blotting has confirmed that BCRP migrates as a 140 kDa band in non-denaturing conditions, as opposed to a 72 kDa band expected from monomers (Ni et al., 2010a). This suggests it exists as homo-dimers probably involving intermolecular disulfide bridges. Further studies have shown higher order oligomer formation of up to 12 monomers (Xu et al., 2004). But to date, the role of oligomerisation in the function and transport activity of BCRP remains unclear, although it has been proposed that oligomer formation leads to a complex with a larger central pore and a higher degree of transport (Mo and Zhang, 2009).

Characterisation of the translocation pathway has been guided by homology modeling, mutagenesis and biochemical studies (Ni et al., 2010a, 2010b). At present, no crystallographic data are available for BCRP but experimental topology data comparison with related bacterial transporters and the crystal structure of mouse P-gp have been used to build a model of the functional BCRP dimer (Ni et al., 2010a, 2010b). The model predicts the presence of a large substrate binding cavity which can be accessed directly from the inner bilayer leaflet or the cytoplasm. Membrane partitioning was found to be important in the interaction at the substrate binding site (Matsson et al., 2007). Accessibility from the cytoplasm is also consistent with the transport by BCRP of hydrophilic anion conjugates such as sulfated drugs, which are unlikely to partition into the bilayer (Ni et al., 2010a). The homology model, together with molecular docking

studies also indicate the presence of multiple drug binding sites. This supports data from competition studies which show the inability of some substrates to reciprocally inhibit each other's transport. For example, it was found that topotecan was unable to inhibit the efflux of mitoxantrone, despite a 23-fold molar excess (Nakanishi et al., 2003). The TMDs forming the binding pocket are seen to be lined with numerous hydrophobic aromatic residues and hydrogen bond donors similar to the P-gp binding cavity, which may explain the substrate overlap between the two transporters (Ni et al., 2010a, 2010b).

1.2.2.2 Tissue distribution and function

Mice without functional BCRP develop normally and do not present with any obvious abnormalities (Jonker et al., 2002). However, they develop serious phototoxic skin lesions upon exposure to ultra-violet light (Jonker et al., 2002). It was found that they have higher plasma concentrations of the phototoxic compound pheophorbide A, a chlorophyll-breakdown product which is present in the mouse diet but virtually undetectable in the plasma of wild-type mice. It was demonstrated that pheophorbide A is an efficient substrate of BCRP, suggesting that BCRP plays a role in its absorption and possibly its renal and hepatic clearance (Jonker et al., 2002).

It is now considered that the main physiological function of BCRP is tissue defense against xenobiotics (Borst and Elferink, 2002). Expression studies in mice and humans show high BCRP expression in the major pharmacological barriers (Huls et al., 2009; Szakács et al., 2008a). Currently it is known that BCRP in humans is highly expressed in the placenta and small intestines. It is also present in the BBB, liver, kidneys, mammary glands, lungs, blood-testis-barrier, adrenal and sweat glands (Schnepf and Zolk, 2013). In polarised cells such as liver hepatocytes and enterocytes; BCRP is expressed at the apical side of the membrane (Huls et al., 2009; Mennone et al., 2010). The direction of transport is away from the circulation and into either the gut lumen, or the bile duct. In the placenta, BCRP effluxes substrates into the maternal circulation, limiting drug entry to the fetus (Mao, 2008). Similarly, endothelial cells forming the BBB express BCRP at the apical side, effluxing substrates towards the systemic circulation and away from the brain (Nicolazzo and Katneni, 2009).

Studies in mice clearly demonstrate an impact of BCRP on the absorption and distribution of substrate drugs, as well as on their renal and hepatic clearance. Fetal-to-maternal plasma ratios

were increased 2- to 5-fold when pregnant mice lacking BCRP were given either topotecan, nitrofurantoin or glyburide and BCRP KO mice had 6-fold higher oral bioavailability of topotecan compared to wild-type (Vlaming et al., 2009; Jonker et al., 2002). In the clinic, serious side effects were associated with the inhibition of BCRP. For example, administration of proton pump inhibitors inhibited the renal clearance of the BCRP substrate, methotrexate (MTX), leading to severe myalgia and bone pain (Santucci et al., 2010; Tröger et al., 2002). Concern for possible adverse DDIs has led the US FDA to require testing of new drugs for BCRP transport and inhibition (Giacomini et al., 2013).

BCRP is also highly expressed in hematopoietic and tissue stem cells where its expression protects these pluripotent cells from potential toxins (Dean, 2009; Huls et al., 2009). It is also considered as a stem cell marker and its efflux of the fluorescent dye Hoechst-33342 is a popular method to identify this sub-population (Nakanishi and Ross, 2012). BCRP also confers a survival advantage to stem cells under the hypoxic conditions that exist in the bone marrow (Krishnamurthy et al., 2004). This lack of oxygen leads to increased heme synthesis which would be toxic if it were not for its efflux by BCRP, which is upregulated through a hypoxia response element in its promoter. This allows stem cells to thrive in these conditions (Krishnamurthy et al., 2004).

BCRP is present and upregulated in mammary glands where it excretes vitamins, such as riboflavin and vitamin K into breast milk during lactation (van Herwaarden et al., 2007). Unfortunately, it also secretes dietary carcinogens or xenobiotics that may be present in the maternal circulation (Nakanishi and Ross, 2012). BCRP may also play a role in folic acid homeostasis since glutamylated forms of folic acid are transported by BCRP and cellular build-up upregulates its expression (Schnepf and Zolk, 2013). The transport of glucuronide and sulfate conjugates of steroid hormones such as estrone-3-sulfate (E3S) and estradiol-17β-D-glucuronide suggests a role of BCRP in steroid hormone metabolism and elimination (Nakanishi and Ross, 2012). Recently, BCRP was demonstrated as an important transporter in the intestinal and renal secretion of uric acid where individuals with a defective BCRP variant had increased incidence of hyperuricemia and were more likely to develop gout (Hosomi et al., 2012; Matsuo et al., 2011).

1.2.2.3 Substrates and inhibitors

Substrates

The range of drugs that BCRP can transport is not as broad as that of P-gp but it includes hydrophilic and anionic molecules including phase II conjugates like glucuronides and sulfates (Robey et al., 2009). In fact, the diversity of BCRP substrates makes it difficult to identify common structural features. Few quantitative structure-activity relationship (QSAR) studies have been conducted for substrate identification, with recent efforts relying mainly on machine learning statistical methods. One of the best models has only 76% accuracy to predict substrates in an external validation set and further refinement is necessary before confident conclusions can be drawn from these models (Hazai et al., 2013).

BCRP shows overlapping substrate specificity with both P-gp and MRP1 despite the TMDs having little sequence homology. Tyrosine kinase inhibitors (TKIs) for example are well-reported to be dual P-gp/BCRP substrates which has implications in attempting to increase their brain penetration in treating CNS metastases (Agarwal et al., 2011; Colabufo et al., 2011). In mice studies, greatly increased brain-to-plasma ratios could only be achieved in dual knockouts, with little effect seen in single KOs of either transporter (Agarwal et al., 2011).

BCRP has been reported to efflux anticancer drugs such as mitoxantrone, camptothecins (topotecan and irinotecan), etoposide, flavopiridol, MTX and TKIs (Table 1-2) (Mao and Unadkat, 2005; Robey et al., 2009, 2011). The interaction of BCRP with TKIs is concentration dependent since at sub-micromolar levels, imatinib and gefitinib are effectively transported by BCRP, whereas at micromolar concentrations BCRP transport is inhibited (Shukla et al., 2012; Pick et al., 2010; Takigawa et al., 2007). It was also noted in *in vitro* studies that BCRP conferred resistance to anthracyclines such as doxorubicin and daunorubicin. It was found that transport was due to a gain-of-function substitution at residue 482 from arginine to either glycine or threonine (Borst and Elferink, 2002). The relevance of this is questionable as the mutation is present only in cancer cell lines and was not observed in the normal population (Meyer zu Schwabedissen and Kroemer, 2011). BCRP is also known to efflux other therapeutic agents including the statins, antibiotics, antiviral drugs, sulfasalazine (SSZ) and dihydropyridines (Table 1-2) (Robey et al., 2011). The statins have been particularly well-studied for pharmacokinetic interactions with BCRP due to

significantly increased plasma concentrations in patients carrying a defective BCRP variant (Schnepf and Zolk, 2013). Both pravastatin and rosuvastatin together with SSZ, are being investigated as *in vivo* probes of BCRP function (Adkison et al., 2010; Meyer zu Schwabedissen and Kroemer, 2011). BCRP also effluxes fluorescent dyes, such as BODIPY FL prasozin and Hoechst-33342, which have been essential in the assessment of BCRP transport *in vitro*, particularly in flow cytometry studies (Robey et al., 2009). These dyes have been used together with mitoxantrone and pheophorbide A which are also fluorescent (Robey et al., 2009).

Protection of BCRP against the diet-derived toxin, pheophorbide A, led to identification of other substrates present in the diet. BCRP was found to efflux dietary carcinogens in cooked meats which include polycyclic aromatic hydrocarbons and heterocyclic amines (van Herwaarden et al., 2006). Aflatoxin B1, a carcinogen in fungi-contaminated grain, is also a substrate (van Herwaarden et al., 2006). BCRP decreases the bioavailability of beneficial plant-derived compounds or phytochemicals and is known to transport anthocyanins and flavonoids which have been linked to a number of health benefits (Dreiseitel et al., 2009; Li and Paxton, 2013). Endogenous substrates (mentioned in the previous section) also include vitamins, urate, and phase II metabolites of steroid hormones and heme.

Table 1-2. Selected BCRP substrates

Anticancer agents	*Fluorescent dyes*
5-Fluorouracil	Hoechst-33342
Methotrexate	BCECF-AM
Mitoxantrone	BODIPY-FL prasozin
Topotecan	
Imatinib	*Hormones*
Gefitinib	Sulfate and glucuronide
Lapatinib	conjugates of estradiol and
Erlotinib	estrone
Nilotinib	
Ortataxel	*Carcinogens*
Irinotecan	Aflatoxin B1
SN-38	PhIP*
Flavopiridol	IQ†
Antivirals	*Flavonoids*
Lopinavir	Quercetin
Nelfinavir	Chrysin
Delavirdine	Genistein
Zidovudine	Malvidin
Abacavir	Petunidin
Statins	*Antibiotics and antifungals*
Rosuvastatin	Ciprofloxacin
Pitavastatin	Ofloxacin
Cerivastatin	Norfloxacin
Calcium channel blockers	*Immunosuppressant*
Azidopine	Sulfasalazine
Dipyramidole	
Nitrendipene	*Cholorophyll metabolite*
	Pheophorbide A

*PhIP – 2-amino-1-methyl-6-phenylimidazo[4,5-b]pyridine
†IQ – 2-amino-3-methylimidazo[4,5-f]quinoline
Compiled from Robey et al., 2009, 2011; Szakács et al., 2008a; van Herwaarden et al., 2006; Li and Paxton, 2013.

Inhibitors

The first identified inhibitors of BCRP were also P-gp inhibitors. These included elacridar, cyclosporine A, biricodar and tariquidar (Robey et al., 2011). Other non-specific inhibitors include the antiretrovirals nelfinavir and ritonavir (Ni et al., 2010a). The first highly selective and potent BCRP inhibitor was the fungal toxin fumitremorgin C (FTC) which showed no activity against P-gp or MRP1-5 (Allen et al., 2002). However, it was toxic and induced tremors and convulsions in mice. Analogue studies led to the discovery of Ko143, which had improved potency and retained the specificity of FTC, without causing neurotoxic effects (Allen et al., 2002). It is currently considered to be the most potent inhibitor of BCRP. The TKIs, imatinib and gefitinib, are also considered potent inhibitors (Pick et al., 2010; Takigawa et al., 2007). Natural compounds and phytochemicals in fruits, vegetables and wine are also reported inhibitors and include curcumin from curry powder, catechins from tea and flavonoids such as chrysin, genistein and quercetin (Li et al., 2010b; Vinod et al., 2013). This has raised the possibility of drug interactions between ubiquitous dietary components and orally administered BCRP substrates (Li et al., 2010b; Morris and Zhang, 2006).

Complex inhibitor interactions due to the presence of multiple drug binding sites are also observed with BCRP. Thus two BCRP substrates may not show competitive inhibition if they bind to different sites in the transporter. For example, zidovudine and abacavir do not affect the transport of prazosin and imatinib (Giri et al., 2009). Multi-site binding has important implications in inhibitor screening as substrate-dependent inhibition is possible. Ejendal and Hrycyna (2005) concluded that cyclosporine A is not a BCRP inhibitor as it did not inhibit the binding of the BCRP substrate [^{125}I]-IAAP (iodoarylazidoprazosin). However, another group has shown BCRP inhibition using pheophorbide A and mitoxantrone as substrates (Gupta et al., 2006). It is likely that cyclosporine A competes at the mitoxantrone binding site but not that of prazosin. This emphasizes the importance of using multiple substrates in inhibitor testing to accurately characterize transporter interactions.

At present, accurate *in silico* prediction of BCRP inhibition remains elusive. Studies have identified structural features that correlate with transport inhibition but these have been conducted using a data set of congeneric compounds and are therefore not universally applicable (Pick et al., 2011;

Zhang et al., 2005). It should be noted that in many QSAR studies, lipophilicity correlated positively with inhibition (Gandhi and Morris, 2009). In a global BCRP inhibition model, 83% of BCRP inhibitors in a test set could be accurately predicted based only on lipophilicity and molecular polarisability (Gandhi and Morris, 2009; Matsson et al., 2007). This agrees with the theory that membrane partitioning is the first step in inhibiting BCRP (Matsson et al., 2007).

1.2.2.4 Regulation of expression

The BCRP promoter has response elements for hypoxia inducible-factor (HIF), hormones, orphan nuclear receptors and transcription factors activated by oxidative stress (Nakanishi and Ross, 2012). Exposure to xenobiotics can lead to increased BCRP expression through a xenobiotic response element bound by the xenobiotic-sensing aryl hydrocarbon receptor (AhR). AhR ligands such as dietary carcinogens (e.g., benzo[a]pyrene) and phytochemicals, upregulate BCRP *in vitro* through this mechanism (Ebert et al., 2005). BCRP is also upregulated by peroxisome proliferator-activated receptor gamma (PPAR-y) agonists (Hoque et al., 2012). Upregulation is also possible through the Nrf2 transcription factor which binds to an antioxidant response element in the promoter (Singh et al., 2010). This is a redox balance sensor activated by oxidative stress. Oxidants such as anticancer drugs (e.g., anthracyclines) can enhance BCRP expression without binding to nuclear receptors.

Sex hormones are known to influence the expression of BCRP but results are contradictory. Estradiol upregulates BCRP mRNA in primary placental trophoblasts but downregulates it in BeWo choriocarcinoma cells (Mao, 2008; Nakanishi and Ross, 2012). Estradiol also reduced BCRP gene and protein expression in isolated rat brain capillaries (Mahringer and Fricker, 2010). Estradiol effects may depend on the estrogen receptor subtypes present in the cell. Estrogen receptor-alpha binding induced expression while binding to the beta subtype decreased expression (Ee et al., 2004; Mahringer and Fricker, 2010; Mao, 2008). Progesterone also regulates BCRP expression. Activation of the progesterone receptor β-subtype induced expression and is likely the mechanism for increased placental BCRP expression during pregnancy, when high progesterone concentrations are observed and the progesterone receptor is upregulated in placenta (Wang et al., 2008). However, contradictory results have also been reported (Wang et al., 2008; Wu et al., 2012).

BCRP expression can be induced by growth factors via the epidermal growth factor receptor (EGFR) and human epidermal growth factor 2 receptor (HER2) (Nakanishi and Ross, 2012; Nakanishi et al., 2010). The NF-κB protein complex, which is a downstream target of EGFR and HER2, was shown to directly bind to the BCRP promoter region and activate gene transcription (Nakanishi and Ross, 2012; Qiao et al., 2013; Somers-Edgar et al., 2011; Wang et al., 2010b; Yadav et al., 2010, 2012a). Increased BCRP expression in cell lines has been observed through this pathway and may be one mechanism for tumours to overexpress BCRP (Nakanishi and Ross, 2012; Nakanishi et al., 2010). Hypoxia, a common feature in solid neoplasms, can also induce BCRP through HIF-1α binding to a hypoxia response element in the BCRP promoter (Krishnamurthy et al., 2004). Stress kinases may also be activated (e.g., c-Jun N-terminal kinases or JNKs) which increase expression (Tomiyasu et al., 2013). Interleukin-6 in the tumour microenvironment can act through X-box binding protein-1 (XBP-1) and induce expression while transforming growth factor-beta (TGF-β) represses transcription through Smad2/3 direct binding of the BCRP promoter, thus linking the immune mediators with BCRP expression (Natarajan et al., 2012). Demethylation and histone acetylation can induce BCRP expression and is a possible mechanism of resistance to BCRP substrates in cancer cell lines (Nakanishi and Ross, 2012; Natarajan et al., 2012). Resistance also resulted from cells expressing transcripts with a truncated 3'-untranslated region, preventing binding of regulatory microRNA (miRNA) that repress expression (Nakanishi and Ross, 2012). The levels of mRNA and BCRP protein expression do not often correlate as observed with acute myelogenous leukemia (AML) samples (Suvannasankha et al., 2004). This suggests post-transcriptional and post-translational mechanisms may be the main determinant of tissue expression in certain cases.

Post-translational regulation of BCRP includes phosphorylation at threonine-362 by the proto-oncogene serine/threonine-protein kinase-1 (Pim-1). Phosphorylation promotes multimer formation of the transporter and translocation to the plasma membrane (Xie et al., 2008). Interference of signaling through the phosphoinositide 3-kinase/Akt (PI3K/AKT) pathway leads to internalisation and a reduction in BCRP present at the cell surface. This was observed with the phosphoinositide 3-kinase (PI3K) inhibitors, LY294002 and wortmannin, where reduced surface immunolabeling was seen without changes to total protein levels (Takada et al., 2005). In KO mice lacking AKT, BCRP localised to the cytoplasm of stem cells with no transporters present at the surface (Mogi et

al., 2003). The mechanism linking PI3K/AKT and BCRP cell surface expression is currently unknown (Nakanishi and Ross, 2012).

1.2.3 Multidrug resistance-associated protein 1 and 5

1.2.3.1 Structure

MRP1 is 1531 amino acids long and runs as a 190 kDa protein in immunoblots (Cole, 2013; He et al., 2011). It is larger than P-gp due to an extra N-terminal domain known as TMD0 (Figure 1-1). The topology in the membrane from computer-assisted hydropathy plots and biochemical studies is N-TMD0-L0-TMD1-NBD1-TMD2-NBD2-C (Figure 1-1) (He et al., 2011). Seventeen TM helices are embedded in the bilayer with 5 comprising TMD0 (helices 1-5) and 6 each for TMD1 (helices 6-11) and TMD2 (helices 12-17). The L0 or linker region connects TMD0 and TMD1 (Figure 1-1). MRP1 has the typical ABC transporter functional core of two TMDs (TMD1 and TMD2) and two NBDs. Deletion of the entire TMD0 results in a protein with functional transport activity and correct trafficking to the basolateral membrane of polarised cells (Bakos et al., 1998). In contrast, deletion or mutations in the linker region L0 significantly reduces transport activity and MRP1 trafficking to the membrane (Bakos et al., 2000). Transport of leukotriene C4 (LTC_4), a classical high affinity MRP1 substrate is completely abolished by an L0 deletion (He et al., 2011).

The translocation pathway is thought to be formed by helices 6-17 from both TMD1 and TMD2; with contribution from L0 and other cytoplasmic loops. Basic residues (e.g., lysines), project into this binding pocket, explaining the transport of anionic substrates (Maeno et al., 2009). A large binding pocket with multiple binding sites is predicted (He et al., 2011). Maeno and colleagues have proposed the presence of at least three distinct binding sites for substrates and modulators (Maeno et al., 2009). Mutation of specific residues was found to abolish transport of certain substrates but not of others. For example, a mutation in Lys332 affected GSH transport but not MTX or E3S (Maeno et al., 2009). Different substrates were also found to label different residues of the transmembrane helices, supporting the presence of multiple binding sites (Bakos and Homolya, 2007).

MRP5 lacks the extra TMD0 of MRP1 (Borst et al., 2007; Slot et al., 2011). It is 1437 amino acids in length, arranged in a similar N-TMD1-NBD1-TMD2-NBD2-C configuration to that of P-gp (Figure 1-1). Little is known of its structure as efforts have focused on tissue distribution, physiological function, role in cancer resistance and substrate/inhibitor characterization. Only homology models of MRP5 based on bacterial and mouse P-gp are present (Ravna et al., 2008; Sager et al., 2012).

These models show a large substrate binding pocket with an overall positive charge from electronic potential surface analysis. This agrees with its activity as an organic anion transporter. Two drug binding sites within the pocket have been predicted centered on two basic residues, Lys448 and Arg232 (Ravna et al., 2008). Docking studies using the MRP5 substrate, cyclic guanosine monophophate (cGMP), identified residues that have been put forward for site-directed mutagenesis experiments (Ravna et al., 2008). Although these models still need to be validated biochemically, they have been useful in the search for novel MRP5 inhibitors. Recently, a homology model of MRP5 was successfully used to find new inhibitors of cGMP efflux (Sager et al., 2012).

1.2.3.2 Mechanism of transport

Biochemical studies of MRP1 support a similar substrate transport cycle to those in P-gp and BCRP (He et al., 2011). A key difference is that substrate access to the binding pocket occurs directly from the cytoplasm rather than in the bilayer (He et al., 2011). MRP1 transports hydrophilic anions which are not expected to partition into the membrane.

MRP1 shows glutathione (GSH) dependent transport that is not observed with either P-gp or BCRP (Cole, 2013; He et al., 2011). Certain compounds cannot be transported in the absence of GSH and for others like vincristine, efflux proceeds slowly but is greatly stimulated by GSH addition (Rothnie et al., 2008). Vincristine in turn, cross-stimulates the efflux of GSH by MRP1, leading to observed co-transport of both compounds. However, not all GSH-dependent substrate transport by MRP1 occurs through a co-transport mechanism. For example, GSH is required to stimulate the efflux of E3S but GSH itself is not transported (Borst et al., 2007; Cole, 2013). A heterotropic/homotropic cooperativity model proposed by Borst et al. (2006) suggests that a modulatory (M) site is present that is distinct from the substrate binding (S) site. In the case of co-transport between vincristine and GSH, both compounds have affinity for the M and S sites and can therefore alternate as modulator and substrate. This results in cross-stimulation and transport of both compounds. In the case of E3S, where cross-stimulation does not occur, it is assumed that E3S binds only to the S-site. It does not stimulate the transport of GSH efflux while GSH binds to the M-site and enhances E3S transport. Stimulation of GSH efflux by bioflavonoids such as apigenin might result from binding of apigenin to the M-site but not the S-site, thus increasing the

affinity of GSH to the S-site without apigenin being transported (Borst et al., 2006). It should be emphasized that GSH-conjugates and other compounds such as MTX are transported by MRP1 without the need for exogenous GSH (Cole, 2013). In the case of GSH-conjugates, it is possible that the GSH-moiety of the molecule binds to the M-site and stimulates its own efflux (Borst et al., 2006; He et al., 2011).

A biochemical characterization of the MRP5 transport cycle has not been conducted. From transport studies, although MRP5 is able to efflux GSH, it does not seem to show the complex GSH-dependent transport observed with MRP1 (Borst et al., 2007).

1.2.3.3 Tissue distribution and function

MRP1

MRP1 is more ubiquitously expressed than P-gp and BCRP and is present in all major tissues, with the highest expression in the lungs, testes, kidneys, heart, choroid epithelium of the blood-cerebrospinal fluid-barrier and placenta (He et al., 2011). Moderate expression was found in the gut, BBB, haematopoietic cells of the bone marrow and peripheral blood mononucleated cells (He et al., 2011). In contrast to P-gp and BCRP, little-or-no MRP1 is present in human liver (Borst et al., 2000). The expression of MRP1 in polarised cells is basolateral rather than apical and only in endothelial cells of the BBB is MRP1 found in the apical membrane (Cole, 2013; Girardin, 2006; He et al., 2011). Hence, in pharmacological barriers such as the gut and lung epithelium, MRP1 transports substrates into the blood circulation rather than to the luminal side of the barrier. MRP1 is primarily thought to protect specific cells from xenobiotic exposure rather than as a general host defense mechanism (Borst and Elferink, 2002). As a consequence of its expression pattern, MRP1 has a limited impact on substrate pharmacokinetics, but may affect substrate distribution (Wijnholds et al., 1998).

MRP1 does not appear to be involved in critical physiological functions since KO mice are healthy and fertile when raised in a protected environment (Wijnholds et al., 1997). The role in tissue protection was highlighted when such mice were administered the MRP1 substrate, etoposide. Increased toxicity was observed compared to wild-type mice which did not occur via pharmacokinetic changes (Wijnholds et al., 1998). The observed tissue damage mirrored MRP1 expression patterns. Toxicity was seen in bone marrow, seminiferous tubules and tubular cells of

the kidney which normally express high levels of MRP1 (Wijnholds et al., 1998, 2000a). KO mice also had reduced response to inflammatory stimuli and impaired migration of dendritic cells due to decreased secretion of the inflammatory response mediator, LTC_4, by mast cells, dendritic cells and eosinophils (Borst and Elferink, 2002; Wijnholds et al., 1997).

MRP1 can transport the oxidised form of GSH (glutathione disulfide, GSSG) with a 10-fold higher affinity than GSH (Suzuki and Sugiyama, 1998). This has important implications in protection against oxidative stress. The presence of an oxidant or electrophile can lead to an intracellular buildup of GSSG which itself has deleterious pro-oxidant effects (Ballatori et al., 2009; Cole, 2013). The export of GSSG by MRP1 is therefore thought to limit cellular damage. It should be noted that certain xenobiotics (e.g., verapamil, apigenin) can considerably enhance the efflux of GSH by MRP1 (Borst et al., 2006; Cole, 2013). This leads to MRP1 sensitising cells to oxidant damage rather than conferring protection (Cole, 2013). MRP1 is also thought to play a role in apoptosis where cells rapidly extrude GSH via an MRP1-mediated process (Hammond et al., 2007). Whether MRP1 inhibitors can slow down apoptosis and increase cell survival needs further investigation. This may have negative implications in combining MRP1 inhibitors with anticancer drugs whose effectiveness relies on their ability to induce apoptosis in cancer cells.

The MRP1 transport of GSH and of glucuronide and sulfate conjugates makes it an important transporter for the cellular efflux of endogenous metabolites and products of drug detoxification reactions (Leslie et al., 2005). Metabolites are hydrophilic and cannot exit the cell via passive diffusion. Although MRP2 can also efflux these conjugates, MRP1 is more ubiquitously expressed and is the transporter likely to mediate efflux from most tissues (Cole, 2013; He et al., 2011; Leslie et al., 2005). However, MRP1 does not directly secrete conjugates into urine, bile or the gut lumen due to its basolateral expression and its absence in the liver (Cole, 2013). Instead it may act cooperatively with MRP2 which is apically expressed in these organs (Keppler and Konig, 1997).

MRP5

The tissue distribution of MRP5 is not as well-characterized as that of MRP1 and MRP5 mRNA is ubiquitously expressed but at low levels (Keppler, 2011). Very few tissue distribution studies have been conducted. The highest expression levels were observed in brain endothelial cells, pyramidal neurons, astrocytes and skeletal muscles (Slot et al., 2011). MRP5 protein was also detected in

placenta, urethra, erythrocytes and corneal epithelial cells (Keppler, 2011; Zhou, 2008a). Expression in polarised cells is basolateral except in brain endothelial cells where expression is apical (Hartz and Bauer, 2010). The implications of the MRP5 expression pattern on substrate disposition are unknown. Very few *in vivo* studies have been published examining the impact of gene knockout or pharmacological inhibition on the pharmacokinetics of substrates (Keppler, 2011).

The physiological function of MRP5 is currently being elucidated. KO mice are healthy and viable, suggesting little involvement in essential physiological processes (Borst et al., 2007). MRP5 is unlikely to function in host defense to xenobiotic exposure due to (a) its low expression in organs critical for xenobiotic entry and elimination (b) its basolateral membrane expression and (c) its very limited substrate range (He et al., 2011). MRP5 may be more relevant in specific tissue protection against xenobiotics. For example, MRP5 expression in skeletal muscle may be protective against statin-induced rhabdomyolysis by preventing statin accumulation (Knauer et al., 2010). The presence of MRP5 in corneal epithelium and its rapid efflux of the anti-glaucoma drugs, bimatoprost and latanoprost; may also affect treatment response in glaucoma (Karla et al., 2009).

MRP5 is best known as a cGMP export pump (Borst et al., 2007). Similar to cyclic adenosine monophosphate (cAMP) (also an MRP5 substrate), cGMP acts as a second messenger in signal transduction pathways and is involved in the regulation of apoptosis, ion channel conductance, glycogenolysis and smooth muscle relaxation (Fallahian et al., 2011; Rybalkin et al., 2003). However, the role of MRP5 in regulating cGMP intracellular levels has been questioned. High affinity cGMP export (K_m = 2.1 μM) reported by Jedlitschky et al. (2000) was not reproduced by other groups which observed only low affinity transport, suggesting that it may instead function as a cGMP overflow pump (Borst et al., 2007). MRP5 is known to export the extracellular matrix component, hyaluronan, but KO mice continue to secrete hyaluronan via the CFTR protein (Schulz et al., 2007, 2010). MRP5 is also able to transport folic acid but at low affinity (Wielinga et al., 2005). MRP5 is not likely to function as an efflux pump for Phase II conjugated metabolites as most GSH and glucuronide conjugates were not found to be substrates (Zhou, 2008a).

1.2.3.4 Substrates and inhibitors

Substrates

MRP1

Anticancer drugs were the first MRP1 substrates to be identified. They include anthracyclines (e.g., doxorubicin), etoposide, vincristine, folate-based antimetabolites (e.g., MTX), flutamide, topoisomerase inhibitors and tyrosine kinase inhibitors (e.g., imatinib) (Table 1-3) but not taxanes (e.g., paclitaxel) (Cole, 2013; He et al., 2011). As with P-gp and BCRP, TKIs show a concentration-dependent interaction with MRP1 (Shukla et al., 2012). They act as substrates at low concentrations but are inhibitory at higher concentrations. In addition to these drug classes, MRP1 can affect the intracellular accumulation of alkylating agents such as chlorambucil, melphalan and cyclophosphamide via efflux of their GSH conjugates (Cole, 2013; Morrow et al., 1998). Other MRP1 substrates include antiretrovirals, antimalarials, antibiotics, environmental toxins, flavonoids and fluorescent dyes (e.g., calcein-AM) used *in vitro* to evaluate MRP1 transport activity (Table 1-3) (Cole, 2013; Szakács et al., 2008a). MRP1 also transports ^{99m}Tc-sestamibi, which has been used to directly image the transport activity of P-gp (Vergote et al., 2002). Endogenous substrates include GSSG and GSH, conjugated prostaglandins, sulfated and glucuronidated sex steroids, folic acid, bilirubin and leukotrienes (Cole, 2013; He et al., 2011). The leukotriene LTC_4, involved in the inflammatory response, is the prototypical MRP1 substrate with the highest affinity to the transporter (Jedlitschky and Keppler, 2002). It has little affinity for P-gp and BCRP but can be effluxed by MRP2 and MRP3 (He et al., 2011; Slot et al., 2011).

Despite little homology in the TMDs, MRP1 shows some substrate overlap with both P-gp and BCRP (Szakács et al., 2008a); thus compensatory efflux by these transporters for certain MRP1 substrates is possible if MRP1 is inhibited. However, neither P-gp nor BCRP can function as redundant efflux pathways for organic anions, which are the preferred substrates for MRP1 (He et al., 2011).

As mentioned previously (Section 1.2.3.2), MRP1 substrates are either transported in a GSH-dependent or independent manner. Most of the hydrophobic and cationic compounds (and some glucuronide and sulfate conjugates) tend to require GSH for transport, while GSH conjugates and hydrophilic compounds like MTX do not (Cole, 2013). This has implications *in vitro* as substrates

like doxorubicin and vincristine will not be transported by MRP1 in cell-free assays unless GSH is added to the buffer (Xia et al., 2007a). This also means that the rate of substrate efflux can be affected by factors that influence intracellular GSH concentrations in studies that use whole cells. Treatment of cell lines with the GSH synthesis inhibitor, buthionine sulfoximine, has been shown to inhibit the efflux of a number of MRP1 substrates (Perek et al., 2002). Conversely, increased GSH synthesis can enhance MRP1-mediated transport (Cole, 2013).

Table 1-3. Selected MRP1 and MRP5 substrates

MRP1	**MRP5**
Anticancer agents	*Anticancer agents*
Doxorubicin	5-Fluorouracil
Daunorubicin	Gemcitabine
Epirubicin	6-Thioguanine
Idarubicin	6-Mercaptopurine
Methotrexate	Methotrexate
Melphalan	Raltitrexed
Etoposide	Pemetrexed
Vincristine	
Vinblastine	*Antivirals*
Chlorambucil	Adefovir
Cyclophosphamide	Abacavir
Ortataxel	
Irinotecan	*Antiglaucoma*
	Bimatoprost
Antivirals	Latanoprost
Saquinavir	
Ritonavir	*Endogenous substrates*
Indinavir	Folic acid
	Cyclic AMP
Antibiotics	Cyclic GMP
Ciprofloxacin	Hyaluronan
Difloxacin	
	Fluorescent dyes
Fluorescent dyes	BCECF
Calcein	CFDA
Fluo-3	
CFDA	
Endogenous substrates	
Glutathione	
Leukotriene C_4	
Folic Acid	
Bilirubin	
Sex steroid conjugates	
Antimalarials	
Chloroquine	
Flavonoids	
Quercetin	
Kaempferol	
Naringenin	

Compiled from Cole, 2013; He et al., 2011; Szakács et al., 2008a; Borst et al., 2007; Karla et al., 2009; Slot et al., 2011.

MRP5

MRP5 is an organic anion transporter like MRP1 but with a considerably more limited range of substrates (Table 1-3) (Borst et al., 2007; Keppler, 2011). MRP5 can efflux GSH but does not seem to transport most GSH, glucuronidated and sulfated conjugates, with the exception of the glucuronide conjugates of estradiol and MTX (Borst et al., 2007). MRP5 has very little, if any, substrate overlap with P-gp and BCRP, and has distinct differences in substrate selectivity compared to MRP1 (Borst et al., 2007; Slot et al., 2011). MRP5 transports analogues of purine and pyrimidine bases, nucleosides and nucleotides, a characteristic shared only with MRP4 and MRP8 (Borst et al., 2007).

The anticancer drug substrates of MRP5 are also limited. It is known to transport the base analogues 6-thioguanine, 6-mercaptopurine, MTX and its polyglutamate conjugates, 5-fluorouracil (5-FU) and the nucleoside analogue gemcitabine (Table 1-3) (Borst et al., 2007; Hagmann et al., 2010b; Li et al., 2011; Wielinga et al., 2005). However, it is unable to efflux natural anticancer drugs such as doxorubicin and vincristine (Zhou, 2008a). Although there is evidence that it transports platinum drugs, this has yet to be reproduced by other laboratories (Pratt et al., 2005). The narrow substrate range of MRP5 suggests a lesser role in cancer MDR than P-gp, BCRP and MRP1 (Borst et al., 2007). However, it continues to be relevant especially in pancreatic cancer resistance where it is upregulated and able to transport the two drugs central for treatment, gemcitabine and 5-FU, which are poor substrates of P-gp, BCRP, MRP1 and MRP4 (Borst et al., 2007; Cole, 2013; Hagmann et al., 2010a, 2010b; Zhou, 2008b). Non-anticancer drug substrates of MRP5 include the antivirals, adefovir and acyclovir and the antiglaucoma drugs, bimatoprost and latanoprost (Borst et al., 2007; Karla et al., 2009). The fluorescent dyes 2,7-bis-(2-carboxyethyl)-5-(and-6)-carboxyfluorescein acetoxymethyl ester (BCECF-AM) and carboxy dichlorofluorescein diacetate (CFDA) are effluxed by MRP5 and are used *in vitro* to assess transport activity (Li et al., 2011; Wu et al., 2005). Endogenous substrates of MRP5 include the cyclic nucleotides cGMP and cAMP, folic acid and hyaluronan, as mentioned previously (Section 1.2.3.3).

Inhibitors

MRP1

MRP1 inhibitors include general organic anion transport inhibitors (e.g., probenecid), leukotriene receptor antagonists (e.g., MK-571), antimalarials such as chloroquine and mefloquine, the P-gp inhibitors verapamil, cyclosporine A, biricodar and dofequidar, natural compounds (e.g., flavonoids and curcumin), non-steroidal anti-inflammatory drugs (e.g., diclofenac and ketoprofen), and reverse transcriptase inhibitors abacavir and lamivudine (Cole, 2013; He et al., 2011; Shukla et al., 2008). Potent and selective experimental compounds have also been developed and include the pyrrolopyrimidines, analogues of GSH-conjugated ethacrynic acid and tricyclic isoxazoles (Cole, 2013; Pajeva et al., 2009).

Most of these inhibitors tend to be non-specific with inhibitory activity against either P-gp, BCRP or other members of the ABCC family (Cole, 2013; He et al., 2011). Organic anion transport inhibitors, such as probenecid can inhibit almost all ABC transporter mediated organic anion efflux (Cole, 2013; He et al., 2011). They also inhibit uptake transporters, introducing confounding factors in MRP1 inhibition assays (Tahara et al., 2006). The leukotriene antagonist MK-571 is currently the most popular MRP1 inhibitor for *in vitro* transport studies (Cole, 2013). It has improved potency (micromolar range) and does not affect uptake transporters. Although it has little activity against P-gp and BCRP, MK-571 inhibits most members of the ABCC family including MRP1, MRP4 and MRP5 (Cole, 2013). The lack of selectivity of MK-571 and the need for compounds of greater potency led to the discovery of the tricyclic isoxazoles, LY475776 and LY465803, which inhibit MRP1 at nanomolar concentrations with little effect on other MRPs (Norman et al., 2005). However, these compounds are not yet commercially available.

Due to the presence of multiple binding sites, complex inhibitor interactions with MRP1 may occur (Maeno et al., 2009). To rule out substrate-specific inhibition, investigational compounds should be tested against a panel of MRP1 substrates before being categorized as an inhibitor. Another consequence of multiple binding sites is that the potency order of inhibitors can change depending on the substrate, as was observed with a panel of flavonoids tested for MRP1 inhibitory activity (Zhou, 2008a).

Inhibition of MRP1 is also complicated by the dependence of certain inhibitors on GSH. For example, LY465803 has potent inhibitory activity only in the presence of millimolar concentrations of GSH (Maeno et al., 2009). For such inhibitors, GSH depletion may affect their efficacy. In addition dependence of substrate transport on GSH levels also means that GSH depleting agents like buthionine sulfoximine can act as inhibitors *in vitro* (Perek et al., 2002).

MRP5

Few compounds have been identified as inhibitors of MRP5 transport activity, and currently there are no specific MRP5 inhibitors available. Like MRP1, the general organic anion transporter inhibitors probenecid, sulfinpyrazone and benzbromarone all inhibit MRP5 but at low potency (Borst et al., 2007). The leukotriene antagonist MK-571 also inhibits MRP5, although much less effectively compared to MRP1, yet it remains a popular inhibitor of MRP5 for *in vitro* assays (Karla et al., 2009; Li et al., 2011). A CFTR modulator, 5-nitro-2-(3-phenylpropylamino)benzoate (NPPB), is another widely used MRP5 inhibitor and is currently considered the most potent inhibitor of MRP5 (Pratt et al., 2006). Other potent inhibitors include the cGMP phosphodiesterase inhibitors, zaprinast, trequinsin and sildenafil, which were reported to inhibit MRP5-mediated cGMP transport in the nanomolar range (Jedlitschky et al., 2000). However, these results remain controversial as potent inhibition has not been reproduced by other laboratories. Pratt et al. (2006) confirmed that these compounds inhibited MRP5 transport but at inhibitory concentrations (IC_{50}) that are 2-3 orders of magnitude higher than previously reported. Other inhibitors include natural compounds such as curcumin and genistein suggesting the possibility of MRP5 modulation by dietary components (Dallas et al., 2004; Li et al., 2010b).

It is unclear yet if the complex inhibitor interactions observed with P-gp, BCRP and MRP1 also occur with MRP5. Homology models show a large binding pocket predicted to have multiple binding sites, but to date a GSH-dependent mechanism of substrate transport and inhibition has not been observed for MRP5 (Ravna et al., 2008).

1.2.4 Role of ABC transporters in cancer chemotherapy

ABC transporters were first discovered in the context of cancer drug resistance where expression undoubtedly confers an MDR phenotype in cancer cells *in vitro*. Since then, research has focused on their contribution to chemotherapy resistance in the clinical setting and whether inhibition can lead to clinical benefits. This section will present data supporting ABC transporters as valid targets for improving cancer chemotherapy. Clinical studies correlating ABC transporters with poor treatment outcome will be outlined, with a focus on AML, breast cancer and pancreatic cancer. Studies indicate that ABC transporters are likely to contribute to chemotherapy resistance in these diseases. Also, the protective role of ABC transporters in cancer stem cells will be discussed. These are an intrinsically resistant, highly proliferative subpopulation in tumours considered key to cancer repopulation and recurrence. Discussions in this section will be limited to P-gp, BCRP, MRP1 and MRP5, although other ABC transporters have also been implicated in chemotherapy resistance (e.g., MRP8) (Yamada et al., 2013).

1.2.4.1 Acute myeloid leukemia

AML is the most well-studied cancer in terms of correlation between treatment outcome and ABC transporter expression. It is mainly treated by anticancer drugs that are good ABC transporter substrates (e.g., daunorubicin, epirubicin, mitoxantrone, etoposide), and patient samples such as blast cells, are relatively easy to collect from blood or bone marrow (Xia and Smith, 2012). In preclinical *in vitro* studies, ABC transporters were upregulated in AML cancer cells that have become resistant after constant exposure to anticancer drugs (e.g., doxorubicin, vincristine) (Calcagno and Ambudkar, 2010). This resistance can be reversed by the addition of ABC transporter inhibitors (Baines et al., 1994; Marie et al., 1991; Motomura et al., 1998). In patient samples, ABC transporters such as P-gp, BCRP and MRP1 were present in leukemia cells and expression was found to be higher than in normal bone marrow (Nakanishi and Ross, 2012; Takeshita et al., 1996).

Transporter expression at diagnosis has been significantly linked to a higher rate of intrinsic resistance to induction therapy and inferior outcomes. For AML, P-gp and BCRP expression are considered predictive of poor chemotherapy response and decreased overall survival (OS) (Nakanishi and Ross, 2012; Tiwari et al., 2011; Xia and Smith, 2012). In a study of 63 patients,

only 53% had complete remission (CR) in a group with P-gp positive blast cells prior to chemotherapy. In the P-gp negative group, CR was significantly higher at 89% (Pirker et al., 1991). P-gp expression was also linked with decreased overall survival (OS) in AML. Schaich et al. (2005) found both a lower CR rate in P-gp positive patients (31% $P\text{-}gp^+$ vs 56% $P\text{-}gp^-$), and significantly lower OS (13% $P\text{-}gp^+$ vs. 29% $P\text{-}gp^-$ after 6 years). For BCRP, a study in 149 AML patients found that in the BCRP-positive group, the CR rate was 43% and 4-year OS, 19% (Benderra et al., 2004). In contrast, patients that were BCRP-negative had a significantly higher CR rate of 69% and 4-year OS of 38% (Benderra et al., 2004). In this study, the prognostic value for BCRP was only seen in patients treated with mitoxantrone, a good BCRP substrate. In patients receiving anthracyclines (poor substrates of wild-type BCRP), no associations were seen with outcome, suggesting effects may be transport-mediated rather than BCRP acting as a marker. The study also highlighted that P-gp and BCRP co-expression is a better prognostic marker with greater differences and stronger associations observed between double-positive vs. double-negative patients for OS and CR.

It should be noted that for both P-gp and BCRP, other studies have shown a complete lack of correlation with treatment outcome (Tiwari et al., 2011). Possible explanations for the discrepancy include the use of different methodologies such as reverse transcription polymerase chain reaction (RT-PCR), western blots or functional assays (e.g., flow cytometry). RT-PCR is especially problematic as mRNA does not always correlate with protein expression and function (Nakanishi and Ross, 2012). Nonetheless, the majority of studies support that P-gp and BCRP are prognostic in AML treatment outcome (Shaffer et al., 2012; Tiwari et al., 2011; Xia and Smith, 2012). As for the role of MRP1, most studies suggest no association between expression and treatment response (Tiwari et al., 2011).

1.2.4.2 Breast cancer

Chemotherapy in breast cancer uses drugs that are ABC transporter substrates including anthracyclines, taxels, vinca alkaloids, mitoxantrone, 5-FU and MTX (Wind and Holen, 2011). Exposure of breast cancer cell lines to these drugs has led to resistance through ABC transporter upregulation (Wind and Holen, 2011). This has also been observed in *in vivo* mice models of breast cancer where in one study, mice lacking genes for breast cancer 1, early onset (BRCA1)

and p53 spontaneously developed mammary carcinomas that became resistant after repeated exposure to doxorubicin (Pajic et al., 2009). It was found that P-gp mRNA was upregulated 5-fold in resistant vs. untreated tumours and the addition of the P-gp inhibitor tariquidar reversed doxorubicin resistance in this model (Mistry et al., 2001). These mice were also seen to upregulate BCRP in response to topotecan treatment and tumour-specific ablation of BCRP led to a reversal of the resistance to topotecan (Zander et al., 2010). These studies therefore provide *in vivo* confirmation that cancer cells upregulate ABC transporter as a protective mechanism against anticancer drugs. Furthermore, it highlighted that even modest mRNA increases in tumours can lead to significant resistance and does not require the hundred- to thousand-fold increase in expression levels typically seen in drug-selected cell lines (Pajic et al., 2009).

In breast cancer patients, ABC transporters were found to be expressed in tumour biopsies. In one study, 58% and 92% of tumours were positive for P-gp and MRP1 mRNA, respectively (Tiwari et al., 2011). Expression of both transporters was significantly linked with decreased response rate, progression-free survival (PFS) and OS (Surowiak et al., 2005; Vishnukumar et al., 2013; Wind and Holen, 2011). Burger and colleagues found that the overall treatment response in tumours with high P-gp expression was only 17% compared to 68% in patients with low P-gp expression (Burger et al., 2003). In this study, P-gp positive tumours were also significantly correlated with poor PFS. A lower response rate to treatment expression was also previously observed in a meta-analysis of 31 studies in addition to an increased proportion of P-gp positive patients after chemotherapy (Trock et al., 1997). Like P-gp, MRP1 expression was increased by chemotherapy and its expression was associated with a higher risk of relapse. In a study of 104 patients, high MRP1 expression significantly correlated with decreased PFS and OS (Wind and Holen, 2011). For BCRP, studies have shown low expression in breast cancer (Tiwari et al., 2011; Wind and Holen, 2011). Although BCRP mRNA was detectable in tumours, it varied greatly between samples and did not change pre- or post-treatment (Tiwari et al., 2011). Most studies have not found a significant correlation with treatment outcome (Tiwari et al., 2011; Wind and Holen, 2011). Nonetheless, BCRP was thought to play a role in relapse as it was highly expressed in a small subpopulation of cancer stem cells isolated from breast cancer tumours (Al-Hajj et al., 2003; Hirschmann-Jax et al., 2004).

As with AML, there are also studies that show no correlation between P-gp and MRP1 expression in breast cancer treatment. These tend to utilise RT-PCR rather than immunohistochemistry (Wind and Holen, 2011). It is also known that ABC transporters are subject to post-transcriptional regulation and the lack of correlation between mRNA and protein expression may account for this variation. In one study for example, 98% of samples were positive for MRP1 mRNA but only 53% was positive for the protein (Filipits et al., 2005). In addition, because drugs used in breast cancer are effluxed by multiple ABC transporters, the contribution of a single transporter may be too weak to detect. In a number of studies, significant association with treatment outcome was only found when co-expression of two or more transporters was considered (Beck et al., 1998; Kovalev et al., 2013; Wind and Holen, 2011).

Triple-negative breast cancer

Triple-negative breast cancer (TNBC) is a an aggressive breast cancer subtype that is negative for the estrogen, progesterone and HER2 receptors (Griffiths and Olin, 2012; Isakoff, 2010). It cannot be treated by endocrine therapy or anti-HER2 agents (e.g., trastuzumab and lapatinib), and relies on non-targeted chemotherapy regimens that involve classic ABC transporter substrates (Anders et al., 2013; Griffiths and Olin, 2012; Isakoff, 2010). These include anthracyclines (e.g., doxorubicin, epirubicin), taxels (e.g., paclitaxel, docetaxel), MTX, cyclophosphamide and 5-FU (Griffiths and Olin, 2012; Isakoff, 2010). As previously outlined, there is evidence that ABC transporters contribute to chemotherapy resistance in breast cancer, a contribution which may be even greater in the TNBC subtype, as recent studies have shown significantly increased ABC transporter expression compared to other types of breast cancer. For example, Britton et al. (2012) demonstrated that TNBC samples had the highest expression of BCRP compared with receptor positive tumours (ER+, PR+, HER2+ and ER+, PR+, HER2- samples). Yamada et al. (2013) in a study of 281 breast cancer tumour samples, also found that BCRP and MRP1 were more frequently expressed and at higher levels in TNBC tumours compared to less aggressive subtypes (e.g., luminal A). At present, only MRP1 and MRP8 expression in tumour samples has been linked with a shorter disease-free survival (Yamada et al., 2013). Although BCRP expression in the tumour bulk does not correlate with survival, a recent study has found that TNBC tumours are more frequently positive for cancer stem cell-like side population cells (see Section 1.2.4.4) than

other subtypes. Since BCRP expression is a marker for these cells, it may play a role in protecting this highly tumourigenic sub-population from anticancer drugs (Britton et al., 2012).

1.2.4.3 Pancreatic cancer

The treatment of pancreatic cancer relies primarily on two nucleoside analogues, gemcitabine and 5-FU (Tokh et al., 2012). These two drugs are not P-gp substrates (likely due to their hydrophilicity), but both are effluxed by MRP5 (Hagmann et al., 2010b). In pancreatic cancer cell lines, MRP5 mRNA and protein are strongly expressed and exposure to 5-FU and gemcitabine upregulates MRP5 expression (Hagmann et al., 2009; Li et al., 2011). Gene silencing or inhibition of MRP5 transport activity resensitises cells to both drugs (Hagmann et al., 2010b; Li et al., 2011; Nambaru et al., 2011). A possible role of MRP5 in clinical resistance was further supported by the detection of mRNA in patient tumour samples (König et al., 2005; Mohelnikova-Duchonova et al., 2013). These tumours have significantly upregulated MRP5 expression compared to surrounding normal tissue. Also, an MRP5 polymorphism has been identified that significantly correlated with OS in gemcitabine-treated patients (Tanaka et al., 2011). At present, very few clinical studies have investigated MRP5 expression in patient samples and, so far, none have significantly linked expression with treatment response (Guo et al., 2009; Steinbach et al., 2003).

Both P-gp and MRP1 were also found to be expressed in pancreatic cancer samples. O'Driscoll et al. (2007) found that in 45 pancreatic tumour samples, 93% were P-gp positive with 31% also co-expressing MRP1. The significance of this is not clear as neither are good transporters of 5-FU or gemcitabine. Unsurprisingly, in a study of 67 pancreatic cancer samples, no significant correlation with disease progression or OS was linked to either P-gp or MRP1; despite protein expression in 52% and 84% of samples respectively (Lee et al., 2012). In this study however, BCRP was expressed in 73% of tumours and high expression significantly correlated with early recurrence (hazard ratio = 2.43) and poor survival (hazard ratio = 2.63). Although BCRP is not known to transport gemcitabine, it has been shown to efflux 5-FU (de Wolf et al., 2008; Yuan et al., 2009). The link between BCRP and early recurrence has been hypothesized to result from the high expression of BCRP in putative pancreatic cancer stem cells (Du et al., 2011; Zhou et al., 2008).

1.2.4.4 Cancer stem cells

According to the cancer stem cell (CSC) theory, CSCs are a subpopulation in tumours with unlimited self-renewal capacity that are thought to be the main drivers of tumour growth (Gupta et al., 2009; Moitra et al., 2011). These cells divide asymmetrically, renewing the CSC pool and also give rise to more differentiated daughter cells that make up the tumour bulk. Unlimited cell division is thought to be an exclusive property of CSCs, with the rest of the tumour having little or no proliferative capacity (Gupta et al., 2009). As CSCs are highly resistant to both radiotherapy and chemotherapy, they are considered to play a major role in chemotherapy resistance and patient relapse (Alison et al., 2012; Borst, 2012). Initial chemotherapy is thought to target the sensitive tumour bulk while leaving the small, highly resistant CSC subpopulation intact. An objective response is seen but patient relapse occurs due to the residual CSCs repopulating the tumour. To completely eradicate cancer, CSCs have to be eliminated together with non-CSC cells.

Resistance of CSCs to chemotherapy is multifactorial but the most well-known mechanism is high expression of P-gp and BCRP (Alison et al., 2012). In fact, BCRP is considered a CSC marker and efflux of the BCRP substrate dye, Hoechst-33342, is a commonly used method to isolate stem cell enriched fractions called the side population, from tumour samples (Moitra et al., 2011; Shaffer et al., 2012). Isolated CSCs are resistant to anticancer drugs that are ABC transporter substrates, and addition of P-gp and BCRP inhibitors, like verapamil or dofequidar, reversed this resistance (Katayama et al., 2009; Loebinger et al., 2008). CSCs have been identified and isolated from a number of solid tumours including breast, lung, pancreatic and colon cancer, as well as leukemias (Nakanishi and Ross, 2012; Tiwari et al., 2011; Visvader and Lindeman, 2008). CSCs identified from these cancers all highly express BCRP with some also co-expressing P-gp (e.g., AML) (Borst, 2012; Moitra et al., 2011). Inhibition of ABC transporters is therefore considered to help sensitise these resistant cells to chemotherapy and may improve treatment outcome in a range of different cancers.

1.2.5 Inhibition of ABC transporters in the clinic

1.2.5.1 Clinical trials of P-gp inhibitors

Clinical trials of ABC transporter inhibitors have focused exclusively on P-gp. The first generation of P-gp inhibitors were approved drugs already in use to treat other conditions (Falasca and Linton, 2012; Palmeira et al., 2012a). These included the calcium channel blocker verapamil, the immunosuppressant cyclosporine A and the antimalarial quinine (Table 1-4) (Palmeira et al., 2012a; Zhou, 2008b). These compounds were of low potency which meant that the plasma concentrations required to inhibit P-gp also caused toxicities from their primary pharmacology. This applied especially to verapamil where initial phase I studies conducted in ovarian cancer patients led to presentation of heart block, cardiac failure and hypotension in the verapamil arm (Ozols et al., 1987). In addition to toxicity, negative results were observed with verapamil and chemotherapy combinations in multiple myeloma, lung and ovarian cancer, thus reducing interest in the drug as a chemosensitiser (Dalton et al., 1995; Hendrick et al., 1991; Milroy, 1993). However, it should be noted that more recent Phase II trials have shown some benefit in adding verapamil to chemotherapy regimens in lung and breast cancers (Belpomme et al., 2000; Huang et al., 2013; Timcheva and Todorov, 1996).

For cyclosporine A, positive results were seen in a number of studies. Improved outcome was observed in retinoblastoma when cyclosporine A was combined with chemotherapy. In addition, recurrence-free and OS were increased in AML patients by adding cyclosporine A to doxorubicin and cytarabine regimens in a phase III study (Chan et al., 1996; List et al., 2001). Li et al. (2009) also observed increased complete remission rate in AML patients with cyclosporine A and idarubicin/cytarabine combinations. Other trials however, failed to observe any improvements, leading to questions of its suitability as a chemosensitiser (Sonneveld et al., 2001; Warner et al., 1995; Weber et al., 1995).

Other issues with first-generation inhibitors include pharmacokinetic interactions and side effects such as nephrotoxicity, neurotoxicity, increased myelosuppression and hyperbilirubinemia (Darby et al., 2011; Ries and Dicato, 1991; Yahanda et al., 1992). Some of these adverse reactions were suspected to result from the non-specific inhibition of other ABC transporters in physiological

tissue (e.g., bone marrow, kidneys and liver), leading to demands for new inhibitors with greater specificity for P-gp (Coley, 2010; Darby et al., 2011; Palmeira et al., 2012a).

The second-generation ABC transporter inhibitors were derivatives and stereoisomers of first-generation compounds. They lack the pharmacological properties of the parent compounds while retaining or improving upon P-gp inhibitory activity (Palmeira et al., 2012a). These include dexverapamil, the D-isomer of verapamil, with reduced calcium channel blocking activity; the analogue of cyclosporine A, valspodar; dofequidar, a quinidine analog; and biricodar, a derivative of tacrolimus (Table 1-4)(Yu et al., 2013). Despite improved potency and lack of immunosuppressive or cardiac effects with valspodar and dexverapamil respectively; these compounds were disappointing in clinical trials (Coley, 2010; Palmeira et al., 2012a; Shaffer et al., 2012). In most trials, the drugs failed to produce any benefits in treatment outcome while other studies were terminated early due to increased toxicity in the experimental arm. Valspodar, dexverapamil and biricodar are also cytochrome P450 (CYP) enzyme substrates which may have decreased the clearance of concurrent anticancer drugs (Coley, 2010). For example, in trials with valspodar, pharmacokinetic interactions caused greater chemotherapy related toxicity such as myelosuppression (Palmeira et al., 2012a). In response, the doses of co-administered drugs were reduced by 30-50% resulting in under-dosing which was probably responsible for the inferior outcomes of the valspodar treated groups in phase III studies (Palmeira et al., 2012a; Shaffer et al., 2012). Inhibition of the physiological function of other ABC transporters by valspodar and biricodar was also considered a problem and was thought to contribute to toxicity (Palmeira et al., 2012a).

The third-generation inhibitors showed enhanced potency, improved specificity for P-gp and did not inhibit CYP enzymes (e.g., CYP3A4) (Palmeira et al., 2012a; Yu et al., 2013). Inhibitors include elacridar, tariquidar and zosuquidar (Table 1-4). For these compounds, toxicity continued to be a problem despite the apparent lack of pharmacokinetic interactions (Fox and Bates, 2007; Palmeira et al., 2012a). Tariquidar, a potent P-gp inhibitor, increased the toxicity of chemotherapy regimens in two phase III lung cancer trials without affecting drug clearance (Fox and Bates, 2007). This caused early termination of both studies as toxicities became unacceptable, and the development of tariquidar was eventually discontinued. The enhanced toxicity may have resulted from dual

Table 1-4. P-gp inhibitors investigated in clinical trials.

First generation
Verapamil
Cyclosporine A
Tamoxifen
Quinine
Nifedipine
Tacrolimus
Second generation
PSC-833 (valspodar)
VX-710 (biricodar)
Dexverapamil
YMB1002 (tesmilifene)
MS209 (dofequidar)
Third generation
LY3335979 (zosuquidar)
OC144-093 (ontogen)
XR9576 (tariquidar)
GF120918 (elacridar)
R101933 (laniquidar)
CBT-1

Compiled from Palmeira et al., 2012a; Sharom, 2011.

inhibition of P-gp/BCRP, increasing the sensitivity of bone marrow to chemotherapy. Tariquidar was initially considered P-gp specific but was later found to inhibit BCRP (Robey et al., 2004). Zosuquidar was more potent with no activity against MRP1 and BCRP (Palmeira et al., 2012a; Shaffer et al., 2012). It had a better safety profile than tariquidar and also did not cause pharmacokinetic interactions (Shaffer et al., 2012). However, large phase III trials have failed to show a benefit when added to chemotherapy (Palmeira et al., 2012a; Shaffer et al., 2012; Yu et al., 2013). Ironically, failure was in part attributed to the lack of MRP1 and BCRP inhibition, previously observed to be upregulated and co-expressed with P-gp in AML and other cancers (Palmeira et al., 2012a).

1.2.5.2 Reasons for the failure of inhibitors in clinical trials

As mentioned previously, reasons for the failure of the ABC transporter inhibitors in clinical trials include increased toxicity from primary pharmacology, pharmacokinetic interactions and increased sensitivity of normal tissue to toxicity, particularly bone marrow. Improved safety was observed with specific P-gp inhibitors such as zosuquidar, but at the expense of the inability to inhibit compensatory efflux of the co-administered anticancer drugs by BCRP and MRP1 (Cripe et al., 2010). As multiple ABC transporters are often overexpressed in cancers, a broad ABC transporter inhibitor may be more desirable; although this would have to be targeted to the tumour to prevent toxicities. Recently, studies on encapsulating paclitaxel and tariquidar into nanoparticles and liposomes to improve tumour targeting are being explored (Patil et al., 2009).

Other suggested reasons for the apparent lack of benefit in clinical trials include shortcomings with the design of the trials themselves, a major criticism being the lack of patient pre-selection for P-gp expression (Steinbach and Legrand, 2007; Yu et al., 2013). In one study by Becton et al. (2006), only 14% of patients overexpressed P-gp making it difficult to show a significant benefit of cyclosporine A addition. Parallels have been drawn with clinical trials for trastuzumab, where a clear benefit was observed only with patients who were HER2-positive (Darby et al., 2011). It has been suggested that patient tumours should be checked for P-gp efflux using *in vivo* imaging agents (e.g., ^{99m}Tc- sestamibi) as mRNA and protein expression does not always correlate with transport function (Robey et al., 2010). Another contributor to variability in the outcomes of clinical trials may be the lack of consideration of P-gp polymorphisms. A reduced function P-gp haplotype which also decreases affinity for inhibitors such as verapamil and cyclosporine is present in as high as 25-40% of Caucasians and Asians (Robey et al., 2010). In this sub-population, addition of a P-gp inhibitor is unlikely to affect tumour response, while it may increase toxicity in normal tissues. Also, a number of studies have used a run-in phase or cross-over study design where patients receive multiple rounds of chemotherapy prior to treatment with inhibitors (Amiri-Kordestani et al., 2012). This may have allowed multiple resistance mechanisms to develop in addition to enhancing P-gp efflux. Also, in some studies, inhibitors have been combined with drugs that are poor transporter substrates such as in a terminated phase III lung cancer trial where tariquidar was administered with carboplatin (Fox and Bates, 2007). Since platins are not substrates of either P-gp or BCRP, this may have confounded results with tariquidar (Borst, 2012).

There is also evidence that some compounds, such as tesmelifine and biricodar, have proceeded to clinical testing without being thoroughly tested for activity in established tumour models of MDR (Yu et al., 2013). Lastly, for some phase III trials, inadequate dosing of the inhibitor has been blamed for lack of efficacy. In a phase III Eastern oncology cooperative group trial for zosuquidar in AML, no benefit was observed in the zosoquidar arm, possibly due to the short zosuquidar infusion time of 6 h (Cripe et al., 2010). Previous studies found that an infusion time of at least 12 h was required to sufficiently reverse anthracycline resistance (Robey et al., 2010; Yu et al., 2013). Similarly, in a phase III trial in AML, no benefit was observed in patients receiving cyclosporine A at 5 mg/kg/day compared to 16 mg/kg/day in a study by the Southwest oncology group (SWOG) (List et al., 2001; Shaffer et al., 2012; Liu Yin et al., 2001). The SWOG study reported a significant improvement in 2-year OS of AML patients with the higher dose of cyclosporine.

Although three generations of P-gp inhibitors have failed in Phase III trials, it is clear that there were major shortcomings with many of the studies (Palmeira et al., 2012a; Shaffer et al., 2012). It is therefore premature to conclude as some have that inhibition of ABC transporters should be abandoned as an adjunct to chemotherapy (Libby and Hromas, 2010). Many phase II studies have shown positive results with inhibitors suggesting that ABC transporters can lead to improved outcomes in resistant cancers (Belpomme et al., 2000; Huang et al., 2013; List et al., 2001; Timcheva and Todorov, 1996). Results of phase III trials would perhaps have been much more favourable had a non-specific, tumour-targeted inhibitor been used in a selected patient population with tumours showing ABC transporter-mediated efflux of the administered anticancer drugs.

1.2.5.3 Phytochemicals as transporter modulators

The high incidence of toxicity especially with earlier generations of P-gp inhibitors has caused a search for alternative compounds with improved safety profiles (Coley, 2010; Palmeira et al., 2012a). When it was found that part of the reason for food-drug interations was ABC transporter inhibition, research was conducted on diet-derived compounds that could modulate ABC transporters (Li et al., 2010b; Molnár et al., 2010; Nabekura, 2010). Phytochemicals (secondary plant metabolites) were later found to have inhibitory activity against P-gp and other ABC transporters (Li et al., 2010b). These phytochemicals are present in dietary components that are consumed on a daily basis such as fruits, vegetables, wine and tea. Examples of well-studied phytochemicals include: resveratrol present in grapes and red wine; quercetin which is ubiquitously found in fruits and vegetables; catechins, such as epigallo-catechin gallate (EGCG) present in tea; and curcumin which has been isolated from turmeric and used as a spice and component of herbal medicines (Li and Paxton, 2013; Nabekura, 2010; Vinod et al., 2013).

Phytochemicals are an attractive option as modulators as they have an excellent safety profile. The wider population is exposed to these compounds on a daily basis at amounts of up to several hundred milligrams with no adverse effects on health (Li et al., 2010b). In fact, positive health benefits have been associated with high intake of phytochemicals including a reduction in the risk of cancer, cardiovascular events, strokes, cataracts, diabetes and neurodegenerative diseases such as Alzheimer's (Liu, 2013). Another possible advantage of phytochemicals is their ability to inhibit multiple ABC transporters. For example, curcumin, quercetin and resveratrol, are reported to inhibit all three major ABC transporters, P-gp, BCRP and MRP1 (Li et al., 2010b). They also modulate other MRPs such as MRP2, MRP4 and MRP5 (Li and Paxton, 2013; Li et al., 2011). This non-specific inhibition may counter the upregulation of multiple ABC transporters in tumours. In addition to increased safety and non-specific inhibition, some phytochemicals appear to possess intrinsic anticancer activity and are known to modulate multiple signaling pathways involved with cell proliferation, apoptotic resistance, angiogenesis, cell invasion and metastasis (Palmeira et al., 2012b; Vinod et al., 2013; Wang et al., 2012). Phytochemicals may therefore act as 'dual-role chemosensitisers' with both anticancer activity and inhibitory effects against ABC transporters. They may also address multiple MDR mechanisms making them ideal candidates as chemosensitisers. Of the phytochemicals studied for both anticancer activity and ABC transporter

inhibition, the diarylheptanoid compound, curcumin, is arguably the best characterized both *in vitro* and *in vivo* (Li et al., 2010b; Limtrakul, 2007; Vinod et al., 2013).

1.3 Curcumin as an MDR reversal agent

1.3.1 Curcumin

Curcumin (or diferuloylmethane) is the main active ingredient of turmeric, a spice derived from the plant *Curcuma longa*, endemic to South and Southeast Asia (Gupta et al., 2012, 2013a). Turmeric is used heavily in South Asian cuisine and herbal medicine and is becoming popular worldwide as an herbal supplement (Gupta et al., 2013a). Turmeric contains 2-5% by weight of curcuminoids, a mixture of curcumin and its demethoxylated analogues, demethoxycurcumin and bisdemethoxycurcumin (Figure 1-4) (Gupta et al., 2011, 2012). Curcumin has been the subject of enormous research interest due to its interactions with a large array of proteins and signalling pathways involved in a range of different diseases (Gupta et al., 2011). The reported biological effects of curcumin include antibiotic, antiinflammatory, antioxidant, anticancer, antiparasitic, antinociceptive, antimalarial, hypoglycaemic and wound healing properties (Gupta et al., 2012; Kunnumakkara et al., 2008). In animal studies, curcumin was found to have activity against cancer, diabetes, neurodegenerative disease, obesity, psychiatric disorders and diseases of the eye, liver, lung and cardiovascular system (Gupta et al., 2012). Phase I and II clinical trials with curcumin alone or in combination with other drugs have established that curcumin has activity in the clinic and is remarkably safe (Gupta et al., 2013b). Doses as high as 12 g/day for 3 months have been administered with little or no toxicity. Curcumin has therefore been currently labelled by the FDA as GRAS (generally recognised as safe) (Gupta et al., 2013b).

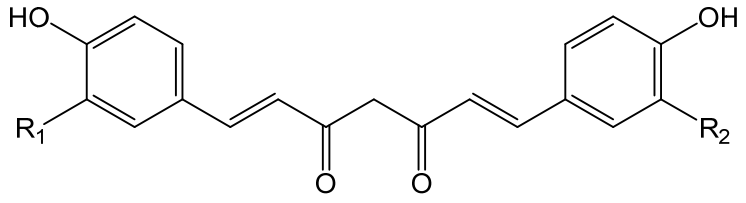

CUR: R1 = R2 = OCH_3
demethoxy-CUR: R1 = H; R2 = OCH_3
bisdemethoxy-CUR: R1 = R2 = H

Figure 1-4. Structure of curcumin (CUR), and its demethoxylated analogues. Used with permission from (Metzler et al., 2013)(Appendix V).

1.3.2 Molecular structure

Curcumin is made up of two ortho-methoxylated phenols connected by a conjugated heptadione linker chain (Figure 1-5) (Metzler et al., 2013; Vyas et al., 2013). This 7-membered linker contains a central β-diketone moiety which can undergo keto-enol tautomerism. Using nuclear magnetic resonance (NMR) and liquid chromatography-mass spectroscopy (LC-MS) studies, curcumin was shown to exist predominantly in the enol form in solution, which has increased stability due to the formation of an intramolecular hydrogen-bond, and extended conjugation over the enol chain (Kawano et al., 2013; Kolev et al., 2005; Payton et al., 2007). Both the keto and enol forms of curcumin contain α,β-unsaturated carbonyl groups which act as Michael acceptors to nucleophilic attack, allowing curcumin to bind to thiol groups (Gupta et al., 2011; Sun et al., 2009). Michael additions are reversible, which may explain the safety of curcumin by minimising the deleterious effects of forming irreversible protein adducts (Grynkiewicz and Ślifirski, 2012; Sun et al., 2009). The two hydrophobic phenyl rings on both ends are thought to participate in pi-pi hydrophobic stacking with aromatic protein side chains (Gupta et al., 2011). The flexibility of the linker chain allows the molecule to adopt different conformations to optimally interact with proteins (Gupta et al., 2011). The two phenolic 4'-hydroxyl groups at both ends of the molecule and the central enolic hydroxyl group (of the enol form) are also thought to participate in hydrogen bonding. These groups are thought to underlie the interactions with macromolecules such as DNA, by hydrogen bonding to the minor groove of AT-rich regions (Gupta et al., 2011).

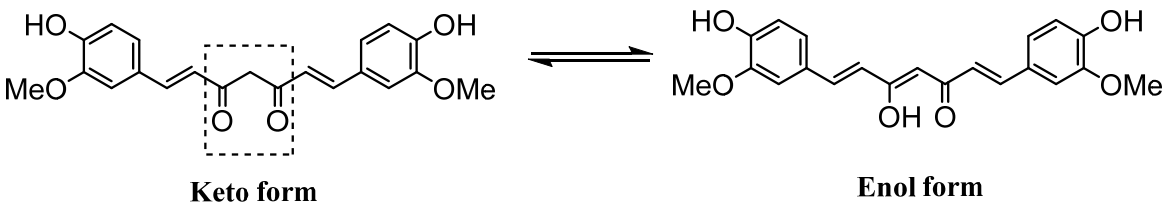

Figure 1-5. Keto-enol tautomerism of curcumin. The β-diketone moiety of the ketone form is indicated by a box.

1.3.3 Anticancer and chemosensitising activity

Curcumin has anticancer activity as a single agent *in vitro* and in tumour xenografts (Gupta et al., 2011). It has also been used to chemosensitise resistant cancer cells when combined with an established anticancer drug (Goel and Aggarwal, 2010). Curcumin can induce apoptosis, cause cell-cycle arrest, inhibit cell invasion and metastasis, and interfere with angiogenesis (Kunnumakkara et al., 2008; Ravindran et al., 2009). Apoptosis induction involves curcumin effects on both the extrinsic and intrinsic apoptosis signaling pathways (Kunnumakkara et al., 2008; Saha et al., 2012). Curcumin is known to increase the expression of death receptors such as DR5, downregulate antiapoptotic proteins (e.g., survivin and Bcl-2) and upregulate pro-apoptotic factors (e.g., Bax) (Saha et al., 2012). Curcumin causes cell-cycle arrest by inhibiting the expression of cyclins and the upregulation of cyclin-dependent kinase inhibitors (Ravindran et al., 2009). Modulation of tumour invasion and metastasis is due to suppression of matrix metalloproteinases (MMPs) which breakdown the extracellular matrix allowing cancer cell release from the primary tumour and metastasis to distal sites (Saha et al., 2012; Shehzad et al., 2013). Curcumin also affects angiogenesis in tumours by suppressing expression of key molecules such as the vascular endothelial growth factor (VEGF) (Kunnumakkara et al., 2008).

As a chemosensitiser, curcumin enhanced the effectiveness of co-administered anticancer drugs against chemo-resistant cell lines and tumour xenografts (Goel and Aggarwal, 2010; Vinod et al., 2013). This occurred through modulation of multiple pathways, the most important include the PI3K/AKT and nuclear factor kappa-light-chain-enhancer of activated B cells (NF-κB) pathways (Goel and Aggarwal, 2010; Saha et al., 2012). Curcumin is a potent inhibitor of EGFR, an activator of the PI3K/AKT signaling pathway (Kunnumakkara et al., 2008; Saha et al., 2012). It also inhibits a key step in the pathway (AKT phosphorylation) through EGFR-independent mechanisms (Gupta et al., 2011; Kunnumakkara et al., 2008). In colorectal cancer cell lines (HCT-116 and HT-29) resistant to first-line combination treatment with folinic acid, 5-FU and oxaliplatin (FOLFOX); addition of curcumin significantly increased apoptosis induction (Patel et al., 2010). This occurred via inhibition of EGFR signaling and decreased AKT activation (Patel et al., 2010; Saha et al., 2012). NF-κB signaling in cancer is associated with chemotherapy resistance and is induced by anticancer drugs (Vinod et al., 2013). Curcumin inhibits NF-κB translocation from the cytoplasm to the nucleus, where it upregulates the expression of genes involved in apoptotic resistance (Bcl-2),

cell proliferation (cyclin D1), angiogenesis (VEGF) and inflammation (pro-inflammatory cytokines and cyclooxygenase, COX-2) (Gupta et al., 2011; Saha et al., 2012). In cisplatin resistant ovarian cancer cells, a 6 h pretreatment with curcumin increased cisplatin sensitivity by ten-fold through an NF-κB mediated mechanism (Saha et al., 2012; Yallapu et al., 2010). NF-κB inhibition by curcumin also caused chemosensitization of cancer cell lines to drugs such as paclitaxel, melphalan, 5-FU, gemcitabine, docetaxel, vincristine and vinblastine (Goel and Aggarwal, 2010; Vinod et al., 2013). In fact, due to its many downstream effects, it has been suggested that potent NF-κB inhibition is the key mechanism of curcumin-mediated chemosensitisation (Goel and Aggarwal, 2010; Vinod et al., 2013). It should be noted that the PI3K/AKT pathway also causes translocation of NF-κB to the nucleus so that some of the effects of PI3K/AKT modulation may therefore be NF-κB mediated (Sun et al., 2010; Vinod et al., 2013).

Another possible mechanism for curcumin's reversal of MDR is activity against the highly-resistant CSC tumour sub-population (Section 1.2.4.4). Curcumin is known to modulate pathways that drive CSC self-renewal. These include the Wnt/β-catenin, Hedgehog, Notch, STAT3 and PI3K/AKT pathways (Gupta et al., 2013a; Saha et al., 2012). In breast cancer stem cells, curcumin-mediated suppression of Wnt/β-catenin inhibited proliferation without affecting differentiated cells (Kakarala et al., 2010). A dasatinib and curcumin combination inhibited growth and colonosphere formation of FOLFOX-resistant colon cancer cells. It also significantly reduced the number of CSCs as observed by the significant decrease in cells carrying stem cell markers (CD133, CD44) (Nautiyal et al., 2011). Curcumin alone was seen to inhibit the proliferation of pancreatic, colon and glioblastoma CSCs which was dependent on hedgehog, STAT3 and insulin-like growth factor (Gupta et al., 2013a). Recently, curcumin was reported to enhance the effectiveness of cisplatin in a laryngeal carcinoma cell line by markedly decreasing the percentage of CD133+ cancer stem cells (Zhang et al., 2013).

1.3.4 Inhibition of ABC transporters

The chemosensitising effect of curcumin was also attributed to inhibition of ABC transporter-mediated drug efflux. Curcumin inhibits P-gp, BCRP, MRP1 and MRP5 *in vitro*, with animal and clinical studies confirming P-gp and BCRP inhibition *in vivo*. Curcumin at concentrations in the range 5-50 μM, can reverse the resistance to P-gp substrate drugs in drug-selected cancer cell lines overexpressing the transporter (Chearwae et al., 2004; Hou et al., 2008; Nabekura et al., 2005; Tang et al., 2005). Inhibition was found to be dose-dependent and curcumin did not affect drug sensitivity of the corresponding parental cells. In cervical carcinoma cells, addition of 15 μM curcumin decreased the IC_{50} of vinblastine from 1.7 to 0.3 μM in P-gp overexpressing, human cervical carcinoma KB-V1 cells but no enhancement of vinblastine cytotoxicity was observed in drug sensitive KB-3-1 parental cells (Chearwae et al., 2004). Curcumin was also shown to inhibit the efflux and increase the intracellular accumulation of fluorescent P-gp substrates including rhodamine-123, calcein-AM and daunorubicin, using flow cytometry and spectrofluorimetry (Chearwae et al., 2004; Hou et al., 2008; Nabekura et al., 2005). The mechanism of inhibition may involve competition at the substrate binding site. Curcumin was able to inhibit the photo-affinity labeling of P-gp by [125I]-IAAP (Chearwae et al., 2004). The latter is a prazosin analog and P-gp substrate which labels the substrate-binding site when photo-activated. Curcumin inhibited IAAP binding with an IC_{50} of 5.8 μM. Interference with ATP-binding at the NBD by curcumin has been ruled out as a mechanism of inhibition since labeling with the photoactivatable ATP analog, 8-azido-ATP-biotin, was not affected by curcumin addition (Sreenivasan et al., 2013).

Although curcumin binds to the substrate binding site, it does not seem to be transported by P-gp. In cytotoxicity assays with parental and P-gp overexpressing cells, expression of the transporter did not increase cellular resistance to the cytotoxic effects of curcumin (Chearwae et al., 2004; Efferth et al., 2002). Low concentrations of curcumin (0.5-1.0 μM) stimulated P-gp ATPase activity (which occurs when substrates are being transported), but higher concentrations inhibited this activity (Chearwae et al., 2004). Direct P-gp transport studies with radiolabeled curcumin have not been conducted, making it difficult to draw definitive conclusions. In addition to transport modulation, long term exposure of P-gp expressing cells to curcumin (e.g., 3 – 4 days) caused downregulation of P-gp mRNA and protein expression (Choi et al., 2008; Ganta and Amiji, 2009; Hou et al., 2008). This could have contributed to resistance reversal in 72 h cytotoxicity assays.

Downregulation was found to be dependent on curcumin inhibition of the transcription factor activator protein 1 (AP-1) and the PI3K/AKT/NF-κB pathway (Choi et al., 2008; Hou et al., 2008). In animal studies, oral administration of curcumin increased the plasma area-under-the-curve (AUC) of co-administered P-gp substrates in rats and mice. The effects of curcumin were often observed when animals were pretreated for a few days prior to addition of substrate and not when dosed 30 min before (Ganta et al., 2010; Zhang et al., 2007; Zhao et al., 2010). Thus, downregulation of intestinal P-gp appeared to have a greater impact on substrate AUC than direct modulation of transport activity. In the clinic, curcumin was also observed to modulate P-gp transport. A significantly greater AUC of the drug talinolol (a P-gp substrate with minimal CYP3A4 affinity/metabolism), was observed in healthy male volunteers given 1 g of curcumin capsules daily for 14 days prior to talinolol administration (He et al., 2012).

Curcumin inhibition of BCRP has been characterised both *in vitro* and *in vivo.* Chearwae et al. (2006a) found that curcumin can reverse the resistance of mitoxantrone, SN-38 and topotecan in BCRP transfected human embryonic kidney (HEK293) cells with no effect observed in empty vector-transfected controls. They found using flow cytometry that curcumin inhibited efflux and increased intracellular accumulation of mitoxantrone and pheophorbide A in transfected cells with IC_{50} values of 1.77 and 1.73 μM respectively. Inhibition was likely through competition at the substrate binding site as curcumin inhibited BCRP labeling by IAAP with an IC_{50} of 0.54 μM. This was significantly more potent than the IC_{50} of 5.8 μM for P-gp labeling (Chearwae et al., 2004).

Similar to P-gp, curcumin had no effect on the binding of 8-azido-ATP to the BCRP NBD (Chearwae et al., 2006a). This suggests that transport inhibition is not mediated by NBD interactions. Although curcumin competes with IAAP at the BCRP drug binding pocket, it was not found to be a substrate. Both vector-transfected and BCRP transfected HEK293 cells had similar sensitivity to curcumin cytotoxicity (Chearwae et al., 2006a). Also, there was no significant reduction in the intracellular accumulation of radiolabeled curcumin in the transfected cells (Chearwae et al., 2006a). In the same study, incubation of adriamycin-selected MCF7-AdVp3000 breast carcinoma cells with 10 μM curcumin for 72 h did not affect BCRP expression, suggesting that the effects were not caused by a reduction in protein expression. However, Ebert et al. (2007) demonstrated increased BCRP protein expression after 24 h treatment of wild-type MCF-7 cells

with 25 μM curcumin. This was not observed in AhR-deficient MCF-7 breast carcinoma cells, suggesting AhR-dependent induction.

In vivo curcumin inhibition of BCRP was demonstrated in studies using wild-type and BCRP KO mice (Shukla et al., 2009). It was found that oral curcumin (400 mg/kg) 1 h prior to an oral dose of the substrate, SSZ, significantly increased the maximum plasma concentration (C_{max}), bioavailability and AUC of SSZ in wild-type but not BCRP KO mice; suggesting that the effect was BCRP-mediated. Since curcumin was only administered 1 h prior to SSZ, increased plasma AUC was likely due to direct transport modulation and not downregulation of transporter expression. Similar results were observed in human volunteers also using SSZ as a BCRP probe substrate. In 8 healthy subjects, SSZ $AUC_{0\text{-}24h}$ increased an average of 3.2-fold when subjects were given 2 g curcumin 30 min prior to a therapeutic oral dose of SSZ, compared to no curcumin pretreatment in the same subjects (Kusuhara et al., 2012).

Inhibition of MRP1 by curcumin was observed in uptake studies using radiolabeled GSH conjugates of ethacrynic acid ([^{14}C]EASG) into inside-out membrane vesicles (Wortelboer et al., 2003). In these vesicles, MRP1 pumps substrates into the vesicular lumen rather than outwards. Curcumin inhibited [^{14}C]EASG uptake with an IC_{50} of 15 μM, a similar potency to that of the pan-MRP inhibitor MK-571 (Wortelboer et al., 2003). However, in the same study the IC_{50} of inhibition of transport in MRP1 transfected Madin-darby canine kidney (MDCKII) cells was 3-fold higher. In these cells, curcumin was rapidly conjugated to GSH to form less potent metabolites (Wortelboer et al., 2003). In another study, Chearwae et al. (2006b) found that 10 μM curcumin could reverse MRP1-mediated etoposide resistance in transfected HEK293 cells. Curcumin also increased the accumulation of the MRP1 fluorescent substrates calcein-AM and fluo4-AM with IC_{50} of transport inhibition in the range 10 - 12.5 μM. Curcumin was not found to affect protein expression levels in this study. No photoaffinity labeling studies have been conducted at the substrate binding site, making it unclear if curcumin inhibits efflux by competing with MRP1 substrates. At the NBD, curcumin was unable to inhibit 8-azido-ATP binding, making it unlikely for competition with ATP at the NBD as the mechanism of inhibition (Chearwae et al., 2006b; Sreenivasan et al., 2013). Curcumin does not appear to be an MRP1 substrate as overexpression of MRP1 does not confer resistance to curcumin in HEK293 cells. Curcumin's monoglutathione conjugates however, were

found to be effluxed by the transporter (Wortelboer et al., 2003). A docking simulation study of curcumin has suggested possible binding to the homology modeled substrate binding site of MRP1, but this requires experimental confirmation (Sreenivasan et al., 2013).

Only a few studies have produced experimental evidence of MRP5 inhibition by curcumin. Our group found that curcumin at 5 and 10 μM increased the intracellular accumulation of the MRP5 fluorescent substrate, BCECF-AM, in MRP5-transfected HEK293 cells and pancreatic cancer cells expressing MRP5 (Li et al., 2011). Curcumin also sensitised transfected cells to the MRP5 substrates 6-thioguanine and 5-FU, with no effect observed in parental cells. Curcumin was also able to inhibit the MRP5-mediated export of hyaluronan from human fibroblasts with an IC_{50} of 17 μM (Prehm, 2013). It is not known if curcumin inhibits substrate binding or interacts with the NBD of MRP5. Molecular docking studies have predicted high affinity binding of curcumin to a site overlapping the ATP binding site formed by the NBDs, suggesting non-competitive inhibition (Prehm, 2013). Further experiments are needed to validate these predictions. It is possible that curcumin downregulates MRP5 protein expression since curcumin is known to inhibit the PI3K/AKT pathway and PI3K inhibitors were previously found to decrease MRP5 expression (Duong et al., 2013; Gao et al., 2013).

Apart from curcumin, natural analogues such as demethoxycurcumin and bisdemethoxycurcumin (Figure 1-4) present in commercial curcumin preparations, are also inhibitors of P-gp, BCRP and MRP1, although they have lower potencies (Chearwae et al., 2004, 2006a, 2006b; Wortelboer et al., 2005). As demethoxycurcumin lacks one of the two methoxy groups of curcumin, and bisdemethoxycurcumin lacks both groups, this indicates that the methoxy groups are not essential for ABC transporter inhibition, but do appear to contribute to potency. Tetrahydrocurcumin (THC), a more stable *in vivo* metabolite where curcumin's conjugated heptadione linker is completely saturated (Figure 1-7), was also found to inhibit P-gp, BCRP and MRP1 (Limtrakul et al., 2007). Its potency however is less than that of curcumin's which suggests that although the double bonds in the linker region are not essential for transport inhibition, they do affect inhibitory potency.

1.3.5 Instability *in vitro* and *in vivo*

Despite promising *in vitro* results as an MDR reversal agent, curcumin has poor stability both *in vitro* and *in vivo*. This poses a major problem for the clinical use of curcumin. Oral doses are poorly absorbed with low bioavailability, and i.v. curcumin is rapidly cleared with a short plasma half-life (Metzler et al., 2013). This makes it difficult to achieve sufficiently high curcumin concentrations in peripheral tissue for a prolonged period.

In vitro, curcumin is rapidly degraded in solutions at neutral-basic pH, and by ultra-violet irradiation and auto-oxidation. Wang et al. (1997) found that 50% of curcumin degraded within 10 min in a pH 7.2 phosphate buffer at 37°C. A similar degradation rate was observed in serum-free media. However, in human blood or media containing 10% serum, curcumin half-life was increased to 8 h (Wang et al., 1997). Albumin can bind curcumin and was thought to stabilize the compound (Grynkiewicz and Ślifirski, 2012; Metzler et al., 2013). The rapid degradation at neutral-basic pH is thought to be caused by proton abstraction from the phenolic hydroxyl groups and auto-oxidation since methylation of both phenolic hydroxyl groups decreased or prevented auto-oxidation and increased compound stability (Gordon and Schneider, 2012; Griesser et al., 2011; Metzler et al., 2013). The auto-oxidation reaction leads to formation of a bicyclopentadione which is the major degradation product (Figure 1-6) along with vanillin, ferulic acid and feruloylmethane as minor products (Gordon and Schneider, 2012). Formation of the major product, bicyclopentadione, involves interconversion between the keto-enol and diketone forms and the minor products result from cleavage at the β-diketone linker chain (Griesser et al., 2011; Metzler et al., 2013; Zhao et al., 2013). It has thus been proposed that the β-diketone moiety plays an important role in curcumin instability (Zhao et al., 2013).

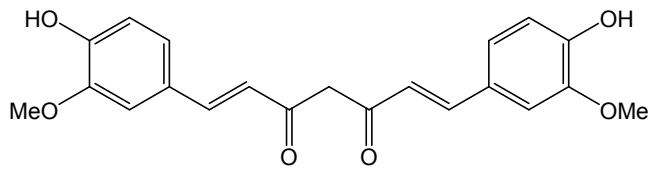

curcumin

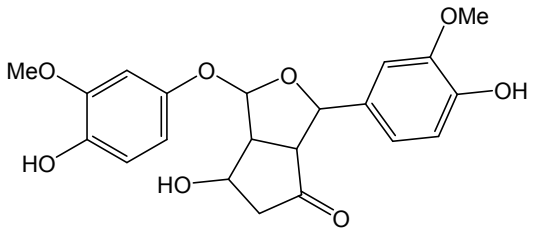

bicyclopentadione

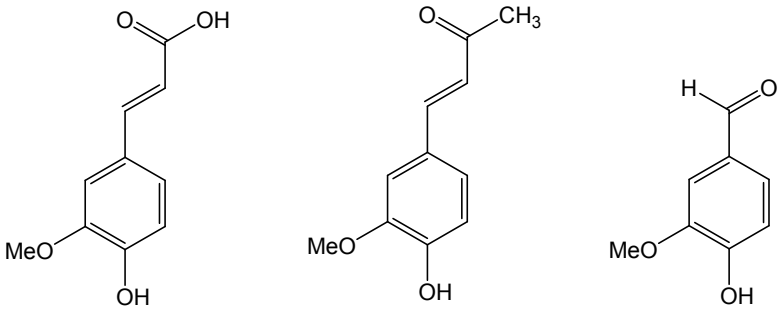

ferulic acid **feruloyl methane** **vanillin**

Figure 1-6. Curcumin and the products of its auto-oxidation. Used with permission from Metzler et al., 2013 (Appendix V).

In animal and clinical studies, curcumin is poorly absorbed and is rapidly metabolised and excreted. Poor absorption in particular, is well documented. In rats administered a 1 g/kg oral curcumin dose, 65-85% remained in the intestines and were excreted unchanged in the faeces after 72 h (Kurita and Makino, 2013). Plasma concentrations in these rats were less than 5 ng/ml or 13.6 nM. In another rat study, a 500 mg/kg oral dose gave 1% bioavailability compared to an intraperitoneal (i.p.) dose (Kurita and Makino, 2013). The C_{max} achieved was 160 nM after 40 min. Similar poor bioavailability was also observed in clinical studies. In one study of patients with pre-malignant lesions, large doses of between 4 - 8 g curcumin were given daily for 3 months (Cheng et al., 2001). An average peak serum curcumin concentration of only 1.76 µM was achieved in the group receiving 8 g, which is considerably less than the IC_{50} required for P-gp inhibition *in vitro*, which lies in the range 5 – 50 µM (Chearwae et al., 2004; Hou et al., 2008; Nabekura et al., 2005).

In another study, 12 healthy volunteers were administered a single oral dose of 10 - 12 g (Vareed et al., 2008). Only one subject had detectable free curcumin in plasma after 30 min with a C_{max} of 50 ng/mL (136 nM). The glucuronide and sulfate conjugates of curcumin were also measured, with C_{max} values of 2 μg/mL (3.7 μM) and 1 μg/mL (1.9 μM) respectively, recorded after 4 hours. Other studies with similar large doses of oral curcumin have reported very low concentrations of both free compound and its reduced and conjugated metabolites, suggesting that absorption and first-pass metabolism/degradation are the main obstacles to oral dosing (Kurita and Makino, 2013; Metzler et al., 2013).

Although poor oral bioavailability may be circumvented by parenteral routes of administration, rapid systemic metabolism and excretion in animal studies suggest that this approach may fail to result in sustained high concentrations of curcumin in plasma. Curcumin rapidly undergoes successive reduction of the four double bonds of the conjugated heptadione linker. The reduced metabolites include dihydrocurcumin, tetrahydrocurcumin (THC), hexahydrocurcumin (HHC) and octahydrocurcumin (Figure 1-7) (Grynkiewicz and Ślifirski, 2012; Metzler et al., 2013). In addition, curcumin itself and its reduced metabolites are subject to glucuronidation, sulfation and GSH conjugation (Figure 1-7) (Grynkiewicz and Ślifirski, 2012; Metzler et al., 2013). Curcumin, however, is not a substrate for the cytochrome P450 enzymes (CYPs) as no demethylation or hydroxylation were observed in microsomal studies (Grynkiewicz and Ślifirski, 2012; Metzler et al., 2013). Efficient excretion and metabolism were seen in a study of i.v. administered tritiated curcumin (^{3}H-CUR) in rats (Holder et al., 1978). Up to 50-60% of the radiolabel was recovered in bile, with greater than 95% of the label present as glucuronides. In addition, treatment with β-glucuronidase found that the major species was not curcumin but its reduced forms, THC and HHC, highlighting the susceptibility of the compound to reduction. Similar studies in bile duct cannulated rats led to biliary recovery of >80% and >85% of i.p. or i.v. administered ^{3}H-CUR within 8 h, providing further evidence of efficient biliary excretion (Metzler et al., 2013). Metabolism and biliary excretion are thought to underlie the short elimination half-life (28 min) of curcumin in rats and also likely contribute to its poor bioavailability due to first-pass metabolism (Yang et al., 2007). Efficient metabolism of curcumin was also observed in clinical trials. Administration of 2 - 4 g curcumin daily for 24 weeks to patients with Alzheimer's disease led to detection of curcumin, curcumin-

glucuronide, THC and THC-glucuronide with curcumin-glucuronide and THC-glucuronide present at 14- and 38-fold higher plasma concentrations than curcumin (Ringman et al., 2012).

It is not exactly clear which specific mechanisms contribute to the extensive metabolism of curcumin. It is known that glucuronidation of the phenolic hydroxyl groups occurs, suggesting that substitution of these groups may prevent conjugation (Metzler et al., 2013). Formation of reduced metabolites, such as THC and HHC is thought to be mediated by alcohol dehydrogenases in the liver (Figure 1-7) (Kurita and Makino, 2013; Metzler et al., 2013). Zhao et al. (2013) have argued that since some *in vivo* studies have observed that as low as 10% of the total oral dose of curcumin could be accounted for by known metabolic pathways (glucuronidation and reduction), other mechanisms of degradation may also occur. They have proposed that the β-diketone moiety of curcumin is a target for the aldo-keto reductases and dioxygenases in the liver and that this is a major contributor to its *in vivo* instability. Recent studies have indicated that these liver reductases could reduce and clear compounds with β-diketone structures rapidly and specifically (Jin and Penning, 2007). It was also found that the numerous oxidoreductases present in the liver have iron as the prosthetic group (Straganz et al., 2003; Zhao et al., 2013). The high affinity of β-diketones for iron may make curcumin a suitable substrate for these enzymes. As the β-diketone was also thought to be involved in the alkaline hydrolysis, auto-oxidation and GSH-mediated nucleophilic attack of curcumin, it has therefore been suggested that removal of this structure may result in analogues with increased stability (Griesser et al., 2011; Metzler et al., 2013; Zhao et al., 2013).

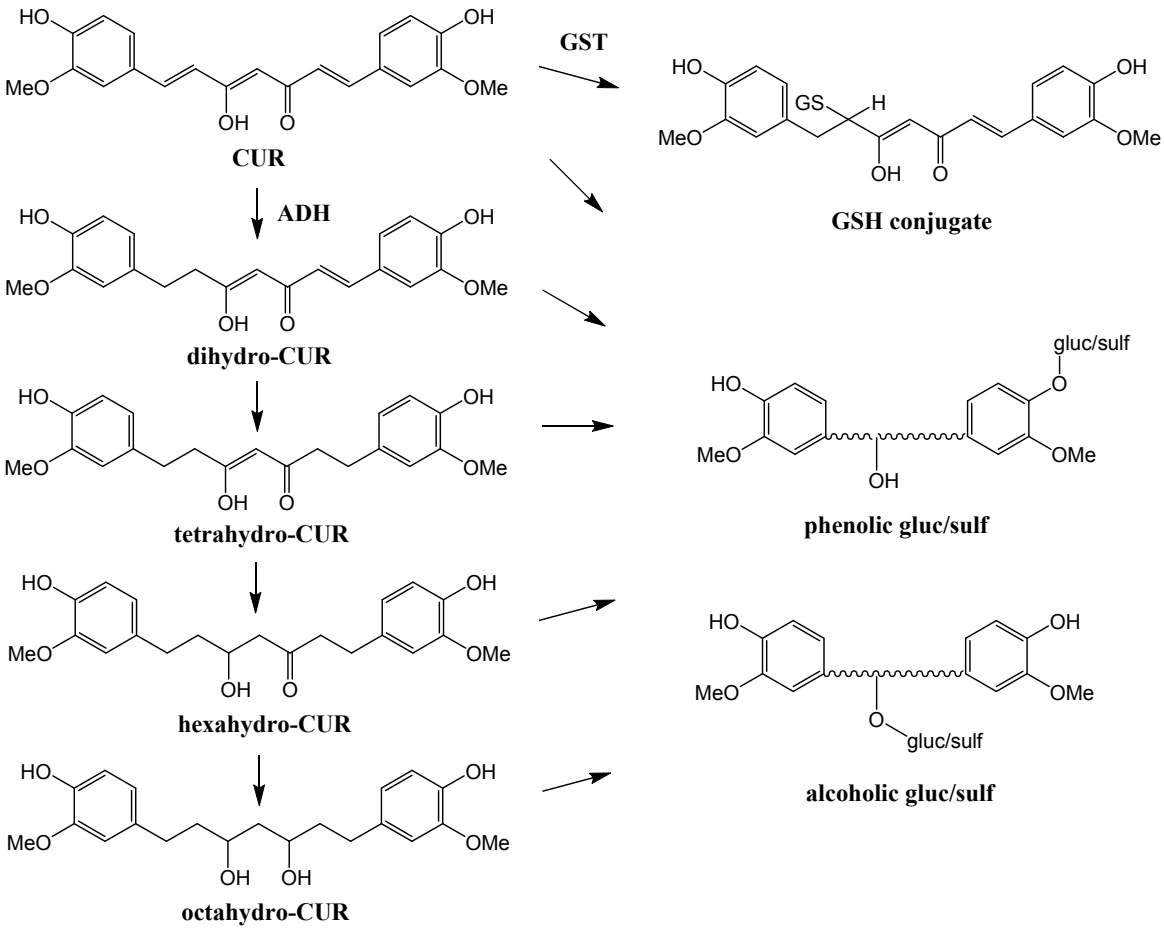

Figure 1-7. Reductive and conjugative metabolism of the enol form of curcumin (CUR). ADH, alcohol dehydrogenase; GST, glutathione-S-transferase; gluc, glucuronide; sulf, sulfate. Used with permission from Metzler et al., 2013 (Appendix V).

1.3.6 Biostable monocarbonyl analogues of curcumin

Monocarbonyl analogues of curcumin (MACs) do not contain the β-diketone moiety and have improved stability *in vitro* and *in vivo* (Figure 1-8) (Liang et al., 2009; Zhao et al., 2013). Liang et al. (2009) replaced the β-diketone containing heptadione spacer with a 5-carbon linker with either a cyclopentanone, acetone or cyclohexanone core, and compared the *in vitro* stability of 20 analogues with curcumin in pH 7.4 phosphate buffer at 37°C for a period of 75 h. After the incubation period, 64% of curcumin was degraded while all 20 analogues degraded to a lesser extent than curcumin (range 0-60%). Eight of these analogues degraded by less than 30%. In the *in vivo* rat studies that followed, greatly improved pharmacokinetic profiles were observed with the two analogues (B02 and B33) tested (Liang et al., 2009). B02 differs from curcumin by removal of the β-diketone and replacement with an acetone group (Figure 1-8). At a 500 mg/kg oral dose, B02 had a 9-fold higher peak plasma concentration, a significantly lower clearance rate of 125.4 L/h/kg compared to 835.2 L/h/kg; and a 7.3-fold higher plasma AUC than curcumin.

An even better pharmacokinetic profile was observed with B33 which has the same acetone linker as B02 but lacks the phenyl methoxy and alcohol groups of curcumin (Figure 1-8). Instead, an ortho-positioned bromine is present on both phenyl rings. For B33, C_{max} was 45-fold higher than curcumin, clearance rate was 21-fold less, and the AUC was increased 22-fold (Liang et al., 2009). It is likely that the improved pharmacokinetic profile of B33 compared to B02 may be caused by the absence of hydroxy substituents in the aromatic rings. As mentioned previously, these are the sites for glucuronide conjugation (Metzler et al., 2013). From the *in vivo* data, it is therefore clear that the issues of poor absorption, low stability and rapid clearance of curcumin could be addressed by removal of the β-diketone group and by changes in the phenyl ring substituents.

It has been speculated that removal of the β-diketone group might abrogate the biological effects of curcumin (Grynkiewicz and Ślifirski, 2012; Priyadarsini, 2013; Vyas et al., 2013). At present, numerous studies have demonstrated that the β-diketone is not essential for anticancer activity (Adams et al., 2004; Zhao et al., 2013). In the previously mentioned study by Liang et al. (2009), MACs were tested against a panel of 7 cancer cell lines along with curcumin and cisplatin. Most analogues had activity against the cell lines with some showing significantly greater potency than curcumin and cisplatin. Of the 41 analogues, 8 were more potent than curcumin against the KB

human cervical carcinoma cell line and 4 were more potent against HeLa cells. The B02 analogue was 5-fold and 1.7-fold more potent than curcumin against nasopharyngeal carcinoma CNE and colon cancer LS 174T cells, respectively. The B33 analogue was equipotent with curcumin against BGC 823 (gastric cancer), LS 174T and PC3 (prostate cancer) cell lines. Other MACs, such as EF24 (Figure 1-8), was 10-fold more potent than cisplatin against mouth cancer *in vitro*, while having greatly improved pharmacokinetics and an excellent safety profile (Adams et al., 2004). In a review of 607 MACs, increased antioxidant, antitumour, antiviral, antiangiogenesis and antiinflammatory activity were observed together with improved metabolic stability but no increased toxicity (Zhao et al., 2013).

Whether the removal of the β-diketone moiety affects ABC transporter inhibitory activity remains unknown and it is unclear if the β-diketone structure underlies the inhibition of curcumin against P-gp, BCRP, MRP1 and MRP5. No studies have so far been conducted that specifically examine the inhibitory activity of MACs against these transporters.

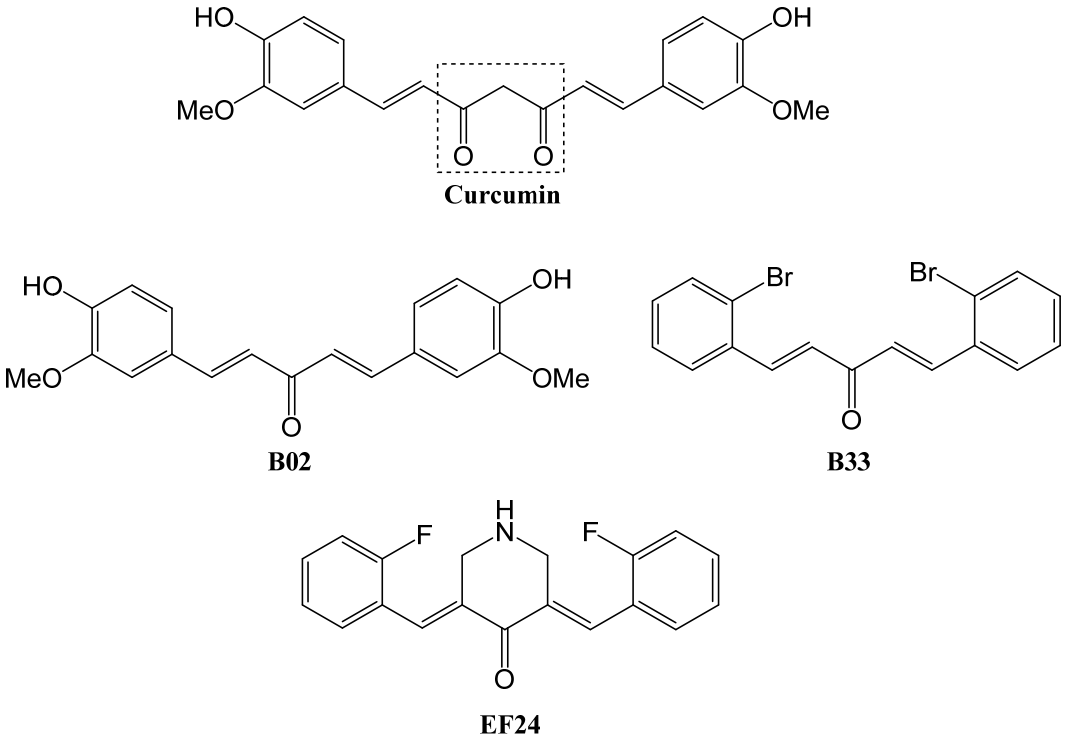

Figure 1-8. The structure of selected monocarbonyl curcumin analogues. The β-diketone moiety of curcumin is indicated by a box.

1.4 Cyclohexanone analogues of curcumin

A series of 24 MACs with heterocyclic cyclohexanone structures were synthesised and tested for anticancer activity by the Rosengren group at the University of Otago (Gandhy et al., 2012; Somers-Edgar et al., 2011; Yadav et al., 2010). These compounds were based on the biostable MACs synthesised by Liang et al. (2009), but with modifications to the aromatic groups and the central monocarbonyl core to improve cytotoxic activity against breast cancer cells. Previous studies from related MACs and structure-activity analysis suggest that these compounds could potentially inhibit ABC transporter efflux pumps.

1.4.1 Structure and anticancer activity

The heterocyclic cyclohexanone curcumin analogues were synthesised for improved activity against estrogen receptor negative (ER-negative) breast cancer, including the TNBC subtype (see Section 1.2.4.2). Members of the analogue series have 5-carbon spacers connecting the aromatic groups with the β-diketone replaced by either a cyclohexanone, N-methylpiperidone, tropinone, cyclopentanone or butoxycarbonyl piperidone core (see Figure 1-9 for the structures of selected analogues) (Gandhy et al., 2012; Somers-Edgar et al., 2011; Yadav et al., 2010). The aromatic groups of these compounds include methoxylated phenols similar to curcumin, pyridines, five-membered nitrogen containing aromatic rings and tri- and dimethoxyphenyls. Cytotoxicity studies show superior activity of these compounds compared to curcumin against a number of breast cancer cells, including the hormone-therapy resistant TNBC cell line, MDA-MB-231 (Somers-Edgar et al., 2011; Yadav et al., 2010). It was found that 12 compounds had greater cytotoxicity than curcumin, with the analogues B1 and B10 having 9.5- and 25-fold lower IC_{50} values respectively (Figure 1-9) (Yadav et al., 2010). Twelve analogues were also more potent than curcumin at inhibiting NF-κB activation. As mentioned previously (Section 1.3.3), NF-κB suppression is thought to be central to the chemosensitising effect of curcumin, suggesting possible chemosensitising activity for these analogues. Potent inhibitors of the PI3K/AKT pathway were also identified (Somers-Edgar et al., 2011; Yadav et al., 2012a, 2012b). This pathway has been implicated in cancer stem cell proliferation (Martelli et al., 2011). In addition to *in vitro* activity, an 8.5 mg/kg oral dose of B1 (referred to as RL66) in mice xenografts significantly decreased mean tumour size by 48% compared to control after 10 weeks (Yadav et al., 2012b).

Despite significantly increased cytotoxicity and *in vivo* activity, these compounds do not seem to be toxic against untransformed and normal epithelial cells. The analogues A1 (RL91) and A2 (RL90) (Figure 1-9) were significantly more potent than curcumin at inhibiting the proliferation of MDA-MB-231 and HER2+ SKBr3 breast cancer cells (Somers-Edgar et al., 2011). Interestingly, both analogues showed no antiproliferative effects against non-cancerous MCF10A breast cancer epithelial cells after 5 days, despite being used at concentrations 50-fold higher than their IC_{50} against MDA-MB-231 cells. In the *in vivo* mice study with B1, no toxicity was observed in mice after 10 weeks of daily dosing at 8.5 mg/kg (Yadav et al., 2012b).

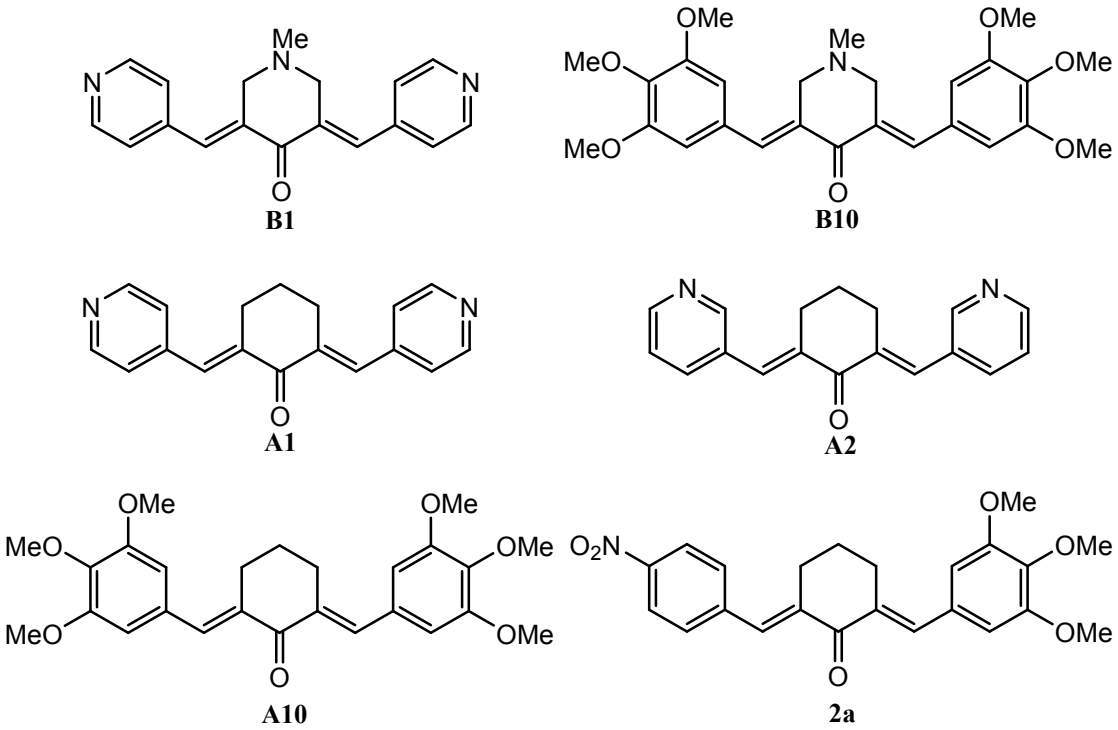

Figure 1-9. Structures of selected cyclohexanone analogues synthesised by Yadav et al. (2010) (B1, B10, A1, A2, A10) and Dimmock et al. (2005) (2a).

1.4.2 Potential inhibition of ABC transporters

It is possible that the cyclohexanone analogues may inhibit ABC transporter activity, as there has been evidence of P-gp inhibition by MACs. Dimmock et al. (2005) synthesised a series of 1,3-diarylidene-2-tetralones which included cyclopentanone and cyclohexanone compounds similar in structure to the analogues synthesised by Yadav et al. (2010). For example, the "2a" analogue has a 5-carbon linker with a cyclohexanone core connecting two phenyl groups (Figure 1-9). The substituents of the phenyl rings are asymmetric unlike the cyclohexanone analogues. Analogue 2a has a 4-nitro functional group in one ring, while the other is 3,4,5-trimethoxylated. The structure is similar to analogue A10 reported by Yadav et al. (2010), except A10 has both phenyl rings 3,4,5-trimethoxylated (Figure 1-9). In the study by Dimmock et al. (2005), a number of the tested monocarbonyl analogues (including 2a) increased accumulation of the P-gp fluorescent substrate rhodamine-123 in mouse lymphoma cells transfected with the MDR1 gene. They found that cyclohexanone structures and trimethoxylated phenyl groups were favourable features for P-gp inhibition. Since the cyclohexanone series by Yadav et al. (2010) included multiple compounds with trimethoxylated substituents, modulation of P-gp may occur.

Um et al. (2008) also observed P-gp inhibition with a series of MACs. These analogues are asymmetrical with a 3-carbon rather than 5-carbon linker as with the cyclohexanone analogues. One of the phenyl rings was unchanged from curcumin while the other contains a para-positioned amide group. It was reported that these analogues could reverse the resistance of P-gp overexpressing KBV20C cervical carcinoma cells to the substrates, vincristine and paclitaxel. Selected compounds were also found to increase accumulation of rhodamine-123, achieving a similar effect as the P-gp inhibitor, verapamil (Um et al., 2008). Although the structures of these compounds may be dissimilar to the cyclohexanone analogues, it provides further evidence that MACs lacking the β-diketone can modulate P-gp activity.

Structure-activity studies of P-gp inhibitors have identified a number of physicochemical and structural properties that are considered important for inhibition. These include; high lipophilicity (Log P > 2.9), the presence of Type I/Type II hydrogen bond acceptor groups and a tertiary nitrogen protonated at physiological pH (Liu et al., 2013; Seelig, 1998; Wang et al., 2003). Lipophilicity is essential as it is thought that compounds must partition into the lipid bilayer to

access the P-gp binding site (Seelig, 1998). Type I/Type II units are hydrogen bond acceptor pairs (oxygen, nitrogen) spaced 2.5 Å or 4.6 Å apart, that are thought to interact with hydrogen bond donors lining the substrate translocation pathway (Seelig, 1998). Lastly a protonated nitrogen is considered necessary to engage in ionic interactions with negatively charged residues in the drug binding cavity (Liu et al., 2013; Wang et al., 2003). Of the cyclohexanone analogues, the majority have partition coefficients (Log P) greater than 2.9, most contain multiple Type I/Type II units and a subset contain tropinone backbones with protonated nitrogens at physiological pH (Yadav et al., 2010). Structure-activity studies therefore predict interactions with P-gp.

For BCRP, transport inhibition by MACs has not been determined. Structure-activity studies however, suggest possible BCRP modulation by the cyclohexanone analogues. In a global model of BCRP inhibition derived from 150 registered drugs, Matsson et al. (2007) could predict inhibitors with 80% accuracy in an external test set using only two parameters, octanol-water distribution co-efficient at pH 7.4 ($LogD_{7.4}$), and molecular polarisability. They found that high polarisability and lipophilicity significantly correlated with transport inhibition. Hence, it may be these properties of curcumin which determine BCRP inhibition and not the presence of the β-diketone. In fact, removal of the β-diketone and replacement with a cyclohexanone increases lipophilicity. A majority of the cyclohexanone analogues have greater calculated $LogD_{7.4}$ values than curcumin, with some also having greater polarisability (Gandhy et al., 2012; Yadav et al., 2010). Matsson et al. (2007), also identified the ability to form pi-pi interactions and the number of nitrogen atoms as related with inhibition. All the cyclohexanone analogues have two aromatic groups (like curcumin) which can engage in pi-pi stacking; and 3 of the 6 core backbones of the series contain nitrogen, as well as 8 out of 13 end aromatic groups which include pyrrole, pyridine and imidazoles (Yadav et al., 2010). BCRP interactions with the cyclohexanone analogues may therefore be possible.

No studies have experimentally determined MRP1 and MRP5 inhibition by MACs. Both MRP1 and MRP5 are known to transport anionic compounds (Cole, 2013). As most cyclohexanone analogues contain nitrogens and may carry a positive charge at physiological pH, their interaction with both transporters may be limited, at least, at the substrate-binding sites. There remains the possibility that these analogues may interact at the NBDs, similar to that of other phytochemicals (e.g, quercetin) (Li and Paxton, 2013). Also, because curcumin is a reported inhibitor of both

transporters, structural features involved with MRP1 and MRP5 inhibition may have been conserved in some of the cyclohexanone analogues. Thus, there is a possibility that inhibitors of both transporters might be identified in these analogues.

In summary, it seems likely that the cyclohexanones analogue synthesised by the Rosengren group may inhibit P-gp and BCRP. For MRP1 and MRP5, inhibitors may also be identified due to structural similarities with curcumin, a reported modulator of both transporters.

1.4.3 Possible implications of ABC transporter inhibition

If the cyclohexanone analogues are demonstrated to inhibit the ABC transporters, these could be used as more bio-stable alternatives to curcumin as ABC transporter inhibitors. More importantly, as some of these analogues have potent anticancer activity (see Section 1.4.1), analogues may be identified that could be used as 'dual-role' chemosensitisers, which have intrinsic anticancer activity and MDR-reversal effects. Such compounds may be more effective chemosensitisers than current ABC transporter modulators that have undergone clinical trials, which are highly potent inhibitors, but do not have anticancer activity. ABC transporter inhibition would be particularly exciting for the cyclohexanone analogues in their planned application in TNBC, as ABC transporters are considered to play a key role in the resistance of this aggressive breast cancer subtype to chemotherapy (see Section 1.2.4.2).

Transporter inhibition by the cyclohexanone analogues will also provide proof that the β-diketone moiety does not underlie the interaction of curcumin with multiple ABC transporters. Currently, this question remains unanswered as very few studies have examined the inhibitory activity of analogues against these transporters. For BCRP and MRP1, no reports of inhibition by MACs have been published. If it is clearly shown that the β-diketone is not essential to transport inhibition, it may encourage investigation of the ABC transporter modulatory activity of the ≥ 600 monocarbonyl analogues reported in the literature (Zhao et al., 2013). Like the cyclohexanone analogues, these compounds have improved pharmacokinetic profiles and pleiotropic effects including potent anticancer activity (Zhao et al., 2013). This could aid in the discovery of drugs which combine potent cytotoxicity and MDR reversal activity. In addition, design of novel ABC transporter inhibitors based on the curcumin scaffold may omit the β-diketone group to improve compound stability.

1.5 Summary and aims of the thesis

MDR to chemotherapy is a major obstacle to the effective treatment of cancer. One of the main mechanisms that contribute to MDR is the cellular efflux of structurally unrelated anticancer drugs by ABC transporters. Clinical studies have shown that ABC transporters are overexpressed in many cancers and expression was correlated with poor treatment outcome. Inhibition of ABC transporters has been demonstrated *in vitro* and *in vivo* xenograft models to reverse MDR and resensitise cells and tumours to chemotherapy. Clinical trials of ABC transporter inhibitors however, have been disappointing, partly due to the problem of intrinsic toxicity of the inhibitor. This has led to a search for transporter modulators with an improved safety profile. Many natural compounds, known as phytochemicals have been found to have inhibitory activity against ABC transporters. Since these compounds are ubiquitously present in our diet, they are considered relatively non-toxic and safe for humans. One of the most promising phytochemicals with inhibitory activity is curcumin. It inhibits multiple ABC transporters including P-gp, BCRP, MRP1 and MRP5, has intrinsic anticancer activity, and also modulates signalling pathways that contribute to MDR. Its application in the clinic however, has been hampered by its unfavourable pharmacokinetic profile. Clinical studies have repeatedly shown low or undetectable plasma curcumin concentrations despite large oral doses of up to 12 g. It has been proposed that the β-diketone moiety of curcumin was responsible for its poor stability, low oral bioavailability and rapid metabolism *in vivo*. Synthesis of compounds that replace the β-diketone with monocarbonyl groups found significant improvements in both *in vitro* and *in vivo* stability. Removal of the β-diketone did not increase toxicity or abrogate anticancer activity. However, it was not known if absence of the β-diketone affected ABC transporter inhibition. No studies have been conducted which specifically aimed to examine inhibition of ABC transporters by monocarbonyl analogues.

Cyclohexanone curcumin analogues have monocarbonyl core structures in place of the β-diketone. They were synthesised by the Rosengren group for activity against aggressive, receptor-negative breast cancer cell lines and were found to have superior anticancer activity than curcumin and more potent inhibition of NF-κB, an important transcription factor in MDR. It is not known if these analogues also inhibit ABC transporter activity. Experiments with structurally related compounds and structure-activity studies suggest that these analogues may show ABC transporter interactions.

The main aim of this research was to determine whether the 24 heterocyclic cyclohexanone analogues obtained from the Rosengren lab retained the inhibitory effects of curcumin against the ABC transporter efflux pumps (P-gp, BCRP, MRP1 and MRP5), with the purpose of finding more stable alternatives to curcumin as ABC transporter inhibitors. As some of these analogues had potent anticancer activity, it was hoped that 'dual-role chemosensitisers' with potent anticancer and MDR-reversal activity, would be identified. It is likely that such analogues would be superior antitumour agents compared to the highly potent ABC transporter inhibitors in clinical trials, as the former would be active as a single agent, while increasing the activity of co-administered substrate drugs.

The specific aims of this study were:

- Flow cytometry screening of all 24 heterocyclic cyclohexanone analogues for inhibition of fluorescent dye efflux in P-gp, BCRP, MRP1 and MRP5 transfected cells. (Chapter 2)

- Confirmation of ABC transporter modulation by determining the ability of identified inhibitors to reverse MDR in cell proliferation assays. (Chapter 3)

- Membrane vesicle assays to determine inhibitory effects using a cell-free system (Chapter 4)

- Total protein expression studies using Western blotting to determine effects on ABC transporter expression. (Chapter 5)

- Cell surface staining studies to determine the effects of identified inhibitors on the cell surface expression of ABC transporters (Chapter 6)

2. Flow cytometry screening of curcumin analogues for ABC transporter inhibition

2.1 Introduction

Flow cytometry screening is a rapid, simple and cost-effective method that can be applied to the identification of ABC transporter inhibitors. It is a widely-used assay that has helped characterise transporter interactions with natural compounds, therapeutic drugs and environmental toxins (Matsson et al., 2007; Nabekura et al., 2005; Pavek et al., 2005). Flow cytometers stream cells from a suspension, one at a time through a laser and an electronic detector (Krishan and Hamelik, 2005; Shapiro, 2005a). They can be equipped with multiple lasers and fluorescence filters and can quantify cell size, intracellular complexity and fluorescence at multiple emission wavelengths at a rate of hundreds to thousands of cells per second (Shapiro, 2005a). The ability to measure fluorescence in individual cells is used to track the intracellular accumulation of ABC transporter probe substrates. Cells overexpressing the transporter of interest accumulate less probe and have reduced fluorescence compared to parental or empty vector-transfected cells (Figure 2-1A). Transporter inhibitors are identified through increased probe accumulation and cellular fluorescence from the inhibition of transporter-mediated probe efflux (Figure 2-1B).

The use of a probe substrate to identify inhibitors is referred to as an 'indirect setup' and can proceed via two different modes (Nabekura et al., 2005; Szakács et al., 2008a; Wang et al., 2000a). Inhibition can be monitored in either the accumulation phase or efflux phase. The efflux phase (or the retention assay) involves the initial loading of transporter-expressing cells with a fluorescent probe substrate, followed by a wash step (Lai et al., 2010; Olson et al., 2001). The cells are then incubated in probe-free media and the decrease in intracellular fluorescence is measured at different time points with or without the presence of test compound (Wang et al., 2000a). Inhibition of probe efflux slows the rate of fluorescence decrease compared to media-only controls. Although relatively straightforward, a number of issues have been identified with this method. The probe can leak out of the membranes via passive diffusion, independent of transporter-mediated efflux (Wang et al., 2000a). This results from a higher probe concentration

within cells compared to the surrounding media. For rapidly effluxed substrates, there is less tolerance for missed time points and precise time-keeping is required to reduce variability (Neyfakh, 1988). To reduce assay time, the efflux assay has been conducted using a single rather than multiple time points per test compound (Durand and Olive, 1981). Nonetheless, due to the initial probe loading step, it remains more time-consuming than other assays.

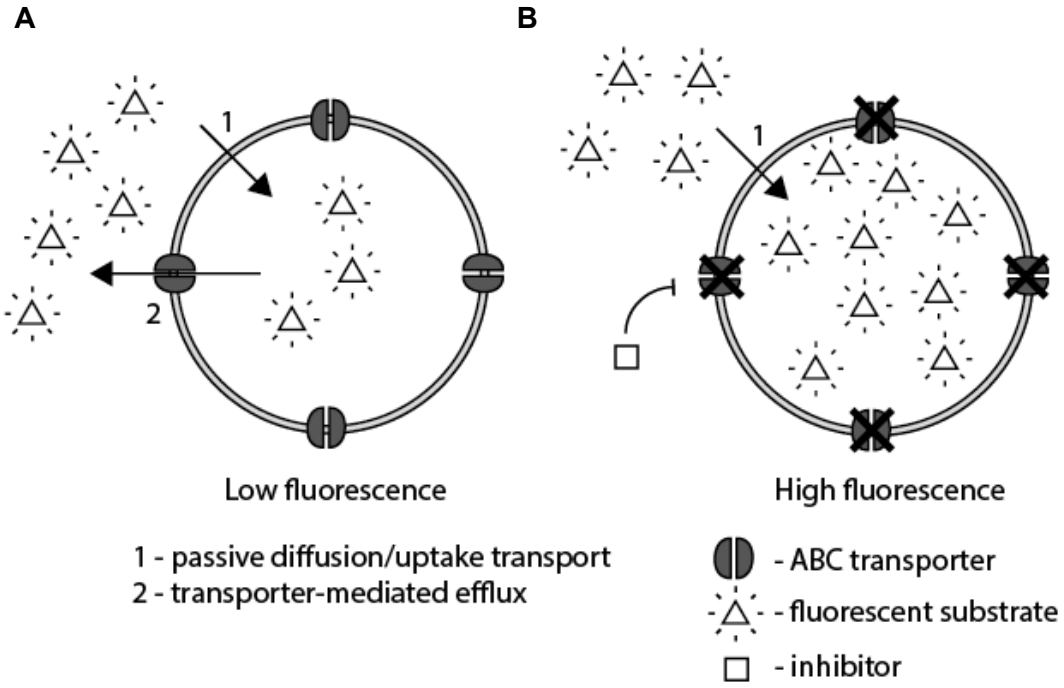

Figure 2-1. Diagram of fluorescent probe substrate accumulation in ABC transporter expressing cells. Probe substrate enters cells through passive diffusion or through an uptake transporter and is actively effluxed. This causes reduced intracellular accumulation and low cell fluorescence (**A**). Addition of ABC transporter inhibitor decreases probe efflux and increases probe accumulation, leading to increased cellular fluorescence (**B**).

The alternative and more common method is the accumulation assay (or steady-state accumulation assay) (Durand and Olive, 1981; Xia et al., 2007a). This does not require a loading step and is preferred over the efflux assay for rapidly screening large numbers of compounds (Matsson et al., 2007; Wang et al., 2000a). In the latter, the probe is allowed to accumulate in transporter overexpressing cells together with test compound and the reaction is stopped after the probe reaches steady-state accumulation (Nabekura et al., 2005; Xia et al., 2007a). Cells are then washed multiple times to remove both extracellular probe and test compound prior to flow cytometric analysis. If the test compound inhibits the probe efflux, the influx/efflux equilibrium is shifted and a higher steady-state probe concentration is achieved. If transport is completely

inhibited, probe concentrations are restored to similar levels as in parental or empty vector-transfected cells (Brouwer et al., 2013; Xia et al., 2007a).

Unlike the efflux assay, membrane leakage through passive diffusion is less of an issue as probe concentrations are higher in the extracellular media than within cells. Since samples are assayed when the probe is at steady-state, variability from the use of a single time-point is reduced compared to the efflux assay (Varma et al., 2003; Wang et al., 2000a).

Numerous studies have successfully used the accumulation assay to identify new ABC transporter inhibitors. Nabekura et al. (2005) screened dietary chemopreventive phytochemicals for P-gp inhibitory activity with this method. Matsson et al. (2007) examined BCRP interactions with 123 registered drugs using mitoxantrone as the probe and a BCRP-transfected Saos-2 cell line. Tan et al. (2013a) screened 56 phytochemicals for BCRP inhibition with mitoxantrone and BCRP-transfected HEK293 cells.

The use of the accumulation assay for inhibitor screening requires a careful study design to limit artifacts and confounding factors. It is critical that the experiments are conducted in parallel with parental or empty vector-transfected cells (Brouwer et al., 2013; Xia et al., 2007a). This helps to identify non-specific effects of the test compound that are separate from transporter interactions. For example, an increased probe influx rate caused by the test compound can be falsely interpreted as efflux inhibition. In such a case, the test compound would increase fluorescence in both transporter-expressing and parental cells as the effect does not depend on the presence of the transporter (Xia et al., 2007a). Another important factor to consider is the possible intrinsic fluorescence of the test compounds (Matsson et al., 2007; Tan et al., 2013a). Strong fluorescence at the same emission wavelength as the probe could be mistaken for increased intracellular accumulation of the probe itself, leading to false positives.

It is also important that the incubation period corresponds to the time needed to reach steady-state (Wang et al., 2000a; Xia et al., 2007a). Failing to do this introduces variability as the reactions are halted while the probe is still accumulating. The time to steady-state should be determined for each probe in each cell line to be used, since accumulation kinetics may vary with each (Krishan et al., 1997a; Xia et al., 2007a). Probe concentrations also need optimisation as high concentrations

may cause cell toxicity or saturate the transporter efflux activity, while low concentrations could result in a poor signal-to-noise ratio (Krishan and Hamelik, 2005; Shapiro, 2005a, 2005b).

In inhibitor screening, transfected cells are preferred over drug-selected cells since the selection process may upregulate multiple efflux pumps and change the expression profile of influx transporters (Calcagno and Ambudkar, 2010). Test compound concentrations should be selected that do not cause excessive toxicity in the time-frame of the experiments. Dead and necrotic cells tend to have increased cellular fluorescence as the cell membranes are compromised and become permeable to extracellular probe substrate (Krishan and Hamelik, 2005; Shapiro, 2005b). Although early apoptotic cells maintain intact cell membranes, they become condensed compared to viable cells and this decreased volume increases intracellular probe concentrations (Shapiro, 2005b). Thus, non-viable apoptotic and necrotic cells need to be excluded to lessen false-positive events. Cell aggregation is another source of false-positives. Cells that are stuck together (e.g., doublets) are read as single events with increased fluorescence (Wersto et al., 2001). Flow cytometry gating strategies that select for single cells (e.g., pulse height vs. area techniques) should be applied to exclude aggregates (Wersto et al., 2001). Cell density is also known to affect intracellular probe concentrations. High density samples may accumulate less probe than low-density samples due to decreased extracellular probe concentrations (Durand and Olive, 1981). This parameter must be kept uniform to allow for valid comparisons and limit variability. Another source of data variation is the use of cells in different phases of growth or passage numbers which may affect ABC expression levels and probe efflux activity (Krishan et al., 1997a, 1997b). Highly confluent cells and excessively high passage numbers may reduce transporter levels and should be avoided.

Taking into account the previously mentioned factors, the flow cytometry accumulation assay was used to screen 24 heterocyclic cyclohexanone curcumin analogues for inhibitory activity against P-gp, BCRP, MRP1 and MRP5. Curcumin was included in the studies for comparison. Stably transfected cell lines were used, together with the corresponding parental cells. These were obtained from the Netherlands Cancer Institute and have been extensively characterised in transport studies (Beedholm-Ebsen et al., 2010; Evers et al., 1998; Pavek et al., 2005; Wijnholds et al., 2000b; de Wolf et al., 2008). Well-reported and established probe substrates were used, including rhodamine-123 for P-gp activity, mitoxantrone for BCRP, calcein-AM and BCECF-AM for

MRP1 and MRP5, respectively (Efferth et al., 1989; Lai et al., 2010; Minderman et al., 2002; Olson et al., 2001; Wu et al., 2005).

As a positive control, verapamil was selected to inhibit rhodamine-123 efflux (Tsuruo et al., 1981; Wang et al., 2000a). Although verapamil is also an MRP1 inhibitor, when combined with the P-gp selective substrate, rhodamine-123, and a P-gp overexpressing cell line, it can reliably determine P-gp mediated transport (Loe et al., 2000). Mitoxantrone is preferentially effluxed by BCRP but has also been reported to be a substrate of P-gp and MRP1 (Minderman et al., 2002; Morrow et al., 2006). It was therefore used with the potent and specific BCRP inhibitor, Ko143, to accurately determine BCRP-mediated efflux (Allen et al., 2002). Calcein-AM (acetomethoxy derivative of calcein) is a non-fluorescent permeable compound which can enter cells rapidly through passive diffusion (Olson et al., 2001). It is converted by non-specific esterases in viable cells to the fluorescent species, calcein, which is an excellent substrate for MRP1 (Olson et al., 2001). Calcein-AM, but not calcein, is also a good P-gp substrate (Legrand et al., 1999). To specifically detect MRP1 efflux activity, the MRP selective inhibitor MK-571 was used which has no inhibitory activity against P-gp (He et al., 2011). Similarly, BCECF-AM rapidly accumulates in cells and is cleaved to its fluorescent form (BCECF) by intracellular esterases (Bachmeier et al., 2004). Free BCECF is a selective and efficient MRP5 substrate (McAleer et al., 1999; Olson et al., 2001). Its lipophilic ester, however, is also a substrate for P-gp and BCRP (Bachmeier et al., 2004). The selective MRP inhibitor MK-571 does not inhibit either transporter and was used to assess MRP5-mediated efflux in transfected HEK293 cells (Gekeler et al., 1995).

2.2 Materials and Methods

2.2.1 Curcumin analogues

Twenty-four MACs were obtained from the Rosengren group at the University of Otago (Table 2-1). Their chemistry and synthesis have been described (except for RL92) (Gandhy et al., 2012; Yadav et al., 2010). These analogues have cyclic ketone cores in place of the β-diketone structure (Figure 2-2). Five distinct ketone cores comprise the backbone of the analogues: series A – cyclohexanone core; series B – N-methylpiperidone core; series C - tropinone core; series D – cyclopentanone core and series E – butoxycarbonyl piperidone core (Figure 2-2). These core structures were linked through methylidene groups to two identical aromatic groups on each end of the molecule. Thirteen different aromatic groups were synthesised. These include pyridines, fluorine substituted pyridines, N-methylpyrroles, N-methylimidazoles, N-methylindole and trimethoxyphenyl and dimethoxyphenyl substituents (Figure 2-2). In addition, a new investigational analogue, RL92, was included in the transport inhibition studies. The latter's structure is protected by intellectual property and has not yet been disclosed.

All analogues were isomerically pure and existed as *E,E* isomers based on nuclear magnetic resonance (NMR) spectroscopy and x-ray crystallographic data (Gandhy et al., 2012; Yadav et al., 2010). They were found to be stable and soluble in dimethyl sulfoxide (DMSO). Analogues were received in powder form at ≥95% purity. Prior to use, they were dissolved in DMSO and stored as 20 mM stock solutions at -80°C. New stock solutions were made every 6 months from powder form.

Table 2-1. List of 24 cyclohexanone and cyclopentanone curcumin analogues obtained from the Rosengren lab.

A series	A1*, A2, A3, A4, A5, A6, A7, A8, A9, A12, A13
B series	B1, B2, B5, B8, B10, B11, B12
C series	C1, C2, C10
D series	D2
E series	E12
RL series	RL92 (proprietary structure)

* - Analogues are coded with alpha-numeric designation. Letters indicate the central core backbone structure. Numbers represent the aromatic substituents. Refer to Figure 2-2 for structures.

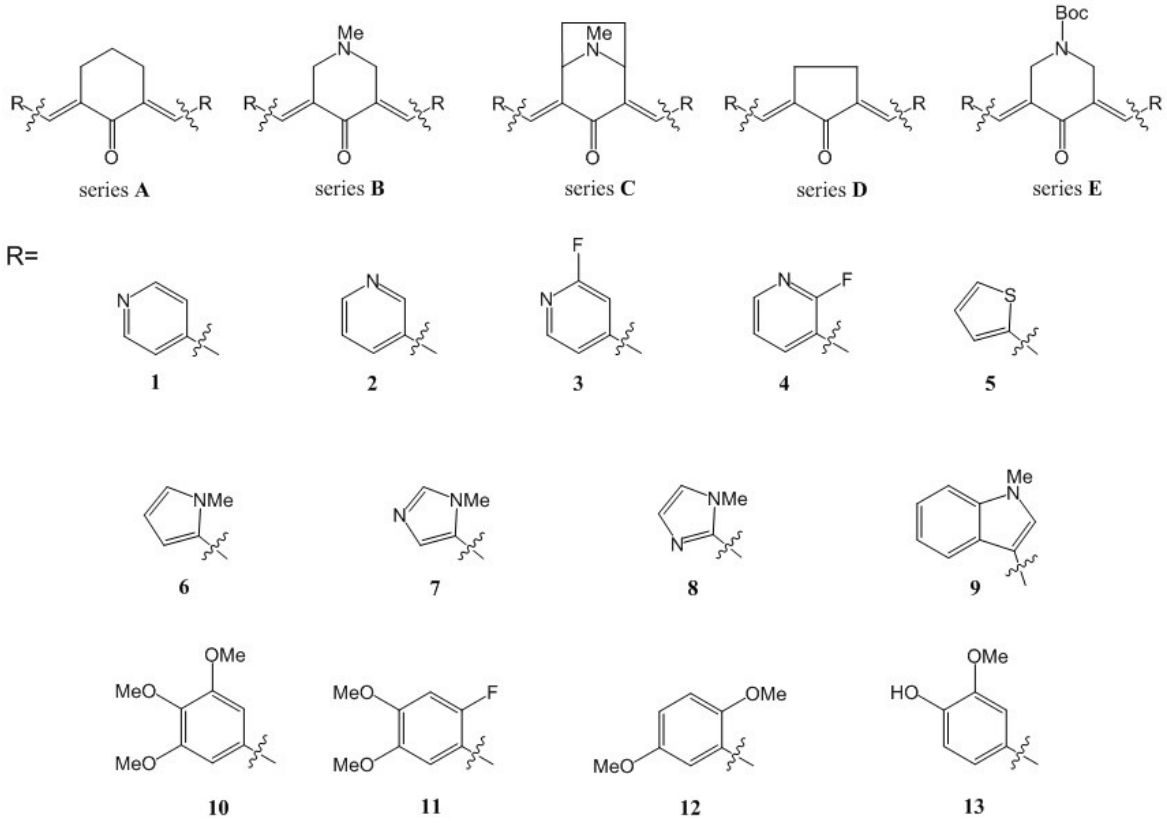

Figure 2-2. Structures of the cyclohexanone analogues. Boc - tert-Butyloxycarbonyl.

2.2.2 Chemicals and reagents

Materials (purity indicated) were purchased from the following sources: mitoxantrone (≥97.0%), calcein-AM (≥90.0%), BCECF-AM (1 mg/mL solution), rhodamine-123 (≥85.0%), propidium iodide (≥94.0%), verapamil (≥99.0%), Ko143 (≥98.0%), DMSO (≥99.9%) and paraformaldehyde (PFM) from Sigma-Aldrich, St Louis, MO; high purity curcumin I (≥98.5%) from Enzo Life Sciences, Farmingdale, NY; MK-571 (≥95.0%) from Cayman Chem, Ann Arbor, MI.

Phenol-red and phenol-red free Dulbecco's modified eagle's medium (DMEM), TrypLE™ cell dissociation enzyme (trypsin substitute), Trypan blue solution (0.4%), penicillin-streptomycin solution (pen-strep) (100x), phosphate buffered saline (PBS) solution, and sterile-filtered fetal bovine serum (FBS) were purchased from Life Technologies (Auckland, NZ).

2.2.3 Cell lines

Parental human embryonic kidney cells (HEK/P) and Madin-Darby canine kidney II cells (MDCKII/P) and the corresponding human ABC transporter transfected cell lines MDCKII/P-gp, MDCKII/BCRP, HEK/BCRP, HEK/MRP1, HEK/MRP5 were generously provided by Professor Piet Borst (The Netherlands Cancer Institute, the Netherlands). Cell lines all stably overexpress the wild-type form of each transporter. Transduction and overexpression in the cell lines were carried out by the Borst and Schinkel groups at the Netherlands Cancer Institute. Publications outlining transfection procedures are outlined in Table 2-2.

Table 2-2. ABC-transporter overexpressing cell lines

Cell line	Promoter	Publication
MDCKII/P-gp	CMV[a]	Evers et al., 1998
MDCKII/BCRP	MMLV[b]	Pavek et al., 2005
HEK/BCRP	MMLV	de Wolf et al., 2008
HEK/MRP1	CMV	Beedholm-Ebsen et al., 2010
HEK/MRP5	CMV	Wijnholds et al., 2000b

[a]cytomegalovirus [b]moloney murine leukemia virus

Both MDCKII and MDCKII/P-gp from the Borst group were previously investigated for P-gp expression using western blots and real-time PCR (Kuteykin-Teplyakov et al., 2010). Expression of MRP1 in HEK/MRP1 cells was previously confirmed using real-time PCR (not shown). Overexpression of MRP5 protein in HEK/MRP5 cells was observed through immunocytochemistry (Li et al., 2011). BCRP expression in MDCKII/BCRP and HEK/BCRP were determined in Chapters 5 and 6. Tan et al. (2013a) have previously confirmed BCRP expression in HEK/BCRP cells.

2.2.4 Cell culture

All cell culture procedures were conducted in a Class II tissue culture hood using sterile techniques.

2.2.4.1 Revival from frozen stocks

Cells were revived from frozen stocks by quick thawing in a 37°C water bath. The cryovials were spun at 500 g, 4°C for 5 min to pellet the cells. Freezing media was aspirated and cells resuspended in 10 ml phenol-red complete DMEM in T_{75} flasks (BD Falcon, Auckland, NZ). Complete DMEM was supplemented with 10% FBS and 1% pen-strep (stock solution: 10,000 units/mL penicillin, 10,000 µg/mL streptomycin). Cells were allowed to grow until confluent (~3 - 4 days) in a humidified incubator at 37°C and 5% CO_2.

2.2.4.2 Cell maintenance and splitting

At confluence, cells were split by washing twice with 5 ml warm PBS solution and adding 2 mL of TrypLE to dissociate the cells from the flask. HEK293 and MDCKII cells were incubated for 5 min and 15 min, respectively, in the 37°C incubator. TrypLE was neutralised by adding 8 mL of complete DMEM. Cells were transferred to 15 mL tubes and spun for 5 min, 4°C at 500 g. Media was discarded and cells were resuspended in 5 mL complete DMEM.

The number of viable cells was determined using the Trypan blue exclusion method. A 20 µl cell suspension aliquot was mixed with 20 µl 0.4% Trypan blue. A 10 µl aliquot was placed in a haemocytometer and cells excluding the dye were counted. Cells were seeded to a new T_{75} flask at a density of 6.0 x 10^5 cells/T_{75} flask for MDCKII/P, MDCKII/BCRP and MDCKII/P-gp; 7.5 x 10^5 cells/T_{75} flask for HEK293/P and 1.0 x 10^6 cells/T_{75} for HEK/MRP1 and HEK/MRP5 (due to the slower doubling times of HEK293 cells) in 10 mL total volume of complete phenol-red DMEM. Cells were grown to ~80 - 90% confluence (3 days) and were either split or used in downstream applications (e.g., flow cytometry, cell proliferation assays). All cells were discarded after a passage number of 20 and similar passage numbers of parental and transfected cell lines were used.

2.2.5 Flow cytometry

Work flow of the flow cytometry screening studies.

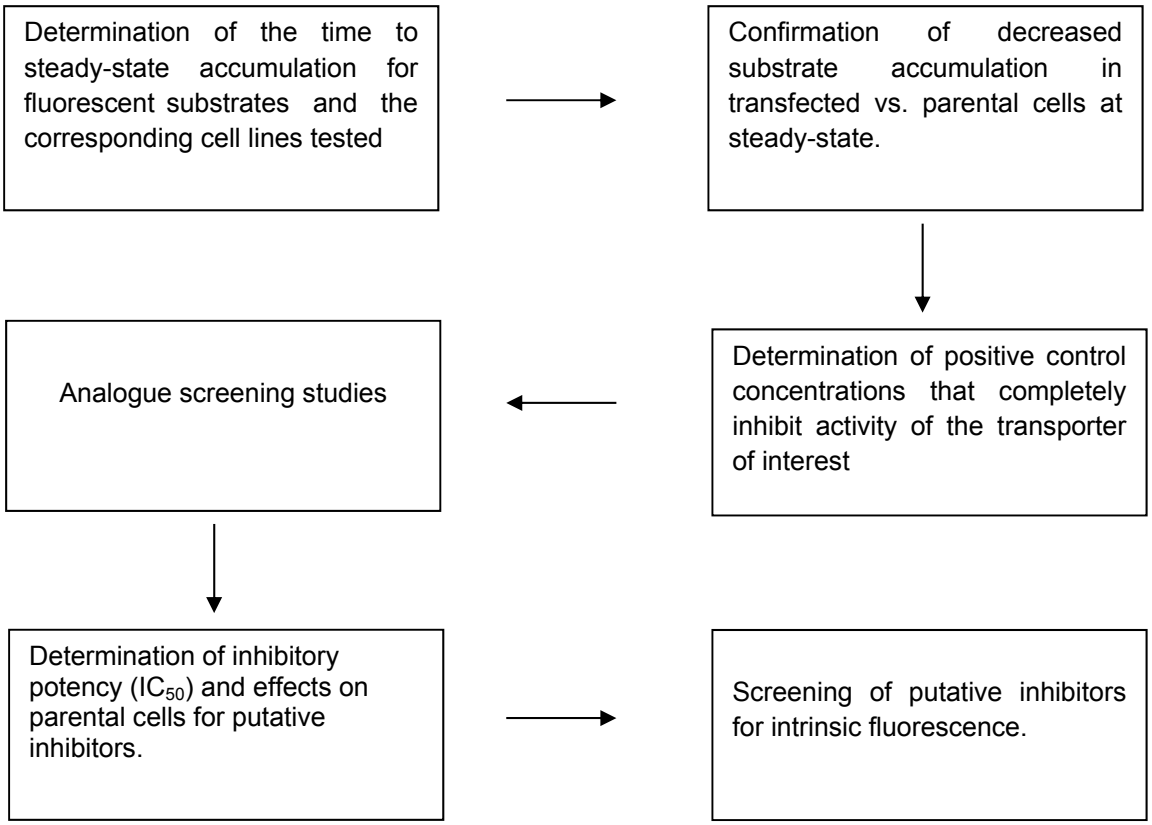

2.2.5.1 Determination of time to steady-state for fluorescent probes

Cells from a T_{75} flask at ~80 - 90% confluence 3 days after seeding were washed twice with PBS and trypsinised (see Section 2.2.4.2). TrypLE was neutralized with 8 mL phenol-red free complete DMEM, transferred to a 15 mL tube and centrifuged at 500 g for 5 min at 4°C. Media was discarded and the cells were resuspended in 5 ml phenol-red free DMEM only, without FBS/Pen-strep. Unsupplemented DMEM was used from this point onwards. Use of phenol-red free DMEM was to minimise intrinsic fluorescence from the media. Viable cells were then counted as in Section 2.2.4.2. Cells were transferred to a 50 mL falcon tube and resuspended in the appropriate volume of DMEM to achieve a cell density in suspension of 5 x 10^5 cells/mL. At this density, a typical T_{75} flask of HEK293 cells would yield a total volume of 14 - 16 mL (7 – 8 million cells). For MDCKII cells, a higher yield of between 16 - 18 mL (8 – 9 million cells) was often observed. For a steady-state accumulation experiment with 6 time points done in duplicates, 1 T_{75} flask was required per cell line.

The cells in the 50 mL falcon tube were allowed to equilibrate at 37°C in the incubator for 10 min. The lid was kept loose to allow for 5% CO_2 to diffuse into the media and keep the pH at 7.4. After 10 min, the tube was shaken to resuspend the cells and 2 x 1 mL cell suspension was transferred to test tubes. These samples represent time 0 min (T_0). Fluorescent substrates were then added into the remaining cell suspension in 50 mL falcon tubes at a 1:1000 dilution. The samples were then gently vortexed, the timer was started and the samples replaced in the 37°C incubator. Samples and stock solutions were wrapped in aluminum foil and the experiment was conducted with minimal light exposure to prevent fluorescence bleaching. Table 2-3 shows the fluorescent substrates used for each cell line, the final substrate concentration in media and the final DMSO concentrations. The fluorescent substrates were previously prepared from powder form by dissolving in pure reagent-grade DMSO to make up 1000x stock solutions. Solutions were made sterile by filtration through a 0.22 µM Whatman syringe filter (Global Science, Auckland, NZ). Stocks were kept at -20°C, protected from light, for 6 months before being discarded. Final substrate concentrations used in this assay were based on previous reports from the literature: rhodamine-123 (Chearwae et al., 2004; Limtrakul et al., 2007; Yumoto et al., 1999), mitoxantrone (Robey et al., 2001; Tan et al., 2013a), calcein-AM and BCECF-AM (Li et al., 2011; Limtrakul et al., 2007; Wu et al., 2005).

Table 2-3. Fluorescent substrates in steady-state accumulation studies

	Fluorescent substrate			
	Rhodamine-123	**Mitoxantrone**	**Calcein-AM**	**BCECF-AM**
Cell lines	MDCKII/P MDCKII/P-gp	MDCKII/P MDCKII/BCRP HEK/P HEK/BCRP	HEK/P HEK/MRP1	HEK/P HEK/MRP5
Stock solution	2.5 mM	5.0 mM	100 µM	250 µM
Final concentration	2.5 µM	5.0 µM	0.1 µM	0.25 µM
Final DMSO concentration	0.1%	0.1%	0.1%	0.1%

Duplicate samples (1 mL cell suspension) were collected in clear round-bottom polypropylene test tubes (BD Biosciences, Auckland, NZ) at specified time points (see Table 2-4). These were immediately placed on ice and the suspensions diluted with 3 mL ice-cold PBS. The cells were centrifuged at 500 g for 5 min at 4°C, and again resuspended in ice-cold PBS. This was repeated twice to wash off excess fluorescent dye. After the cells were pelleted and the PBS was discarded, they were resuspended in 500 µl cold PBS by pipetting up and down multiple times. Once fully resuspended, 500 µl freshly prepared cold 2% paraformaldehyde (PFM) solution in PBS was added for a final concentration of 1%. Prior resuspension of cells was necessary to prevent significant cell loss as direct addition of PFM solution to the pellet caused substantial cell adhesion to the test tube. After addition of PFM, the tubes were gently vortexed and were incubated on ice, protected from light for 15 min. After fixation, 3 mL cold PBS was added per tube and the cells spun down at 500 g for 5 min, followed by resuspension with 500 µl DMEM, and then placed on ice. After all samples were collected and processed, cell fluorescence was read within 1 h with a flow cytometer. The time to reach steady-state accumulation for each substrate dye was used in the inhibitor screening studies.

Table 2-4. Time points for sample collection in steady-state accumulation studies

	Time points (min)			
	Rhodamine-123	**Mitoxantrone**	**Calcein-AM**	**BCECF-AM**
Sample 1	0	0	0	0
2	15	30	15	5
3	30	60	30	15
4	45	90	45	30
5	75	120	60	45
6	120	180	75	60

2.2.5.2 Determining complete transport inhibition by positive controls

Transfected cells and the corresponding parental cells were trypsinised and resuspended in media at a density of 5 x 10^5 cells/mL (see Section 2.2.5.1). Known ABC transporter inhibitors were added to transfected cells at two concentrations which were several-fold higher than their reported IC_{50} values in the literature (Allen et al., 2002; Munić et al., 2010; Wortelboer et al., 2003; Wu et al., 2005). The inhibitors used were verapamil (25 & 50 µM) for P-gp, Ko143 (5 & 10 µM) for BCRP and MK-571 (45 & 60 µM) for MRP1 and MRP5. DMSO-only controls of parental and transfected cells were included in all experiments. All inhibitors were dissolved in DMSO and filtered. Final DMSO concentrations in media were 0.4% for MK-571 samples and 0.2% for verapamil and Ko143 treated samples and were kept uniform with corresponding controls. After addition of inhibitors, cells were pre-incubated for 15 min at 37°C. Fluorescent substrates were then added and incubated for the appropriate time to achieve steady-state as determined in Section 2.2.5.1. This was 75 min for rhodamine-123; 120 min for mitoxantrone; 30 min for calcein-AM; and 15 min for BCECF-AM. After the incubation, the reaction was stopped with ice-cold PBS and the cells washed three times to remove excess substrate and inhibitors (see Section 2.2.5.1). Cells were then resuspended in 500 µl DMEM without fixation and placed on ice and analysed within 1 h.

2.2.5.3 Transport inhibition screening studies and determination of IC_{50} values

MDCKII/P-gp, MDCKII/BCRP, HEK/MRP1 and HEK/MRP5 cells were trypsinised and resuspended in phenol-red free DMEM as outlined in Section 2.2.5.1. Density was adjusted to 5 x 10^5 cells/mL and aliquots of 1 mL cell suspension were transferred to 15 mL tubes. Curcumin analogues, stored as 20 mM stock solutions in DMSO, were added at a 1:1000 dilution (final concentration of 20 µM). Direct dissolution of either curcumin or the analogues with culture media was not possible due to precipitate formation. However, all analogues were soluble in media at 20 µM with no precipitation observed, if first dissolved in DMSO before dilution with media. Using this procedure, A13 and RL92 were also soluble up to 40 µM and curcumin up to 100 µM in media. Samples were incubated for 15 min at 37°C in an incubator. Fluorescent substrates were added and samples were further incubated in the 37°C incubator. Concentration of fluorescent substrates, incubation times, positive controls and final DMSO concentrations are reported in Table 2-5. DMSO concentrations for experimental samples and their corresponding DMSO-only controls were kept uniform.

Table 2-5. Reagent concentrations and incubation period for inhibitor screening studies

	Fluorescent substrate			
	Rhodamine-123	**Mitoxantrone**	**Calcein-AM**	**BCECF-AM**
Cell lines	MDCKII/P MDCKII/P-gp	MDCKII/P MDCKII/BCRP HEK/P HEK/BCRP	HEK/P HEK/MRP1	HEK/P HEK/MRP5
Incubation time	75 min	120 min	30 min	15 min
Substrate concentration	2.5 µM	5.0 µM	0.1 µM	0.25 µM
Positive control	25 µM verapamil	5 µM Ko143	60 µM MK-571	60 µM MK-571
Final DMSO concentration	0.2%	0.2%	0.5%	0.5%

After the incubation, the reaction was stopped with ice-cold PBS, and the cells were washed three times with PBS (Section 2.2.5.1), followed by resuspension in 500 µl DMEM and storage on ice in the dark until analysis.

The same protocol was used to produce concentration-response curves of identified inhibitors using 5-6 concentrations of the test compounds. Both DMSO controls and the corresponding positive controls were included. The highest inhibitor concentrations used in the potency calculations were also tested against the corresponding parental cells (either HEK/P or MDCKII/P) to rule out non-transporter-mediated effects.

2.2.5.4 Flow cytometry analysis

Samples were analysed with a BD LSRII flow cytometer (BD, San Jose, CA) using BD FACSDiva software and FlowJo (Treestar, Ashland, OR).

Selection of viable cells

Viable cells were enriched from the total cell population using forward and side scatter parameters. Forward scatter measures cell size while side scatter is a measure of intracellular complexity or granularity and increases with greater particle density within cells. Non-viable, necrotic and apoptotic cells have decreased cell size and greater intracellular particle density compared to viable cells due to cell shrinkage and other processes such as chromatin condensation (Bertho et al., 2000; Ohnuma et al., 2006; Al-Rubeai et al., 1997). In a 2D-plot of forward vs. side scatter, non-viable cells appear in an area to the left or upper-left of viable cells due to their lower forward scatter and higher side scatter. These can be excluded from subsequent analysis by forming a "gate" around the viable cells only and instructing the flow cytometer to count and analyse events that only fall within a specified forward and side scatter range.

Prior to the start of each experiment, the position of the viability gate (referred to as P1) in the 2D forward vs. side scatter plot was determined using healthy, untreated and unstained cells (either HEK293 or MDCKII cells). Since the samples were from a homogenous cell population, viable cells clustered into a single high density area of the 2D plot (Figure 2-3A). The P1 gate was placed around this population. To confirm that the gate represented the viable cell fraction, the whole sample population was stained with the fluorescent dye, propidium iodide (PI). PI binds to dsDNA but only penetrates cells with compromised membranes (i.e., non-viable cells). PI was added 10 min prior to analysis at a final concentration of 1 µg/mL in PBS to the untreated, unstained samples. Figure 2-3B is a representative experiment showing low PI staining of the P1 population while positive staining was seen in non-viable cells identified from the 2D scatter plot (Figure 2-3A).

It should be noted that the fixation process in the steady-state accumulation studies kills the cells. The same gating method (but without PI staining) was also applied in these samples, since fixation accurately preserves forward and side-scatter.

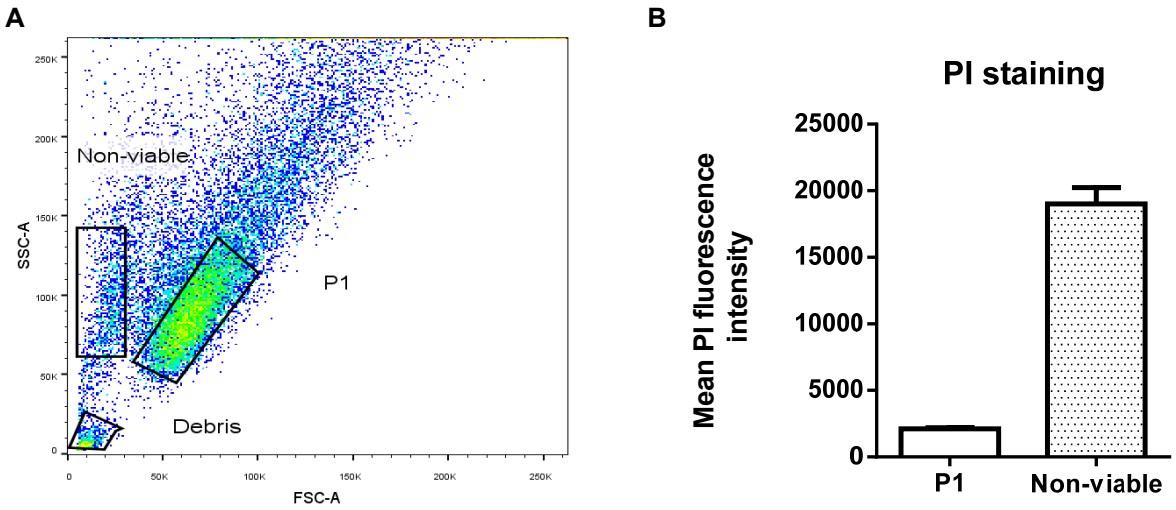

Figure 2-3. (A) Representative scatter plot of MDCKII cells showing P1 viable cell gating. Non-viable cells and subcellular debris are also indicated. **(B)** Propidium iodide (PI) staining of the P1 and non-viable populations. Mean ± standard error of N=3 independent experiments. Mean fluorescence represents 5000 cell events. Y-axis is the mean PI fluorescence intensity.

Doublet exclusion

To ensure fluorescence intensity was measured from single cells only, doublets were gated out using the doublet exclusion method (Wersto et al., 2001). Forward scatter area vs. height signal (FSC-A vs FSC-H) and side scatter area vs. height (SSC-A vs SSC-H) were used. The area of the pulse signal for either forward scatter or side scatter increases proportionally to signal height in single cells. From the viable population P1 (Figure 2-4A), an FSC-A vs. FSC-H plot was made and a gate was constructed in the cell population with proportional area vs. height increase (Figure 2-4B). This population was designated P2. From P2 the same process was repeated using SSC-A vs SSC-H to isolate the P3 population. Thus, this population was composed only of single cells (Figure 2-4C).

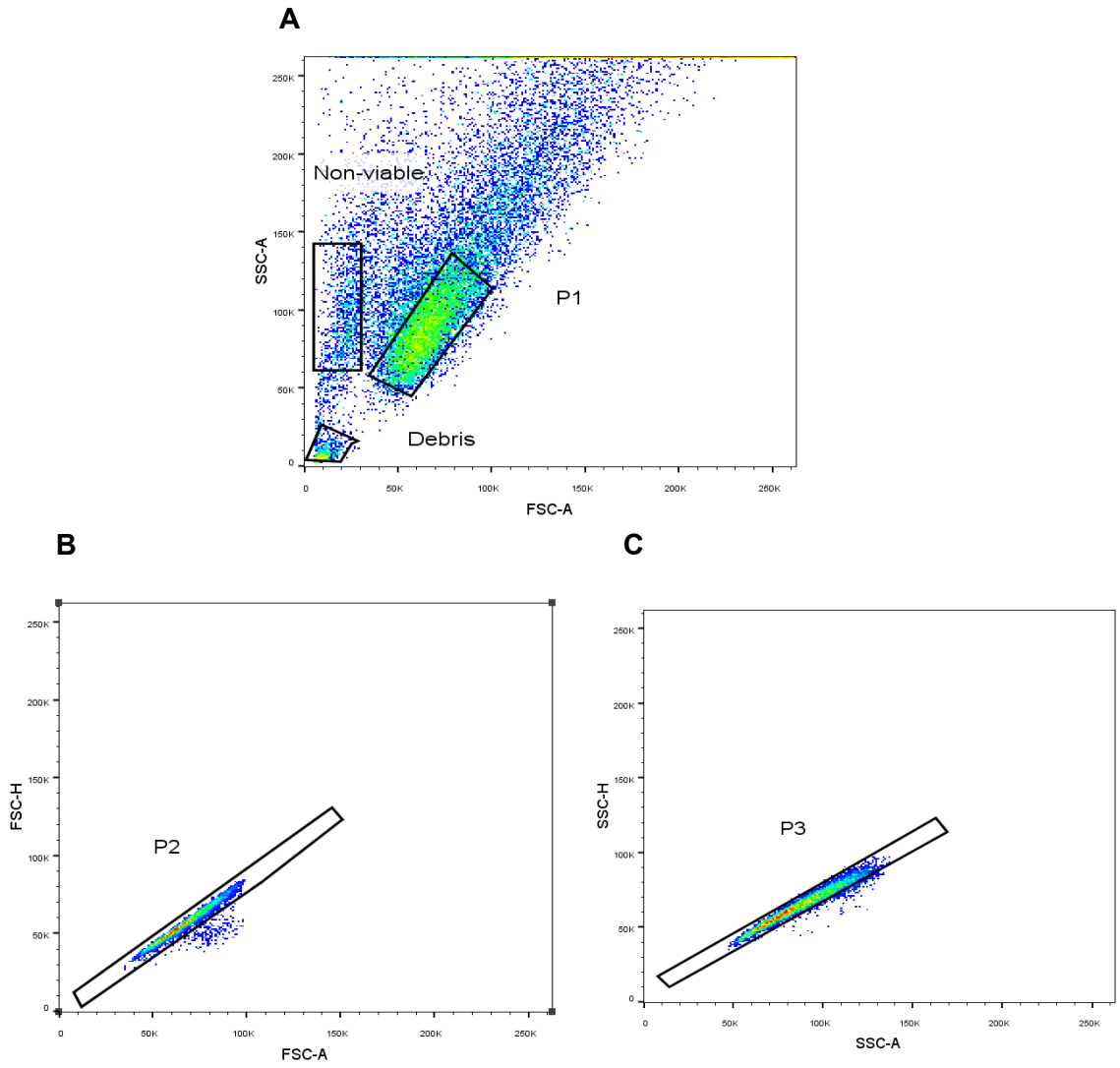

Figure 2-4. Doublet exclusion method **(A)** Scatter plot of MDCKII cells showing the viable population (P1). **(B)** FSC-A vs FSC-H of P1. A new gate P2 was constructed for cells with proportional area vs height signal increase. **(C)** SSC-A vs SSC-H of the P2 population. A new gate P3 represents the single cell population within viable cells (P1).

Data analysis

For all samples, mean fluorescence was measured only in the P3 single, viable cell population from 5000 cellular events. The flow cytometer channels used were FITC (fluorescein isothiocyanate) for rhodamine-123, calcein-AM and BCECF-AM. The APC (allophycocyanin) channel was used for mitoxantrone. The FITC channel uses 488 nm excitation and a bandpass emission filter 530 ± 30 nm. The APC channel uses 633 nm excitation and bandpass emission filter 660 ± 20 nm.

For the steady-state accumulation assay, fluorescence data was presented as a percentage (Y) of the maximum fluorescence observed for each experiment (Equation 2-1).

$$Y = \left(\frac{SF - BF}{MF - BF}\right) \times 100\% \qquad \textbf{Equation 2-1}$$

Where SF = sample fluorescence, MF = maximum fluorescence and BF is background fluorescence (fluorescence from cells + DMSO-only controls).

In inhibition studies with positive controls (Section 2.3.2), mean fluorescence values were presented for substrates and the cell line pairs tested. Values were background substracted using cells + DMSO-only controls.

For the flow cytometry screening assay, Equation 2-2 was used to determine the extent of transport inhibition (Y) by each analogue, expressed as a percentage of the net fluorescence increase of transfected cells + fluorescent substrate + positive controls (100% inhibition). Mean fluorescence in transfected cells + fluorescent substrate + DMSO-only samples were therefore set as 0% inhibition.

$$Y = \left(\frac{A - C}{B - C}\right) \times 100\% \qquad \textbf{Equation 2-2}$$

Where A = (Fluorescence in transfected cells + substrate + test compound). B = (Fluorescence in transfected cells + substrate + positive control). C = (Fluorescence in transfected cells + substrate + DMSO-only). Subtraction of C from A and B takes into account background fluorescence.

Intrinsic fluorescence

HEK293 or MDCKII transfected cells were incubated with 20 μM of the analogues alone without addition of fluorescent probe (Section 2.2.5.2). The same protocol was then followed as with the inhibitor screening studies (Section 2.2.5.3). Data are presented as mean fluorescence values without normalisation. Mean fluorescence of DMSO-only controls and transfected cells incubated with fluorescent substrate were included for comparison.

The intrinsic fluorescence of the identified inhibitors from the screening assays were also determined using a Spectramax fluorescence plate reader (Molecular Devices, Sunnyvale, CA). The analogues (listed in Table 2-6) were added to unsupplemented phenol-red free DMEM at a

final concentration of 20 µM. These were aliquoted to opaque 96-well plates at 200 µl/well in triplicate and fluorescence scanned at 488 nm excitation and 530/20 nm emission at room temperature, corresponding to the excitation/emission wavelengths of the FITC channel of the BD LSRII flow cytometer. DMEM with 2.5 µM rhodamine-123 was used as positive control with DMSO-only DMEM as blank. Analogues were also scanned at 630 nm excitation and 660 nm emission wavelengths, corresponding to the APC channel used in the mitoxantrone accumulation assays. DMEM with 5 µM mitoxantrone was used as positive control.

Table 2-6. Analogues tested for intrinsic fluorescence using a fluorescence spectrometer

Fluorescence channel	Curcumin analogues
FITC	A12, A13, B11, C10, RL92
APC	A12, A13, B11, RL92

2.2.6 Structure-activity studies

BCRP inhibition has been previously correlated with the octanol-water distribution coefficient $LogD_{7.4}$, and molecular polarisability (Matsson et al., 2007). Both parameters were calculated for all analogues using the Marvin chemistry suite (ChemAxon, Cambridge, MA). The product of $cLogD_{7.4}$ and molecular polarisability were then calculated for each analogue. A non-parametric Spearman correlation was conducted against the ranks of [$cLogD_{7.4}$ * polarizability] and BCRP inhibition [% inhibition of maximum] for the analogue series. A rank correlation was carried out using Graphpad Prism 6 software (Graphpad software, La Jolla, CA). Values for $cLogD_{7.4}$, polarisability and BCRP inhibition can be found in Appendix I, Table A-1. Protonation calculations at physiological pH were also conducted using the Marvin software.

2.2.7 Statistical analysis and IC_{50} calculation

All curve-fitting, IC_{50} determinations and statistical analysis were carried out using Graphpad Prism 6 software. All results were from at least 3 independent experiments unless otherwise stated. Data are presented as mean ± standard error (SE). Multiple comparisons between control and different treatment groups were done using one-way analysis of variance (ANOVA) with Dunnett's post-hoc test. A p-value <0.05 was considered significant.

For steady-state accumulation studies, a one-phase exponential accumulation curve was fitted to the data using Equation 2-1 (see Figure 2-5). Time to steady-state was the first time-point in the plateau phase of the curve.

For IC_{50} calculations, normalised mean fluorescence values from three independent experiments were obtained (The best-fit non-linear regression curve of Log (inhibitor concentration) vs. normalised fluorescence was defined by the equation:

$$Y = \frac{100}{\{1 + 10\text{^}[(\text{LogIC50} - X) * \text{Hill Slope}]\}} \qquad \textbf{Equation 2-3}$$

The IC_{50} is the X-value at Y = 50 and represents the absolute IC_{50}, i.e., the concentration of analogue which causes 50% of the inhibition compared to positive control (defined as complete inhibition). This is in contrast to the relative IC_{50} which calculates the midway point between minimum and maximum response of a compound. Since the maximum response of some analogues may be lower than the complete inhibition observed with positive controls, relative and absolute IC_{50} will differ. In all cases, absolute IC_{50} values are presented.

2.3 Results

2.3.1 Assay optimisation

2.3.1.1 Steady-state accumulation of fluorescent probes

Accumulation studies were conducted to determine the time to reach steady-state for each fluorescent probe in the cell lines tested. These time points were used in subsequent screening studies. The studies also helped confirm transport activity in transfected cells and indicated that probe concentrations were not saturating transporter efflux.

The accumulation studies indicated that rhodamine-123 reached steady-state in parental and MDCKII/P-gp cells after 75 min (Figure 2-5A). Accumulation of rhodamine-123 was 3.5-fold lower in MDCKII/P-gp cells compared to the parental cells. For mitoxantrone, accumulation reached steady-state after 120 min in both parental and MDCKII/BCRP cells (Figure 2-5B). MDCKII/BCRP had 3.2-fold lower fluorescence at steady-state than MDCKII/P cells. Mitoxantrone accumulation was also determined in HEK cells (Figure 2-5C). A faster time to steady-state of 60 min was observed compared to MDCKII. HEK/BCRP cells accumulated 1.9-fold lower mitoxantrone compared to HEK/P cells.

Calcein (the hydrolysed fluorescent form of calcein-AM), accumulated rapidly in HEK/P and HEK/MRP1 cells, reaching steady-state after 30 min (Figure 2-5D). HEK/MRP1 accumulated considerably less probe (8.9-fold) compared to parental cells. For BCECF, steady-state was reached after 15 min in both parental and MRP5 transfected cells (Figure 2-5E). Transfected cells accumulated 3.8-fold lower BCECF than parental cells. For all the fluorescent substrates tested, no significant increase in the proportion of non-viable cells (or a decrease in viable cells) was observed at the longest time points (determined using the P1 viability gate, see Section 2.2.5.4).

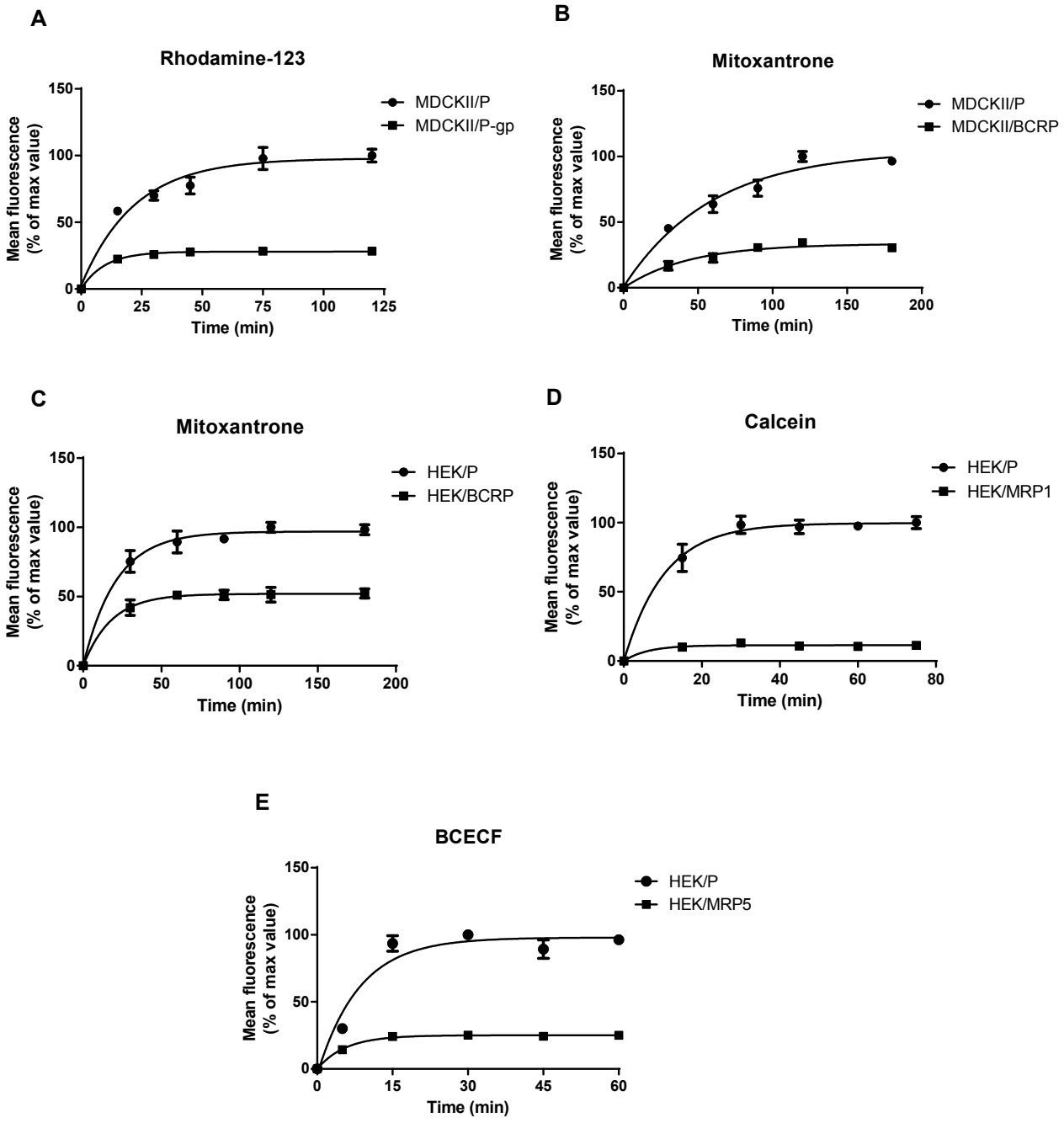

Figure 2-5. Time course of the accumulation of fluorescent probes: 2.5 µM rhodamine-123 (**A**), 5 µM mitoxantrone (**B,C**), 0.1 µM calcein (**D**), and 0.25 µM BCECF (**E**) in parental (●) and ABC-transporter overexpressing cells (■). Data presented are mean fluorescence expressed as % of the maximum value observed in the samples. Results are mean ± standard error of n = 2 independent experiments in duplicates.

2.3.1.2 Complete inhibition of transport activity by positive controls

The positive control concentrations needed to completely inhibit the efflux activity of ABC transporters were determined. These were identified as the ability to restore intracellular accumulation of fluorescent probe in transfected cells to similar levels as the parental cells. These concentrations were subsequently used in the screening studies to represent 100% inhibition of transport activity.

Results showed that MDCKII/P-gp cells accumulated significantly lower (5.8-fold, $p < 0.001$) rhodamine-123 than DMSO treated MDCKII/P control cells (Figure 2-6A). Co-incubation with 25 μM verapamil completely restored intracellular fluorescence in transfected cells to similar values as parental cells. No increased inhibition was seen with a higher verapamil concentration of 50 μM. Higher mean fluorescence was observed in the verapamil treated cells than parental cells but the differences were not statistically significant. Thus, verapamil at 25 μM was used in the flow cytometry screening studies.

In Figure 2-6B, Ko143 at 5 μM completely eliminated the 4.5-fold difference in mitoxantrone accumulation between MDCKII/P and MDCKII/BCRP. Increasing Ko143 concentrations to 10 μM did not further increase mitoxantrone fluorescence. Ko143 at 5 μM also restored the intracellular fluorescence of mitoxantrone in HEK/BCRP cells to similar values as HEK/P cells (Figure 2-6C). For both cell types, 5 μM Ko143 was used as positive control in subsequent experiments. Similar to observations in the steady-state accumulation study (Section 2.3.1.1), the difference in mitoxantrone fluorescence between parental and transfected cells was lower in HEK (2.5-fold) than MDCKII (4.5-fold).

In HEK/MRP1 cells, a 3.9-fold lower accumulation of calcein was observed compared to HEK/P (Figure 2-6D). Co-incubation of 45 μM MK-571 with HEK/MRP1 completely restored intracellular fluorescence to parental values. Increasing the concentration to 60 μM did not cause a further increase in calcein fluorescence. For HEK/MRP5 cells, BCECF accumulated 9.6-fold lower than in HEK/P (Figure 2-6E). Co-incubation with 45 μM MK-571 significantly increased ($p < 0.001$) BCECF fluorescence in HEK/MRP5 cells but did not restore fluorescence to parental values. This was only observed with 60 μM MK-571. For both HEK/MRP1 and HEK/MRP5, 60 μM MK-571 was used as the positive control.

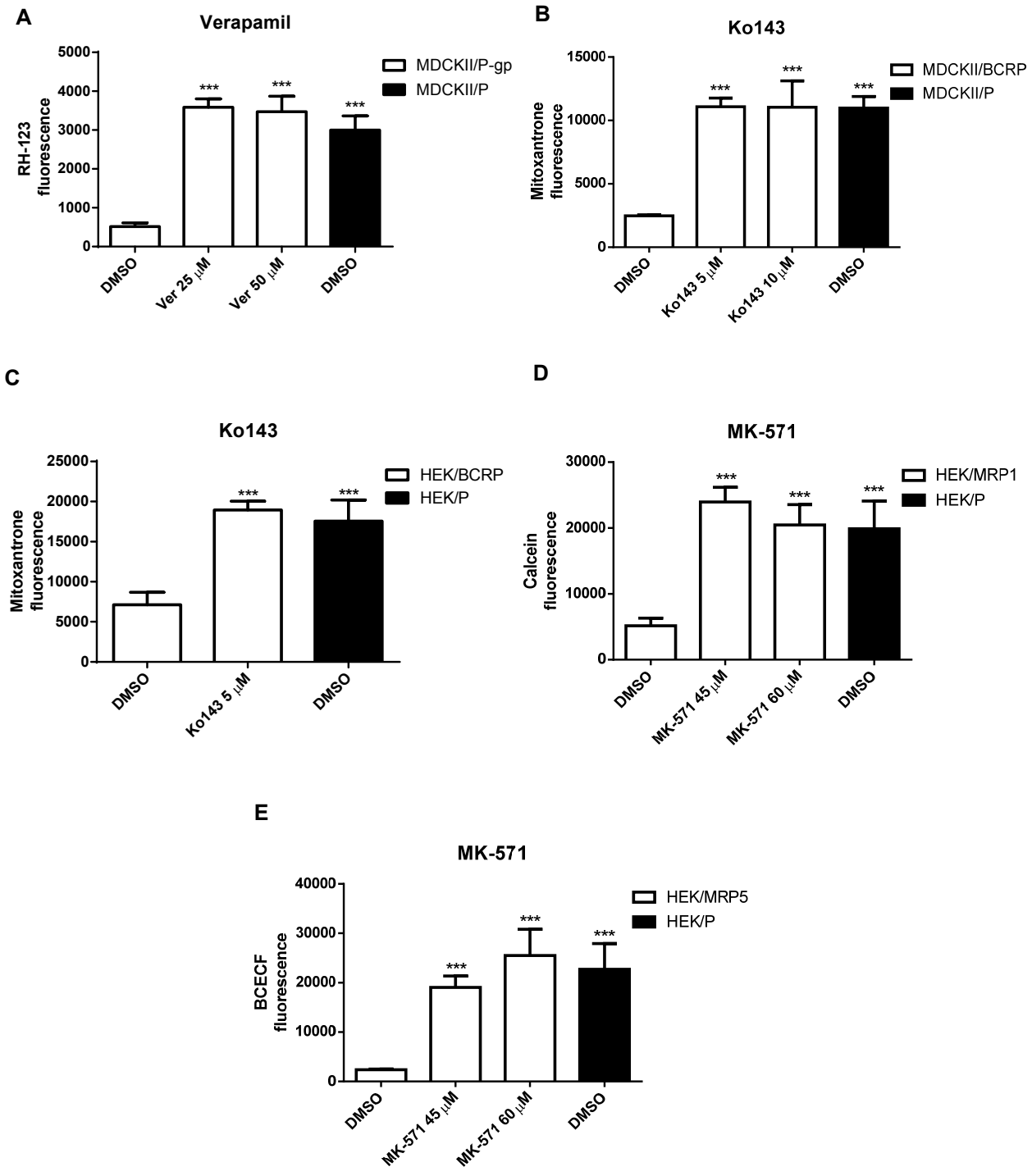

Figure 2-6. Intracellular fluorescence of ABC transporter substrates at steady-state in parental cells (■) co-incubated with DMSO only and transfected cells (□) co-incubated with DMSO or positive control. Verapamil (Ver) (**A**), Ko143 (**B,C**) and MK-571 (**D,E**) were used as positive controls. Cell lines are indicated in the figures. Results are presented as mean ± standard error of fluorescence values subtracted by background (cells + DMSO only without substrate). n ≥ 3 independent experiments. ***p<0.001 significantly different from the control group (DMSO-only transfected cells) using one-way ANOVA. Dunnett's post-hoc test was used to compare means of each treatment against the control group. RH-123 – rhodamine-123.

2.3.2 Flow cytometry screening

2.3.2.1 Inhibition of P-gp by curcumin analogues

Analogue screening

After assay optimisation, all 24 analogues and curcumin were tested at 20 μM for inhibition of rhodamine-123 efflux in MDCKII/P-gp cells. In Figure 2-7, 8 out of 24 analogues significantly inhibited ($p < 0.001$) P-gp activity, observed as an increase in rhodamine-123 accumulation. Inhibition was observed for A, B, C and E-series analogues, as well as the new investigational compound RL92.

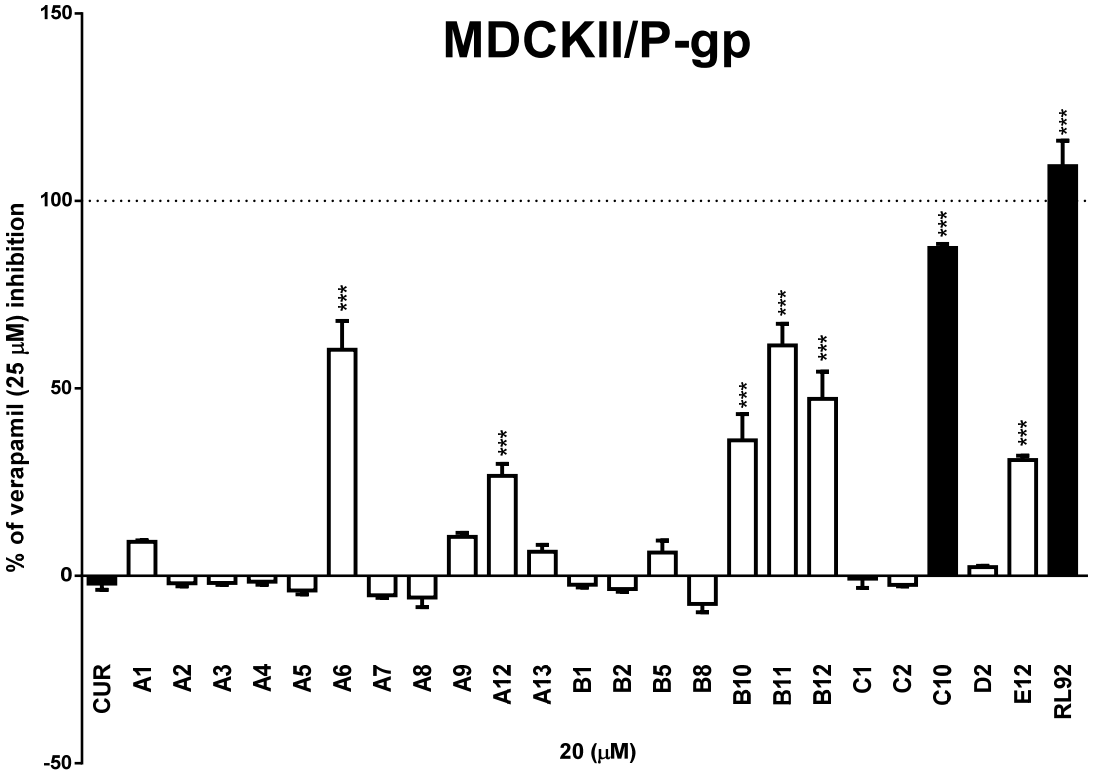

Figure 2-7. Inhibition of rhodamine-123 (2.5 μM) efflux in MDCKII/P-gp cells by curcumin and cyclohexanone analogues. Data are presented as a percentage of the inhibition by 25 μM verapamil (100% inhibition). Results are mean ± standard error of n ≥ 3 independent experiments. CUR – curcumin. ***p<0.001 significantly different from the control group (cells incubated with substrate and DMSO-only (0% baseline)), calculated using one-way ANOVA and Dunnett's post-hoc test. Solid columns represent analogues further studied for potency and for effects on parental cells. Representative fluorescence histograms for C10 and RL92 can be found in Appendix II.

For the A-series analogues, A6 and A12 (which have pyrrole and dimethoxylated phenyl rings, respectively) caused partial but significant ($p < 0.001$) increase in rhodamine-123 accumulation. For the B-series analogues, only the compounds with methoxylated phenyl rings (B10, B11, B12) significantly inhibited P-gp ($p < 0.001$). Of the C-series analogues, the trimethoxyphenyl-carrying C10 inhibited P-gp to a similar extent as 25 μM verapamil (see Figure 2-8 for C10 structure). The analogue E12 with dimethoxylated substituents also significantly inhibited P-gp ($p < 0.001$), as did RL92, with the latter completely inhibiting rhodamine-123 efflux. In contrast, curcumin did not significantly affect rhodamine-123 efflux. As C10 and RL92 were the best inhibitors in the series, their potency was investigated in concentration-response studies.

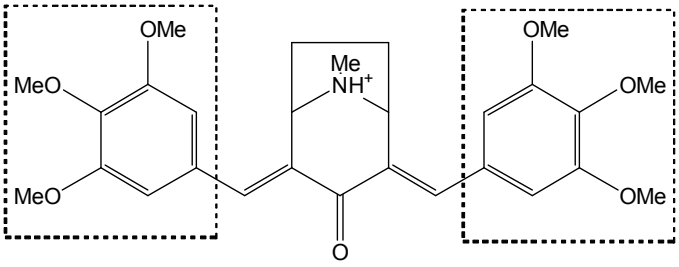

C10

Figure 2-8. The structure of C10 with the trimethoxyphenyl groups bounded by boxes and the tertiary nitrogen depicted in the protonated state.

Concentration-dependent P-gp inhibition and potency of C10 and RL92

To show concentration-dependent inhibition and determine the potency of C10 and RL92 (IC_{50} value), the % of P-gp inhibition was plotted against the Log concentration of each analogue and a non-linear regression curve was fitted to the data. For comparison, the potency of curcumin was also determined. Figure 2-9 shows concentration-dependent inhibition of rhodamine-123 efflux in MDCKII/P-gp cells by C10, RL92 and curcumin. The regression curve for C10 follows the single-site binding model with a Hill slope close to 1 (Hill slope of 1.4) (Figure 2-9A). Complete inhibition of rhodamine-123 efflux was observed at the highest concentration of 20 μM ($10^{-4.7}$ M) and the curve plateaued at 100% of verapamil inhibition. A steeper regression curve was seen for RL92 with a Hill slope >1 (Hill slope of 3.0) (Figure 2-9B). The curve was not found to plateau at the concentration range used, although the highest concentration of RL92 (20 μM) completely inhibited efflux.

For curcumin, a very steep regression curve with a Hill slope of 10.5 was seen (Figure 2-9C). Curcumin could only partially inhibit rhodamine-123 efflux as the regression curve plateaued at ~70% inhibition at a concentration of 60 μM ($10^{-4.2}$ M). Higher concentrations of 80 μM ($10^{-4.1}$ M) and 100 μM ($10^{-4.0}$ M) did not show any further increase in effect.

The IC_{50} values calculated from the regression curves indicated that C10 was 18-fold more potent (IC_{50} of 2.8 ± 0.4 μM vs. 50.5 ± 4.7 μM) and RL92 6-fold more potent (IC_{50} of 8.7 ± 0.8 μM vs. 50.5 ± 4.7 μM) as P-gp inhibitors compared to curcumin (Table 2-7).

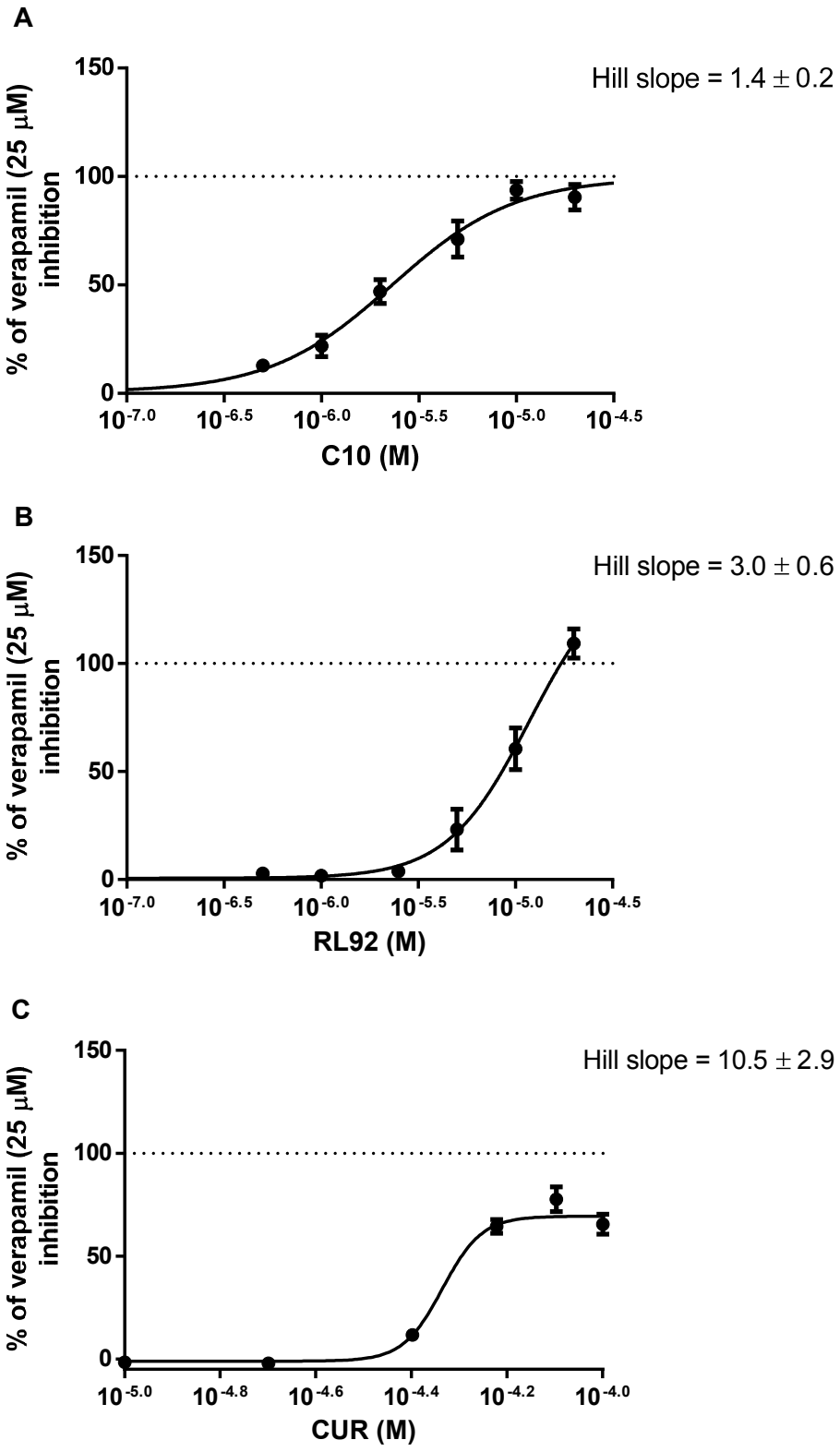

Figure 2-9. Log concentration-response curves of rhodamine-123 (2.5 μM) efflux inhibition by C10 (**A**), RL92 (**B**) and curcumin (CUR) (**C**) in MDCKII/P-gp cells. Data are presented as % of the inhibition produced by 25 μM verapamil (100% inhibition). Results are mean ± standard error of n ≥ 3 independent experiments. Non-linear regression fit of the data was done using Graphpad prism 6.0. The calculated IC_{50} values from the curve fit are presented in Table 2-7. The Hill slope ± standard error of each curve is indicated.

Table 2-7. IC_{50} values of curcumin, C10 and RL92 in inhibiting rhodamine-123 efflux by MDCKII/P-gp cells.

Compound	IC_{50} ± SE[a] (μM)
Curcumin	50.5 ± 4.7
C10	2.8 ± 0.4***
RL92	8.7 ± 0.8***

[a] Mean ± standard error of 3 independent experiments.***p<0.001 significantly different from curcumin IC_{50} calculated using one-way ANOVA and Dunnett's post-hoc test.

Effects on parental cells

To demonstrate that the increased intracellular rhodamine-123 accumulation caused by C10, RL92, curcumin and verapamil was via a P-gp-mediated mechanism, their effects on rhodamine-123 accumulation in parental cells was determined.

Figure 2-10 shows that C10, RL92 and verapamil (at concentrations that significantly increased rhodamine-123 accumulation several-fold in transfected cells) also increased rhodamine-123 accumulation in parental cells but not significantly. In contrast, 80 μM curcumin significantly increased rhodamine-123 accumulation ($p < 0.05$), suggesting the involvement of non-P-gp mediated mechanisms. Fluorescence was increased an average of 63% of the DMSO-only controls. However, the effect on parental cells was considerably less than the 400-500% increase in rhodamine-123 accumulation observed in MDCKII/P-gp cells with curcumin co-incubation.

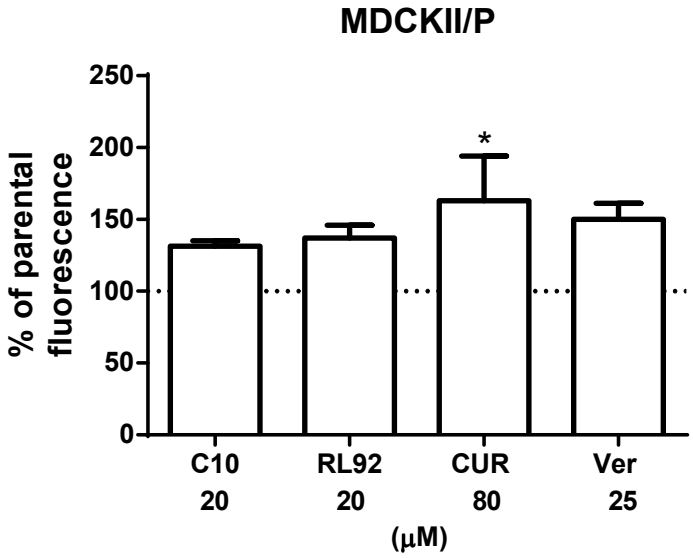

Figure 2-10. Effects of C10, RL92, curcumin (CUR) and verapamil (Ver) on the intracellular accumulation of rhodamine-123 (2.5 μM) in MDCKII/P cells. Concentrations used were previously shown to inhibit rhodamine-123 efflux in transfected cells (Figure 2-9). Data are presented as a % of the mean fluorescence in MDCKII/P cells treated with substrate and DMSO-only (100%). Results are mean ± standard error of n = 3 independent experiments. *$p<0.05$ significantly different from the control group (MDCKII/P + substrate + DMSO (100% fluorescence)), calculated using one-way ANOVA and Dunnett's post-hoc test.

2.3.2.2 Inhibition of BCRP by curcumin analogues

Analogue screening

In the BCRP inhibition screening assay (Figure 2-11), 13 of the 24 analogues significantly increased mitoxantrone accumulation ($p < 0.01$). Four of these analogues (A12, A13, B11 and RL92) increased mitoxantrone accumulation to a similar extent as the positive control (Ko143) and were further studied for potency and effects on parental cells (see Figure 2-12 for structures). BCRP inhibition was not limited to a specific core backbone, as compounds from the A, B, C and E series all showed significant inhibition. All analogues with methoxylated phenyl rings (A12, A13, B10, B11, B12, C10 and E12) significantly inhibited mitoxantrone efflux ($p < 0.001$). Analogues with sulfur-containing thiophene rings (A5), pyrrole (A6), imidazole (A7) and indole (A9) substituents also inhibited transport. Curcumin significantly increased mitoxantrone accumulation ($p < 0.001$) but was less effective than the analogues and Ko143. Ten of the analogues (A7, A9, A12, A13, B10, B11, B12, C10, E12, RL92) had equal or greater inhibition of mitoxantrone efflux compared to curcumin. Although BCRP inhibition was not associated with a specific core backbone or aromatic substituent, it significantly correlated with the molecular polarisability and lipophilicity of the analogues. A significant Spearman correlation coefficient of 0.8 ($p < 0.00001$) was observed when the ranks of the product of the distribution coefficient and polarisability [$cLogD_{7.4}$ * polarisability] of the analogues were plotted against the ranks of the analogues for inhibiting BCRP (Figure 2-13). It was found that the most lipophilic and polarisable compounds also best inhibited mitoxantrone transport.

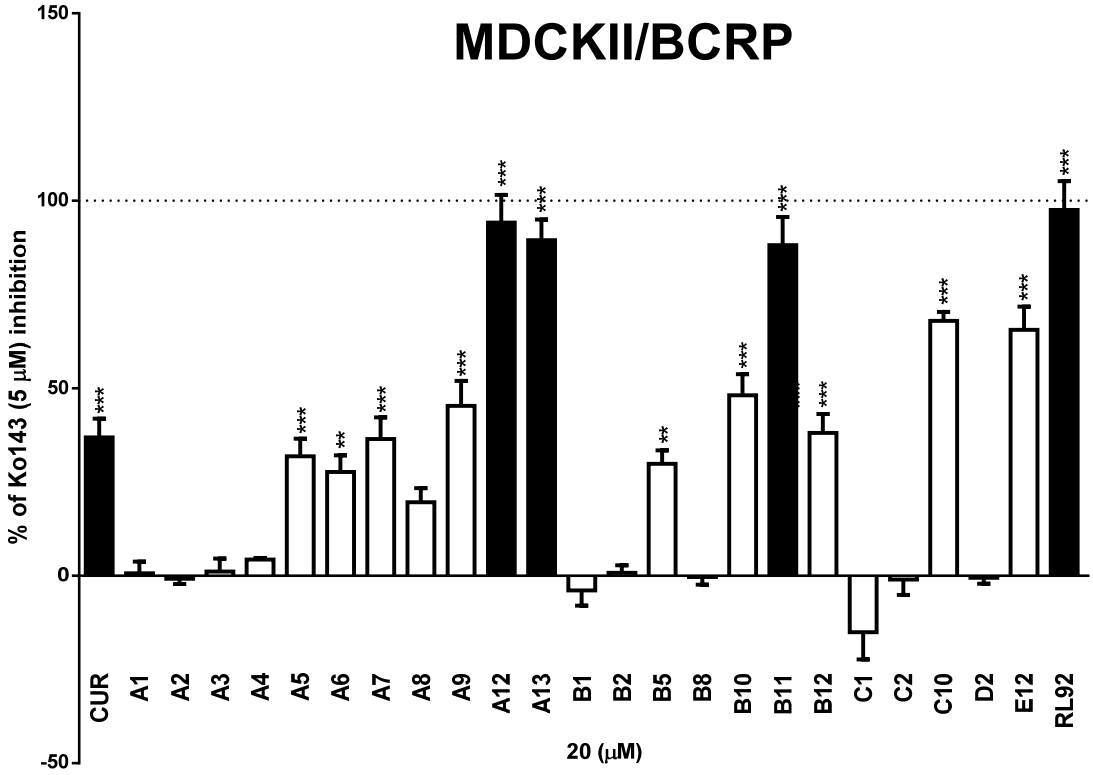

Figure 2-11. Inhibition of mitoxantrone (5 μM) efflux in MDCKII/BCRP cells by curcumin and 24 cyclohexanone analogues. Data are presented as a percentage of the inhibition by 5 μM Ko143 (100% inhibition). Results are mean ± standard error of n ≥ 3 independent experiments. **p<0.01, ***p<0.001 significantly different from the control group (cells incubated with substrate and DMSO only (0% baseline)), calculated using one-way ANOVA and Dunnett's post-hoc test. Solid columns represent analogues further studied for potency and for effects on parental cells. CUR – curcumin. Representative fluorescence histograms for A12, A13, B11 and RL92 can be found in Appendix II.

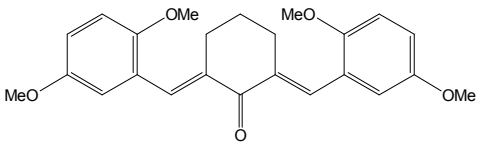

A12

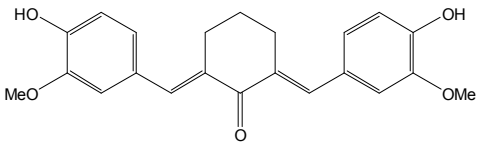

A13

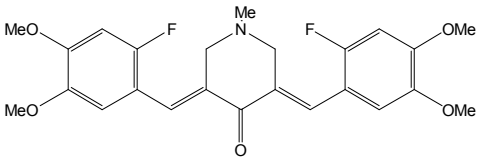

B11

Figure 2-12. Structures of A12, A13 and B11.

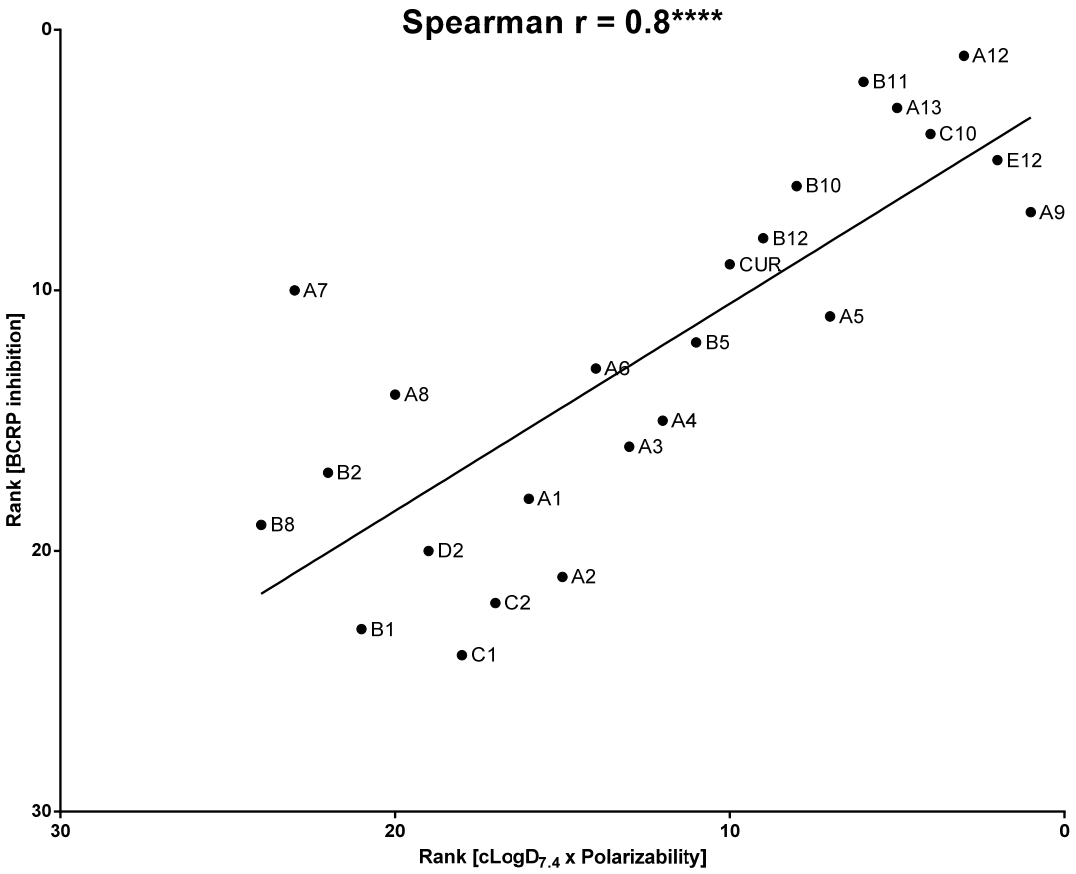

Figure 2-13. Correlation of lipophilicity * polarisability of curcumin analogues with inhibition of BCRP-mediated mitoxantrone transport. The analogues were ranked on the extent of BCRP inhibition at 20 µM from the flow cytometry screening assay and from the product of their $cLogD_{7.4}$ and polarisability. The ranks were plotted on the y- and x-axis respectively. BCRP inhibition decreases from top to bottom and lipophilicity/polarisability increases from left to right. The Spearman non-parametric rank correlation coefficient was calculated using Graphpad prism 6 sofware and corresponds to the slope of the linear regression line. (**** = $p<0.0001$). Calculated $LogD_{7.4}$ and polarisability values for each analogue can be found in Appendix I, Table A-1.

Concentration-dependent BCRP inhibition and potency of A12, A13, B11 and RL92

Concentration-dependent inhibition and potency of the best BCRP inhibitors (A12, A13, B11 and RL92) were determined using non-linear regression curve fits of the Log concentration-response data from MDCKII/BCRP cells (Figure 2-14). Concentration-response curves of A12, A13 and curcumin were also determined in HEK/BCRP cells as previous studies of curcumin transporter interactions were conducted in this cell line (Chearwae et al., 2006a). Figure 2-14A shows clear concentration-dependent inhibition of mitoxantrone efflux by A12 in both MDCKII/BCRP and HEK/BCRP. The response-curves were identical in both cell lines with Hill slopes close to 1.0. The regression curve plateaued at 100% of Ko143 inhibition with complete inhibition of mitoxantrone efflux at the highest concentration. The potency of A12 was similar in both cell lines with calculated IC_{50}s of 1.2 ± 0.1 μM in MDCKII/BCRP and 1.1 ± 0.1 μM in HEK/BCRP (Table 2-8). In Figure 2-14B, a clear concentration-dependent effect was also seen for A13. The regression curves of A13 differed between MDCKII/BCRP and HEK/BCRP cells, with greater potency observed in HEK/BCRP cells. The calculated IC_{50} in HEK/BCRP was 5.4-fold lower (0.8 ± 0.1 μM) than in MDCKII/BCRP (4.3 ± 0.7 μM) (Table 2-8). The regression curves of A13 in both cell lines reached a plateau at 100% inhibition in HEK/BCRP; while slightly less than maximal inhibition was observed with MDCKII/BCRP.

Greater inhibitory potency in HEK/BCRP than in MDCKII/BCRP was also observed with increasing concentrations of curcumin (Figure 2-14C). The calculated IC_{50} in HEK/BCRP cells was 13.9-fold less than in MDCKII/BCRP (2.3 ± 0.5 μM vs. 32.0 ± 4.2 μM) (Table 2-8). Neither regression curves were found to plateau at the concentration range used (1 μM – 60 μM or $10^{-6.0}$ M – $10^{-4.2}$ M) (Figure 2-14C). Curcumin at 60 μM increased mitoxantrone accumulation in HEK/BCRP 76% higher than co-incubation with 5 μM Ko143; the latter representing complete inhibition of BCRP-mediated mitoxantrone efflux. This effect was not observed in MDCKII/BCRP cells. For both B11 and RL92, clear concentration-dependent inhibition of mitoxantrone efflux was observed in MDCKII/BCRP cells (Figure 2-14D & E) . The regression curves for both analogues did not plateau at concentrations from 0.1 μM to 20 μM ($10^{-7.0}$ – $10^{-4.7}$), although similar inhibition to Ko143 was achieved at the highest concentrations used.

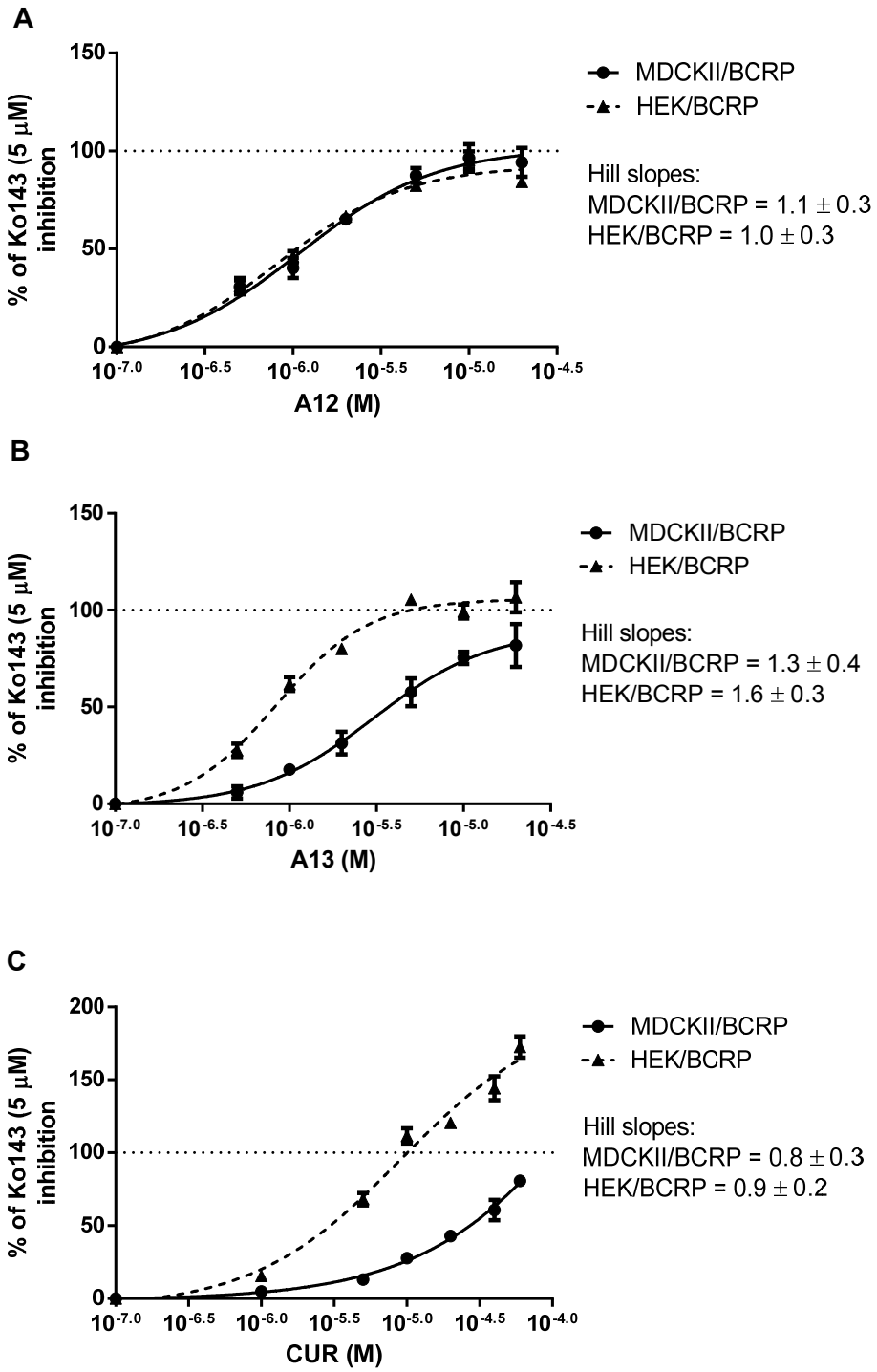
A
% of Ko143 (5 μM) inhibition
150
100
50
0
10-7.0
10-6.5
10-6.0
10-5.5
10-5.0
10-4.5
A12 (M)
MDCKII/BCRP
HEK/BCRP
Hill slopes:
MDCKII/BCRP = 1.1 ± 0.3
HEK/BCRP = 1.0 ± 0.3
B
% of Ko143 (5 μM) inhibition
150
100
50
0
10-7.0
10-6.5
10-6.0
10-5.5
10-5.0
10-4.5
A13 (M)
MDCKII/BCRP
HEK/BCRP
Hill slopes:
MDCKII/BCRP = 1.3 ± 0.4
HEK/BCRP = 1.6 ± 0.3
C
% of Ko143 (5 μM) inhibition
200
150
100
50
0
10-7.0
10-6.5
10-6.0
10-5.5
10-5.0
10-4.5
10-4.0
CUR (M)
MDCKII/BCRP
HEK/BCRP
Hill slopes:
MDCKII/BCRP = 0.8 ± 0.3
HEK/BCRP = 0.9 ± 0.2

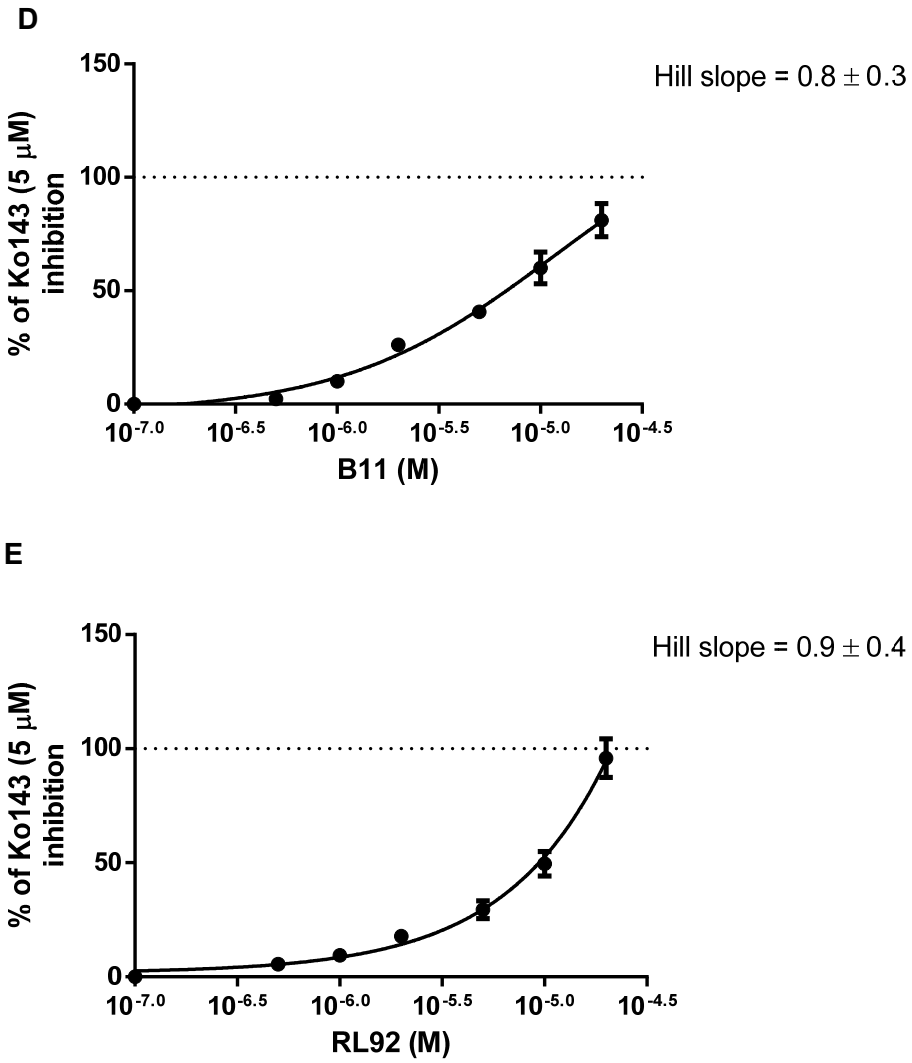

Figure 2-14. Log concentration-response curves of mitoxantrone (5 μM) efflux inhibition in MDCKII/BCRP (●) and HEK/BCRP (▲) cells by A12 (**A**), A13 (**B**), CUR (**C**), B11 (**D**) and RL92 (**E**). Data is presented as % of the inhibition produced by 5 μM Ko143 (complete inhibition). Results are mean ± standard error of n = 3 independent experiments. Non-linear regression fit of the data was done using Graphpad prism 6.0. The calculated IC_{50} values from the curve fit are presented in Table 2-8. The Hill slope ± standard error of each curve is indicated.

A summary of the calculated IC_{50} values are presented in Table 2-8. All four analogues tested (A12, A13, B11 and RL92) were significantly more potent than curcumin ($p < 0.001$) in MDCKII/BCRP. The order of potency was A12 > A13 > B11 > RL92 > curcumin. Compounds A12 and A13 were the most potent analogues, and had 27- and 7-fold lower IC_{50} than curcumin, respectively. B11 was 6-fold more potent (IC_{50} 5.2 ± 0.4 μM) while the least potent analogue, RL92, had a 3.3-fold lower IC_{50} (9.7 ± 0.8 μM) than curcumin (32.0 ± 4.2 μM).

In contrast to results in MDCKII/BCRP cells, no large potency differences were observed between A12, A13 and curcumin in HEK/BCRP cells (Table 2-8). A12 was found to be only 2.1-fold more potent than curcumin in HEK/BCRP cells, and the difference in IC_{50} values was not statistically significant (1.1 ± 0.1 μM vs. 2.3 ± 0.5 μM, respectively). A13 was significantly more potent than curcumin ($p < 0.05$) in HEK/BCRP but only had a 2.9-fold lower IC_{50} compared to a 7-fold difference in MDCKII/BCRP cells. As seen with the regression curves (Figure 2-14A–C), the lack of significant differences in IC_{50} values was due to the greatly improved potency of A13 and curcumin in HEK/BCRP, while the IC_{50} of A12 remained unchanged.

Table 2-8. IC_{50} values for curcumin and selected analogues in inhibiting mitoxantrone efflux by MDCKII/BCRP and HEK/BCRP cells.

Compound	**IC_{50} ± SE[a] (μM)**	
	MDCKII/BCRP	**HEK/BCRP**
Curcumin	32.0 ± 4.2	2.3 ± 0.5
A12	1.2 ± 0.1***	1.1 ± 0.1
A13	4.3 ± 0.7***	0.8 ± 0.1*
B11	5.2 ± 0.4***	n.d.
RL92	9.7 ± 0.8***	n.d.

[a] Mean ± standard error of n=3 independent experiments. n.d – not determined. *p<0.05, ***p<0.001 significantly different from the curcumin IC_{50} in each respective cell line, calculated using one-way ANOVA and Dunnett's post-hoc test.

Effects on parental cells

To rule out non-BCRP mediated factors, putative inhibitors were tested for effects on mitoxantrone accumulation in MDCKII/P and HEK/P cells (Figure 2-15). Concentrations of analogues, curcumin and Ko143 that significantly increased mitoxantrone accumulation in BCRP-transfected cells, failed to show significant effects in MDCKII parental cells (Figure 2-15A). In HEK/P cells, co-incubation with A12, A13 and Ko143 increased mean fluorescence but this was not statistically significant (Figure 2-15B). Only curcumin (40 μM), significantly increased mitoxantrone accumulation in HEK/P cells ($p < 0.05$).

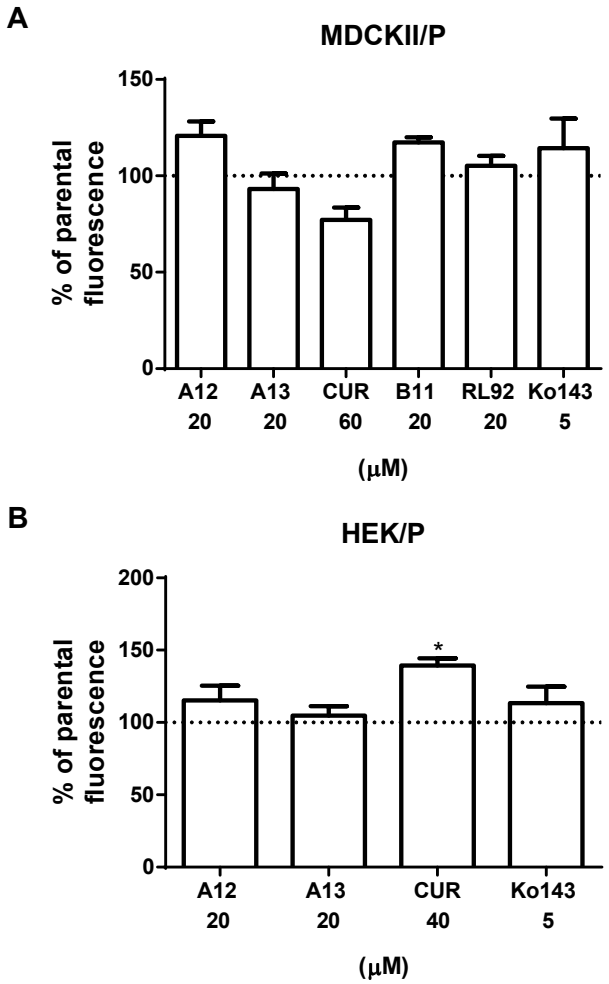

Figure 2-15. Effects of A12, A13, curcumin (CUR), B11, RL92 and Ko143 on the intracellular accumulation of mitoxantrone (5 μM) in MDCKII (**A**) and HEK293 parental cells (**B)**. Concentrations used were previously shown to inhibit mitoxantrone efflux in transfected cells (Figure 2-14). Data are presented as a % of the mean fluorescence in MDCKII/P (**A**) or HEK/P (**B**) cells treated with substrate and DMSO only (100%). Results are mean ± standard error of n = 3 independent experiments. *p<0.05 significantly different from the control group (HEK/P + substrate + DMSO (100% fluorescence)), calculated using one-way ANOVA and Dunnett's post-hoc test.

2.3.2.3 Inhibition of MRP1 & MRP5 by curcumin analogues

Analogue screening

MRP1 inhibitor screening indicated that 4 analogues (A13, RL92, B10 and C10) significantly increased calcein accumulation in HEK/MRP1 cells ($p < 0.001$) (Figure 2-16A). Two of the analogues (B10 and C10), both with trimethoxylated phenyl rings, showed only weak inhibition (<50% inhibition). The compound RL92 achieved greater inhibition but did not completely inhibit transport at 20 μM. Only analogue A13 completely inhibited calcein efflux, similar to that observed with MK-571. Curcumin (20 μM) also showed similar inhibition as 60 μM MK-571. Both curcumin and A13 were the only compounds tested with hydroxyl groups in the aromatic substituents (Figure 2-17).

From the screening study in HEK/MRP5 cells, four analogues (A5, A6, A13, RL92) significantly inhibited BCECF efflux, two of which (A5 and A6), showed only weak inhibition (<50%) (Figure 2-16B). Compounds A13 and RL92 showed similar inhibition to 60 μM MK-571, as was found with MRP1. Similarly, curcumin at 20 μM was able to completely inhibit BCECF efflux.

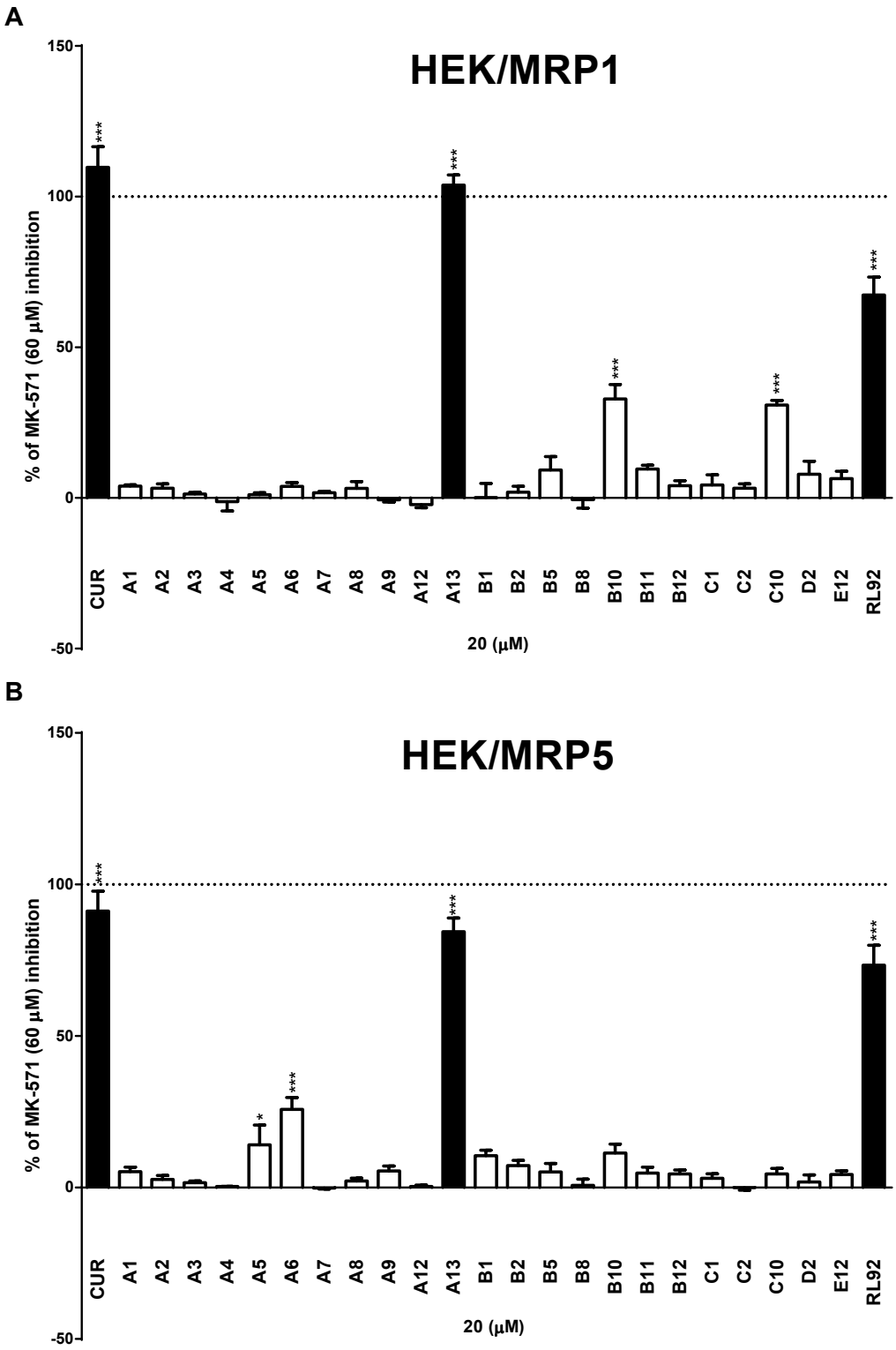

Figure 2-16. Inhibition of calcein (0.1 µM) and BCECF (0.25 µM) efflux in HEK/MRP1 (**A**) and HEK/MRP5 (**B**) cells respectively by curcumin and 24 cyclohexanone analogues. Data are presented as a percentage of the inhibition by 60 µM MK-571 (complete inhibition). Results are mean ± standard error of n ≥ 3 independent experiments. CUR – curcumin. *p<0.05, ***p<0.001 significantly different from the control group (cells incubated with substrate and DMSO-only (0% baseline)), calculated using one-way ANOVA and Dunnett's post-hoc test. Solid columns represent analogues further studied for potency and for effects on parental cells. Representative fluorescence histograms for A13 and RL92 can be found in Appendix II.

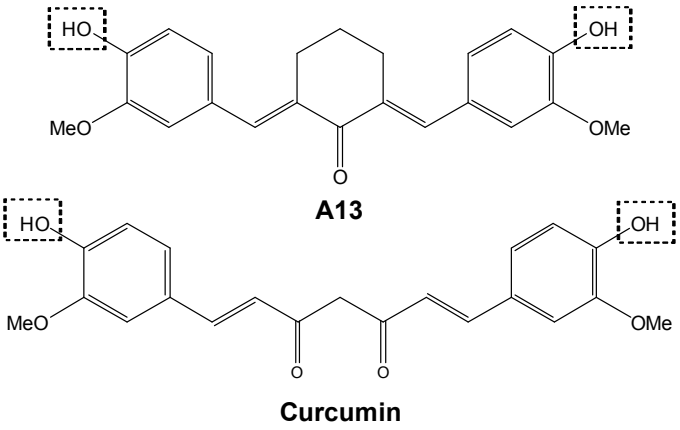

Figure 2-17. The structure of A13 and curcumin (keto form) with the 4'-hydroxyl groups bounded by boxes.

Concentration-dependent inhibition and potency of A13 and RL92 in HEK/MRP1 and HEK/MRP5

Concentration-dependent inhibition and potencies of the two analogues that showed complete inhibition in the MRP1 and MRP5 screening studies (A13, RL92), were determined using non-linear regression of the Log concentration-response data (Figure 2-18). A13 showed concentration-dependent inhibition of both MRP1 and MRP5 transport activity (Figure 2-18A). The regression curves increased sharply with a Hill slope >1 (5.1 and 3.5 for HEK/MRP1 and HEK/MRP5 respectively), indicative of cooperative rather than one-site binding to the transporters. Both curves plateaued at 100% of MK-571 inhibition, showing complete inhibition of transport at the highest concentrations used (40 μM or $10^{-4.4}$ M). Steep regression curves with Hill slopes >1 were also observed for MRP1 and MRP5 inhibition by RL92 (Hill slopes of 2.5 and 5.8 respectively) (Figure 2-18B). The RL92 regression curve plateaued at close to 100% inhibition in HEK/MRP5 cells while only partial inhibition (72%) was observed at the highest concentration of 40 μM ($10^{-4.4}$ M) in HEK/MRP1 cells. For curcumin, steep concentration-response curves were observed for MRP1 and MRP5 inhibition (Hill slopes of 12.0 and 7.2 respectively) suggesting cooperativity (Figure 2-18C). Curcumin completely inhibited transport activity of both transporters at the highest concentration of 40 μM.

The calculated IC_{50} values of the regression curves show that A13 was significantly more potent than curcumin at inhibiting HEK/MRP1 ($p < 0.01$) and HEK/MRP5 ($p < 0.05$) transport activity

(Table 2-9). The differences in IC_{50} values, however, were marginal, with A13 having a 1.4-fold lower IC_{50} at inhibiting both MRP1 and MRP5 (11.9 vs. 16.1 μM for MRP1; 11.7 vs 16.9 μM for MRP5) compared to curcumin. RL92 was 1.4-fold less potent than curcumin at inhibiting MRP1 (IC_{50} of 22.5 ± 2.7 μM vs. 16.1 ± 0.8μM for curcumin) but was equipotent at inhibiting MRP5.

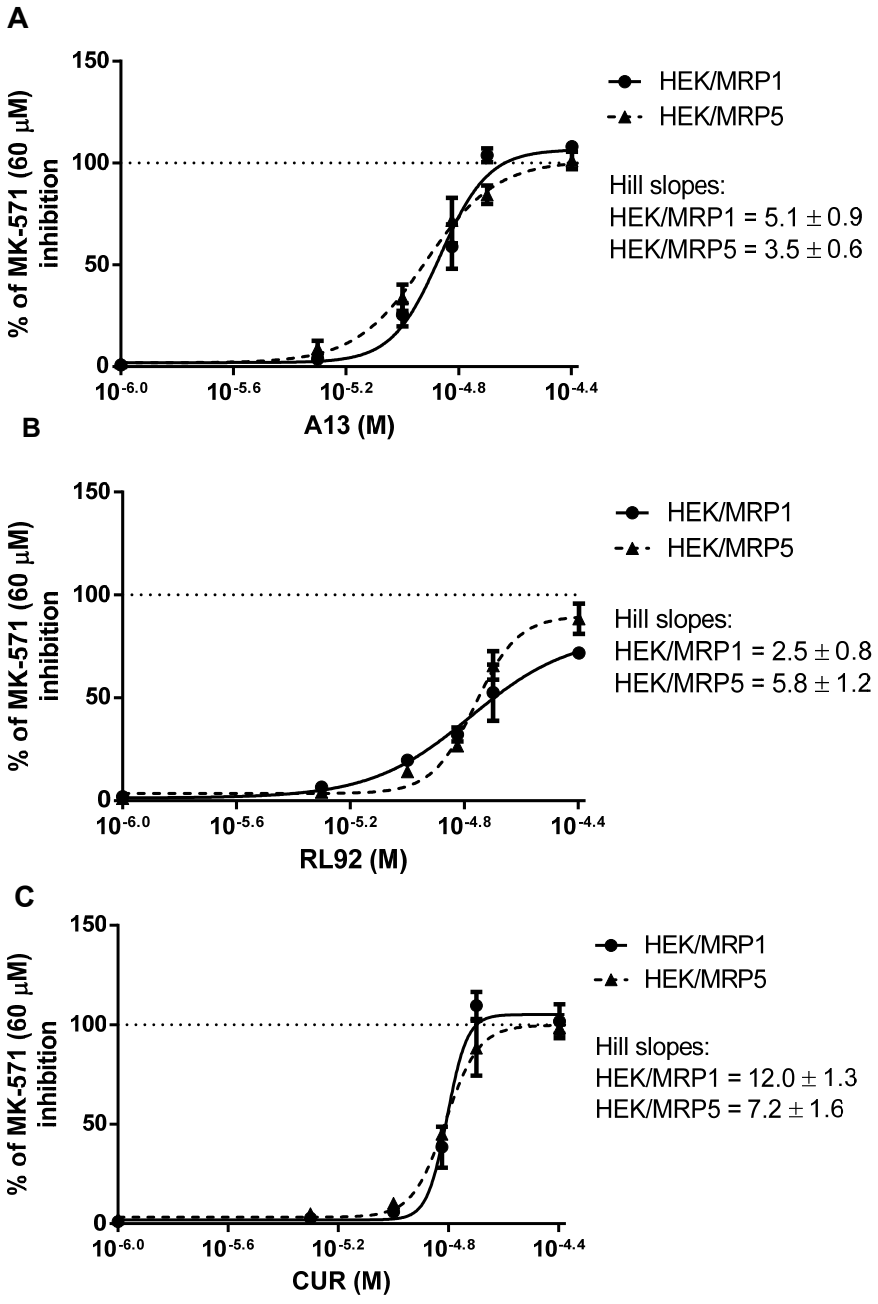

Figure 2-18. Log concentration-response curves of calcein (0.1 μM) and BCECF (0.25 μM) efflux inhibition in HEK/MRP1 (●) and HEK/MRP5 (▲) cells respectively by A13 (**A**), RL92 (**B**) and CUR (**C**). Data are presented as % of inhibition by 60 μM MK-571 (complete inhibition). Results are mean ± standard error of n = 3 independent experiments. Non-linear regression fit of the data was done using Graphpad prism 6.0. The calculated IC_{50} values from the curve fit are presented in Table 2-9. The Hill slope ± standard error of each curve is indicated.

Table 2-9. IC_{50} values of curcumin, A13 and RL92 in inhibiting calcein efflux by HEK/MRP1 and BCECF efflux by HEK/MRP5 cells.

Compound	IC_{50} ± SE[a] (μM)	
	HEK/MRP1	HEK/MRP5
Curcumin	16.1 ± 0.8	16.9 ± 0.9
A13	11.9 ± 0.7**	11.7 ± 1.3*
RL92	22.5 ± 2.7*	16.8 ± 1.8

[a] Mean ± standard error of n=3 independent experiments. *p<0.05, **p<0.01 significantly different from the curcumin IC_{50} in each respective cell line, calculated using one-way ANOVA and Dunnett's post-hoc test.

Effects on parental cells

Neither A13, RL92, curcumin, nor MK-571 significantly affected the intracellular accumulation of calcein or BCECF in HEK/P cells (Figure 2-19) using the highest concentrations from the concentration-response studies (Figure 2-18). RL92 slightly decreased the mean fluorescence of calcein in parental cells but this was not statistically significant.

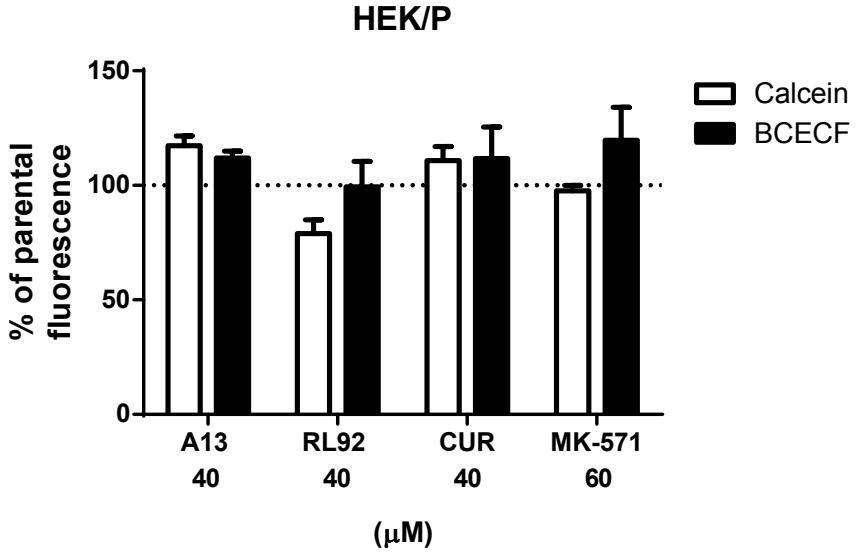

Figure 2-19. Effects of A13, RL92, curcumin (CUR) and MK-571 on the intracellular accumulation of calcein (0.1 μM) (□) and BCECF (0.25 μM) (■) in HEK/P cells. Concentrations used were previously shown to inhibit calcein and BCECF efflux in transfected cells (Figure 2-18). Data are presented as a % of the mean fluorescence in HEK/P cells treated with substrate and DMSO-only (100%). Results are mean ± standard error of n = 3 independent experiments.

2.3.3 Intrinsic fluorescence

To ensure that the identified inhibitors in the screening assays were not false positives due to intrinsic fluorescence of the analogues themselves, the fluorescence of cells + analogues-only were monitored in the FITC channel and the APC channel.

2.3.3.1 FITC channel

Since the fluorescence of rhodamine-123, calcein and BCECF were quantified using the FITC channel of the flow cytometer, analogues that showed significant inhibition of P-gp, MRP1 and MRP5 in the screening studies were also monitored for intrinsic fluorescence in this channel using both a flow cytometer and a fluorescence plate reader (methods in Section 2.2.5.4). The same protocols were followed as for the screening assays.

Results in Figure 2-20A show no significant intrinsic fluorescence of MDCKII/P cells treated with 20 μM curcumin analogues compared to DMSO-only controls in the FITC flow cytometer channel. Addition of rhodamine-123 (2.5 μM) resulted in a >2-log higher fluorescence compared to DMSO controls. Similarly, a lack of intrinsic fluorescence was observed in HEK/P cells treated with either curcumin or the cyclohexanone analogues (Figure 2-20B). Calcein-AM treated cells had 2-3 log higher fluorescence than analogues or DMSO-treated samples.

Intrinsic fluorescence of curcumin and selected analogues dissolved in unsupplemented DMEM (no cells) were also measured using 96-well plates and a fluorescence plate reader at the FITC excitation/emission wavelengths. No differences in fluorescence between DMEM only and DMEM with 20 μM of A12, A13, C10 or RL92 were seen (Figure 2-21). The positive control 2.5 μM rhodamine-123 had 2-3 log higher fluorescence than DMEM-only samples.

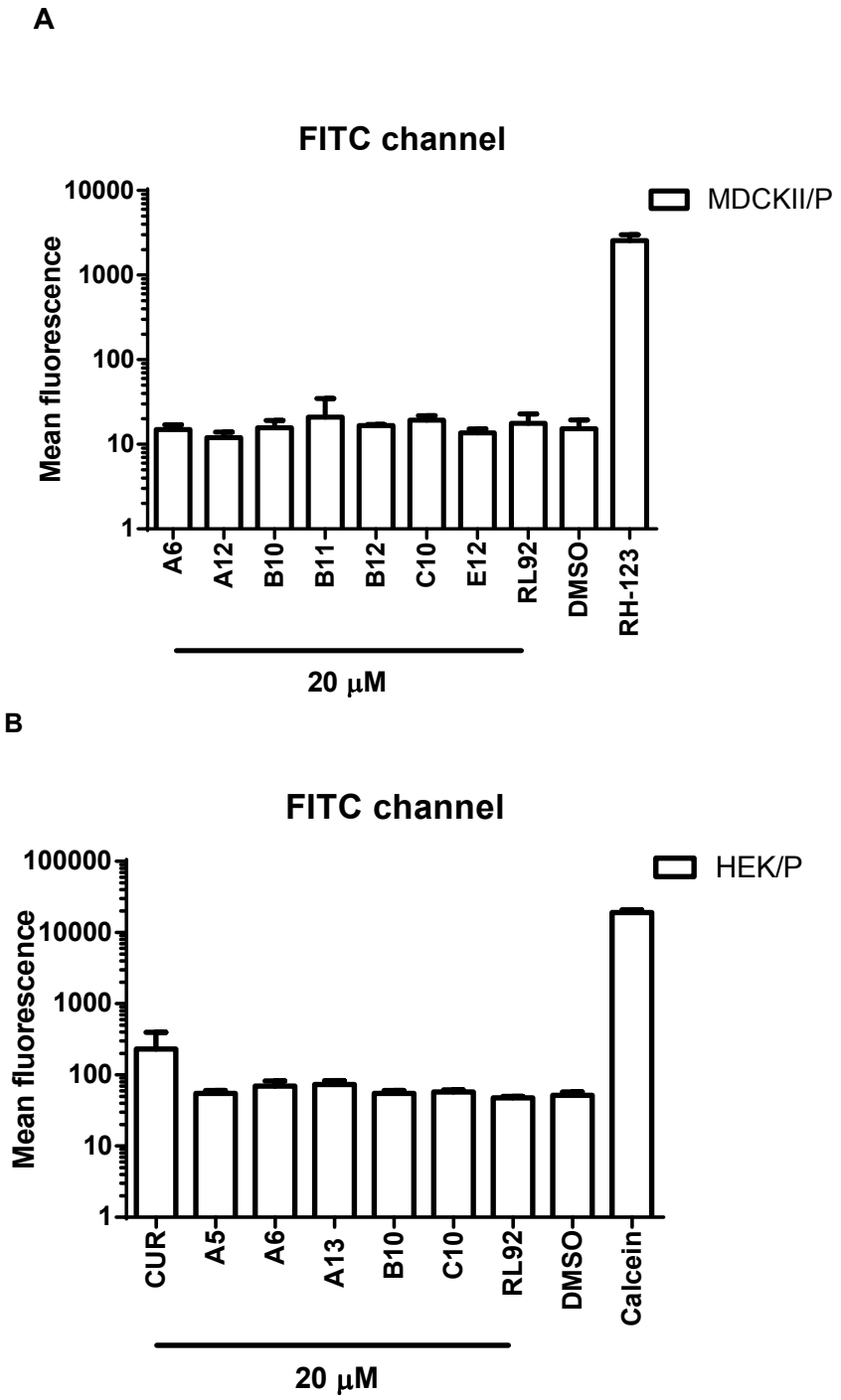

Figure 2-20. Fluorescence of MDCKII/P (**A**) and HEK/P (**B**) cells incubated with 20 μM curcumin (CUR) and cyclohexanone analogues only. Rhodamine-123 (RH-123) (2.5 μM) and calcein (0.1 μM) were included as positive controls. Incubation times were 75 min for MDCKII/P and 30 min for HEK/P. Fluorescence was read using the FITC channel of the flow cytometer (488 nm excitation/ 530 nm emission wavelength). Data are expressed as mean fluorescence values of n = 2 independent experiments. Error bars represent standard error. Y-axis is in Log scale.

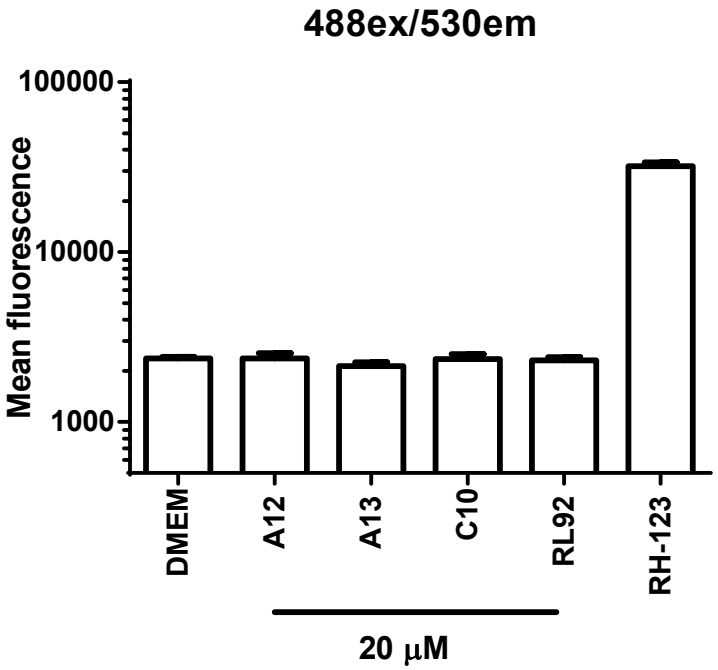

Figure 2-21. Fluorescence of DMEM media with or without curcumin analogues. Rhodamine-123 (RH-123) (2.5 μM) was included as positive control. Samples were read using a fluorescence plate reader at 488 nm excitation/530 nm emission wavelength, corresponding to the FITC channel in flow cytometry studies. Results are presented as mean fluorescence of n = 2 independent experiments in triplicate. Errors bars represent standard error. Y-axis is in Log scale.

APC channel

The APC channel of the flow cytometer was used to monitor the fluorescence of mitoxantrone in the BCRP inhibitor screening studies. Identified inhibitors were checked for intrinsic fluorescence in this channel by incubating MDCKII/P cells with analogues only.

Little to no fluorescence was observed in the APC channel for MDCKII/P cells treated with 20 μM curcumin, A12, A13, B11 and RL92. This is in contrast to the 2-Log higher fluorescence in mitoxantrone-treated cells (Figure 2-22).

DMEM with 20 μM curcumin, A12, A13, B11 or RL92 were also observed to have little fluorescence at the APC excitation/emission wavelengths using a 96-well plate format and a fluorescence plate reader (Figure 2-23). DMEM with 5 μM mitoxantrone displayed strong fluorescence at these wavelengths.

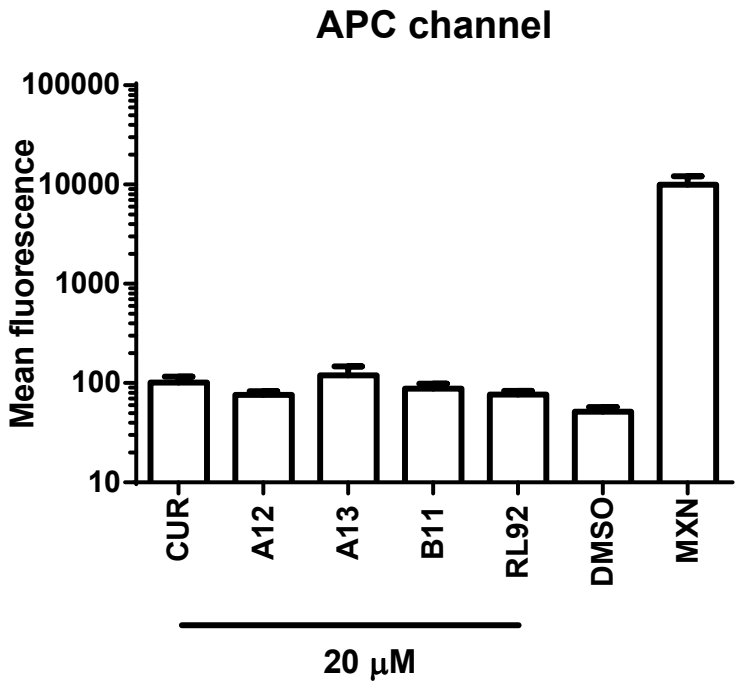

Figure 2-22. Fluorescence of MDCKII/P cells incubated with 20 μM curcumin (CUR) and cyclohexanone analogues only. Mitoxantrone (MXN) (5 μM) was included as positive control. Incubation time was 120 min. Fluorescence was read using the APC channel of the flow cytometer (633 nm excitation/ 660 nm emission wavelength). Data is expressed as mean fluorescence values of n = 2 independent experiments. Errors bars represent standard error. Y-axis is in Log scale.

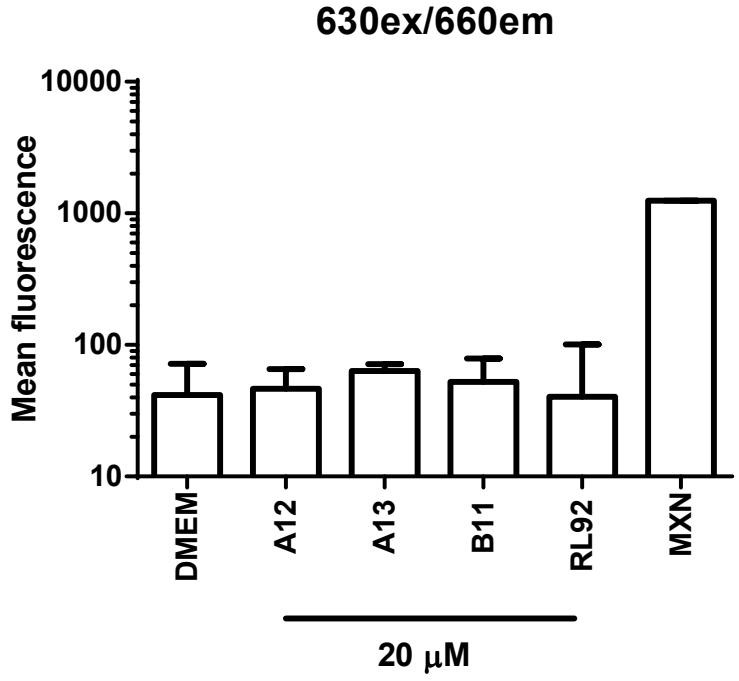

Figure 2-23. Fluorescence of DMEM media with or without curcumin analogues. Mitoxantrone (MXN) (5 μM) was included as positive control. Samples were read using a fluorescence plate reader at 630 nm excitation/660 nm emission wavelength, corresponding to the APC channel in flow cytometry studies. Results are presented as mean fluorescence of n = 2 independent experiments in triplicates. Errors bars represent standard error. Y-axis is in Log scale.

2.4 Discussion

To initially screen the analogues for ABC transporter inhibition, the flow cytometry-based accumulation assay was used. This is a common method for the screening of ABC transporter inhibitors as it is relatively simple, highly reproducible and is rapid compared to other methods. When combined with selective or specific probes and inhibitors with transfected cell lines, the assay can measure ABC-transporter functional activity in a specific manner.

Prior to screening the cyclohexanone curcumin analogues for inhibition, the accumulation assay was optimised to address issues typically encountered in screening studies (see Section 2.1). A protocol was used that took into account the effects from doublets, non-viable cells, solubility of the test compounds, growth phase of the cells and their density in suspension, passage numbers and presence of organic solvents (i.e., DMSO) (see Section 2.2). Experiments were conducted in stably transfected rather than drug-selected cell lines, minimising possible problems from the upregulation of other transporters; and established probe substrates and positive control inhibitors were selected that allowed specific assessment of efflux activity of the transporter of interest (Section 2.2).

Steady-state accumulation studies clearly demonstrated ABC transporter-mediated efflux of probe substrates as evidenced by significantly reduced fluorescence in transfected vs. parental cells (Section 2.3.1.1). The decreased fluorescence could be completely restored to parental levels by co-incubation with ABC transporter inhibitors. The effects of these inhibitors on probe substrate accumulation were saturable, further supporting a transporter-mediated process.

After assay optimisation which included determining the time to steady-state for each probe substrate and finding positive control concentrations that completely inhibited efflux activity, analogues were then screened for ABC transporter inhibition.

P-gp inhibition

From the screening assay, cyclohexanone analogues were found to significantly increase rhodamine-123 accumulation in MDCKII/P-gp cells. Of the 24 analogues tested, 8 were positive hits, including the new investigational compound RL92 (unreleased structure) (Section 2.3.2.1) (Figure 2-7). This was in contrast to curcumin which did not show any effects at the screening

concentration of 20 μM. The results suggest that the β-diketone structure does not underlie curcumin interactions with P-gp. Inhibition was observed for analogues with A, B and C cores (Figure 2-2). Even E12, which has a large butoxycarbonyl piperidone core, displayed significant inhibition. Examining the aromatic substituents flanking the core structure, 6 of the 7 inhibitors (excluding RL92) have methoxylated phenyl rings in this position. The best inhibitor, C10 had 3 methoxy groups in the flanking phenyl rings (Figure 2-8). Similar results were found by Dimmock et al. (2005) who reported that the trimethoxyphenyl-containing analogues were the most potent P-gp inhibitors. SAR studies have also previously correlated methoxy groups with P-gp inhibition (Liu et al., 2013; Palmeira et al., 2012b; Seelig and Gatlik-Landwojtowicz, 2005). The methoxy groups act as hydrogen bond acceptors and are thought to interact with donor groups in the P-gp binding cavity (Palmeira et al., 2012b).

It was observed that the analogue C10 was more potent than B10, despite having the same trimethoxylated aromatic substituents (Figure 2-7). C10, however, has a tropinone backbone with a protonated tertiary nitrogen at physiological pH (structure in Figure 2-8). SAR studies have identified this moiety to be a critical feature for highly efficient P-gp inhibition due to ionic interactions with negatively charged residues in the P-gp binding site (Liu et al., 2013; Palmeira et al., 2012b). Both C1 and C2 are the only other analogues with this feature but they have greatly decreased lipophilicity compared to C10 due to their pyridine substituents (Appendix I). As high lipophilicity was determined by SAR studies as an important requirement for inhibition, this may explain their lack of activity (Liu et al., 2013; Palmeira et al., 2012b; Seelig, 1998). All identified inhibitors in this screening assay were lipophilic, with $cLogD_{7.4}$ values >2.9 (Appendix I). This was the cutoff point for P-gp inhibitors determined by Palmeira et al. (2012b) in a comprehensive review of SAR studies.

Of the 8 positive hits, only C10 and RL92 completely inhibited rhodamine-123 efflux (Figure 2-7). To see if these analogues were more effective P-gp inhibitors than curcumin, their potencies were determined from non-linear regression curves of Log concentration-response data. The results show that both analogues were significantly more potent than curcumin at inhibiting rhodamine-123 efflux ($p < 0.001$) (Table 2-7). C10 was 18-fold more potent than curcumin, while RL92 was 6-fold more potent. Their concentration-response curves suggest that both analogues differ in their

mechanism of inhibition (Figure 2-9). The regression curve for C10 had a Hill slope of 1.4 ± 0.2, suggesting inhibition via a classic one-site binding (Prinz, 2010). In contrast, a steeper Hill slope of 3.0 was seen for RL92, indicating cooperativity and multi-site binding interactions. Although further studies are required to confirm such an interaction (e.g., radioligand binding studies), cooperative inhibition of P-gp is common and has been reported for a number of P-gp inhibitors (Martin et al., 2000; Wang et al., 2000b). In a flow cytometry study by Wang et al. (2000b) in P-gp overexpressing cells, 13 out of 15 compounds inhibited P-gp activity with Hill slopes greater than 1 (range of 1 – 11). This included well-known P-gp inhibitors, such as verapamil and quinidine.

Although curcumin did not inhibit P-gp at 20 μM in the screening assays, concentration-dependent inhibition was observed at higher concentrations (Figure 2-9C). A very steep inhibition curve with a Hill slope of 10.5 was recorded, also suggesting a cooperative mechanism of inhibition. However, the regression curve of curcumin plateaued at ~70% of verapamil inhibition, indicating that it is only a partial inhibitor of rhodamine-123 transport. This contrasted with complete transport inhibition with C10 or RL92 treatment. This partial inhibition by curcumin may be due to non-competitive inhibition, such as binding to a distinct negative allosteric site (Martin et al., 1997, 2000; Wang et al., 2000b). Alternatively, rhodamine-123 may have multiple binding sites in P-gp and curcumin may only compete at one site. Previous studies however, support rhodamine-123 binding to a single site (Martin et al., 2000; Shapiro and Ling, 1997). Another possible explanation for curcumin's apparent partial inhibition could be limited aqueous solubility, which is a known cause of plateau effects for lipophilic compounds (Weiss and Haefeli, 2006). However, curcumin dissolved in DMSO and diluted to the maximum concentration of 100 μM in media was a clear solution with no precipitate. Concentrations up to 400 μM has been previously used in cell culture media with no issues (LoTempio et al., 2005).

Previous studies examining curcumin inhibition of rhodamine-123 efflux have used only one-to-two concentrations of curcumin, and thus this study is the first to propose negative heterotropic cooperativity and partial inhibition of rhodamine-123 transport by curcumin (Chearwae et al., 2004; Nabekura et al., 2005; Tang et al., 2005; Zhang and Lim, 2008). However, further studies, such as displacement of radiolabeled rhodamine-123 are required to elucidate this inhibitory mechanism.

Accumulation studies in MDCKII/P cells found that C10, RL92, verapamil and curcumin all increased rhodamine-123 fluorescence, although the effect was only significant for curcumin ($p < 0.05$) (Figure 2-10). This increased accumulation of rhodamine-123 was likely due to the expression of low levels of endogenous canine P-gp in MDCKII cells (Kuteykin-Teplyakov et al., 2010; West and Mealey, 2007). The extent of fluorescence increase was small (30-70%) compared to that in transfected cells (400-700%), and hence, it was concluded that the increased accumulation in the screening assays was predominantly caused by inhibition of the transfected human P-gp transporter. In addition, no intrinsic fluorescence of curcumin, C10 or RL92 was observed in either the flow cytometry or the plate-based methods that could have interfered with these results.

BCRP inhibition

In the BCRP screening assay, 13 of the cyclohexanone analogues significantly increased the accumulation of mitoxantrone in MDCKII/BCRP cells (Section 2.3.2.2). Four of these (A12, A13, B11 and RL92) inhibited efflux to the same extent as 5 μM Ko143. A partial inhibition (<50%) was observed for curcumin at 20 μM, with 8 analogues showing greater inhibition than curcumin (Figure 2-11). A greater structural diversity of identified inhibitors was observed compared to P-gp inhibitors, with no specific structural motif associated with inhibition. All methoxylated-phenyl-ring containing analogues showed significant activity, as well as those with pyrrole, thiophene, imidazole and indole substituents. Inhibition was also not limited to a specific backbone structure, as inhibitors were seen with A, B, C and E-series compounds. In a large-scale screening assay of over 100 compounds, Matsson et al. (2007) reported that BCRP inhibition was significantly correlated with lipophilicity and molecular polarisability. To investigate whether a similar correlation applied to this data from the screening assay, the rank of the distribution coefficient and polarisability of each analogue was plotted against its BCRP inhibition rank and the Spearman correlation coefficient was determined (Figure 2-13). A significant positive correlation was observed between the lipophilicity and polarisability product and BCRP inhibition, suggesting a relative tolerance to changes in the curcumin structure, provided that analogues maintained high lipophilicity and polarisability.

The potency of A12, A13, B11 and RL92 were determined in MDCKII/BCRP cells and all were found to be significantly more potent than curcumin ($p < 0.001$) (Table 2-8). The potency order was A12 > A13 > B11 > RL92 > curcumin. However the observed IC_{50} for curcumin in MDCKII/BCRP was considerably higher (32.0 vs 1.8 μM) compared to that reported by Chearwae et al. (2006a) in HEK/BCRP cells. To examine if this apparent discrepancy was caused by differences in assay conditions or was dependent on cell line, the IC_{50} values of curcumin, A12 and A13 were also determined in HEK/BCRP cells (Figure 2-14). A much lower IC_{50} of curcumin was observed using the same assay conditions as the MDCKII/BCRP studies, which was similar to that obtained by Chearwae et al. (2006a) (2.3 vs 1.8 μM). Interestingly, the potency of A12 remained unchanged; while A13 IC_{50} decreased 5-fold in HEK/BCRP cells. As a result, all 3 compounds were equipotent at inhibiting mitoxantrone efflux in HEK/BCRP cells.

The reasons for this increased potency in HEK/BCRP compared to MDCKII/BCRP cells is not known, but could have resulted from lower BCRP expression levels (Szakács et al., 2008a; Wang et al., 2000a; Xia et al., 2007a). Results in Sections 2.3.1.1 and 2.3.1.2 show less functional transport activity in HEK/BCRP than MDCKII/BCRP cells based on differences in mitoxantrone accumulation between transfected and parental cells. However, a lower BCRP expression level would have also caused the potency of A12 to increase. The fact that the potency of A12 remained unchanged indicates that other factors may be responsible. A more plausible explanation could be that curcumin, A12 and A13 do not differ significantly in their affinity for BCRP, and that the potency differences in MDCKII/BCRP cells were due to intracellular metabolism. Wortelboer et al. (2003) have previously reported that curcumin was rapidly conjugated to glutathione in MDCKII cells. This was responsible for the greatly decreased potency of curcumin at inhibiting MRP2 in these cells compared to cell-free membrane vesicles. In MDCKII/BCRP cells, both curcumin and A13 may have been conjugated to glutathione, causing a decrease in potency compared to A12. In contrast, little to no conjugation would have occurred in HEK/BCRP cells, leading to improved potency for both curcumin and A13, without affecting the potency of A12. To test this mechanism, the affinity of these compounds to BCRP would have to be determined, as well as their susceptibility to glutathione conjugation in MDCKII/BCRP cells.

An examination of the concentration-response curves of the selected analogues indicates that all inhibited BCRP-mediated mitoxantrone efflux via binding to a single site on the transporter (Figure 2-14). Curcumin and the analogues A12, A13, B11 and RL92 had regression curves with Hill slopes ~1 in MDCKII/BCRP. As expected, similar Hill slopes were seen for A12, A13 and curcumin in HEK/BCRP cells, providing further support for a single-site binding mode for these compounds.

It was observed in the concentration-response studies that curcumin at 60 μM increased mitoxantrone accumulation in HEK/BCRP cells up to 76% greater than 5 μM Ko143 (Figure 2-14C). Since Ko143 at 5 μM completely inhibited BCRP-mediated mitoxantrone efflux, this increased mitoxantrone accumulation caused by curcumin suggests the involvement of non-BCRP mediated mechanisms. This was further supported by the significant 39% increase ($p < 0.05$) in mitoxantrone accumulation in HEK/P cells on co-incubation with 40 μM curcumin. However, these "non-specific" effects may be limited to the higher concentrations of curcumin (40 μM and 60 μM). At 10 μM (10^{-5} M), curcumin inhibited mitoxantrone efflux in HEK/BCRP to a similar extent as Ko143 (Figure 2-14C), but at this concentration it did not affect mitoxantrone accumulation in HEK/P cells (not shown). This indicates that the observed effect proceeds via a BCRP-mediated mechanism. In MDCKII/BCRP cells, the inhibition by curcumin was BCRP-specific, as it did not increase mitoxantrone accumulation in parental cells at 60 μM. Curcumin also was not fluorescent in the APC channel which could have confounded the results.

The cyclohexanone analogues (A12, A13, B11 and RL92) did not significantly increase mitoxantrone accumulation in MDCKII/P cells (Figure 2-15). Both A12 and A13 also did not affect mitoxantrone accumulation in HEK/P cells. None of the selected analogues were intrinsically fluorescent in the flow cytometry or plate-based assays. These results confirm that the effects of these analogues on mitoxantrone accumulation were specific to BCRP.

MRP1 and MRP5 inhibition

A lesser number of inhibitors were identified in the MRP1 screening assay, probably because most of the analogues were either neutral or positively charged (most had nitrogen containing groups), while MRP1 is mainly an organic anion transporter (He et al., 2011). In the screening assay, only A13 and curcumin completely inhibited calcein efflux (Figure 2-16A). Interestingly, A13 has the same phenyl ring group as curcumin, and both were the the only two compounds tested which

contained hydroxy substituents located at the 4'-position of the phenyl rings, and the only ones with hydrogen bond donor groups (Figure 2-17). RL92 also showed substantial, but partial inhibition of MRP1, but whether RL92 also contains a hydroxy substituent or a donor group is not known as the structure has yet to be released. Similar results were observed with the MRP5 screening assays. Only CUR, A13 and RL92 completely inhibited the efflux of BCECF by HEK/MRP5 (Figure 2-16B).

From these results, it is apparent that a hydrogen bond donor group is required for MRP1 and MRP5 inhibition, but whether this has to be a hydroxy group cannot be concluded from the screening assay. It is also not known if the positioning of the donor group is important for inhibitory activity. The inclusion of other analogues with non-hydroxy donor groups (e.g., primary or secondary amines) and analogues with hydroxy groups in different positions of the molecule and attached to different aromatic rings would help address these questions.

Molecular docking studies have suggested that the 4'-positioned hydroxy group in the phenyl rings of curcumin are important for MRP1 and MRP5 interactions (Figure 2-17). Docking of curcumin to a homology model of MRP1 showed that the 4'-hydroxy group of the phenyl ring was involved in hydrogen bonding interactions with the glutamine-450 residue of the MRP1 substrate-binding site (Sreenivasan et al., 2013). Similarly, docking of curcumin in a MRP5 homology model demonstrated that the 4'-hydroxy group of both phenyl rings hydrogen-bonded with asparagine-548 and tryptophan-471 residues at the ATP-binding site between NBD1 and NBD2 (Prehm, 2013). Both studies are consistent with the results from the MRP1 and MRP5 screening assays. As A13 and curcumin were the only compounds with 4'-hydroxylated phenyl rings, they were the only ones that efficiently inhibited transport activity (not considering RL92).

However, the concentration-response curves of A13 and curcumin appeared to contradict the proposed interaction from the docking studies (Figure 2-18). Both studies identified a single binding site for curcumin in MRP1 and MRP5 whereas the regression curves of curcumin and A13 suggested cooperativity and multi-site binding, with Hill slopes considerably greater than 1 (range 3.5-12.0). Experimental binding data for A13 and curcumin are therefore needed to accurately determine the stoichiometry of binding to both transporters and site-directed mutagenesis is

necessary to confirm the curcumin interactions proposed by the molecular docking studies. This could establish the importance of the phenolic 4'-hydroxy group in transport inhibition.

It should be mentioned that GSH-depletion by RL92 and curcumin is unlikely to be the mechanism of inhibition. This is because calcein efflux by MRP1 is not GSH-dependent (Feller et al., 1995).

The concentration-response curves indicate that A13 was a significantly more potent inhibitor of MRP1 ($p < 0.01$) and MRP5 ($p < 0.05$) than curcumin, although the difference in IC_{50} values was marginal (1.4-fold for both transporters) (Table 2-9). RL92 was slightly less potent than curcumin at inhibiting MRP1 but was equipotent at inhibiting MRP5. Studies in HEK/P showed a lack of effect by A13, RL92, curcumin and MK-571 on calcein and BCECF accumulation, confirming that inhibition was MRP1 and MRP5 specific (Figure 2-19). In addition, no intrinsic fluorescence was observed for any of the analogues or curcumin at the excitation/emission wavelengths used to quantify calcein and BCECF (Figure 2-20).

Limitations

Although the flow cytometry assay identified inhibition of probe efflux by the analogues, it gave little information into the mechanisms involved in this inhibition. For example, these analogues could be substrates and compete at the substrate binding site; or the mechanism could be non-competitive with inhibition of ATP binding to the NBD. Radioligand displacement assays, transport kinetic studies and photoaffinity labeling are needed to identify the mechanism of inhibition. These assays could also confirm results which suggested partial inhibition and cooperativity by curcumin and some of its analogues.

The flow cytometry screening assays were conducted using a single probe substrate for each transporter. Due to the presence of multiple-binding sites, it remains possible that analogue inhibition was specific to the probe used (Clark et al., 2006; Maeno et al., 2009; Martin et al., 2000). This is particularly applicable to rhodamine-123 and mitoxantrone which are known to be transported by P-gp and BCRP, respectively, via binding sites distinct from other substrates (Clark et al., 2006; Shapiro and Ling, 1997; Shapiro et al., 1999). To ensure that the analogues could inhibit the efflux of a broad range of substrates, inhibition needs to be confirmed using additional probes.

In this study, analogues were incubated for a short time frame of between 30 - 135 min, including the 15 min pre-incubation period. This would have detected direct interactions with the transporter but would have failed to identify any inhibition caused by downregulation of transporter expression which may occur at longer incubation times. In addition, whether the analogues themselves, or an intracellular metabolite, were responsible for the inhibition, is not known. For example, Wortelboer et al. (2005) found that some α,β-unsaturated carbonyl compounds, similar in structure to the curcumin analogues, required activation to an active metabolite to inhibit MRP1 in MDCKII transfected cells. This requirement for bioactivation was found by comparing activity with a cell-free membrane vesicle assay.

It should also be noted that, as the accumulation assay was cell-based, the potency of the analogues did not necessarily reflect the affinity for the transporter of interest. The calculated IC_{50} value is a function of affinity and other factors, such as intracellular degradation/activation and cellular uptake. It is therefore difficult to identify the reasons why the analogues have improved potency compared to curcumin. For example, it cannot be determined if the increased potency of C10 in inhibiting P-gp was due to reduced susceptibility to intracellular metabolism, greater cellular uptake, or increased affinity for the transporter. Binding studies using cell-free systems are thus needed to accurately compare the affinities or dissociation constants (Kd) between compounds to help elucidate the reasons underlying the potency differences.

These experiments were all conducted in DMEM-only media (without FBS) to represent unbound drug concentrations. The extent of protein binding of these analogues is not known. For highly protein bound analogues, the calculated IC_{50} in this assay may overestimate potency (Margulis et al., 2010). Also, as the half-life of curcumin in serum-free media was reported to be 10 min, substantial degradation of curcumin may have occurred, especially for the P-gp and BCRP screening assays which have incubation times of between 75 – 120 min (Wang et al., 1997). Since the concentrations of free curcumin or the analogues were not quantified before and after the experiments, there remains the possibility that the improved transport inhibition was merely a result of greater media stability of the analogues.

Summary

The flow cytometry accumulation method demonstrated significant inhibition of P-gp, BCRP, MRP1 and MRP5 by cyclohexanone curcumin analogues. Identified inhibitors were found to have either superior or equal potency to curcumin, and some also inhibited multiple ABC transporters. For example, A13 completely inhibited BCRP, MRP1 and MRP5 at 20 μM; while RL92 inhibited all four transporters at similar low μM concentrations. The selected analogues inhibited the investigated ABC transporters in a specific manner with no significant effects on parental cells.

Some structure-activity insights have been gained from the screening assays. The β-diketone backbone appears to play little role in determining ABC transporter inhibition, as analogues of various core structures showed potent transport inhibition. Methoxylated phenyl groups and a protonated tertiary nitrogen were associated with P-gp inhibition whereas BCRP inhibition significantly correlated with lipophilicity and polarisability. MRP1 and MRP5 inhibition by the analogues was associated with the presence of a phenyl ring with a 4'-hydroxy substituent. This moiety was previously demonstrated by molecular docking studies to be involved in curcumin binding to both transporters. However, discrepancies between molecular docking and the experimental data in this study (the former proposes single-site binding while the latter suggests multi-site binding of curcumin to both MRP1 and MRP5) warrants further investigation into the role of this substituent.

Although inhibition of ABC transporter-mediated efflux was clearly demonstrated by these accumulation studies, the mechanism of inhibition remains unclear, as do the reasons why the analogues have improved potency over curcumin. Substrate-specific effects also could not be discounted and the role of intracellular metabolism requires further clarification.

3. Confirmation of ABC transporter inhibition in resistance reversal assays

3.1 Introduction

The plate-based resistance reversal assay is another commonly used method for the identification of ABC transporter inhibitors. Although not as rapid, nor as high throughput as flow cytometry, the results may be more relevant in the search for MDR reversal agents as it directly measures the reversal of ABC-transporter mediated resistance to cytotoxic or cytostatic drugs (Brouwer et al., 2013; Szakács et al., 2008a; Xia et al., 2007a). In its simplest form, a cell line overexpressing the transporter of interest, either through drug selection or cDNA transfection, is seeded onto a multi-well plate and incubated with a range of concentrations of a cytotoxic substrate (Sarkadi et al., 2006; Szakács et al., 2008a). Due to ABC-transporter mediated efflux, these cells maintain lower intracellular concentrations of the substrate and are more resistant to anti-proliferative effects than the parental or empty vector-transfected cells (Sarkadi et al., 2006; Szakács et al., 2008a; Xia et al., 2007a). Test compounds are then added, and if the transporter of interest is inhibited, substrate efflux is reduced and resistance is decreased. If ABC-transporter mediated efflux is the sole cause of resistance, complete transport inhibition will restore the sensitivity of the transporter-expressing cells to that of parental or untransfected cells. The assay can also be used to identify ABC transporter substrates (Chearwae et al., 2006a; Wielinga et al., 2005). This requires that the test compound has anti-proliferative activity and is carried out by comparing the sensitivity of transporter-expressing vs. parental or untransfected cells to the cytotoxic/cytostatic effects of the compound. Increased resistance in the transporter-expressing cells is observed if the compound is effluxed.

The sensitivity (or resistance) of cells to anti-proliferative effects is quantified using a number of methods. Viability assays, such as MTT [3-(4,5-dimethylthiazol-2-yl)-2,5-diphenyltetrazolium bromide], resazurin or trypan blue can measure the total number of viable or surviving cells after the incubation period (Niles et al., 2008). Assays, such as the lactate dehydrogenase (LDH) assay, can directly measure cytotoxicity while cell proliferation assays such as SYBR green I and

sulforhodamine B can measure the total amount of cell proliferation over the length of the incubation period (Myers, 1998; Niles et al., 2008). A concentration-response curve can be constructed and the IC_{5o} (or EC_{50} for the cytotoxicity assays) can be calculated and compared between different treatments (Chearwae et al., 2006b; Wielinga et al., 2005; Xia et al., 2007a).

The resistance reversal assay does not require specialised equipment (e.g., a flow cytometer), and is simple and straightforward. However, it has known issues that must be addressed for results to be valid and accurate. Since the assay identifies ABC transporter inhibition as increased cytotoxicity or growth inhibition by the substrate drug, it is crucial that the test compound itself is not cytotoxic or cytostatic at the concentration used. Otherwise, increased cytotoxicity with test compound addition may be interpreted as resistance reversal, leading to false positives. Also, if the test compound is dissolved in an organic solvent such as DMSO, final solvent concentrations should be kept low as these can be cytotoxic to cells (Da Violante et al., 2002; Xia et al., 2007a).

Ideally, the relative resistance of transporter-expressing cells to the substrate should be exclusively due to efflux by the transporter of interest. The presence of other transporters that can influence the intracellular accumulation of the substrate will introduce artifacts into the assay. Transfected cell lines with low endogenous ABC transporter-expression are preferred over drug-selected cells as the latter may also result in the upregulation of other transporters (Szakács et al., 2008a; Xia et al., 2007a). Specific or selective substrates and inhibitors (as positive controls) of the transporter of interest should be used in order to limit contributions from other transporters. Most importantly, resistance reversal assays should be conducted in parallel with parental or untransfected cells. Test compounds which act via an ABC-transporter specific mechanism will reverse substrate resistance only in cells expressing the transporter of interest, without affecting parental or untransfected cells.

Other issues common with plate-based assays must also be considered. Plating densities need to be uniform across the whole plate so that differences in cell survival or cell growth are due to treatment effects and not variations in plating. The plating density for each cell line must be consistent between experiments, as initial seeding density is known to influence growth rates and may affect the calculated IC_{50} or EC_{50} in concentration-response curves (Niles et al., 2008; Sherley et al., 1995; Wang et al., 2010a). Seeding densities also need to be optimised so that wells are not

overgrown with cells at the end of the incubation period. This may lead to an underestimation of toxicity. Plates must also be kept in a humidified incubator so that evaporation effects on culture media are minimal. The peripheral wells of plates should not be used as these are susceptible to 'edge effects' or uneven distribution of cells due to thermal gradients between outer and inner wells (Lundholt et al., 2003).

In this chapter, the plate-based resistance reversal assay was used to confirm the observed ABC transporter inhibition by curcumin analogues in the flow cytometry screening assay (Chapter 2). As a secondary objective, it was also determined if the analogues were substrates of the transporters. C10, A12, A13, B11 and RL92 were selected for further studies as these were considered the most promising inhibitors. Curcumin was included for comparison. The P-gp resistance reversal assays were conducted in MDCKII/P-gp cells, with paclitaxel as the cytotoxic substrate, due to its selectivity for P-gp (Doyle and Ross, 2003; Jang et al., 2001). This was used together with the P-gp inhibitor, verapamil, as a positive control (Tsuruo et al., 1981). For BCRP, mitoxantrone was selected as the cytotoxic substrate in MDCKII/BCRP cells, together with the BCRP inhibitor, Ko143, as a positive control (Allen et al., 2002; Doyle and Ross, 2003). The assay was also conducted in BeWo choriocarcinoma cells which endogenously overexpress BCRP, to rule out cell-specific inhibition by the analogues (Ceckova et al., 2006). Assays using another substrate, topotecan, were conducted in MDCKII/BCRP cells to ensure that inhibition was not specific to mitoxantrone (Jonker et al., 2000). For MRP1, two cytotoxic substrates, etoposide and doxorubicin were used together with the MRP-selective inhibitor, indomethacin, in HEK/MRP1 cells (Benyahia et al., 2004; Cole, 2013; Draper et al., 1997). For MRP5, the antimetabolite drug raltitrexed was used as a cytotoxic substrate with the reported MRP5 inhibitor, NPPB, as positive control in HEK/MRP5 cells (Pratt et al., 2005; Wielinga et al., 2005).

The selected endpoint for measuring the cytotoxic/cytostatic effects of the substrates was total cell proliferation, quantified using a SYBR green I assay (Leggate et al., 2006; Myers, 1998). The latter measures the fluorescence of the SYBR green I nucleic acid stain, which increases with the amount of double-stranded DNA (dsDNA) that it binds. It was preferred over colorimetric viability assays, such as the MTT assay, due to its improved sensitivity and greater linear dynamic range (2-3 orders of magnitude) (McGowan et al., 2011; Myers, 1998; Wang et al., 2010a). It also does

not involve multiple wash steps which can dislodge cells from the plate; particularly weakly adherent cell lines such as HEK293 (Robbins and Horlick, 1998). Lastly, some viability assays rely on the metabolic status of the cells, which can be affected by the test compounds themselves (Niles et al., 2008; Vistica et al., 1991). This may result in data variability and inaccuracies in determining the anti-proliferative effects of compounds. For example, the polyphenol epigallocatechin gallate (EGCG) greatly increased the activity of mitochondrial enzymes which convert MTT to the coloured formazan dye, leading to an underestimation of its anti-proliferative effects (Wang et al., 2010a). The SYBR green assay does not have such shortcomings as it does not require mitochondrial reduction and is independent of cellular metabolic status (Myers, 1998).

3.2 Materials and methods

3.2.1 Chemicals and reagents

Materials (purity indicated) were sourced from the following: doxorubicin (≥98.0%), topotecan (≥98.0%), indomethacin (≥99.0%), and 5-Nitro-2-(3-phenylpropylamino)benzoic acid (NPPB) (≥98.0%) were from Sigma-Aldrich, St Louis, MO; paclitaxel (≥98%) and etoposide (≥98%) were from Cayman Chem, Ann Arbor, MI; and raltitrexed (≥99.0%) was from Selleck Chem, Houston, TX. All chemicals were dissolved in DMSO, aliquoted and stored at -80°C. New stock solutions were made every 6 months.

Sources for other materials, including mitoxantrone, Ko143, verapamil and cell culture reagents are in Section 2.2.2. Synthesis and chemistry of curcumin analogues are outlined in Section 2.2.1.

3.2.2 Cell lines

Sources for the transfected and parental HEK293 and MDCKII cells are in Section 2.2.3. BeWo choriocarcinoma cells were kindly provided by Dr. Michael Steiner of the Liggins Institute (University of Auckland, NZ) and were originally obtained from American Type Culture Collection (ATCC, Manassas, VA). BeWo cells were cultured using phenol-red and phenol-red free DMEM/F12 (Life Technologies, Carlsbad, CA). Expression of BCRP in BeWo cells was confirmed with Western blots (Chapter 5) and cell surface staining (Chapter 6).

General cell culture methods, including cell maintenance and splitting, are outlined in Section 2.2.4. All cells used were from passage numbers of < 20.

3.2.3 SYBR green I linearity

HEK/P and MDCKII/P cells were trypsinised for 5 and 15 min, respectively, and resuspended in complete phenol-red free DMEM. These were then counted using trypan blue staining and were plated in 96-well plates in triplicate at numbers ranging from 3,000 to 50,000 cells (see Section 2.2.4). Total volume was 200 µl media/well. The plates were incubated for 5 h at 37°C, 5% CO_2 in a humidified incubator to allow cells to attach to the plate. Media was then aspirated and the plates were stored at - 80°C. After thawing, the total cell numbers/well were quantified using a previously reported SYBR green I method (Leggate et al., 2006; Myers, 1998; Reid et al., 2009). A 10,000x

SYBR green I concentrate (Cat # S7563) (Life Technologies, Carlsbad, CA) was diluted 1:1000 with a Tris-EDTA/Triton X-100 cell lysis buffer (10mM Tris HCl, 2.5 mM EDTA, 1% Triton X-100) and 100 µl added to each well, followed by incubation at 4°C for 48 h. The cell lysate in each well was thoroughly mixed by pipetting up and down before the plate was read with a fluorescence plate reader at 485 nm excitation and 535 nm emission wavelength. Background fluorescence was quantified from SYBR green only wells (no cell controls) and subtracted from the readings.

3.2.4 Cell proliferation assay

3.2.4.1 Anti-proliferative effects of curcumin analogues

Cells grown after 3 days (~80 – 90% confluence) were trypsinised, resuspended in complete phenol-red free DMEM (DMEM/F12 for BeWo) and viable cells were counted using the trypan blue exclusion method (see Section 2.2.4). Cells were checked for clumping which causes uneven distribution to the well bottom, causing variations in well proliferation. Cells were then plated at 2000/well (MDCKII) or 3000/well (HEK and BeWo), with the density previously optimised so that wells are not overly confluent after the 96 h total incubation period. Cells were in 100 µl of complete media and allowed to attach to the plate for 24 h. These were then incubated with increasing concentrations of the analogues. Stock solutions in DMSO were dissolved in cell culture media at 2x the final concentration and 100 µl added to the existing 100 µl of culture media in each well, followed by incubation for a further 72 h in the 37°C incubator. Afterwards, total cell numbers/well were quantified using the method in Section 3.2.3. Final DMSO concentrations did not exceed 0.4% and were kept uniform between treatment and control samples. Experiments were done in triplicate and included cells + media only controls.

3.2.4.2 Resistance reversal assays

After cells were plated and allowed to attach for 24 h (see previous section), these were incubated for a further 72 h (37°C, 5% CO_2) with increasing concentrations of the corresponding cytotoxic substrate drugs in the absence or presence of test compound (see Table 3-1). A typical plate layout using a low and high concentration of analogue is shown in Figure 3-1. Analogue concentrations used did not inhibit cell growth from the studies in Section 3.2.4.1. Selected concentrations of test compounds for the resistance reversal assays were further tested for growth

inhibitory effects by incubating cells for 72 h with the test compound only. The total cell numbers were then compared against cells incubated with media only.

Reported ABC transporter inhibitors were used as positive controls of resistance reversal (Table 3-1). All experiments conducted in transfected cell lines were carried out in parallel with parental cells (seeded in separate plates). Final DMSO concentrations did not exceed 0.8% and were kept uniform between the treatment and control samples. After the 72 h incubation period, media was aspirated and cell numbers quantified using the method described in Section 3.2.3.

Table 3-1. Cytotoxic substrates and positive controls used in the resistance reversal studies

	Cell lines				
	MDCKII/P-gp MDCKII/P	**MDCKII/BCRP MDCKII/P**	**BeWo**	**HEK/MRP1 HEK/P**	**HEK/MRP5 HEK/P**
Cytotoxic substrate	paclitaxel	mitoxantrone topotecan	mitoxantrone	doxorubicin etoposide	raltitrexed
Positive control	verapamil 20 µM	Ko143 1 µM	Ko143 1 µM	indomethacin 40 µM	NPPB 40 µM

	Water only										
	No drug	AL	AL+S1	AL+S2	AL+S3	AL+S4	AL+S5	AL+S6	AL+S7	AL+S8	
	No drug	AL	AL+S1	AL+S2	AL+S3	AL+S4	AL+S5	AL+S6	AL+S7	AL+S8	
	No drug	AL	AL+S1	AL+S2	AL+S3	AL+S4	AL+S5	AL+S6	AL+S7	AL+S8	
	No drug	AH	AH+S1	AH+S2	AH+S3	AH+S4	AH+S5	AH+S6	AH+S7	AH+S8	
	No drug	AH	AH+S1	AH+S2	AH+S3	AH+S4	AH+S5	AH+S6	AH+S7	AH+S8	
	No drug	AH	AH+S1	AH+S2	AH+S3	AH+S4	AH+S5	AH+S6	AH+S7	AH+S8	
	Water only										

Figure 3-1. Typical plate layout for a resistance reversal assay in a 96-well plate using a low (AL) and high (AH) concentration of analogue or test compound. Eight increasing concentrations of cytotoxic substrate drug were used (S1-S8). Wells marked AL or AH were cells incubated with media + analogues alone. No-drug wells contain cells incubated with media + DMSO only. Due to edge effects, the peripheral wells were not used. Instead, 300 µl of water was added to to reduce media evaporation. Plates were also incubated in a humidified incubator.

3.2.5 Statistical analysis and IC_{50} calculation

Statistical analysis, non-linear regression and determination of IC_{50} were carried out using Graphpad Prism 6 software. Significant differences between multiple treatment groups and a control group were done using one-way ANOVA with Dunnett's post-hoc test. A p-value < 0.05 was considered significant.

To determine the IC_{50} of the anti-proliferative effects of the analogues, the fluorescence data from the SYBR green assay were normalised to cells + media only samples. These wells had maximal cell proliferation (100%). Samples incubated with the highest concentrations of analogue were set at 0%. At these concentrations, cell proliferation was completely inhibited. A non-linear regression curve was then fit of the normalised fluorescence data using the method outlined in Section 2.2.7 to calculate the IC_{50}.

In the resistance reversal assays, data was normalised to fluorescence in wells incubated with analogue or positive control only without cytotoxic substrate (set as 100%). Samples incubated with the highest concentration of cytotoxic substrate (complete inhibition of proliferation) was set as 0%. A non-linear regression curve was fit and the IC_{50} calculated as in Section 2.2.7.

3.3 Results

3.3.1 Linearity of SYBR Green I proliferation assay

The SYBR green method, used to quantify total cell numbers/well, was verified for linearity at the expected range of cell numbers in the proliferation assays. A linear relationship between SYBR green I fluorescence was observed for MDCKII/P at a range of 0.3 – 5 x 10^4 cells (Figure 3-2A). A similar linear relationship was also observed for HEK/P and BeWo cells (Figure 3-2B & C).

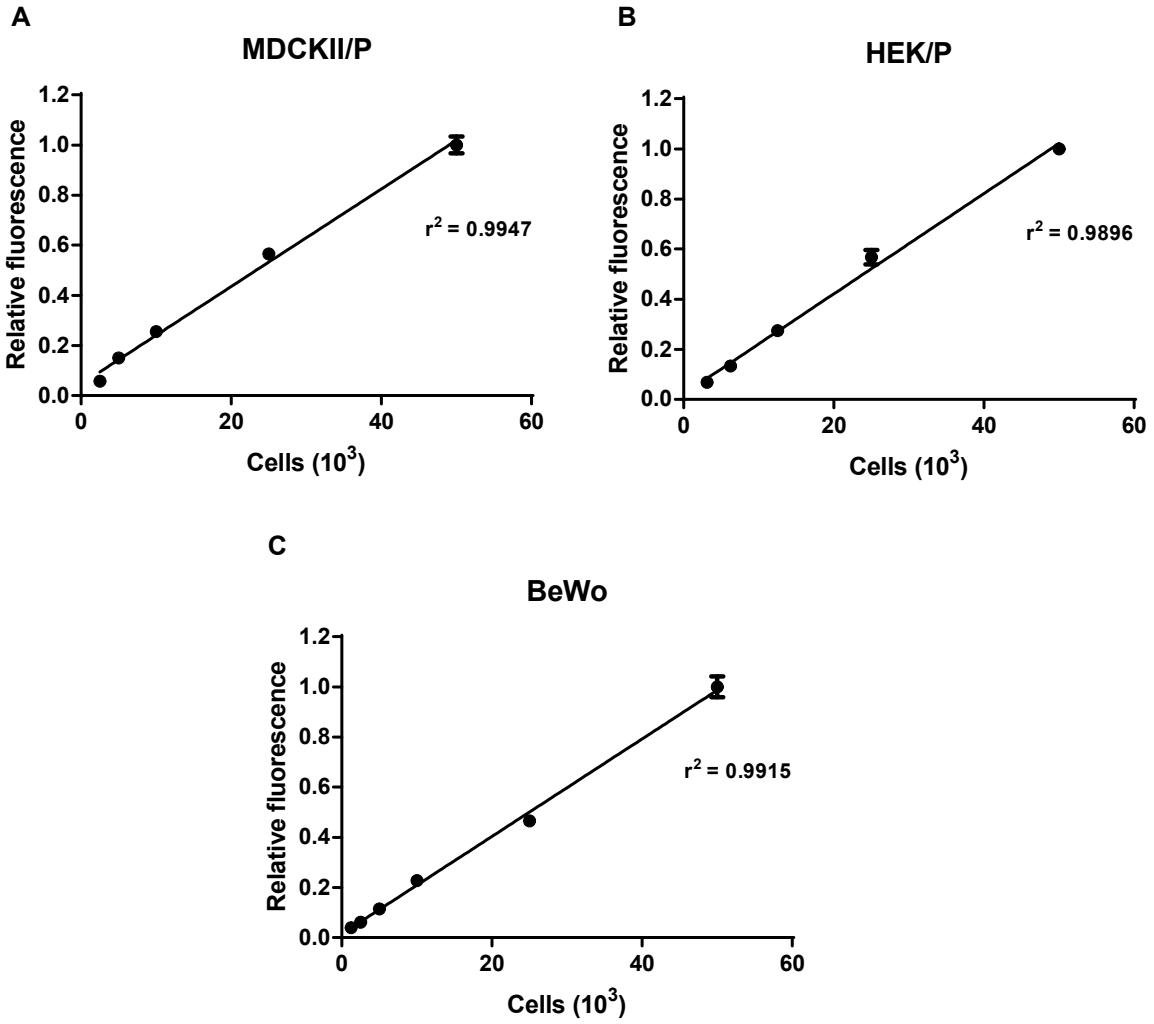

Figure 3-2. Linearity of SYBR Green I fluorescence with increasing cell numbers of MDCKII/P (**A**), HEK/P (**B**) and BeWo cells (**C**). Data are expressed as relative fluorescence from maximum (5 x 10^4 cells). Data are representative of n = 2 independent experiments; mean ± standard error of triplicates.

3.3.2 Anti-proliferative effects of curcumin analogues in parental and transfected cell lines

Prior to the start of resistance reversal studies, the antiproliferative or growth inhibitory effects of curcumin analogues were determined in parental and transfected cells to identify non-cytotoxic/cytostatic concentrations. These also indicated if transporter overexpression conferred a resistant phenotype towards the analogues.

Table 3-2 summarises IC_{50} data from 72 h proliferation assays conducted in MDCKII cells. The identified BCRP inhibitors, A12, A13, B11 and RL92 inhibited the growth of MDCKII/P and MDCKII/BCRP. B11 was the most potent inhibitor, followed by RL92, A13 and A12 in both cell lines. Resistance was not increased in MDCKII/BCRP compared to MDCKII/P. Similarly, the P-gp inhibitors C10 and RL92 inhibited MDCKII/P and MDCKII/P-gp proliferation. MDCKII/P-gp cells were as sensitive to growth inhibition as the parental cells.

Table 3-2. Intrinsic anti-proliferative activity of A12, A13, B11, C10 and RL92 in parental and ABC transporter transfected MDCKII cells.

	IC_{50} ± SE[a] (μM)		
Compounds	**MDCKII/P**	**MDCKII/P-gp**	**MDCKII/BCRP**
A12	22.7 ± 3.0	--	19.5 ± 3.8 (0.9)[b]
A13	10.6 ± 0.9	--	14.1 ± 0.1 (1.3)
B11	1.0 ± 0.1	--	1.3 ± 0.1 (1.3)
C10	2.1 ± 0.3	2.3 ± 0.3 (1.1)	--
RL92	3.3 ± 0.1	3.0 ± 0.1 (0.9)	3.3 ± 0.2 (1.0)

[a] – mean ± standard error of n ≥ 3 independent experiments. [b] – Fold resistance is the IC_{50} divided by the IC_{50} of the analogue in MDCKII/P cells. Spaces left blank – IC_{50} was not determined.

Anti-proliferative effects against HEK cells are summarised in Table 3-3. The analogue A13 inhibited proliferation of HEK/P, HEK/MRP1 and HEK/MRP5. All three cell lines were equally sensitive to A13. HEK/P cells were also more sensitive to growth inhibition by A13 than MDCKII/P (Table 3-2) with a 3-5 fold lower IC_{50} in HEK293 cells. RL92 inhibited the proliferation of all three cell lines with similar potency. Increased resistance to RL92 was not observed in HEK/MRP1 and HEK/MRP5 compared to parental cells.

Table 3-3. Intrinsic anti-proliferative activity of A13 and RL92 in parental and ABC transporter transfected HEK cells.

	IC_{50} ± SE[a] (µM)		
Compounds	**HEK/P**	**HEK/MRP1**	**HEK/MRP5**
A13	3.0 ± 0.5	2.9 ± 0.2 (1.0)[b]	2.5 ± 0.1 (0.8)
RL92	1.2 ± 0.2	1.0 ± 0.1 (0.8)	1.5 ± 0.3 (1.3)

[a] – mean ± standard error of n ≥ 3 independent experiments. [b] – Fold resistance is the IC_{50} divided by the IC_{50} of the analogue in HEK/P cells.

3.3.3 Reversal of P-gp mediated resistance

3.3.3.1 Growth inhibitory effects of test compounds in MDCKII/P-gp

Before conducting the resistance reversal assays, it was first determined if the maximum concentrations of analogues, curcumin and positive control to be used, exhibited growth inhibitory effects. Figure 3-3 shows that incubation of cells for 72 h with media containing C10, RL92, curcumin or verapamil at the indicated concentrations did not significantly affect cell growth compared to media + DMSO-only controls.

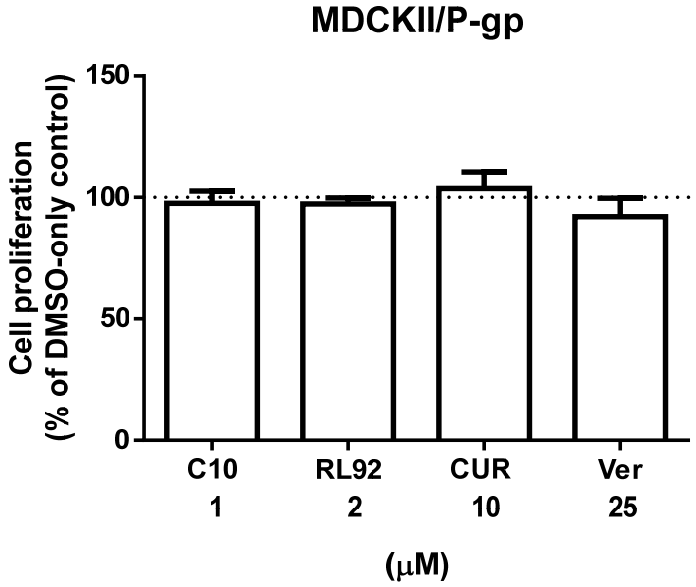

Figure 3-3. Effects of C10, RL92, curcumin (CUR) and verapamil (Ver) on the proliferation of MDCKII/P-gp. Cells were incubated with complete media and the indicated test compounds for 72 h. Data are expressed as a % of the total proliferation in DMSO-only control wells, quantified using SYBR-Green I DNA binding dye. Results are mean ± standard error of n ≥ 3 independent experiments.

3.3.3.2 Reversal of paclitaxel resistance in MDCKII/P-gp cells

To confirm inhibition of P-gp by C10 and RL92 from flow cytometry studies, both analogues were tested for the ability to reverse paclitaxel resistance in MDCKII/P-gp cells in long term 72 h cell proliferation assays. Figure 3-4A shows that C10 at 1 μM sensitised MDCKII/P-gp cells to paclitaxel and decreased the IC_{50} by 28-fold. Figure 3-4B also shows that RL92 at 2 μM could reverse paclitaxel resistance in MDCKII/P-gp cells to similar levels as parental cells. Lower concentrations of C10 and RL92 (0.5 and 1 μM, respectively), also significantly reversed paclitaxel resistance (Table 3-4). The effects of both compounds were less than that of the positive control verapamil (25 μM) which decreased paclitaxel IC_{50} 138-fold and made MDKCII/P-gp cells 13.5-fold more sensitive than parental cells (Figure 3-4A). In contrast, curcumin at 10 μM did not significantly affect paclitaxel IC_{50} and was not found to change the concentration-response curve (Figure 3-4B).

To determine if non-P-gp specific mechanisms were involved in resistance reversal, studies were conducted in parallel in MDCKII/P cells (Table 3-4). Verapamil, C10 and RL92 at low and high concentrations all significantly decreased the IC_{50} of paclitaxel in the parental cells ($p < 0.001$). However, the extent of sensitisation was less compared to MDCKII/P-gp. Verapamil decreased paclitaxel IC_{50} 13.5-fold compared to 138-fold in MDCKII/P-gp. C10 at 1 μM sensitised parental cells 10-fold compared to 28-fold in transfected cells. RL92 at 2 μM decreased paclitaxel IC_{50} 7-fold compared to 23-fold in MDCKII/P-gp. These results suggest a minor contribution by non-P-gp mediated mechanisms.

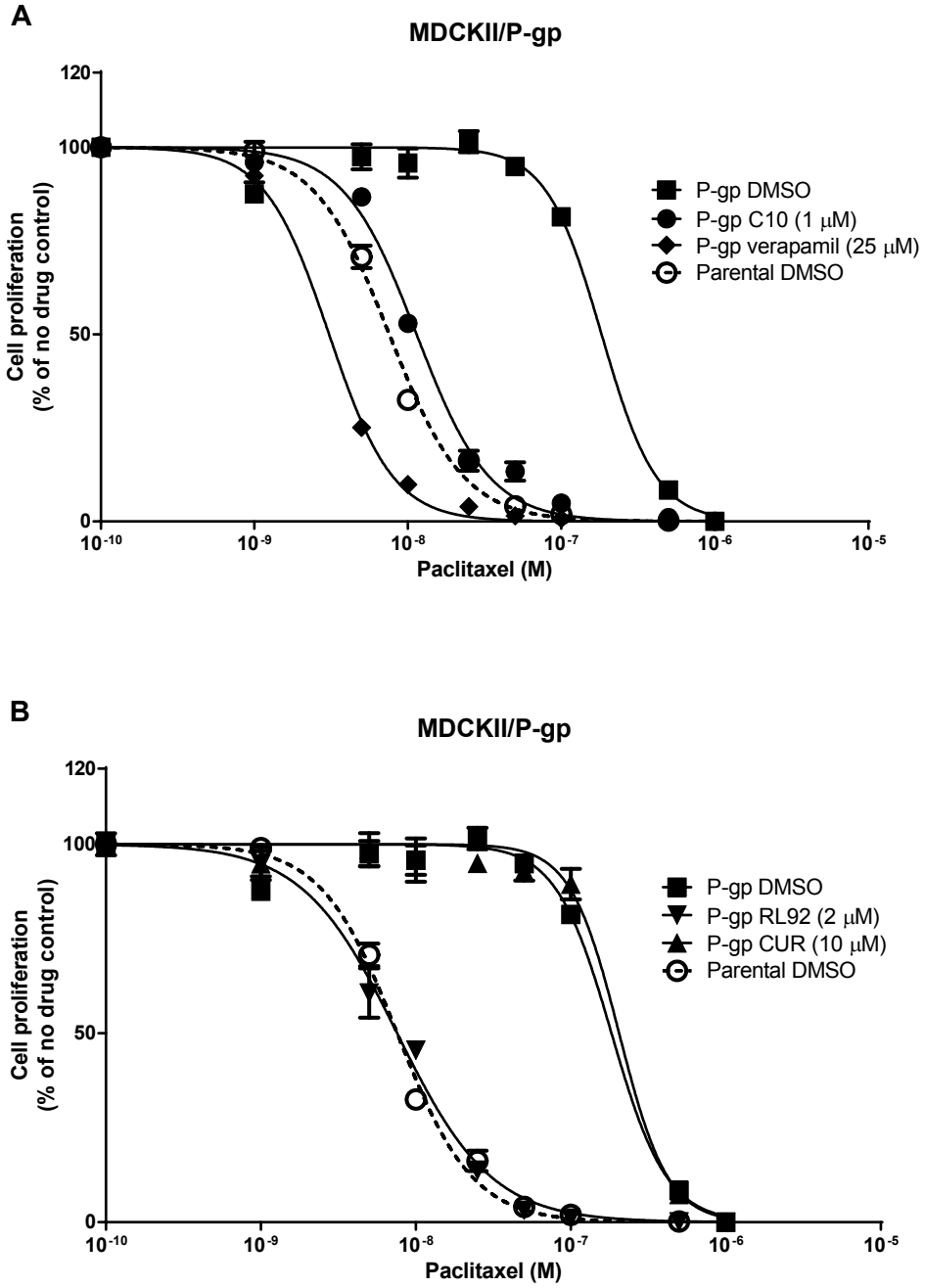

Figure 3-4. Inhibition of MDCKII/P-gp (solid lines) and MDCKII/P (dashed lines) cell proliferation by paclitaxel in the absence or presence of selected curcumin analogues. Paclitaxel was co-incubated with DMSO only (■) and (○); C10 (●) or the positive control, verapamil (◆) (**A**); RL92 (▼) or curcumin (CUR) (▲)(**B**). For simplicity, only paclitaxel concentration-response curves co-incubated with a high concentration of curcumin or analogues are included. Results are total cell proliferation quantified using SYBR green I dsDNA binding dye. Data are presented as % of the fluorescence from no paclitaxel controls and are representative of n ≥ 3 independent experiments. Data points are mean ± standard error of triplicates.

Table 3-4. The effects of curcumin and cyclohexanone analogues on paclitaxel IC_{50} in MDCKII/P and MDCKII/P-gp cells.

	Paclitaxel IC_{50} ± SE[a] (nM)	
Compounds	**MDCKII/P**	**MDCKII/P-gp**
Paclitaxel + DMSO	8.1 ± 0.4	206.6 ± 11.9 (25.5)[b]
+ verapamil (25 μM)	0.6 ± 0.1 (0.07)***	1.5 ± 0.9 (0.2)***
+ CUR (5 μM)	--	240.4 ± 16.4 (29.7)
+ CUR (10 μM)	--	213.8 ± 18.0 (26.4)
+ C10 (0.5 μM)	0.8 ± 0.1 (0.1)***	20.6 ± 2.2 (2.5)***
+ C10 (1 μM)	0.6 ± 0.1 (0.07)***	7.5 ± 2.0 (0.9)***
+ RL92 (1 μM)	1.5 ± 0.6 (0.19)***	36.5 ± 4.4 (4.5)***
+ RL92 (2 μM)	1.2 ± 0.2 (0.15)***	9.1 ± 3.4 (1.1)***

[a] – mean ± standard error of n ≥ 3 independent experiments. [b] – Fold resistance is the IC_{50} value / IC_{50} of paclitaxel alone in MDCKII/P cells. ***$p<0.001$ significantly different from paclitaxel only control for each cell line, calculated using one-way ANOVA and Dunnett's post-hoc test. Spaces left blank – IC_{50} was not determined. CUR – curcumin.

3.3.4 Reversal of BCRP mediated resistance

3.3.4.1 Growth inhibitory effects of test compounds on MDCKII/BCRP and BeWo

The cyclohexanone analogues, curcumin and Ko143 were tested for growth inhibitory effects on MDCKII/BCRP. Figure 3-5A shows that A12, A13, B11, RL92, curcumin or Ko143 did not significantly decrease MDCKII/BCRP proliferation at maximal concentrations to be used in subsequent resistance reversal assays. In BeWo cells, A12, A13 and Ko143 also did not affect cell growth after 72 h at the indicated concentrations (Figure 3-5B).

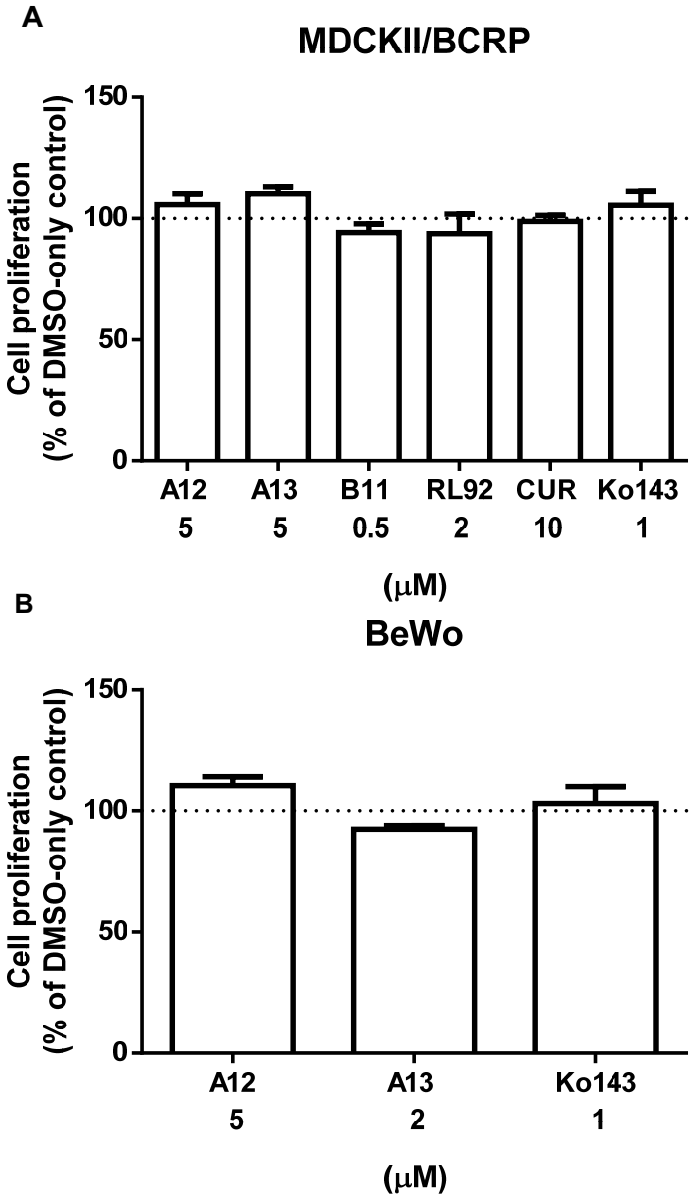

Figure 3-5. Effects of curcumin (CUR), Ko143 and cyclohexanone analogues on the proliferation of MDCKII/BCRP (**A**) and BeWo cells (**B**). Cells were incubated with complete media and the indicated test compounds for 72 h. Data are expressed as a % of the total proliferation in DMSO only control wells, quantified using SYBR-Green I DNA binding dye. Results are mean ± standard error of n ≥ 3 independent experiments done in triplicate.

3.3.4.2 Reversal of mitoxantrone resistance in MDCKII/BCRP

The BCRP inhibitors A12, A13, B11 and RL92 identified from the flow cytometry studies were tested for reversal of MDCKII/BCRP resistance to mitoxantrone in 72 h cell proliferation assays. Figure 3-6A shows that A12 and A13 completely reversed MDCKII/BCRP resistance to similar levels as parental cells. The effect was the same as that observed with the positive control, Ko143. The analogues B11, RL92 and curcumin also significantly decreased mitoxantrone resistance (Figure 3-6B). B11 and RL92 only partially resensitised MDCKII/BCRP cells; while curcumin completely reversed resistance. Both B11 and RL92 were used at 10- and 2.5-fold lower concentrations, respectively, compared to A12 and A13, due to their anti-proliferative effects (see Table 3-2).

All analogues tested (except B11) significantly decreased mitoxantrone IC_{50} in MDCKII/BCRP cells in a concentration-dependent manner (Table 3-5). Neither Ko143, nor any of the analogues, significantly affected the sensitivity of MDCKII/P cells to mitoxantrone.

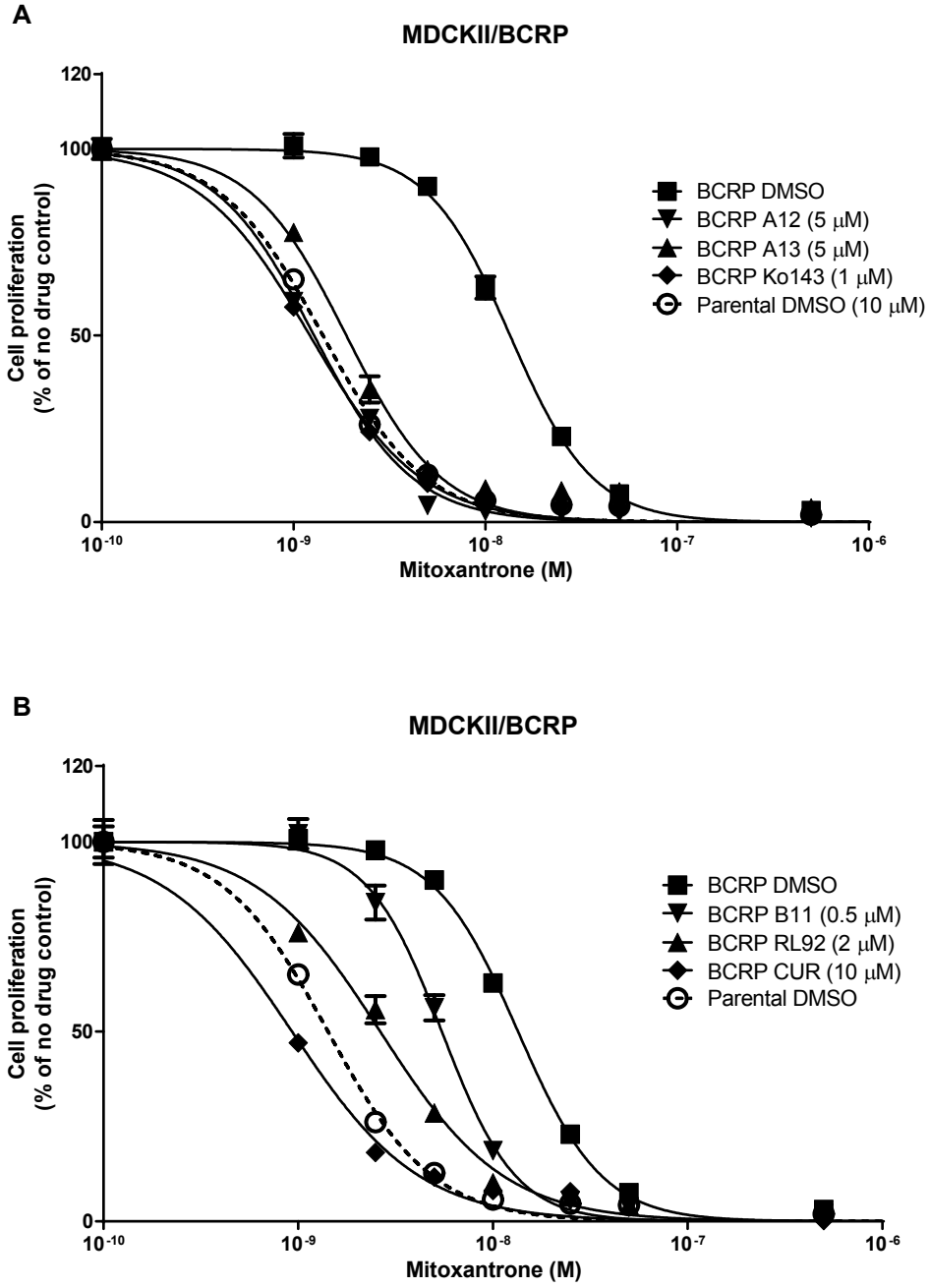

Figure 3-6. Inhibition of MDCKII/BCRP (solid lines) and MDCKII/P (dashed lines) proliferation by mitoxantrone. Mitoxantrone was co-incubated with DMSO only; A12, A13 or positive control, Ko143 (**A**); B11, RL92 or curcumin (CUR)(**B**). For simplicity, only mitoxantrone concentration-response curves co-incubated with a high concentration of curcumin or analogues are included. Results are total cell proliferation quantified using SYBR green I dsDNA binding dye. Data are presented as % of the fluorescence from no mitoxantrone controls and are representative of n ≥ 3 independent experiments. Data points are mean ± standard error of triplicate.

Table 3-5. The effects of curcumin and cyclohexanone analogues on mitoxantrone IC_{50} in MDCKII/P and MDCKII/BCRP cells.

Compounds	Mitoxantrone IC_{50} ± SE[a] (nM)	
	MDCKII/P	MDCKII/BCRP
Mitoxantrone + DMSO	0.9 ± 0.1	13.4 ± 1.7 (14.9)[b]
+ Ko143 (1 μM)	0.9 ± 0.2 (1.0)	1.1 ± 0.2 (1.2)***
+ CUR (5 μM)	0.9 ± 0.1 (1.0)	2.6 ± 0.2 (2.9)***
+ CUR (10 μM)	0.8 ± 0.1 (0.9)	1.6 ± 0.1 (1.8)***
+ A12 (1 μM)	1.5 ± 0.1 (1.7)	5.1 ± 0.4 (5.7)***
+ A12 (5 μM)	1.3 ± 0.3 (1.4)	1.6 ± 0.2 (1.8)***
+ A13 (1 μM)	1.1 ± 0.2 (0.8)	4.3 ± 1.0 (4.8)***
+ A13 (5 μM)	1.8 ± 0.2 (2.0)	1.5 ± 0.2 (1.7)***
+ B11 (0.25 μM)	1.4 ± 0.3 (1.6)	8.5 ± 1.0 (9.4)
+ B11 (0.5 μM)	1.3 ± 0.2 (1.4)	7.0 ± 0.8 (7.8)*
+ RL92 (1 μM)	1.0 ± 0.1 (1.1)	4.7 ± 0.3 (5.2)***
+ RL92 (2 μM)	0.8 ± 0.1 (0.8)	2.8 ± 0.2 (3.1)***

[a] – mean ± standard error of n ≥ 3 independent experiments. [b] – Fold resistance is the IC_{50} value / IC_{50} of mitoxantrone alone in MDCKII/P cells (0.9 ± 0.1 μM). *p<0.05 ***p<0.001 significantly different from the IC_{50} of mitoxantrone only control for each cell line, calculated using one-way ANOVA and Dunnett's post-hoc test. CUR – curcumin.

3.3.4.3 Determination of cell-line and substrate-dependent effects of A12 and A13

The two most potent BCRP inhibitors, A12 & A13, were tested for resistance reversal effects on BCRP overexpressing BeWo choriocarcinoma cells to rule out cell-line specific effects. The ability to reverse MDCKII/BCRP resistance to another BCRP substrate, topotecan, was also determined to show that sensitisation was not specific to mitoxantrone only.

Figure 3-7A shows that both A12 and A13 reversed BeWo cell resistance to mitoxantrone to a similar extent as the positive control, Ko143. Lower concentrations of both analogues also significantly decreased mitoxantrone IC_{50} ($p < 0.01$) (Table 3-6). Figure 3-7B also shows that high concentrations of A12 and A13 reversed MDCKII/BCRP resistance to topotecan similar to that achieved with Ko143. In addition, a high concentration of either analogue made MDCKII/BCRP cells as sensitive to topotecan as MDCKII/P cells (see Table 3-6 footnotes for topotecan IC_{50} value in MDCKII/P cells). A low concentration of either analogue also significantly decreased topotecan IC_{50} in MDCKII/BCRP cells ($p < 0.001$) (Table 3-6).

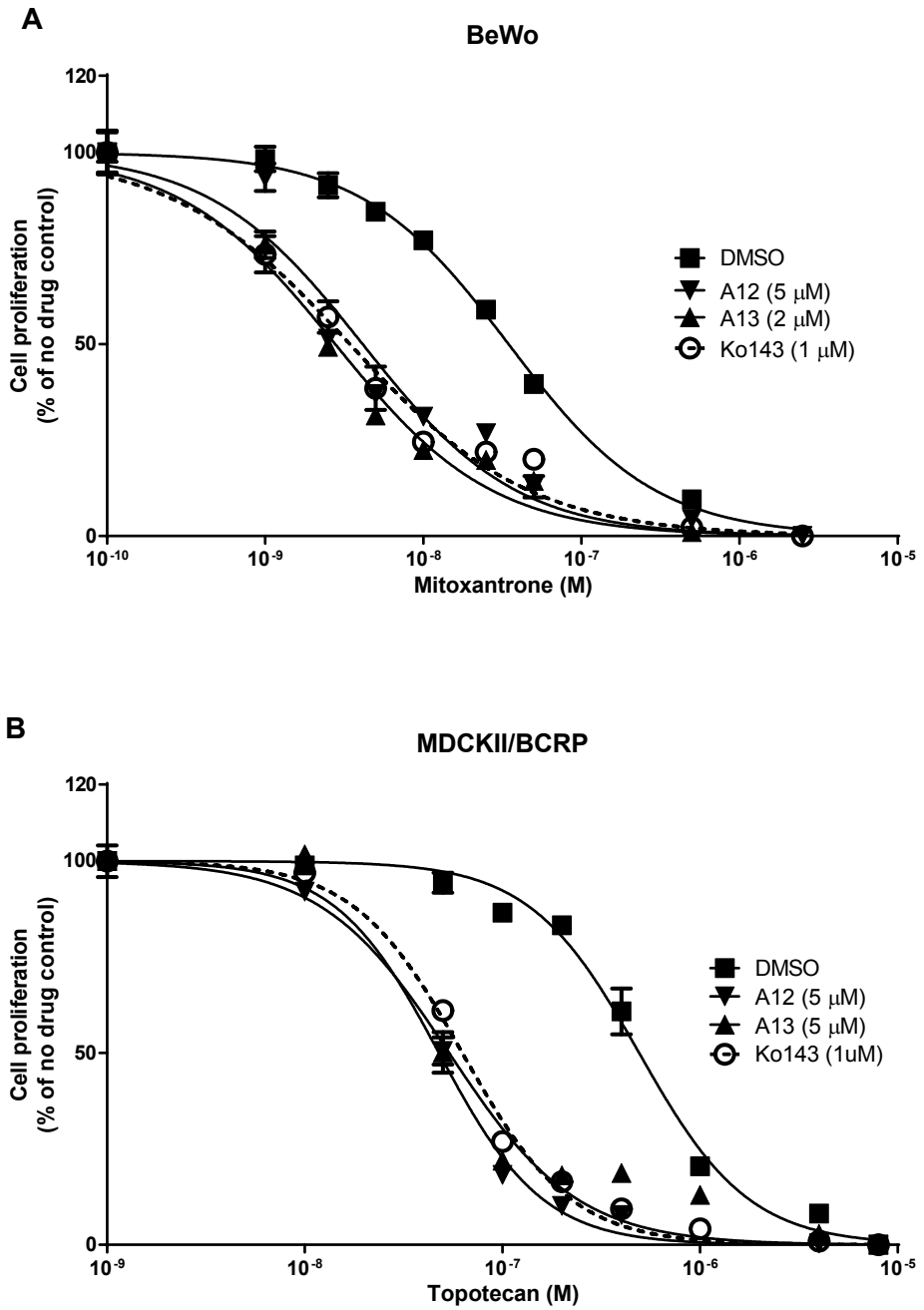

Figure 3-7. Inhibition of BeWo choriocarcinoma (**A**) and MDCKII/BCRP (**B**) proliferation by mitoxantrone and topotecan respectively. Mitoxantrone or topotecan was co-incubated with DMSO only (■) or positive control, Ko143 (O); A12 (▼) or A13 (▲). For simplicity, only mitoxantrone and topotecan concentration-response curves co-incubated with a high concentration of the analogues are included. Results are total proliferation quantified using SYBR green I DNA binding dye. Data are presented as % of the fluorescence from no mitoxantrone or topotecan controls and are representative of n ≥ 3 independent experiments. Data points are mean ± standard error of triplicate.

Table 3-6. The effects of A12 and A13 on the IC_{50} of mitoxantrone in BeWo choriocarcinoma cells and topotecan in MDCKII/BCRP cells.

	IC_{50} ± SE[a] (nM)	
	BeWo	**MDCKII/BCRP**
Compounds	**Mitoxantrone**	**Topotecan**
Mitoxantrone or topotecan + DMSO	28.3 ± 3.7 (7.3)[b]	499.3 ± 8.2 (11.6)[c]
+ Ko143 (1 μM)	3.9 ± 1.2 (1.0)***	59.1 ± 7.5 (1.4)***
+ A12 (1 μM)	8.3 ± 0.5 (2.1)***	174.1 ± 16.7 (4.1)***
+ A12 (5 μM)	5.0 ± 0.4 (1.3)***	57.8 ± 7.9 (1.3)***
+ A13 (1 μM)	7.4 ± 1.4 (1.9)**	173.4 ± 16.9 (4.0)***
+ A13 (2 μM)	4.1 ± 1.3 (1.1)***	--
+ A13 (5 μM)	--[d]	45.1 ± 4.5 (1.1)***

[a] – mean ± standard error of n ≥ 3 independent experiments. [b] – mitoxantrone resistance factor is the IC_{50} value / IC_{50} of mitoxantrone + Ko143 (3.9 ± 1.2 nM). [c] – topotecan resistance factor is the IC_{50} value / IC_{50} of topotecan in MDCKII/P cells (42.9 ± 2.6 nM). [d] – significant cytotoxicity observed, IC_{50} was not determined. **p<0.01 ***p<0.001 significantly different from the IC_{50} of mitoxantrone or topotecan only control, calculated using one-way ANOVA and Dunnett's post-hoc test. Spaces left blank – IC_{50} was not determined.

3.3.5 Reversal of MRP1 and MRP5 mediated resistance

3.3.5.1 Growth inhibitory effects of test compounds on HEK/MRP1 and HEK/MRP5

The highest concentrations of A13, RL92, curcumin (CUR), indomethacin (Indo) and NPPB used in the resistance reversal studies were tested for growth inhibitory effects in HEK/MRP1 and HEK/MRP5. Figure 3-8 shows no significant effects on the proliferation of HEK/MRP1 (A) or HEK/MRP5 (B) after 72 h incubation with the compounds alone.

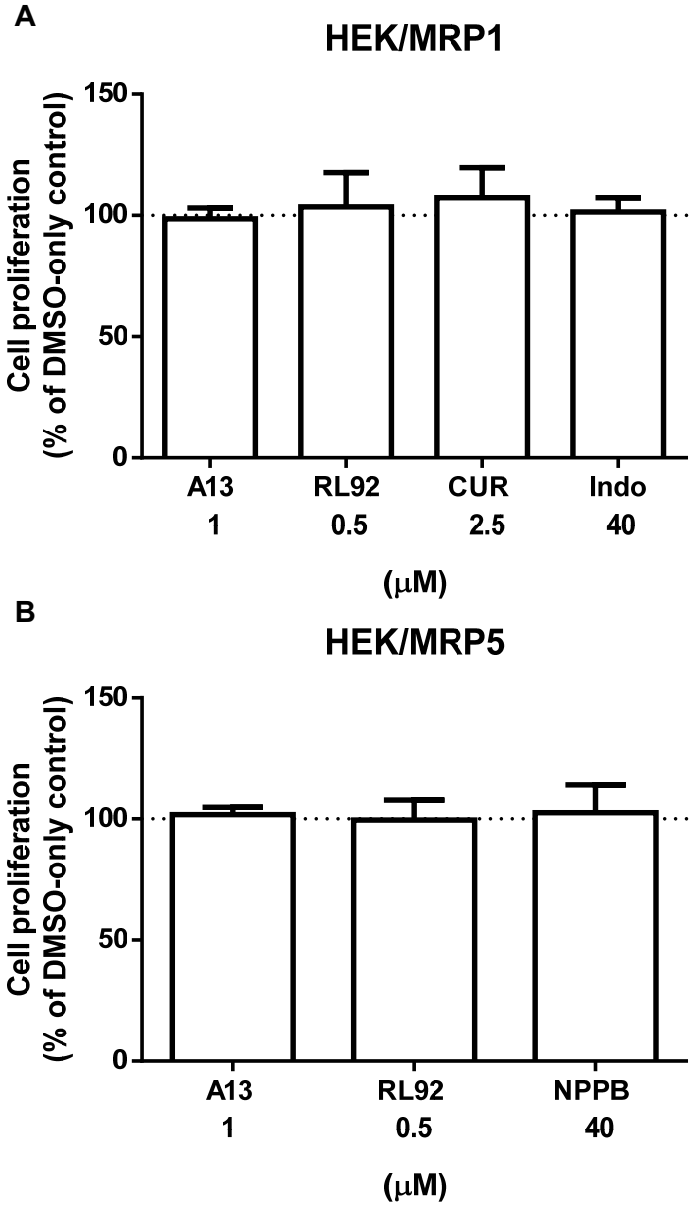

Figure 3-8. Effects of A13, RL92, curcumin (CUR), indomethacin (Indo) and NPPB on the proliferation of HEK/MRP1 (**A**) and HEK/MRP5 cells (**B**). Cells were incubated with complete media and the indicated test compounds for 72 h. Data are expressed as a % of the total proliferation in DMSO only control wells, quantified using SYBR-Green I DNA binding dye. Results are mean ± standard error of n ≥ 3 independent experiments done in triplicate.

3.3.5.2 Reversal of MRP1-mediated etoposide and doxorubicin resistance

The previously identified MRP1 inhibitors, A13 and RL92 (Chapter 2), were tested for reversal effects on HEK/MRP1 resistance to etoposide. Figure 3-9A shows that 1 μM A13 did not significantly affect etoposide IC_{50}. This was in contrast to indomethacin which restored sensitivity similar to parental cells. Both RL92 at 0.5 μM and curcumin at 2.5 μM also did not significantly affect etoposide IC_{50} (Figure 3-9B). The concentrations of A13, RL92 and curcumin were 12-, 45- and 6-fold lower than the recorded IC_{50} in the flow cytometry studies (Table 2-9), due to their anti-proliferative effects at higher concentrations (Table 3-3). A13 was also tested for resistance reversal of another MRP1 substrate, doxorubicin, in HEK/MRP1 cells. No significant effect on doxorubicin IC_{50} was observed with addition of 1 μM A13, but the positive control, indomethacin (40 μM), completely resensitised HEK/MRP1 to similar levels as parental cells (Figure 3-10). The summary of IC_{50} data for etoposide and doxorubicin resistance reversal assays are presented in Table 3-7.

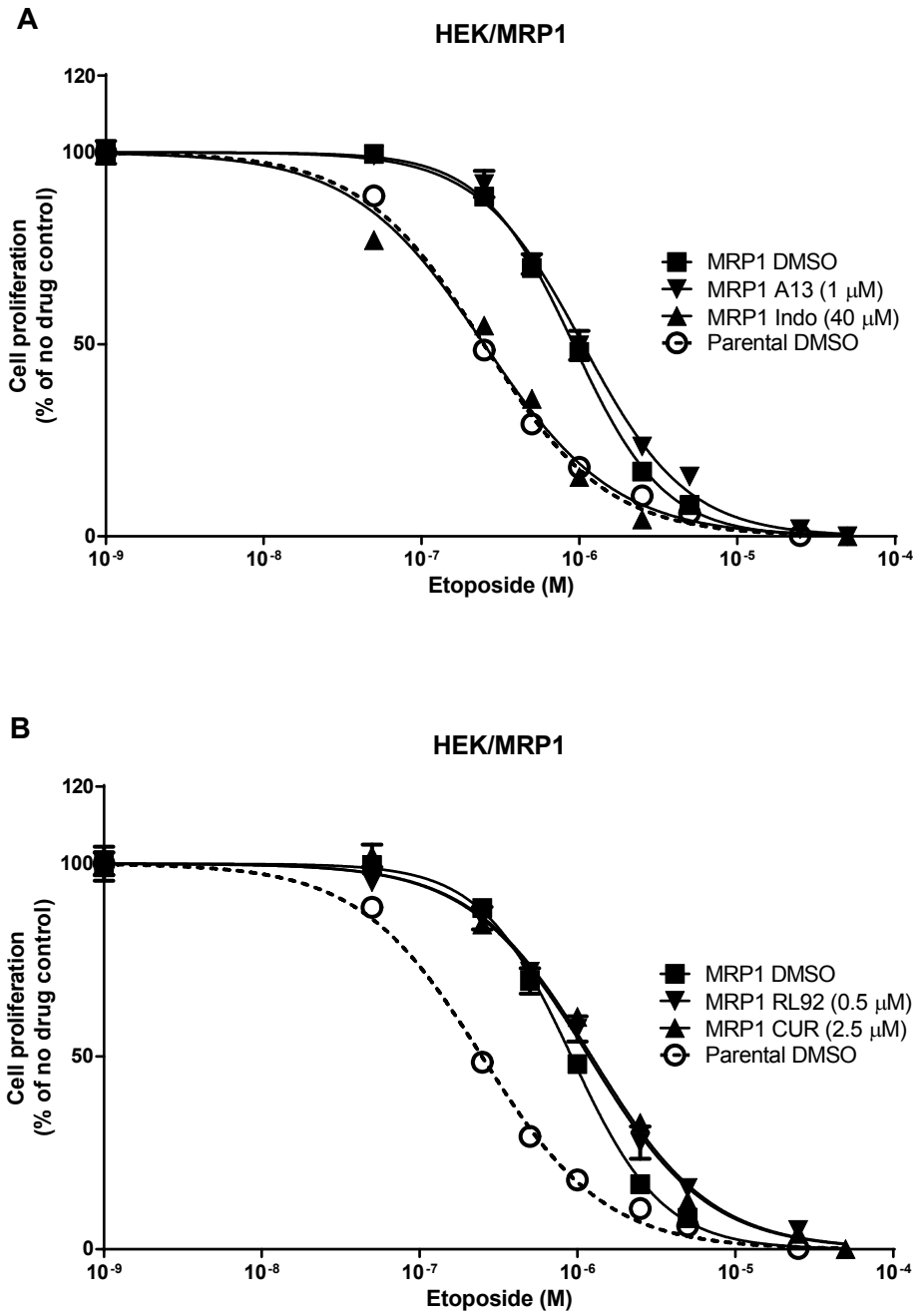

Figure 3-9. Inhibition of HEK/MRP1 (solid lines) and HEK/P (dashed lines) proliferation by etoposide. Etoposide was co-incubated with DMSO only; A13 or positive control, indomethacin (Indo) (**A**); RL92 or curcumin (CUR)(**B**). For simplicity, only etoposide concentration-response curves co-incubated with a high concentration of curcumin or analogues are included. Results are total DNA/well quantified using SYBR green I DNA binding dye. Data are presented as % of the fluorescence from no etoposide controls and are representative of n ≥ 3 independent experiments. Data points are mean ± standard error of triplicate.

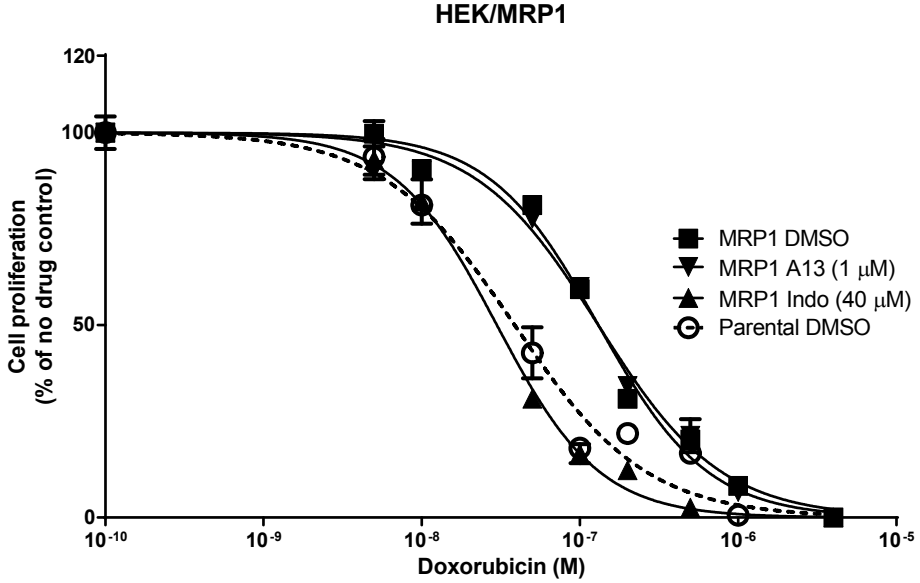

Figure 3-10. Inhibition of HEK/MRP1 (solid lines) and HEK/P (dashed lines) proliferation by doxorubicin. Doxorubicin was co-incubated with DMSO only (■) and (O); A13 (▼) or positive control, indomethacin (Indo) (▲). For simplicity, only the doxorubicin concentration-response curve co-incubated with a high concentration of A13 is included. Results are total DNA/well quantified using SYBR green I DNA binding dye. Data are presented as % of the fluorescence from no doxorubicin controls and are representative of n ≥ 3 independent experiments. Data are mean ± standard error of triplicate.

Table 3-7. The effects of curcumin and cyclohexanone analogues on the IC_{50} of doxorubicin or etoposide in HEK/MRP1 cells and HEK/P cells.

	IC_{50} ± SE[a] (nM)	
Compounds	**Etoposide**	**Doxorubicin**
HEK/MRP1		
Etoposide or doxorubicin + DMSO	986.3 ± 57.1 (4.8)[b]	126.8 ± 3.9 (3.2)[c]
+ Indomethacin (40 μM)	299.3 ± 49.3 (1.5)***	34.6 ± 2.5 (0.88)***
+ CUR (1 μM)	1031.0 ± 184.2 (5.1)	--
+ CUR (2.5 μM)	1080.5 ± 161.2 (5.3)	--
+ A13 (0.5 μM)	1147.9 ± 200.1 (5.6)	117.1 ± 8.1 (3.0)
+ A13 (1 μM)	1243.0 ± 125.2 (6.1)	114.6 ± 8.7 (2.9)
+ RL92 (0.25 μM)	1118.9 ± 102.1 (5.5)	--
+ RL92 (0.5 μM)	1054.9 ± 155.2 (5.2)	--
HEK/P		
Etoposide or doxorubicin + DMSO	204.1 ± 22.6	39.0 ± 2.2
+ Indomethacin (40 μM)	155.7 ± 32.2 (0.8)	--

[a] – mean ± standard error of n = 3 independent experiments. [b] – etoposide resistance factor is the IC_{50} value / IC_{50} of etoposide in HEK/P cells (204.1 ± 22.6 nM). [c] – doxorubicin resistance factor is the IC_{50} value / IC_{50} of doxorubicin in HEK/P (39.0 ± 2.2 nM). ***$p<0.001$ significantly different from the IC_{50} of doxorubicin or etoposide only control, calculated using one-way ANOVA and Dunnett's post-hoc test to compare all treatment groups with the control group. Spaces left blank – IC_{50} was not determined. CUR – curcumin.

3.3.5.3 Reversal of MRP5-mediated raltitrexed resistance

The previously identified MRP5 inhibitors, A13 and RL92 (Chapter 2), were tested for their ability to reverse resistance of the MRP5 substrate, raltitrexed, in HEK/MRP5 cells. Figure 3-11 shows that neither A13 (1 μM), nor RL92 (0.5 μM) increased the sensitivity of HEK/MRP5 cells to raltitrexed. The positive control NPPB (40 μM) only partially reversed raltitrexed resistance, but did not restore sensitivity to similar levels as HEK/P cells. Due to their anti-proliferative effects at high concentrations (Table 3-3), both A13 and RL92 were used at 12- and 34-fold lower concentrations than their reported IC_{50} of MRP5 inhibition from the flow cytometry studies (Table 2-9).

A summary of IC_{50} data from the raltitrexed resistance reversal assay is presented in Table 3-8.

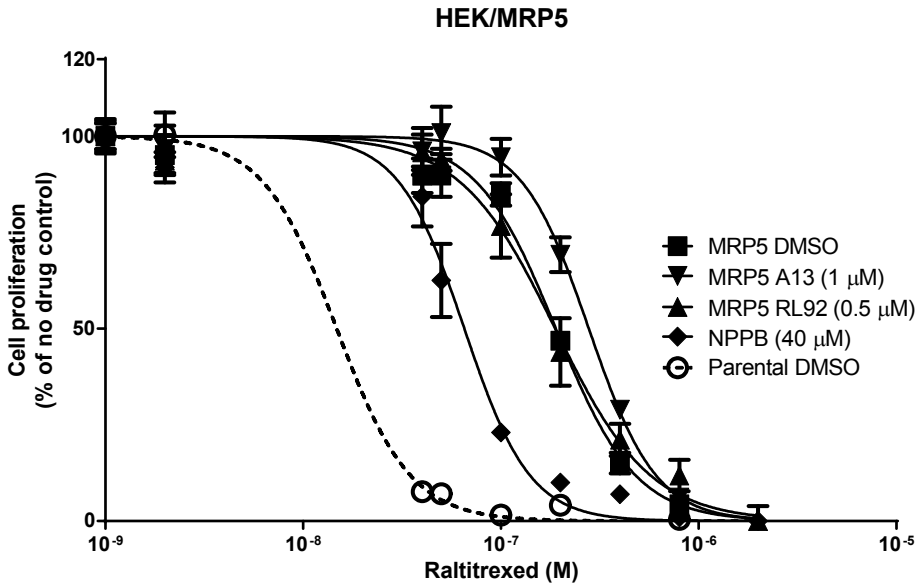

Figure 3-11. Inhibition of HEK/MRP5 (solid lines) and HEK/P (dashed lines) proliferation by raltitrexed. Raltitrexed was co-incubated with DMSO only (■) and (○); A13 (▼), RL92 (▲) or positive control, NPPB (◆). For simplicity, only raltitrexed concentration-response curves co-incubated with a high concentration of the analogues are included. Results are total DNA/well quantified using SYBR green I DNA binding dye. Data are presented as % of the fluorescence from no raltitrexed controls and are representative of n ≥ 3 independent experiments. Data points are mean ± standard error of triplicates.

Table 3-8. The effects of NPPB and cyclohexanone analogues on the IC_{50} of raltitrexed in HEK/MRP5 and HEK/P cells.

	IC_{50} ± SE[a] (nM)
Compounds	**Raltitrexed**
HEK/MRP5	
Raltitrexed + DMSO	182.3 ± 7.7 (12.0)[b]
+ NPPB (40 μM)	65.4 ± 0.1 (4.3)***
+ A13 (0.5 μM)	147.5 ± 8.6 (9.7)
+ A13 (1 μM)	205.3 ± 10.1 (13.5)
+ RL92 (0.25 μM)	169.1 ± 3.15 (11.1)
+ RL92 (0.5 μM)	159.1 ± 14.63 (10.5)
HEK/P	
Raltitrexed + DMSO	15.2 ± 1.8
+ NPPB (40 μM)	12.6 ± 2.8 (0.8)

[a] – mean ± standard error of n ≥ 3 independent experiments. [b] – raltitrexed resistance factor is the IC_{50} value / IC_{50} of raltitrexed in HEK/P (15.2 ± 1.8 nM). ***p<0.001 significantly different from the IC_{50} raltitrexed only control, calculated using one-way ANOVA and Dunnett's post-hoc test to compare all treatment with the control group.

3.4 Discussion

The aim of the resistance reversal studies was to confirm the inhibition of ABC transporter efflux activity by curcumin analogues identified using flow cytometry (Chapter 2). This was accomplished by directly determining the ability of the selected analogues to reverse the ABC-transporter mediated resistance to anticancer drug substrates. A secondary objective was to determine if the analogues were themselves substrates for the ABC transporters by comparing their anti-proliferative effects in transporter-expressing vs. parental cells.

Before commencing these studies, the linear range of the SYBR green assay was determined in the three cell lines used (MDCKII, HEK/P and BeWo) to ensure that the expected cell numbers in the reversal assays were accurately quantified. The SYBR green fluorescence assay was found to be linear at a range of 0.25 – 5 x 10^4 cells for HEK/P and MDCKII/P and 0.125 – 5 x 10^4 cells for BeWo (Section 3.3.1). Given a plating density for MDCKII/P of 2000 cells/well and a reported doubling time of 22 h (www.atcc.org), the expected total cell number after a 96 h period is 4.1 x 10^4 cells; well within the linear range of the assay (Cho et al., 1989). Both HEK/P and BeWo cells were observed to have slower doubling times than MDCKII/P (not shown) and would also be within the linear range. This also applied to transfected cells as they had equal (MDCKII/P-gp, MDCKII/BCRP) or slower growth rates (HEK/MRP1, HEK/MRP5) than parental cells (not shown).

With the linearity of the SYBR green assay established, the growth inhibitory effects of the selected analogues were determined to investigate if they were ABC-transporter substrates, and also to identify possible non-cytotoxic/cytostatic concentrations (Section 3.3.2). All compounds tested (A12, A13, B11, C10, RL92), exhibited growth inhibitory activity against MDCKII and HEK293 cells. This was not suprising as the analogues were previously shown to cause cell-cycle arrest and apoptosis in breast cancer cell lines (Somers-Edgar et al., 2011; Yadav et al., 2010). However, for all analogues, no significant difference in growth inhibition was seen between transfected and parental cells, suggesting that they are not effluxed by these transporters. BCRP overexpression did not confer resistance to A12, A13, B11 and RL92. P-gp expression did not cause resistance to C10 and RL92; nor did MRP1 and MRP5 expression affect cell sensitivity to the growth inhibitory effects of A13 and RL92. These results are similar to those for curcumin, which was reported to be an inhibitor, but not a substrate for P-gp, BCRP and MRP1 (Chearwae et

al., 2004, 2006a, 2006b). As these analogues are being investigated for activity against ER-negative breast cancer, the results suggest that these compounds may be effective against resistant tumors expressing ABC transporters since their cell penetration will not be limited by ABC-transporter mediated efflux (Somers-Edgar et al., 2011; Yadav et al., 2010). Analogues like RL92, which is not a substrate of P-gp, BCRP, MRP1 or MRP5 might be an effective cytotoxic agent against cancer cells that show ABC-transporter mediated MDR.

After the anti-proliferative effects were determined, concentrations of analogues that did not affect cell growth were selected for the resistance-reversal assays, and were further investigated for growth inhibition, together with curcumin and positive controls. None were found to significantly inhibit the proliferation of the cell lines over a 72 h period and were therefore not expected to interfere with the resistance-reversal assays (Figure 3-3, Figure 3-5, Figure 3-8).

For the P-gp resistance-reversal assay (Section 3.3.3.2), it was found that MDCKII/P-gp cells were 26-fold more resistant to paclitaxel antiproliferative effects than parental cells (Table 3-4). This could be completely reversed with the P-gp inhibitor verapamil (25 μM). Co-incubation with either C10 (1 μM) or RL92 (2 μM) significantly decreased paclitaxel resistance ($p < 0.001$) in MDCKII/P-gp cells to a similar level as parental cells. This confirmed the P-gp inhibitory activity from the flow cytometry studies, and in addition provided evidence that transport inhibition is not limited only to rhodamine-123 (see Chapter 2). Paclitaxel sensitivity in MDCKII/P cells was also significantly decreased by verapamil, C10 and RL92 ($p < 0.001$). This likely resulted from inhibition of previously reported endogenous canine P-gp in MDCKII/P although non-P-gp mediated mechanisms cannot be completely discounted (Kuteykin-Teplyakov et al., 2010). The extent of resistance reversal, however, was always greater in MDCKII/P-gp than MDCKII/P. Verapamil, C10 and RL92 decreased paclitaxel resistance 138-, 28- and 23-fold in MDCKII/P-gp cells, respectively, compared to only 14-, 14- and 7-fold in parental cells (Table 3-4). A completely non-specific mechanism would have resulted in an equal extent of reversion in both cell lines.

Curcumin at 10 μM was unable to reverse the IC_{50} of paclitaxel in MDCKII/P-gp cells, indicating that both C10 and RL92 were superior chemosensitisers (Table 3-4). However, the concentration used was 5-fold lower than the IC_{50} of P-gp inhibition from the flow cytometry studies (higher concentrations were cytotoxic), possibly explaining this lack of effect (Table 2-7). It should be

noted that C10 and RL92 were also used at maximum concentrations that were 3- and 4-fold lower, respectively, than their reported IC_{50} values for P-gp inhibition in the flow cytometry studies. Observed sensitisation at such low concentrations may be due to downregulation of the transporter over the long incubation period (Choi et al., 2008; Hou et al., 2008). Alternatively, the longer incubation time may have caused greater conversion to a more potent metabolite. This mechanism of inhibition was observed with caffeic acid in MRP1-transfected MDCKII cells (Wortelboer et al., 2005). Another possibility may be improved stability of C10 and RL92 in complete media compared to serum-free media (used in flow cytometry). For example, binding to albumin was reported to increase curcumin's half-life from 30 min to 8 h in serum-supplemented vs. serum-free media (Wang et al., 1997). However, perhaps the simplest explanation for these differences observed in inhibitory concentrations resides in assay sensitivity, as a consequence of a more prolonged incubation period (72 h vs. 15 – 120 min), and also the use of different probe substrates (paclitaxel vs. rhodamine-123). P-gp immunoblotting, identification of intracellular metabolites and media stability studies would help clarify these issues.

For BCRP, the analogues A12, A13, B11 and RL92 were tested for reversal of MDCKII/BCRP resistance to mitoxantrone (Section 3.3.4). As expected, MDCKII/BCRP cells were 15-fold more resistant to mitoxantrone than parental cells, and sensitivity could be completely restored by the BCRP inhibitor, Ko143. It was found that A12, A13, B11 and RL92, all showed significant concentration-dependent reversal of mitoxantrone resistance in MDCKII/BCRP cells with A12 and A13 at 5 μM completely restoring sensitivity (Table 3-5). This confirmed the results from the flow cytometry studies of BCRP inhibition by these analogues. Curcumin at 10 μM, also completely reversed mitoxantrone resistance, but the sensitisation was inferior to that of the analogues (Table 3-5). At 5 μM, curcumin sensitisation effects were similar to 2 μM of RL92 and less than that observed with similar concentrations of A12 and A13. None of the analogues, curcumin or Ko143 significantly affected mitoxantrone IC_{50} in MDCKII/P cells, indicating that resistance reversal was BCRP specific.

Due to their anti-proliferative effects, most of the analogues were used at concentrations well below their reported IC_{50} values for BCRP inhibition in the flow cytometry studies (Section 3.3.2). It was therefore perhaps surprising that significant resistance reversal was achieved. Complete

resensitisation by 5 μM A13 was unexpected as this concentration only inhibited BCRP transport by 50% in flow cytometry studies (Table 2-8). Similarly, both B11, RL92 and curcumin were used at maximum concentrations that were 10-, 5-, and 3-fold lower respectively than their IC_{50} of BCRP inhibition (Table 2-8), perhaps supporting the previous suggestion that the resistance-reversal assay is more sensitive than the corresponding flow cytometry assay. However, as discussed previously with P-gp inhibitors, other factors, such as increased stability in the media, conversion to a more potent metabolite, or downregulation of the the transporter cannot be ruled out, and further investigations are warranted.

As both the flow cytometry and resistance-reversal assays used the same BCRP substrate, mitoxantrone, there exists the possibility that transport inhibition by the analogues may be substrate-specific. BCRP is known to have multiple drug-binding sites, and substrate-dependent inhibition has been previously reported for BCRP (Ejendal and Hrycyna, 2005; Giri et al., 2009; Gupta et al., 2006). However, the two most potent inhibitors, A12 and A13, were able to concentration-dependently decrease the resistance of MDCKII/BCRP cells to another substrate, topotecan (Table 3-6). This demonstrated that the inhibition by A12 and A13 was not mitoxantrone-specific. Topotecan is also believed to bind to a site distinct from mitoxantrone (Nakanishi et al., 2003), but whether A12 and A13 interfere with transport by binding to a site that overlaps the two distinct binding sites is not known, and would require further radioligand displacement studies to answer this question. Binding to the NBD and blocking ATP hydrolysis could equally explain these results.

It was previously observed that the potency of curcumin differed between BCRP-transfected HEK293 and MDCKII cells, suggesting that inhibition may be cell-line dependent (Table 2-8). To ensure that the effects of the two most potent inhibitors (A12 & A13) were not specific to the canine MDCKII/BCRP cell line, studies were also conducted in human BeWo choriocarcinoma cells. BeWo cells endogenously overexpress BCRP under a native promoter, and thus may be sensitive to resistance reversal through transcriptionally-mediated downregulation unlike viral promoter-controlled BCRP in MDCKII/BCRP (Ceckova et al., 2006; Pavek et al., 2005). Both A12 and A13 were equally effective at sensitising BeWo cells to mitoxantrone, demonstrating that resistance reversal was not limited to MDCKII/BCRP. Whether the analogues affected BCRP

expression in BeWo is not known and would require further Western blotting studies and cell surface staining techniques.

In the MRP1 resistance-reversal assay (Section 3.3.5.2), the cytotoxic drug etoposide was used as substrate to test the sensitisation effects of A13 and RL92. HEK/MRP1 cells were 5-fold more resistant to the drug than the parental cells and they could be resensitised with the positive control, indomethacin (40 μM). In contrast, co-incubation with both A13 (1 μM) and RL92 (0.5 μM) failed to reverse etoposide resistance; similarly the addition of 2.5 μM curcumin had no effect. To rule out a specific issue with the substrate, similar experiments were also conducted using doxorubicin as substrate. HEK/MRP1 cells displayed doxorubicin resistance that was reversible with indomethacin (Table 3-7) but A13 at 0.5 μM and 1 μM had no significant effect on doxorubicin's IC_{50}. However, the inability of A13, RL92 and curcumin to reverse MRP1 resistance is likely due to the low concentrations used. Due to potent anti-proliferative effects on HEK293 cells, A13, RL92 and curcumin were used at maximum concentrations that were 12-, 44- and 6-fold lower respectively, than their IC_{50} values recorded for MRP1 inhibition in the flow cytometry studies (Table 2-9). A similar lack of effect by A13 and RL92 on the resistance of HEK/MRP5 to raltitrexed was observed. Maximum concentrations of A13 and RL92 were 12- and 32-fold lower than their IC_{50} of MRP5 inhibition (Table 2-9). The MRP1 and MRP5 reversal assays were therefore inconclusive and experiments should be repeated in transfected cell lines that are less sensitive to the anti-proliferative effects of these analogues. In addition, transporter inhibition could also be confirmed using cell-free assays, such as membrane vesicle uptake studies.

In summary, these studies using the resistance-reversal assays have confirmed P-gp inhibition by C10 and RL92, and BCRP inhibition by A12, A13, B11 and RL92; all selected from the flow cytometry screening (Chapter 2). In addition, both A12 and A13 were demonstrated to inhibit BCRP in a non cell-line and non-substrate-specific manner. These studies have also indicated that the selected analogues are poor substrates for these transporters, as observed by the lack of resistance of ABC-transporter transfected cells to the anti-proliferative effects of the analogues. Lastly, resistance reversal was not observed for A13 and RL92 in MRP1 and MRP5 overexpressing cell lines. However, the latter studies were considered inconclusive as potent anti-proliferative effects precluded the use of sufficiently high analogue concentrations. Further

experiments, such as the use of more robust transfected cell-lines, are required to accurately determine MRP1 and MRP5 resistance reversal by A13 and RL92.

4. Inhibition of BCRP transport activity in membrane vesicle uptake studies

4.1 Introduction

From the flow cytometry studies and the resistance reversal assays, it was determined that the curcumin analogues were most promising at inhibiting the BCRP transporter. The analogues A12, A13, B11 and RL92 displayed potent inhibition in flow cytometry studies and reversed BCRP-mediated drug resistance at low concentrations (≤ 5 μM), and in a non-substrate or cell line-specific manner. Therefore, the current and subsequent chapters have focused on further characterising the interactions of the analogues with BCRP. In this chapter, BCRP inhibition by A12, A13, B11, RL92 and curcumin was determined using a membrane vesicle assay. The main purpose was to ascertain whether inhibition by these analogues involved a direct interaction with the transporter. This was not apparent from the previous studies which used cell-based techniques (Chapter 2 & 3). In the latter, inhibition of transport activity could have been due to other mechanisms, such as the conversion of the analogue to an active metabolite, or perhaps, indirect modulation of BCRP expression (Glavinas et al., 2008; Nervi et al., 2010). The membrane vesicle assay is a cell-free system, with the transporter directly accessible from the assay buffer, and thus directly detects analogue-transporter interactions. In addition, by using a different model of transport, the vesicle studies will provide further evidence supporting BCRP inhibition by these analogues. Also, by using a different BCRP substrate, such as MTX, these studies will provide extra support that the BCRP inhibition of these analogues is non-substrate dependent.

The membrane vesicle uptake assay is a widely-used, high-throughput method for determining substrates and inhibitors of ABC transporters (Glavinas et al., 2008; Hegedus et al., 2009; Xia et al., 2007a). Membrane vesicles are spherical, bilayer structures formed by the resealing of ruptured plasma membranes from homogenised cells (Glavinas et al., 2008). These membrane vesicles can reseal in two different orientations and can be either right-side-out or inside-out (Figure 4-1) (Glavinas et al., 2008; Hegedus et al., 2009). The former has the bilayer oriented similar to intact whole cells; while the latter has the inner leaflet of the bilayer exposed to the

extravesicular space. Consequently, the ABC transporters present in inside-out vesicles have the cytoplasmic NBDs facing the extravesicular space, while the normally extracellular side of the protein projects into the vesicular lumen. As a result, these transporters mediate the uptake of substrate compounds into the vesicles, in contrast to their usual efflux role (Glavinas et al., 2008; Hegedus et al., 2009).

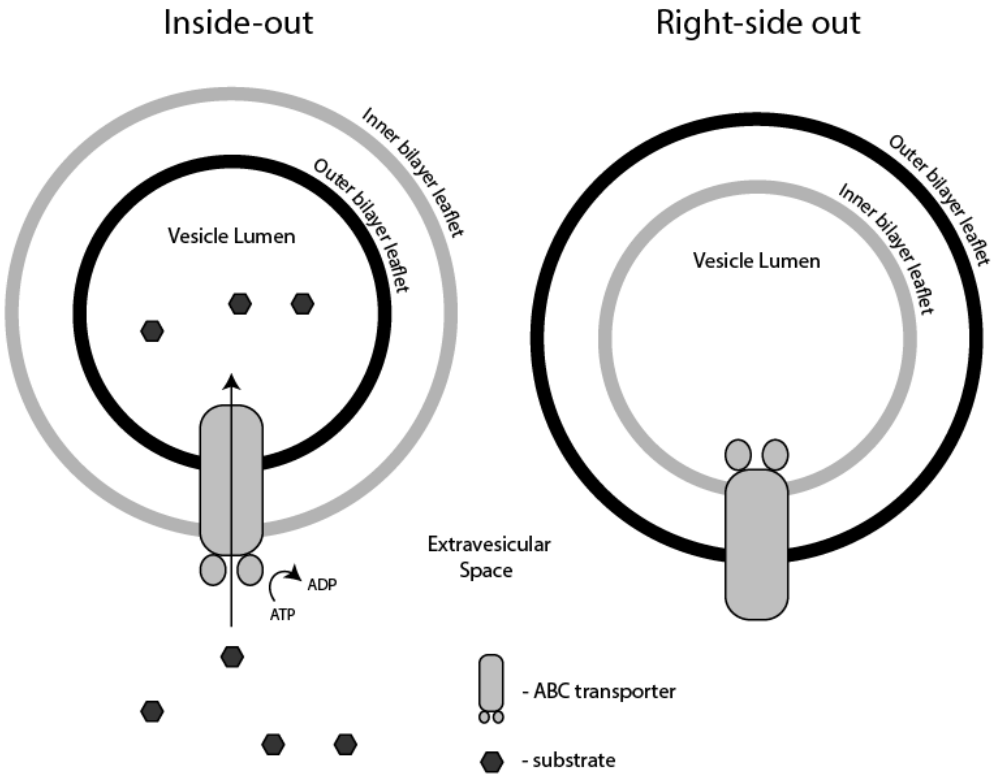

Figure 4-1. Orientation of bilayer leaflets and ABC transporters in inside-out and right-side-out membrane vesicles. In inside-out vesicles, the ABC transporter mediates uptake of the substrate compound into the vesicular lumen using ATP as an energy source. In right-side-out vesicles, the ABC transporter is oriented so that no uptake is observed. The nucleotide-binding domains are also not accessible to ATP present in the extravesicular space. In crude membrane preparations which are a mixture of both types of vesicles, right-side-out vesicles do not contribute to substrate uptake.

In the screening for ABC transporter inhibitors, a probe substrate is used as a reporter of transporter-mediated uptake activity (Brouwer et al., 2013; Glavinas et al., 2008; Xia et al., 2007a). These are often radiolabeled or fluorescent for easy detection and have low passive permeability and minimal non-specific binding to the vesicles (Glavinas et al., 2008). Test compounds are added with the probe together with the necessary co-factors (e.g., ATP), and incubated at 37°C to allow ATP-dependent transport to proceed. After the incubation period, the vesicles are separated

from the buffer by rapid filtration, and the vesicle-encapsulated probe substrate that remains in the filters is quantified by radioactivity counting, or fluorescence detection, or high-performance liquid chromatography and liquid chromatography-mass spectrometry (for unlabeled compounds) (Glavinas et al., 2008). Inhibition of the transporter of interest by the test compound will result in an observed decrease in probe uptake. This setup will not discriminate between substrates and non-transported inhibitors, as both will be able to interfere with probe uptake (Brouwer et al., 2013; Glavinas et al., 2008).

In contrast to cell-based methods like flow cytometry screening, the membrane vesicle assay directly reflects the affinity of the inhibitor for the transporter, as the substrate-binding site and NBDs of the ABC transporters in inside-out vesicles are directly accessible from the assay buffer. The measured IC_{50} values are therefore not affected by intracellular metabolism or by differences in cellular uptake of the test compounds (Glavinas et al., 2008; Nervi et al., 2010). They are also independent of compound lipophilicity, since passive diffusion through both leaflets of the bilayer is not necessary for inhibition (Hegedus et al., 2009; Nervi et al., 2010). Thus, this assay can detect interactions from hydrophilic molecules which are unable to diffuse to the substrate-binding site or NBDs using whole cells (Glavinas et al., 2008). A good example is the hydrophilic phytochemical, hesperidin, which inhibits BCRP in the membrane vesicle assay, but not in the cell-based flow cytometry assay (Tan et al., 2013a). The direct interaction between test compound and transporter makes the membrane vesicle assay suitable for determining transport kinetic parameters (Brouwer et al., 2013). The substrate concentration at half-maximal transport velocity (K_m) and the maximal transport rate (V_{max}) can be easily determined; while the dissociation constant (K_i) and the mechanism of inhibition (e.g., competitive, non-competitive) can be derived from Dixon plots of transport velocity at different probe and inhibitor concentrations (Brouwer et al., 2013).

In this chapter, the inhibition of BCRP by the analogues was characterised using a protocol that was used to screen therapeutic drugs and natural compounds (Ishikawa et al., 2005; Saito et al., 2006; Tan et al., 2013a, 2013b). Radiolabeled MTX, a hydrophilic antifolate with low non-specific binding to membrane vesicles, was used as a probe substrate (Brouwer et al., 2013; Saito et al., 2006; Volk et al., 2002). MTX has a low passive permeability across membranes, allowing for good retention inside vesicles after uptake transport (Hegedus et al., 2009; Volk et al., 2002). It is also

sensitive to displacement from low-affinity or weak inhibitors as it has a very high K_m (millimolar range) in BCRP transport studies (Saito et al., 2006; Volk et al., 2002). The assay used membrane vesicles from Sf9-insect cells transfected with wild-type human BCRP. These cells have an advantage over mammalian expression systems due to very high BCRP expression levels achieved and the lack of interference from mammalian transporters (Sarkadi et al., 1992). A creatine phosphate/creatine phosphokinase-based ATP regeneration system was also included in the assay protocol to ensure that ATP was not depleted during the course of the incubation (Ishikawa et al., 2005; Xia et al., 2007a). In addition, the use of 96-well plates considerably reduced the radioactive waste compared to other methods which use scintillation vials. The use of a rapid filtration technique also reduced assay variability by quickly filtering vesicles after incubation, leading to less MTX leak-back into the buffer (Brouwer et al., 2013). Along with the BCRP-expressing vesicles, parental controls were included to assess the contribution of non-BCRP mediated processes on MTX uptake, and no-ATP controls determined any ATP-dependent component of MTX uptake. Ko143 was used as positive control for BCRP inhibition (Allen et al., 2002).

4.2 Materials and Methods

4.2.1 Chemicals and reagents

Materials (purity indicated) were purchased from the following sources: MTX (≥99.0%) from Selleck Chem, Houston, TX; radiolabeled MTX ($^{[3H]}$MTX) (1 mCi/mL, 1:1 ethanol/water solution) from American Radiolabeled Chemicals, St Louis, MO; adenosine 5′-triphosphate (ATP) disodium salt hydrate (≥99.0%), creatine phosphokinase (≥50 units/mg protein), creatine phosphate (≥98.0%) from Sigma-Aldrich, St Louis, MO. The sources of high purity curcumin, A12, A13, B11, RL92 and Ko143 were previously outlined in Section 2.2.2. Unlabeled MTX was dissolved in pure DMSO as 40 mM stock solution. ATP was dissolved with $MgCl_2$ as a 200 mM MgATP solution using ultrapure Milli-Q water (Merck-Millipore, Billerica, MA). Both creatine phosphate (0.5 M) and creatine phosphokinase (4 mg/mL) were prepared in Buffer A (Table 4-1). All solutions were aliquoted and stored at -20°C.

4.2.2 Membrane vesicles

The membrane vesicles were kindly provided as a crude membrane vesicle preparation (mix of inside-out and right-side-out vesicles, Figure 4-1) by Dr Kee Tan (Plant and Food Research, Auckland, NZ). The membrane vesicles were isolated from parental Sf9 insect cells (Sf9/P) and cells transfected with the human wild-type BCRP transporter (Sf9/BCRP) as previously outlined in detail by Tan et al. (2013a, 2013b), together with the characterisation of BCRP expression and functional transport activity. Upon receipt of the vesicles, total protein concentrations were measured with the Biorad-DC™ protein assay (Biorad, Hercules, CA) and all samples were stored at - 80°C.

4.2.3 Membrane vesicle transport assay

The vesicle transport assay is a modification of the protocol used by Tan et al. (2013a) which was based on the original method by Ishikawa et al. (2005). Membrane vesicles, supplied as a suspension in Buffer A, were thawed at 4°C and diluted with the same buffer to a total protein concentration of 2.78 µg/µl (see Table 4-1 for Buffer A composition). The diluted vesicles were then added to a 96-well plate at a volume of 18 µl/well (50 µg vesicles) (see Figure 4-2 for plate layout). Next, the test compounds at 50x the final concentration (dissolved in DMSO) were added in a volume of 1 µl and the plates were incubated at 37ºC for 5 min. The reaction was started by adding 31 µl of pre-warmed (37ºC) Buffer B (see Table 4-1) and the plates were incubated at 37°C for 20 min. Reaction start and stop times were staggered to take into account the time delays in reagent addition between samples, and to ensure that variations in incubation times were kept to a minimum. After the incubation period, the reaction was stopped by the addition of 150 µl ice-cold Buffer A and the mixture was quickly transferred to a 96-well Multiscreen HTS-FB plate (Merck-Millipore, Billerica, MA). A vacuum was then applied to the filter plate, and 200 µl Buffer A was thrice added to the wells to wash excess radiolabel from the filters. After all the samples were filtered, the plate underdrain was removed and the plate was allowed to dry overnight. The bottom of the plate was then sealed with adhesive film and 50 µl Optiphase supermix scintillation cocktail (Perkin Elmer, Waltham, MA) was added to each well. After sealing the top of the plate with a clear PCR adhesive film, it was incubated for 24 h and then read using a a Wallac Trilux 96-well scintillation counter (Perkin Elmer, Waltham, MA).

All samples in the assay had a final DMSO concentration of 2.25%. This caused a slight (5-10%) but significant decrease ($p < 0.05$) in MTX uptake compared to no-DMSO controls. To account for this, each experiment included DMSO-only controls and the readings from these wells were used to normalise the data (see plate layout, Figure 4-2).

Table 4-1. Composition of Buffer A and Buffer B.

Buffer A	0.25 M sucrose, 10 mM Tris/HEPES, $pH_{7.4}$, 6 mM $MgCl_2$, dissolved in ultrapure Milli-Q water
Buffer B	0.25 M sucrose, 10 mM Tris/HEPES, $pH_{7.4}$, 10 mM $MgCl_2$, 4 mM ATP, 10 mM creatine phosphate, 100 µg/ml creatine phosphokinase, 100 µM MTX, 0.67 µM $^{[3H]}$MTX (specific activity: 15 Ci/mmol), dissolved in ultrapure Milli-Q water

	1	2	3	4	5	6
	Controls		Compound A		Compound B	
A	Parental controls	Parental controls	DMSO	DMSO	DMSO	DMSO
B	Ko143 (1 µM)	Ko143 (1 µM)	A1	A1	B1	B1
C	ATP +	ATP +	A2	A2	B2	B2
D			A3	A3	B3	B3
E			A4	A4	B4	B4
F			A5	A5	B5	B5
G			ATP -	ATP -	ATP -	ATP -
H						

Figure 4-2. Plate layout of a typical experiment with 5 concentrations each of two test compounds done in duplicates. Only half of a 96-well plate is depicted. Parental control wells contain Sf9/P membrane vesicles instead of Sf9/BCRP. Ko143 incubated wells were included as positive inhibition control. ATP+ wells measured MTX uptake without DMSO. DMSO-only wells were used for data normalisation and was set as 100% MTX uptake in concentration-response curves. ATP- controls was used to measure radioactivity from non-active processes and was substracted from the data. It was therefore set as 0% in the concentration-response curves.

4.2.4 Data and statistical analysis

The scintillation counter quantified the extent of radiolabeled MTX uptake into vesicles as counts per minute (CPM). In Section 4.3.1, raw CPM values for the different samples were normalised to the CPM values from DMSO-only incubated Sf9/BCRP vesicles. The latter samples were set as 100% $^{[3H]}$MTX-uptake.

In Section 4.3.2, all data were background substracted using CPM readings from no-ATP control Sf9/BCRP vesicles (set as 0% $^{[3H]}$MTX uptake). The difference, therefore, represented the ATP-dependent MTX uptake. All values were then normalised to the ATP-dependent MTX uptake in DMSO-only control wells (100% $^{[3H]}$MTX uptake).

To determine the IC_{50} value of MTX uptake inhibition, logarithmic concentrations of the analogues were plotted against normalised $^{[3H]}$MTX uptake and a non-linear regression curve was fitted using Graphpad Prism 6.0. The software calculated both the IC_{50} and the Hill slopes using Equation 2-3 (see Section 2.2.7).

Statistical analysis was also carried out using the same software. Statistical significance was determined using one-way ANOVA paired with the Dunnett's control-comparison test. The latter test was used to compare the mean $^{[3H]}$MTX uptake for all treatment groups against the uptake from DMSO-only wells in Figure 4-4. The same test was also used to compare the IC_{50} values of all treatment groups to that of curcumin and to determine if the Hill-slopes of the concentration-response curves significantly differed from -1.0. A p-value of < 0.05 was considered significant.

4.3 Results

4.3.1 Methotrexate uptake in Sf9/BCRP membrane vesicles

Before commencing, the Sf9/BCRP membrane vesicles were first confirmed for ATP-dependent, Ko143-inhibitable uptake of $^{[3H]}$MTX. Figure 4-3 shows that MTX uptake was considerably higher (11.4-fold) in Sf9/BCRP membrane vesicles compared to vesicles isolated from untransfected Sf9/P insect cells. This higher uptake was ATP-dependent, since incubation of Sf9/BCRP with ATP-free buffer resulted in a similar uptake as Sf9/P vesicles. Uptake was also confirmed to be Ko143-inhibitable as the addition of 0.5 µM Ko143 significantly reduced MTX accumulation to 12% ($p < 0.001$) compared to that of DMSO-only controls.

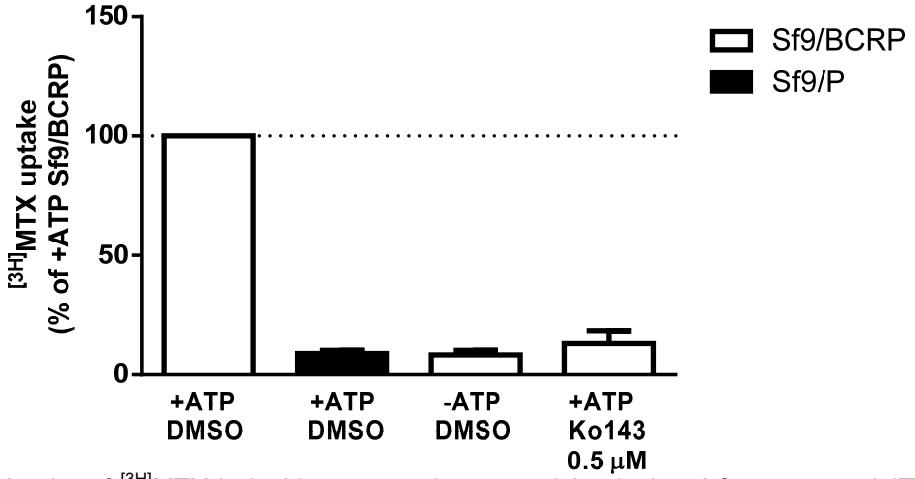

Figure 4-3. Uptake of $^{[3H]}$MTX in inside-out membrane vesicles isolated from parental (■) (Sf9/P) and BCRP-transfected Sf9 insect cells (□) (Sf9/BCRP) in the presence or absence of ATP and BCRP inhibitor (Ko143). Results are counts per minute (CPM) normalised to the CPM of Sf9/BCRP vesicles incubated with ATP and DMSO. Data is presented as mean ± standard error of n = 3 independent experiments, done in duplicate. Final DMSO concentrations for all samples was 2.25%.

4.3.2 Inhibition of methotrexate uptake by curcumin analogues

To gain further insight into analogue-BCRP interactions and provide additional evidence of BCRP inhibition, studies using cell-free membrane vesicles were conducted. These studies demonstrated that the analogues previously reported to inhibit BCRP from flow cytometry and cell proliferation assays (A12, A13, B11, RL92), significantly inhibited the uptake of MTX at 10 μM ($p < 0.001$) (Figure 4-4). Both A12 and A13 decreased uptake to 15% of DMSO-only controls; while curcumin, B11 and RL92 reduced uptake to less than 10%. In addition, 20 μM of A2 and B1 significantly inhibited the uptake of MTX into vesicles to 53% and 59% of DMSO-only controls ($p < 0.001$) (Figure 4-4). The latter two were included for comparison as both compounds lacked any BCRP inhibition in the flow cytometry studies (Chapter 2).

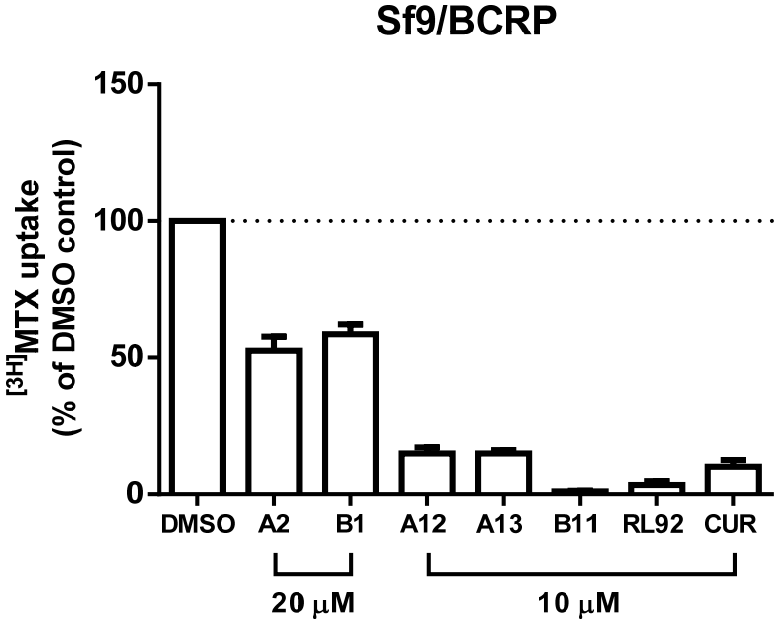

Figure 4-4. Inhibition $^{[3H]}$MTX uptake by curcumin (CUR) and cyclohexanone analogues in Sf9/BCRP inside-out membrane vesicles. Results are counts per minute (CPM) normalised to the CPM in DMSO-only controls. Before data normalisation, raw CPM values were subtracted using the CPM from no-ATP samples; this represented background radioactivity. Data are mean ± standard error of n = 3 independent experiments done in duplicate. Final DMSO concentration for all samples was 2.25%.

The potency of MTX uptake inhibition was determined for A12, A13, B11 and RL92, together with curcumin and the BCRP inhibitor, Ko143. The latter two were used as references to compare analogue potencies with the parent compound (curcumin) and a widely used BCRP inhibitor (Ko143). Figure 4-5 shows that all compounds tested were able to concentration-dependently inhibit the uptake of MTX. Of the analogues, RL92 was found to be the most potent with an IC_{50} of 0.62 ± 0.05 μM; while A12 was the least potent with an IC_{50} of 1.63 ± 0.28 μM. The apparent order of potency compared to curcumin was RL92 > B11 > curcumin > A13 > A12, although a multiple comparison test has not found any significant differences in IC_{50} value between the analogues and curcumin (Table 4-2). In contrast to these results, the IC_{50} of Ko143 (0.025 ± 0.002 μM) was significantly lower ($p < 0.01$) compared to curcumin's (1.04 ± 0.13 μM), making it 42-fold more potent at inhibiting MTX uptake (Table 4-2). Likewise, Ko143 was a superior inhibitor than the most potent analogue, RL92, despite the latter having a sub-micromolar IC_{50}.

From the concentration-response curves, the Hill slopes were also derived to gain an insight into analogue-transporter interactions. It was found that the Hill slopes for A12, A13, RL92 and curcumin, did not significantly differ from -1.0 (single-site binding to the transporter); while significantly greater Hill slopes were observed for B11 and Ko143 ($p < 0.01$), suggesting multi-site binding to BCRP (Table 4-2).

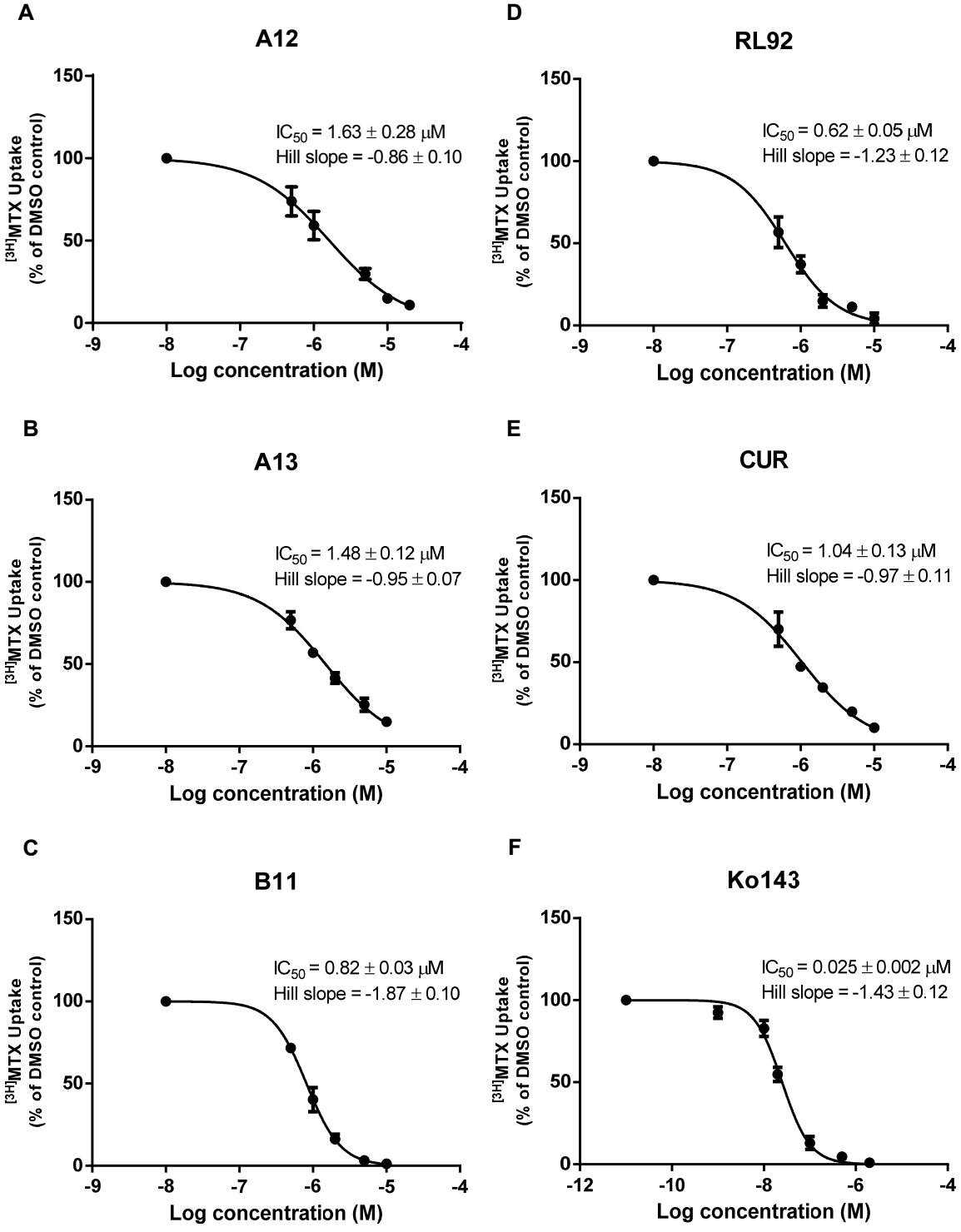

Figure 4-5. Concentration-response curves for the inhibition of [3H]MTX uptake in Sf9/BCRP inside-out membrane vesicles by A12 (**A**), A13 (**B**), B11 (**C**), RL92 (**D**), curcumin (CUR) (**E**) and Ko143 (**F**). Results are normalised to counts per minute (CPM) from DMSO-only control samples. Raw CPM values were subtracted with CPM readings in no-ATP controls (0% baseline) which represent non-specific binding. Data points are mean ± standard error of n = 3 independent experiments done in duplicates. Non-linear regression, IC_{50} and Hill slope values (± standard error) were calculated using Graphpad Prism 6.0. Final DMSO concentration for all samples was 2.25%.

Table 4-2. Summary of IC_{50} and Hill slope values for the inhibition of radiolabeled MTX uptake in Sf9/BCRP inside-out membrane vesicles by curcumin, cyclohexanone analogues and Ko143 (see Figure 4-5).

Compounds	IC_{50} ± SE[a] (μM)	Hill slope ± SE
Curcumin	1.04 ± 0.13	-0.97 ± 0.11
Ko143	0.025 ± 0.002**	-1.43 ± 0.12†
A12	1.63 ± 0.28	-0.86 ± 0.10
A13	1.48 ± 0.12	-0.95 ± 0.07
B11	0.82 ± 0.03	-1.87 ± 0.10†††
RL92	0.62 ± 0.05	-1.23 ± 0.12

[a] – mean ± standard error (SE) of n = 3 independent experiments. **p<0.01 significantly different from the IC_{50} of curcumin, calculated using one-way ANOVA and Dunnett's post-hoc test to compare all treatment with curcumin IC_{50}. †p<0.05, †††p<0.001 Hill slope significantly different from -1.0, one-way ANOVA and Dunnett's post-hoc test.

4.4 Discussion

Both the flow cytometry and resistance-reversal assays have shown that A12, A13, B11 and RL92, inhibited the functional activity of BCRP. However, neither assay has clearly demonstrated a direct interaction between these analogues and the transporter. In the current chapter, the cell-free membrane vesicle assay was used to investigate such an interaction, as well as provide additional evidence of BCRP inhibition by the selected analogues.

The preliminary tests on the vesicle preparations were conducted to ensure that functional BCRP activity was retained after transport and storage (Section 4.3.1). It was also important to demonstrate that MTX uptake in these vesicles was primarily BCRP-mediated, with little interference from other processes, such as passive influx, or the presence of other transporters (Brouwer et al., 2013; Glavinas et al., 2008). These preliminary tests indicated an approximately 11-fold greater MTX accumulation in Sf9/BCRP vesicles compared to the corresponding untransfected, parental Sf9 vesicles (Figure 4-3). This increased accumulation was ATP-dependent, since Sf9/BCRP vesicles incubated in ATP-free buffer had little uptake of radioactivity, similar to that of parental controls. These results were consistent with active uptake transport being responsible for the increased accumulation of MTX. The addition of the highly-selective BCRP inhibitor, Ko143, also decreased accumulation to levels similar to parental or no-ATP controls. This indicated that virtually all of the ATP-dependent MTX uptake was BCRP-mediated, with little-to-no contribution from other active processes. There was some low-level radioactivity observed in parental and no-ATP controls, likely resulting from non-specific binding to vesicles and filters, as well as some passive permeation of the labeled MTX (Glavinas et al., 2008; Hegedus et al., 2009). Thus, the subsequent inhibition experiments included no-ATP controls, which were used to substract background radioactivity from the data, to ensure that only ATP-dependent transport was measured.

The analogues investigated using the Sf9/BCRP vesicles included A12, A13, B11 and RL92 (10 μM), which were identified as BCRP inhibitors from flow cytometry and resistance-reversal studies. In addition, curcumin (10 μM), A2 and B1 (20 μM), were included for comparison, with the latter two being selected due to a lack of activity in the flow cytometry studies (see Figure 2-11). All analogues, including A2, B1 and curcumin, significantly inhibited the uptake of MTX in membrane

vesicles. This provided the first evidence of a direct interaction of these compounds with BCRP, and indicated that the compounds themselves could inhibit the transporter, without requiring conversion to an active metabolite or the existence of an alternative mechanism (e.g., modulation of BCRP expression). Direct inhibition is desirable for inhibitors, as compounds that rely on bioactivation, or downregulation of transporter expression are more likely to exhibit cell-specific effects, since such compounds are only active in cells with the necessary bioactivation pathways or transcription factors. However, it should be noted that although direct transport modulation has been observed, it does not preclude other mechanisms of inhibition. There is a possibility that in some cell lines, the analogues downregulate BCRP expression, as well as directly inhibit BCRP transport. To examine this, protein expression studies using immunoblotting and cell surface staining are needed.

Aside from demonstrating direct inhibition of BCRP, these results further confirm the findings of previous chapters that these analogues are BCRP inhibitors as consistent modulation of transport activity has been seen in three different transport models. Also, the data provides additional evidence of a non-substrate specific effect, since, in addition to mitoxantrone and topotecan, transport inhibition of MTX has been demonstrated. The inhibition of MTX transport is important, as BCRP radioligand binding studies conducted by Clark et al. (2006) have indicated a distinct binding site from that of mitoxantrone. This suggests that these analogues will inhibit other substrates that are transported via the MTX binding site.

It was also interesting to note that the analogues A2 and B1, which lacked activity in the flow cytometry screening (see Figure 2-11), showed significant inhibition ($p < 0.01$) of MTX uptake. It is possible that this was due to substrate-specific inhibition, and that both analogues competed with MTX, but not mitoxantrone binding (the latter being the substrate in flow cytometry). Another explanation is that the weak inhibition by A2 and B1 in whole cells is due to their reduced access to the TMD or NBD of BCRP compared to potent analogues like A12 and A13. Access to these sites in whole cells is dependent on membrane partitioning from the extracellular media to the inner bilayer leaflet, which may be limited for A2 and B1 due to their polar pyridine groups (Figure 2-2). In contrast, these sites are readily accessible to the media/buffer in membrane vesicles, possibly explaining the observed inhibition by both analogues. To help determine which of the two

mechanisms is valid, vesicle studies using radiolabeled E3S could be conducted, which will eliminate the possibility of substrate-specific inhibition (Imai et al., 2012). Mitoxantrone itself cannot be used due to its high passive permeability. E3S is a suitable replacement as it is hydrophilic, and appears to be transported through the same binding site as mitoxantrone (they competitively inhibit each other's transport) (Suzuki et al., 2003).

The IC_{50} values determined for A12, A13, B11 and RL92 in the Sf9/BCRP vesicles varied from 0.6 – 1.6 μM and were not significantly different from each other, nor from that observed for curcumin (1.04 ± 0.13 μM). Only Ko143 had a significantly lower IC_{50} (0.025 ± 0.002 μM, $p < 0.01$), which was similar to that reported by Tan et al. (2013a) (0.026 μM) and Allen et al. (2002) (IC_{90} of 0.023 μM). The results therefore indicated that curcumin and the analogues have a similar affinity towards BCRP. This supports the previous suggestion from the flow cytometry studies (see Section 2.4) that the large potency differences in MDCKII/BCRP cells was caused by differential susceptibility to intracellular metabolism, rather than affinity differences for BCRP.

The Hill slopes for the concentration-response curves of A12, A13, RL92 and curcumin (but not B11), indicated one-site binding to the transporter, which agreed with the data for mitoxantrone inhibition in the flow cytometry studies (Section 2.3.2.2). Whether this single binding site overlaps the mitoxantrone, topotecan and MTX binding sites, or the ATP-binding site, is not known. Further membrane vesicle studies could have helped clarify this issue by identifying competitive or non-competitive inhibition of MTX by the analogues, using methods such as Dixon plots (Brouwer et al., 2013). However, due to the limited supply of membrane vesicles, such studies were not conducted.

It was interesting to note that the Hill slope for B11 indicated cooperativity in the vesicle assay but single-site binding in the flow cytometry studies. The reason for this difference is not known. Binding stoichiometry should have remained consistent regardless of substrate, unless MTX treatment exposed an additional binding site for B11. As the latter is uncommon, this cooperative inhibition needs further confirmation using uptake studies with other substrates, such as radiolabeled estrone-3-sulfate (Imai et al., 2012). Apart from B11, Ko143 also showed cooperative inhibition, consistent with previous studies (Pan et al., 2007; Wanek et al., 2012).

In summary, the membrane vesicle assay has provided evidence that the analogues A12, A13, B11 and RL92 directly inhibit the BCRP transporter, without requiring bioactivation or modulation of transporter expression. These studies have further confirmed the results from previous chapters that these analogues are BCRP inhibitors. In addition, the assay demonstrated transport inhibition of a third BCRP substrate, MTX, supporting non-substrate specific inhibition by these compounds. Some insights into the binding stoichiometry and relative affinity of these analogues for this transporter were also gained. In this cell-free system, the analogues had a similar affinity for a single-binding site on BCRP, supporting a previous suggestion that potency differences between the analogues in the BCRP flow cytometry screening were not due to differences in affinity for the transporter.

5. Modulation of total BCRP protein expression by curcumin and selected analogues

5.1 Introduction

It has been previously observed that the curcumin analogues A12, A13, B11 and RL92 can reverse BCRP-mediated resistance to cytotoxic substrates at concentrations that were too low to directly modulate transporter activity in the flow cytometry studies (Chapter 2). A number of reasons were discussed to account for this discrepancy (Section 3.4). Of these, one possibility was that the curcumin analogues may have downregulated the expression of the transporter at low concentrations. This mechanism was considered as previous studies have shown that curcumin and some related cyclohexanone analogues can modulate signaling pathways and transcription factors that regulate BCRP expression. These include reports of inhibition of the PI3K/AKT pathway which post-transcriptionally upregulates the expression of the transporter and inhibition of the NF-κB protein complex, which directly binds to the BCRP promoter region and activates gene transcription (Nakanishi and Ross, 2012; Qiao et al., 2013; Somers-Edgar et al., 2011; Wang et al., 2010b; Yadav et al., 2010, 2012a). The aim of this study was therefore to determine if BCRP protein downregulation was the reason for the significant reversal of mitoxantrone resistance by A12, A13, B11 and RL92 in the 72 h resistance reversal assays. Showing the downregulatory effects of these compounds is also important as it would complement their direct inhibition of BCRP transport, and enhance their effectiveness as MDR reversal agents.

To determine the downregulatory effects of curcumin and the selected analogues on BCRP expression, sodium dodecyl sulfate – polyacrylamide gel electrophoresis (SDS-PAGE), followed by immunoblotting, were used to resolve and semi-quantitatively measure the protein from isolated membrane fractions of treated cells. This technique is the most widely used assay for detecting downregulation of a protein of interest, and is accurate and reproducible provided that a few important requirements are met (Blancher and Jones, 2001; Madamanchi and Runge, 2001). These include: the need for a highly specific antibody to the target protein; the use of a reliable

loading control to adjust for uneven sample loading and protein transfer; the use of a suitable cell model that is responsive to downregulation; and a sufficiently long incubation period to detect changes in protein expression levels.

In this study, a mouse monoclonal antibody, BXP-21, was used to detect BCRP. It is the most popular antibody for the detection of this transporter, due to its specificity and lack of cross-reactivity against other members of the ABC protein family, such as P-gp, MRP1 and MRP2 (Maliepaard et al., 2001; Xia et al., 2005). BXP-21 has seen extensive application in immunoblotting, and has been used to demonstrate BCRP downregulation by therapeutic drugs, such as tyrosine kinase inhibitors (e.g., gefitinib), experimental compounds such as PI3K inhibitors (e.g., LY294002), endogenous hormones (e.g., estrogen), and phytochemicals (e.g., EGCG from green tea) (Farabegoli et al., 2010; Imai et al., 2005; Pick and Wiese, 2012). In all cases, the antibody specifically detected BCRP, without cross-reacting with other proteins. In addition, the BXP-21 antibody was found to effectively detect both glycosylated and un-glycosylated forms of BCRP, allowing it to measure the total BCRP expression in cells (Maliepaard et al., 2001; Mohrmann et al., 2005).

To fulfill the requirement for a reliable loading control, the current assay avoided the use of traditional house-keeping proteins such as β-actin, tubulin and glyceraldehyde-3-phosphate (Ferguson et al., 2005). This was based on reports that these proteins were not always consistently expressed, and could be influenced by biochemical stimuli and other factors such as cell growth and differentiation (Dittmer and Dittmer, 2006; Gilda and Gomes, 2013; Ruan and Lai, 2007). The use of such high abundance proteins may also result in chemiluminescent detection falling out of the linear range, especially when high amounts of total protein are loaded (Aldridge et al., 2008). The latter may cause the loading control to no longer correlate with protein concentration (Aldridge et al., 2008; Dittmer and Dittmer, 2006). Numerous reports have demonstrated that total protein stains, such as SYPRO ruby, coomassie blue, ponceau S, or amido black and silver staining are superior loading controls compared to traditional house-keeping proteins (Aldridge et al., 2008; Lopez et al., 2000; Romero-Calvo et al., 2010). These stains have a lower susceptibility to variations in protein expression, and a greater linear dynamic range. The SYPRO ruby stain was chosen as it is one of the most sensitive total protein stains

(similar in sensitivity to silver staining), and with the largest linear dynamic range (1 ng – 1 µg protein) (Lopez et al., 2000). SYPRO ruby staining is performed on PVDF or nitrocellulose membranes after the protein transfer step, but before antibody incubation. This allowed for the control of uneven protein transfer and also prevented antibody binding to the membrane which might interfere with the staining (Aldridge et al., 2008).

The two cell lines (MDCKII/BCRP and BeWo choriocarcinoma cells) used in this study, have been successfully used in the past to identify BCRP downregulators, and were considered suitable cell models for detecting downregulation. BCRP downregulation by the tyrosine kinase inhibitor, gefitinib, and the PI3K inhibitor LY294002, was demonstrated in MDCKII/BCRP cells; while BeWo choriocarcinoma cells helped characterise the downregulatory effects of estrogen and 17β-estradiol (Imai et al., 2005; Pick and Wiese, 2012; Wang et al., 2006). Two cell lines were utilised in this investigation because MDCKII/BCRP is sensitive only to post-transcriptional mechanisms of downregulation, since it expresses BCRP under constitutive viral promoter control (Pavek et al., 2005). By using BeWo cells expressing BCRP under the native promoter, the assay can detect both transcriptional and post-transcriptional mechanisms of downregulation (Imai et al., 2005). In addition, the use of both cell lines allows the identification of compounds that downregulate BCRP exclusively through native promoter-dependent transcriptional mechanisms, as an effect would be seen in BeWo, but not in MDCKII/BCRP cells. In the determination of BCRP protein expression, crude membrane fractions were isolated from these cells, rather than whole cell lysates. Membrane fractions are enriched with membrane-bound proteins like BCRP, resulting in a stronger signal compared to cell lysates. A cleaner blot is also obtained, due to less interference from cytosolic proteins.

Due to the long half-life (35 h) of BCRP protein, an incubation period of 72 h was used to better detect downregulation by compounds that inhibit new protein synthesis (Imai et al., 2005). A shorter incubation period (e.g., shorter than the protein half-life) would be less sensitive to such effects, as protein synthesised prior to test compound addition would not have degraded. Thus, a 72 h incubation period would allow for a significant amount of the existing protein to degrade, making it more likely for an effect to be detected.

To summarise, the downregulatory effects of selected curcumin analogues on the BCRP transporter was investigated using an SDS-PAGE and immunoblotting method. The protocol used a highly specific anti-BCRP antibody, an improved assay for avoiding uneven sample loading, and two cell lines that were previously used to detect BCRP downregulation. A long 72 h incubation period was used, allowing for a sufficient time to detect changes in protein expression.

5.2 Materials and Methods

5.2.1 Chemicals and reagents

Complete protease inhibitor cocktail (Cat. # 04693159001) was purchased from Roche, Basel, Switzerland. Radio-immunoprecipitation assay (RIPA) buffer, Tween-20, Tris-HCl and β-mercaptoethanol were from Sigma Aldrich, St Louis, MO. Blotting grade blocker (non-fat dry milk, NFDM), 7.5 % Tris-glycine gel, Laemmli buffer, Tris-base, glycine, sodium dodecyl sulfate and Precision plus Western C™ protein standards were from Bio-rad, Hercules, CA. Magic Mark XP™ molecular weight marker and SYPRO ruby protein stain were from Life Technologies, Carlsbad, CA. The source of curcumin and the synthesis and chemistry of A12, A13, B11 and RL92 are outlined in Section 2.2.1.

5.2.2 Cell culture

The sources of the MDCKII/P, MDCKII/BCRP and BeWo choriocarcinoma cell lines were previously outlined in Sections 2.2.3 and 3.2.2. General cell culture techniques and cell maintenance are outlined in Section 2.2.4.

5.2.2.1 Drug treatment and isolation of crude membrane fractions

MDCKII/BCRP, MDCKII/P or BeWo cells at ~ 80 – 90% confluence were trypsinised, counted, and plated at 1 million cells/dish in 150 mm culture plates, and suspended in 8 mL complete phenol-red free DMEM (DMEM/F12 for BeWo). Each treatment group used 3 x 150 mm dishes to produce sufficient crude membranes for Western blot analysis. The cells were incubated for 24 h at 37°C, before the addition of a further 8 mL media containing either DMSO or test compounds at 2x the final concentration. After a 72 h incubation period, the media was removed and the cells were washed twice in ice-cold PBS. After freeze-thawing once, 5 mL ice-cold PBS was added and the cells were scraped and transferred to a 50 mL tube, with samples in the same treatment group pooled in a single tube. The cell suspension was centrifuged (500 g at 4°C) and resuspended in 5 mL ice-cold hypotonic buffer (0.5mM Na_2HPO_4 + 0.5mM NaH_2PO_4), supplemented with protease inhibitor cocktail. The samples were then freeze-thawed twice, followed by 90 min of constant agitation using a bench-top rotator in a cold room at 4°C (all steps thereafter were at 4°C). The cells were homogenised with a dounce homogeniser and the homogenate was spun at 500 g for

10 min. The supernatant was transferred to ultracentrifuge tubes and samples were spun for 1 h at 100,000 g. The remaining pellet was resuspended in 200 µl RIPA buffer (+ protease inhibitors), aliquoted to PCR strips and stored immediately at - 80°C. Prior to storage, a small aliquot was removed for the determination of total protein concentration using the Biorad DC-protein assay™ (Bio-rad, Hercules, CA).

5.2.3 Gel electrophoresis and immunoblotting

For gel electrophoresis, the crude membrane fractions were first mixed 1:1 with Laemmli buffer containing 5% β-mercaptoethanol, and then heated to 75°C for 15 min to reduce and denature the proteins. The samples were loaded into a 7.5 % Tris-glycine gel and then placed in a vertical electrophoresis system with Tris/glycine/SDS running buffer (25 mM Tris, 192 mM glycine, 0.1 % SDS, pH 8.6). The proteins were allowed to separate for 30 min at 200 V (constant voltage) after which, the gel was removed and the proteins transferred into a PVDF membrane using the Trans-blot turbo™ transfer system (Biorad, Hercules, CA). The PVDF membrane was then air-dried and stained for total protein using the SYPRO ruby protein stain, following the manufacturer's instructions. Total protein staining was visualised using the blue-light illuminator of a LAS-3000 imager (Fujifilm, Tokyo, Japan).

Following imaging of the membrane for total protein, it was re-wet with 100% methanol and washed with TBST buffer (10 mM Tris–HCl, pH 8.0,150 mM NaCl, and 0.1% Tween-20) for 2 x 2 min in an orbital shaker. It was then blocked with 5% NFDM in TBST for 1 h at room temperature and incubated with BXP-21 mouse monoclonal antibody overnight at 4°C (Abcam, Cambridge, UK) (1:5000 dilution in 1% non-fat dry milk, TBST). Excess primary antibody was removed by washing the membrane with TBST 4 x 5 min with agitation, before incubation with an HRP-conjugated rabbit polyclonal secondary antibody for 1 h at room temperature (1:10,000 dilution in 1 % NFDM, TBST) (Abcam, Cambridge, UK). Thereafter the membrane was washed 4 x 5 min with TBST to remove excess antibody and incubated for 5 min with Electrochemiluminescence (ECL) Prime substrate (GE Healthcare, Buckinghamshire, UK). The membrane was imaged for chemiluminescence using a LAS-3000 imager.

5.2.4 Protein densitometry analysis

The protein band densities of the total protein stains and BCRP immunoblots were determined using ImageJ software (NIH, Bethesda, MD). To determine the total protein density for each lane from the SYPRO ruby staining, the method by Alridge et al. (2008) was used which involves using a thin strip spanning the whole length of a lane (Figure 5-1A). This allowed the sampling of all proteins and reduced errors due to lane bending.

In determining BCRP expression, a box which included the bands from glycosylated and un-glycosylated BCRP was used (Figure 5-1B). All forms of BCRP were therefore quantified, thus avoiding issues of sample processing or test compound treatment affecting the relative abundance of the different forms of the transporter.

In comparing BCRP protein expression between control and test compound-treated samples (Section 5.3.3), the BCRP band density values were adjusted using the total protein stain to control for uneven loading of the samples. An adjustment factor was calculated (Equation 5-1) that was used to divide the density value of the treated samples. The new adjusted density value was then normalised to the BCRP band density of the control lane (Equation 5-2).

Equation 5-1

$$\frac{\text{Total protein density (treated sample)}}{\text{Total protein density (control)}} = \text{Adjustment factor}$$

Equation 5-2

$$\left[\left(\frac{\text{BCRP BD (treated sample)}}{\text{Adjustment factor}}\right) \div \text{BCRP BD (control)}\right] \times 100 = \%\ \text{BCRP expression of control}$$

BD – band density

A

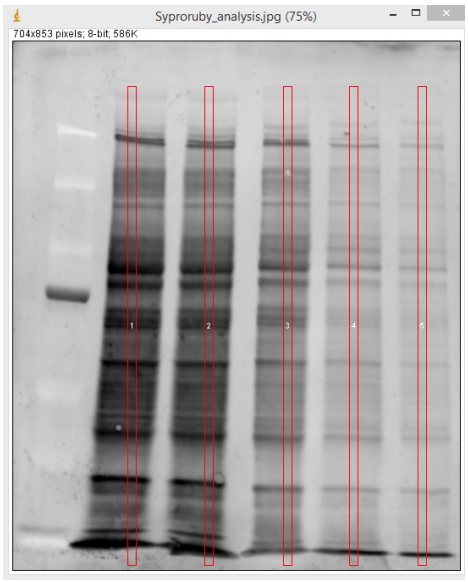

B

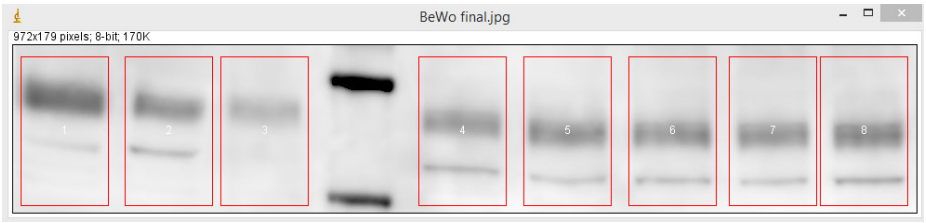

Figure 5-1. A total protein stain (**A**), and a BCRP immunoblot (**B**) showing the area (red boxes) used to analyse protein band densities with ImageJ software. The whole length of the lane was sampled for total protein staining (A), while an area which includes both glycosylated and un-glycosylated BCRP was used to quantify BCRP protein expression (B).

5.2.5 Statistical analysis

One-way ANOVA was used together with Dunnett's post-hoc control-comparison test to determine significant differences between the BCRP expression of test compound-treated samples and DMSO-only control samples. A p-value of < 0.05 was considered significant. Graphpad Prism 6.0 (Graphpad software, La Jolla, CA) was used for statistical analysis.

5.3 Results

5.3.1 The linearity of the total protein stain and the immunoblotting assay

Before investigating the effects of the analogues on protein expression, both the total protein staining and immunoblotting assay were confirmed to be linear over a range of different protein loading quantities. This ensured that both assays accurately measured the changes in total protein and BCRP expression at the range of amounts expected in subsequent experiments.

Figure 5-2A shows the total protein staining of serially diluted MDCKII/BCRP membrane fractions at amounts ranging from 50 - 5 µg protein in the preceding gel electrophoresis step. The calculated total protein band density of each lane, expressed relative to the lane with the lowest density value, was plotted against loaded protein in Figure 5-2B. A line of best-fit shows that total protein band densities determined using the SYPRO ruby stain, decreased linearly (r^2 = 0.997) as the protein sample was serially diluted from 50 to 5 µg.

In Figure 5-3A, an immunoblot with the anti-BCRP BXP-21 antibody is shown using serially diluted MDCKII/BCRP membrane fractions (40 – 5 µg protein), loaded in the preceding gel electrophoresis step. A single ~ 70 kDa band was detected, which corresponds to the reported size of the BCRP protein. The density of the BCRP band for each lane, relative to that of the lowest density BCRP band, was determined and plotted against the amount of total protein loaded (Figure 5-3B). A line of best-fit through the points had an r^2 value of 0.987, showing that the quantified BCRP band density was linear over the serial dilution range.

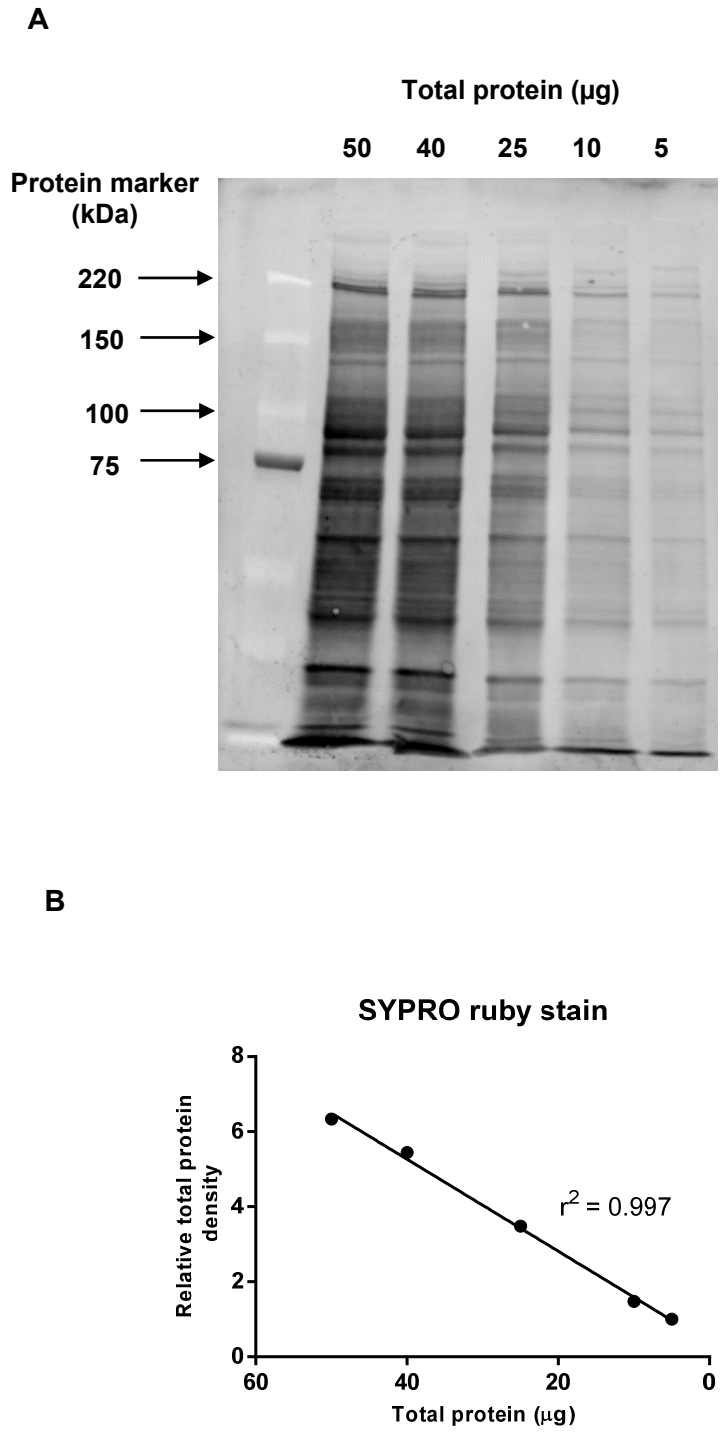

Figure 5-2. Total protein stain of serially diluted MDCKII/BCRP membrane fractions using SYPRO ruby (**A**). The amount of total protein loaded per well is indicated at the top of the image and the size of the protein markers are shown to the left. The stain was imaged using fluorescence detection at 450 nm excitation and 610 nm emission wavelength. A plot of relative total protein density per lane vs. protein amount can be found in (**B**). A line of best-fit with the r^2 value of the goodness-of-fit are shown. Relative protein density was determined using ImageJ software.

A

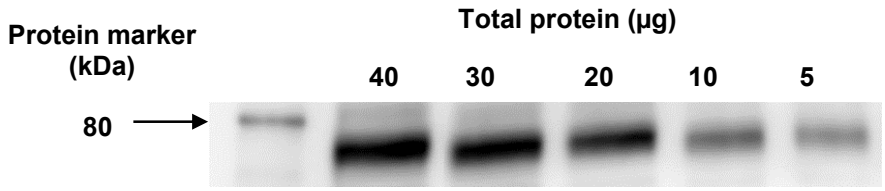

B

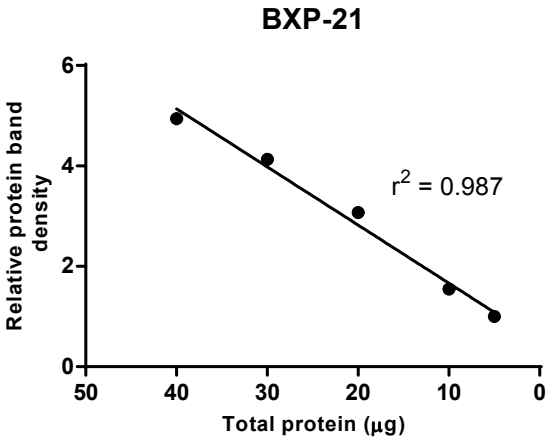

Figure 5-3. An immunoblot of serially diluted MDCKII/BCRP membrane fractions using the BXP-21 anti-BCRP monoclonal antibody (**A**). The 80 kDa molecular weight marker is visible on the leftmost lane. The chemiluminescent image was acquired using a LAS-3000 imager. A plot of BCRP band density relative to lowest density BCRP band vs. total protein amount loaded per lane is shown in (**B**). A line of best-fit and the r^2 value of the goodness-of-fit are shown. Relative band density was determined using ImageJ software.

5.3.2 Detection of BCRP in MDCKII/BCRP, MCDKII/P and BeWo cells by immunoblotting

After the linearity of the total protein staining and the immunoblotting assay were confirmed, a preliminary test was conducted to assess the specificity of the immunoblotting assay for BCRP. This was done by testing against a negative control (parental MDCKII/P cells) and two positive controls (MDCKII/BCRP and BeWo cells). Figure 5-4A shows an immunoblot demonstrating that BXP-21 only detected BCRP bands in MDCKII/BCRP and BeWo membrane fractions, without showing any signal in the negative control MDCKII/P cells. In addition, the detected bands in both the MDCKII/BCRP and BeWo lanes were only those corresponding to BCRP in its glycosylated and un-glycosylated forms, without the presence of other non-specific bands. For MDCKII/BCRP samples, two bands of sizes < 80 kDa were detected, corresponding to the two glycosylated forms of BCRP, previously reported to run as a 75 – 80 kDa and 70 – 72 kDa band, respectively (Imai et al., 2005; Mohrmann et al., 2005). For BeWo cells, a third band was also observed with a size of ~ 60 kDa, this corresponds to the un-glycosylated form of BCRP, previously found to run as a 62 – 66 kDa band (Imai et al., 2005; Mohrmann et al., 2005). A total protein stain of the PVDF membrane in Figure 5-4B shows that all three lanes were evenly loaded with protein, including the lane for MDCKII/P.

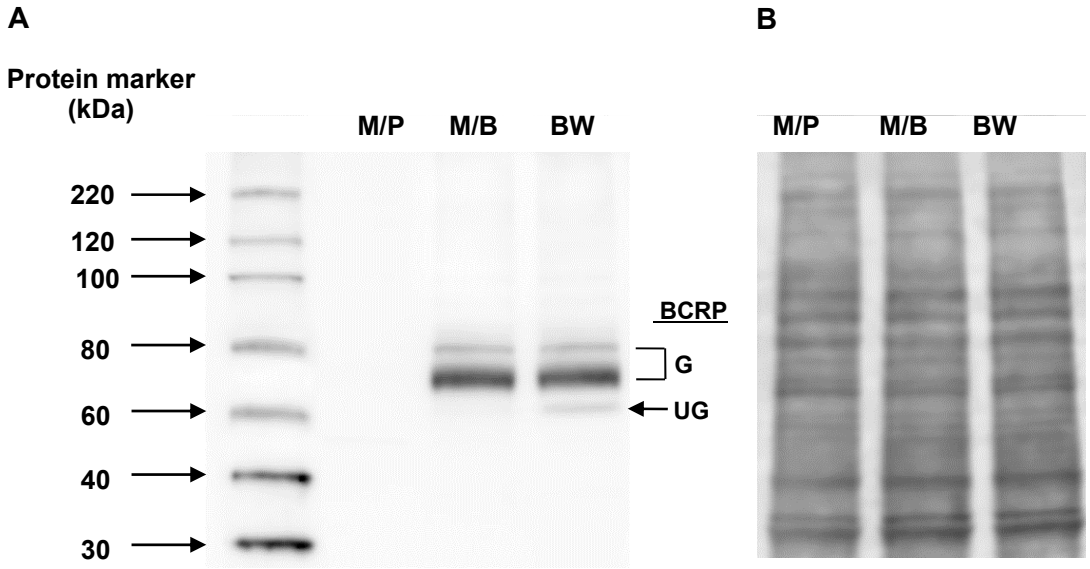

Figure 5-4. Immunoblot (**A**) of membrane fractions from MDCKII/P (M/P), MDCKII/BCRP (M/B), and BeWo (BW) cells using the BXP-21 anti-BCRP monoclonal antibody and an HRP-conjugated anti-mouse secondary antibody. Total protein was loaded at 20 µg per lane. The bands corresponding to the glycosylated (G) and un-glycosylated (UG) forms of BCRP are marked. Molecular weight markers are indicated on the leftmost lane. The total protein stain of the sample-loaded lanes are shown in (**B**).

5.3.3 The effects of curcumin and selected analogues on BCRP total protein expression

After the preliminary experiments, the effects of curcumin, A12, A13, B11 and RL92 on the protein expression of BCRP were determined in BCRP-transfected MDCKII/BCRP cells, and BeWo choriocarcinoma cells.

Figure 5-5 shows a representative immunoblot of membrane fractions isolated from MDCKII/BCRP cells treated for 72 h with either DMSO (control samples) or non-cytotoxic concentrations of curcumin and the selected analogues. The treatment concentrations were 10 μM curcumin, 5 μM A12 or A13, 0.5 μM B11 or 2 μM RL92. The figure shows no obvious differences in band density between control and curcumin or analogue-treated samples, at 20 μg of total protein. As expected, staining was more intense in the lanes loaded with 30 μg of control samples, and lighter in the lanes loaded with 10 μg protein. In the densitometric analysis of n = 4 immunoblots (Figure 5-6), BCRP expression after curcumin, A12, A13, B11 or RL92 treatment was not found to be significantly different from DMSO-only treated controls. The densitometry analysis included both glycosylated and un-glycosylated forms of BCRP, with band densities adjusted to total protein staining to account for uneven transfer and sample loading.

Th effects of curcumin and the analogues on BCRP expression in BeWo cells is shown in Figure 5-7. In contrast to MDCKII/BCRP cells, the test compound concentrations were lower due to the increased sensitivity of BeWo cells to cytotoxicity. The concentrations used in the 72 h incubation were 1 μM of curcumin or RL92, 5 μM A12, 2 μM A13 or 0.25 μM B11. The blot shows that neither curcumin nor analogue treatment caused obvious changes to the BCRP band density in the isolated membrane fractions after 72 h, compared to that of DMSO-treated control samples at 20 μg of total protein. Control samples at 30 μg and 10 μg resulted in darker and lighter bands respectively than the 20 μg control. In the densitometric analysis of n = 3 immunoblots (Figure 5-8), curcumin, A12, A13, B11 and RL92 treatment did not significantly affect total BCRP expression compared to DMSO-only controls.

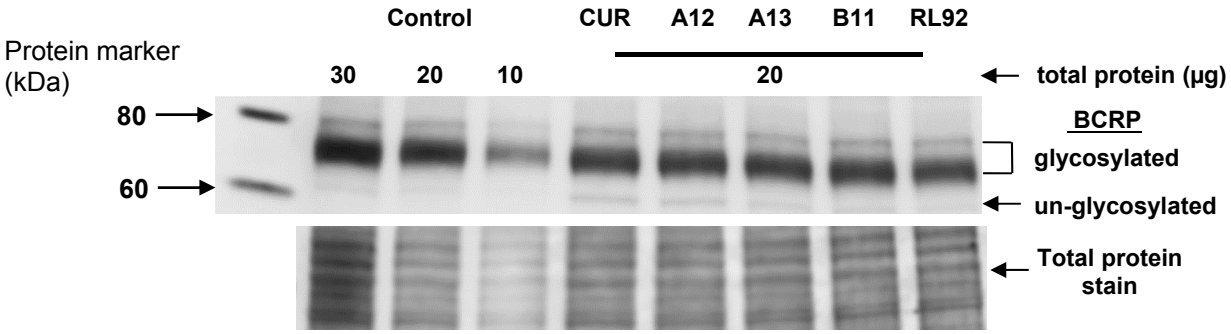

Figure 5-5. Immunoblot of MDCKII/BCRP membrane fractions treated with DMSO (Control), 10 µM curcumin (CUR), 5 µM A12 or A13, 0.5 µM B11, or 2 µM RL92 for 72 h. The amount of total protein loaded per lane is indicated at the top of the figure. The bands corresponding to the glycosylated and un-glycosylated forms of BCRP are indicated. The total protein stain of the PVDF membrane is shown below the blot. The figure is representative of n = 4 independent experiments.

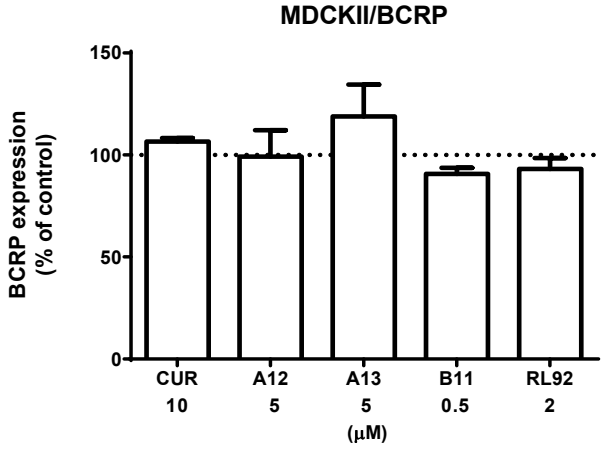

Figure 5-6. Total BCRP expression in MDCKII/BCRP cells, after incubation with 10 µM curcumin (CUR), 5 µM A12 or A13, 0.5 µM B11, or 2 µM RL92 for 72 h. Results are expressed as a percentage of the total BCRP in control cells treated with DMSO only (see Equation 5-2). Total protein density per lane was used as the loading control and both glycosylated and un-glycosylated BCRP were included in the protein density analysis. Data are presented as mean ± standard error of n = 4 independent experiments. Relative band densities were determined using ImageJ software.

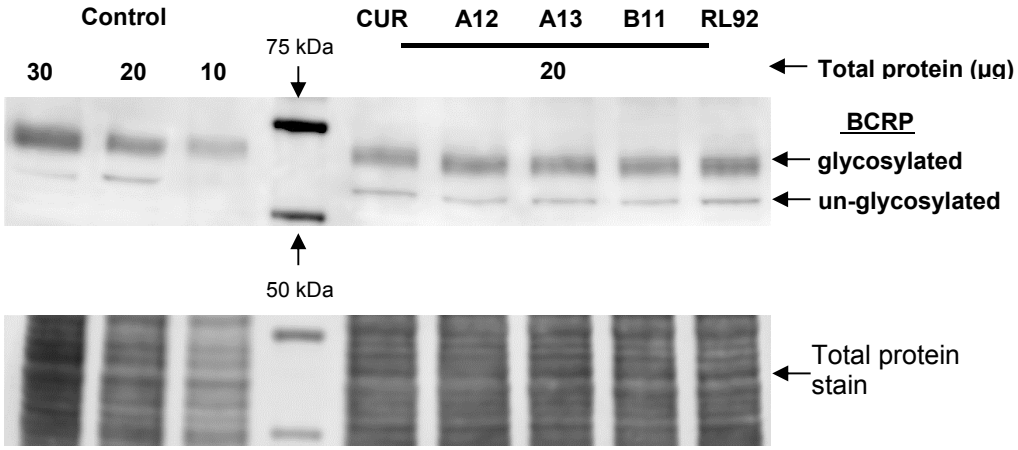

Figure 5-7. Immunoblot of membrane fractions from BeWo choriocarcinoma cells treated with DMSO (Control), 1 µM curcumin (CUR), 5 µM A12, 2 µM A13, 0.25 µM B11, or 1 µM RL92 for 72 h. The amount of total protein loaded per lane is indicated at the top of the figure. The bands corresponding to the glycosylated and un-glycosylated forms of BCRP are indicated. The total protein stain of the PVDF membrane is shown below the blot. The figure is representative of n = 3 independent experiments. Molecular weight markers are indicated.

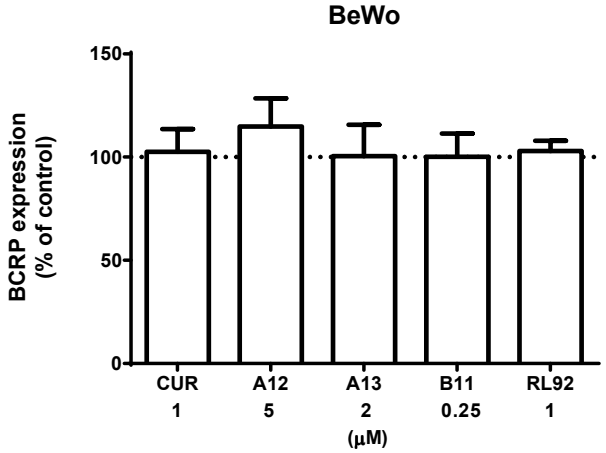

Figure 5-8. Total BCRP expression in BeWo choriocarcinoma cells, after incubation with 1 µM curcumin (CUR), 5 µM A12, 2 µM A13, 0.25 µM B11, or 1 µM RL92 for 72 h. Results are expressed as a percentage of the total BCRP in control cells treated with DMSO only (see Equation 5-2). Total protein density per lane was used as the loading control and both glycosylated and un-glycosylated BCRP were included in the protein density analysis. Data are presented as mean ± standard error of n = 3 independent experiments. Relative band densities were determined using ImageJ software.

5.4 Discussion

It was suspected in the resistance reversal assay (Chapter 3) that curcumin and the putative BCRP inhibitors, A12, A13, B11 and RL92, may have downregulated the protein expression of BCRP. This was due to their ability to reverse resistance to cytotoxic substrates at low concentrations that were not expected to directly inhibit BCRP transport activity. The downregulatory effects of these analogues were therefore determined in MDCKII/BCRP and BeWo cells, using SDS-PAGE and immunoblotting.

Before the downregulation studies were conducted, preliminary experiments validated both assays. Firstly, the linearity of the SYPRO ruby total protein staining was assessed, to see if it correlated with protein loading amount. Figure 5-2 shows that the total protein staining was linear from 5 – 50 µg total protein, and could therefore effectively function as a loading control within this protein range. Next, the linearity of the immunoblotting assay was determined to ensure that the BCRP band density correlated with the amount of protein present per lane. Figure 5-3 shows that the density of the BCRP band decreased linearly with total protein amount from 40 – 5 µg. The immunoblotting assay could therefore accurately detect changes in BCRP expression levels within this range. From these results, the protein loading amount was set at 20 µg in the downregulation studies. This allowed for either a doubling or a halving of BCRP expression to fall within the linear range of the immunoblot assay.

The immunoblot assay was also assessed for the specific detection of the BCRP protein. Figure 5-4A is an immunoblot of isolated membrane fractions from parental MDCKII/P cells (not expressing human BCRP), and BCRP-overexpressing MDCKII/BCRP and BeWo cells. The blot clearly showed that the assay was specific to BCRP, as bands were only seen in the two BCRP-overexpressing cell lines and not in the MDCKII/P-derived samples. The lack of signal in the MDCKII/P lane was consistent with previous studies, and was not the result of the absence of loaded protein, since the total protein staining (Figure 5-4B) clearly showed that protein was present in the lane (Ceckova et al., 2006; Pick and Wiese, 2012). The absence of any signal also indicated that minimal non-specific binding by either the primary or secondary antibody was occurring, which can be caused by insufficient blocking of the membrane, protein overloading, or excessively high antibody concentrations. Lastly, this result indicated that either canine BCRP was

absent (or present in small undetectable amounts) in MDCKII/P cells, or that the BXP-21 antibody did not recognise it. In either case, it was apparent that endogenous canine BCRP was unlikely to have interfered with the results of subsequent experiments.

From the blots, multiple bands were observed in the MDCKII/BCRP and BeWo lanes. This was not due to off-target binding, but was evidence that the immunoblot assay could detect the glycosylated and un-glycosylated forms of BCRP. Three BCRP forms have been characterised in immunoblots; the complex and core glycosylated proteins run at the size ranges of 75 – 80 kDa and 70 – 72 kDa, respectively while the un-glycosylated form has been detected as a 62 – 66 kDa band (Imai et al., 2005; Maliepaard et al., 2001; Mohrmann et al., 2005). In the BeWo membrane fractions, three bands were detected, which corresponded to these three forms (Figure 5-4A). This demonstration that the immunoblot assay specifically detected both glycosylated and un-glycosylated BCRP is important, because N-glycosylation does not affect either protein trafficking to the plasma membrane, or influences its function (Mohrmann et al., 2005; Ni et al., 2010a). Hence, all these forms of BCRP can potentially contribute to transport activity and therefore, all were included in the measurement of total BCRP expression. In doing so, the assay thus avoided false positives and false negatives from test compounds that may have influenced BCRP glycosylation, and altered the relative abundance of the different forms of BCRP without affecting the expression of the transporter.

The downregulation studies were conducted by incubating MDCKII/BCRP cells with curcumin and selected analogues for 72 h, using non-cytotoxic concentrations that were previously used to reverse BCRP-mediated resistance (Section 3.3.4.2). Figure 5-5 and Figure 5-6 show that treatment of MDCKII/BCRP cells for 72 h with 10 μM curcumin, 5 μM A12 or A13, 0.5 μM B11 or 2 μM RL92, did not significantly affect the expression of BCRP. The lack of a downregulatory effect was not due to the treatment groups being overloaded relative to the control group, since total protein staining of the blot showed equal loading. Also, it was unlikely that downregulation was not detected due to oversaturation of the BCRP signal (a result of sample overloading, or overexposure of the blot), since the 30 μg and 10 μg controls resulted in a visibly higher and lower density band, respectively, compared to the 20 μg control.

Because the use of MDCKII/BCRP cells only allows the detecton of post-transcriptional downregulation (due to a viral promoter-controlled BCRP), studies were also conducted in BeWo cells, which express the transporter using the native promoter and are responsive to promoter-mediated downregulation. BeWo cells were incubated for 72 h with 1 μM curcumin, 5 μM A12, 2 μM A13, 0.25 μM B11, or 1 μM RL92. These concentrations were lower than for MDCKII/BCRP cells due to the greater sensitivity of BeWo to cytotoxicity. Neither curcumin nor its analogues significantly altered BCRP expression in BeWo cells (Figure 5-7, Figure 5-8). Total protein staining demonstrated equal loading of the samples and the control lanes indicated that the BCRP band was not oversaturated, since the band densities correlated with protein loading.

Both the MDCKII/BCRP and BeWo studies therefore demonstrated that curcumin, A12, A13, B11 and RL92 at least at the selected concentrations, did not appear to affect the expression of BCRP. Hence, this mechanism could not have caused the significant reversal of BCRP-mediated resistance by these compounds, when used at concentrations lower than their IC_{50} of BCRP inhibition (see Section 3.3.4). Other explanations should therefore be considered to account for this observation.

These results support the argument that the tested curcumin analogues inhibited BCRP transport activity primarily, or exclusively, via a direct interaction with the transporter. Such a mechanism has previously been proposed for curcumin, which directly inhibited photoaffinity labeling of BCRP, without affecting protein expression in BCRP-expressing MCF-7 AdVp3000 breast cancer cells (Chearwae et al., 2006a). However, it should be pointed out that the immunoblot assay cannot rule out the possibility that the analogues caused an internalisation of the protein from the plasma membrane. This could effectively and rapidly decrease BCRP-mediated cellular efflux, without affecting protein expression (Takada et al., 2005). Such an effect should first be investigated (e.g., through cell surface staining), before it can be confidently concluded that direct interaction with BCRP is the main or sole mechanism of transport inhibition for these compounds.

As mentioned previously (Section 5.1), curcumin, A13 and B11 have been reported to inhibit NF-κB activation, a protein complex that binds directly to the promoter region of BCRP to activate transcription (Wang et al., 2010b; Zhang et al., 2011). It was therefore somewhat surprising that no downregulation was observed in BeWo cells, which are responsive to BCRP-promoter mediated

transcriptional regulation (Imai et al., 2005; Wang et al., 2006). The absence of any effect may have resulted from curcumin, A13 and B11 being used at concentrations that were insufficient to inhibit NF-κB. The IC_{50} of NF-κB activation for curcumin, A13 and B11 were 15, 5 and 4 μM, respectively; while the concentrations used in the BeWo studies were much lower, at 1, 2 and 0.25 μM, respectively (Yadav et al., 2010). In addition, it was not known whether an activated NF-κB was driving the expression of BCRP in BeWo cells, and thus significant downregulation may not have occurred, even if NF-κB had been inhibited.

Another signaling pathway involved in BCRP expression, that could be modulated by curcumin and cyclohexanone analogues, is the PI3K/AKT pathway. Inhibition of this pathway with small molecule inhibitors (e.g., LY294002) was previously demonstrated to post-transcriptionally downregulate BCRP expression in MDCKII/BCRP cells, as well as in K562/MX10 leukemia cells (Nakanishi et al., 2006; Pick and Wiese, 2012). Curcumin is a known inhibitor of this pathway, and yet, no downregulation was seen in MDCKII/BCRP (Qiao et al., 2013; Yu et al., 2008). As with NF-κB inhibition, this lack of effect might have been caused by the low concentrations used in the current study. Significant inhibition of PI3K/AKT activation, measured through inhibition of AKT phosphorylation, was observed only at curcumin concentrations > 20 μM (Qiao et al., 2013; Yu et al., 2008). This is higher than the 10 μM curcumin used in the MDCKII/BCRP incubations. However, inhibition of the PI3K/AKT pathway did not always result in BCRP downregulation, as some studies have shown that the transporter is internalised from the plasma membrane, while protein expression remained constant (Goler-Baron et al., 2012; Imai et al., 2012; Mogi et al., 2003; Takada et al., 2005). It would therefore be interesting to use cell surface staining techniques to investigate whether curcumin can cause BCRP internalisation. The analogues A12, A13, B11 and RL92 could also be tested, since PI3K/AKT inhibition appears to be a class effect, due to potent inhibition of the PI3K/AKT pathway by similar in-class compounds A1, A2, B1 and B10 (Somers-Edgar et al., 2011; Yadav et al., 2012a, 2012b).

Finally, although no downregulation of BCRP was observed, neither was there an increase in protein expression. Whether or not these analogues upregulated BCRP expression is important, as this could counteract their MDR reversal activity. Although the results suggest that the analogues did not increase BCRP expression, it should be noted that the cell models used in this

study were not ideal for detecting BCRP induction. For example, the MDCKII/BCRP cells exogenously express very high levels of BCRP, and therefore, are unlikely to respond to further induction (Pavek et al., 2005). Although the BeWo cell line has been successfully used to detect BCRP upregulation by estriol, progesterone and prolactin, it may only be responsive to the most potent inducers due to its high endogenous BCRP expression (Wang et al., 2006, 2008). Cell lines with low but inducible BCRP expression (e.g., MCF-7 breast cancer cells), should be used to confirm the lack of upregulation by the analogues (Ebert et al., 2007).

To summarise, the immunoblotting assay has clearly shown that curcumin, A12, A13, B11 and RL92 do not downregulate the protein expression of BCRP in MDCKII/BCRP and BeWo cells. Decreased transporter expression can therefore be ruled out as the reason for the significant resistance reversal effects of the analogues, observed at concentrations that were less than their IC_{50} values for BCRP inhibition in the flow cytometry studies. The results support a direct interaction with the transporter as the primary mechanism of transport inhibition. However, the immunoblotting assays do not rule out the possibility of BCRP internalisation from the cell surface by the analogues. Lastly, the immunoblotting studies could not conclusively determine if the analogues could upregulate BCRP expression. Further studies in cell lines suitable for determining BCRP induction need to be conducted to clarify this issue.

6. The effects of curcumin and selected analogues on BCRP cell surface expression

6.1 Introduction

The results from the immunoblotting assay (Chapter 5) indicate that downregulation of BCRP protein expression was unlikely to have caused the reversal of BCRP-mediated mitoxantrone resistance by A12, A13, B11 and RL92, when used at concentrations that were lower than their IC_{50} values for BCRP inhibition (determined by flow cytometry). Other explanations, such as the possibility that functional BCRP was internalised from the plasma membrane, were therefore considered. BCRP internalisation can decrease efflux activity, without affecting protein expression, and is undetectable using immunoblotting techniques (Nakanishi and Ross, 2012; Takada et al., 2005). Numerous compounds have been reported to inhibit BCRP transport via this mechanism, with the majority thus far being direct or indirect inhibitors of the PI3K/AKT pathway (Mogi et al., 2003; Nakanishi et al., 2006; Pick and Wiese, 2012; Takada et al., 2005; To and Tomlinson, 2013). This signaling pathway, also implicated in cancer growth and survival, is considered to play an important role in the localisation of BCRP to the plasma membrane (Huang et al., 2014; Mogi et al., 2003; Nakanishi and Ross, 2012). As both curcumin and other cyclohexanone analogues, such as A1, A2, B1 and B10, are inhibitors of this pathway, it is possible that the structurally-similar analogues (e.g., A12, A13, B11 and RL92) might also have inhibitory effects on this pathway, and thus may induce BCRP internalisation (Qiao et al., 2013; Somers-Edgar et al., 2011; Yadav et al., 2012a, 2012b).

To determine if this was so, immunofluorescence staining followed by flow cytometry detection was conducted in BCRP-overexpressing MDCKII/BCRP and BeWo cells. These cell lines were treated under two different conditions, one corresponding to the resistance reversal assay and the other, to the flow cytometry screening. Although the incubation period of the latter was relatively short (2 h), BCRP internalisation has been observed after 90 min, which is within the time-frame of the assay (Takada et al., 2005). Specific detection of surface BCRP was via the 5D3 antibody, which is targeted to an extracellular epitope of the protein (Ozvegy-Laczka et al., 2005; Zhou et al.,

2001). The 5D3 antibody has been used previously in detecting BCRP internalisation caused by compounds such as PI3K and EGFR inhibitors and PPARγ agonists (Pick and Wiese, 2012; To and Tomlinson, 2013).

An indirect immunostaining assay was used, which involved biotin-conjugated 5D3, and detection with streptavidin conjugated with phycoerythrin (PE). Indirect staining was preferred over direct staining (i.e., the fluorophore is directly attached to 5D3), as the former allowed for signal amplification, due to the possibility of multiple streptavidin-PE molecules binding to 5D3. The PE fluorophore was selected as it is one of the brightest fluorescent tags available (high quantum yield), and streptavidin was chosen over avidin to reduce non-specific binding (Chang et al., 2010; Diamandis and Christopoulos, 1991; Oi et al., 1982).

As non-specific binding of the primary antibody and secondary fluorescent detection can lead to false positives, staining with a biotin-conjugated host-matched IgG2b isotype control was included in every experiment (D'hautcourt, 2002; Radbruch, 2000). The isotype control is an antibody targeted to an irrelevant antigen, but of the same isotype as the primary antibody. It allowed for the quantification of the background signal caused by non-specific antibody interactions with cellular proteins, and also determined the non-specific binding of the secondary detection system (Radbruch, 2000). By subtracting the signal from the isotype control with 5D3 staining, the BCRP-specific component of the observed fluorescence was measured. Staining was also conducted in parental MDCKII/P cells as an additional control for non-specific binding, and to confirm that a BCRP-specific signal was only detectable in cells expressing the target protein.

To increase the intensity of the BCRP-specific signal, a paraformaldehyde fixation step was included in the protocol, as Ozvegy-Laczka et al. (2005, 2008) had previously demonstrated that fixation stabilises a high affinity conformation of BCRP to 5D3, greatly increasing the staining intensity compared to non-fixed samples. The fixation step also prevented the internalisation and the capping and shedding of the antibody-transporter complex to the extracellular media, which can decrease staining intensity and may be falsely interpreted as BCRP downregulation (Dyer and Benjamins, 1988; Smit et al., 1974). It should be noted that fixation did not permeabilise the cells (this requires detergent treatment), and hence, large molecules, such as 5D3 or streptavidin-PE, were limited to binding cell surface antigens (Jamur and Oliver, 2010).

To confirm that the immunostaining protocol was sensitive to downregulatory stimuli, two reported downregulators of BCRP surface expression, wortmannin (PI3K inhibitor) and gefitinib (EGFR inhibitor), were included in each experiment. Wortmannin has been found to rapidly induce BCRP internalisation (within 90 min); while gefitinib caused internalisation at longer incubation periods (24 – 72 h) (Pick and Wiese, 2012; Takada et al., 2005). Since gefitinib is not expected to have effects at short incubation periods, it was included in the 2 h studies as negative control.

The immunofluorescence staining was quantified using flow cytometry rather than visual imaging methods, as the former is more quantitative and sensitive at detecting subtle changes in staining than the latter (Tung et al., 2007). As such, many of the precautions that apply to flow cytometry analysis were included in the current protocol (see Section 2.2.5.4). These include: gating strategies to exclude cell doublets, which can artificially increase surface staining; live-gating, to exclude cellular debris and non-viable cells; and checking for intrinsic fluorescence of the test compounds (Bertho et al., 2000; Wersto et al., 2001). Although fixation after drug treatment killed the cells, forward and side scatter information was preserved, hence, gating strategies that rely on these two parameters (e.g., live-gating and doublet exclusion) can be applied to fixed samples (Jensen et al., 2010).

6.2 Materials and methods

6.2.1 Chemicals and reagents

Materials were purchased from the following sources: wortmannin and gefitinib were from LC Labs, Woburn, MA; the primary antibody, anti-BCRP biotin-conjugated mouse monoclonal 5D3 clone (Cat. no. ab95692) from Abcam, Cambridge, UK; the biotin-conjugated IgG2b,κ mouse isotype control (Cat. no. 555741) was from BD Biosciences, San Jose, CA; streptavidin conjugated with phycoerythrin (PE) (Cat. no. 016-110-084) from Jackson Immuno, West Grove, PA; bovine serum albumin from MP Biomedicals, Auckland, NZ. The sources for high-purity curcumin, A12, A13, B11 and RL92 are outlined in Sections 2.2.1 and 2.2.2.

6.2.2 Cell culture and cell surface staining

Sources for the MDCKII/P, MDCKII/BCRP and BeWo choriocarcinoma cell lines are outlined in Sections 2.2.3 and 3.2.2.

6.2.2.1 Preliminary studies

In the preliminary studies (Section 6.3.1), MDCKII/P, MDCKII/BCRP and BeWo choriocarcinoma cells grown in T25 flasks at ~80-90%, were trypsinised, counted and resuspended in phenol red-free DMEM (DMEM/F12 for BeWo) and aliquoted into polystyrene test tubes at 5 x 10^5 cells per tube (see Section 2.2.4 for cell culture techniques). Staining commenced by first centrifuging (500 g) the samples at room temperature (all steps herein were conducted at room temperature, unless otherwise stated), and washing with 1 mL of PBS/1% BSA for 3 x 1 min (500 g) (this wash step was used throughout the assay). The cell pellet was then resuspended with freshly prepared PBS with 1% paraformaldehyde, and incubated for 10 min at 37°C. After fixation, the cells were washed and resuspended in 100 µl PBS/10% fetal calf serum to block non-specific binding sites. The cells were then incubated for 5 min, followed by the addition of 1 µl 0.5 mg/mL 5D3 antibody or 20 µl isotype control (following manufacturer's instructions). After mixing by pipetting up-and-down, the cells were incubated for 1 h at 37°C, followed by washing, resuspension in 100 µl of the same buffer with 2 µl 0.5 mg/mL PE-conjugated streptavidin, mixed, and a further 1 h incubation at 37°C. The cells were then washed, and resuspended in 300 µl DMEM/1% BSA (DMEM/F12 for BeWo)

and stored away from light until analysis (within 2 h). Steps involving the secondary antibody were carried out in low light to reduce photobleaching of the fluorescent label.

To check for intrinsic fluorescence in the PE channel, MDCKII/BCRP cells were treated as in Section 2.2.5.4. Results are in Appendix III.

6.2.2.2 BCRP surface expression studies

In the surface expression studies at low test compound concentrations (Section 6.3.2), MDCKII/BCRP cells were trypsinised, counted, and seeded in 12-well plates at various densities (see Table 6-1) using 1mL complete (10% FBS, 1% penicillin/streptomycin), phenol-red free DMEM. The cells were incubated for 24 h in a 37°C incubator, followed by the addition of a further 1 mL complete DMEM, with 2x the final concentration of test compound. Final DMSO concentrations were 0.8% for all samples (similar to the resistance reversal assays). The cells were then incubated in the 37°C incubator for time periods outlined in Table 6-1. After incubation, the media was aspirated and cells were washed thrice with warm PBS and trypsinised. Cells were resuspended in PBS/1% BSA, counted, and aliquoted at 5 x 10^5 cells per polystyrene test tube. Staining proceeded as in Section 6.2.2.1.

For the surface expression studies at high test compound concentrations (Section 6.3.3), MDCKII/BCRP or BeWo cells grown in T_{75} flasks were trypsinised, resuspended in phenol-red free DMEM or DMEM/F12 (for BeWo), counted, and aliquoted in 15 mL tubes at 1 x 10^6 cells in 1 mL of media. Test compounds were added, the tubes were gently vortexed, and then incubated for 2 h at 37°C. Final DMSO concentrations were 0.2% for all samples (similar to the flow cytometry screening studies). Afterwards, cells were centrifuged and the cell pellet was resuspended in PBS/1% BSA, counted, and 5 x 10^5 cells were aliquoted per polystyrene test tube. Staining proceeded as in Section 6.2.2.1.

Table 6-1. Seeding density and incubation period for the treatment groups in Section 6.3.2.

Treatment group	Seeding density (cells/well)	Incubation period
1	6 x 10^5	2 h
2	3 x 10^5	24 h
3	1 x 10^5	72 h

6.2.3 Flow cytometry and data analysis

Cell surface staining was determined using a BD LSRII flow cytometer (BD, San Jose, CA) and data was analysed with BD FACSDiva software and FlowJo (Treestar, Ashland, OR). Forward and side-scatter parameters were used to exclude dead, non-viable cells, cellular debris, and cell doublets using the method outlined in detail in Section 2.2.5.4. Mean fluorescence intensity (MFI) of 5000 cellular events was measured with the phycoerythrin (PE) channel (488 nm excitation, 562-588 nm emission). The data in Sections 6.3.2 and 6.3.3 were MFI as a % of DMSO-treated control and were calculated using the equation below:

Equation 6-1

$$\left[\frac{\text{MFI (Test sample)} - \text{MFI (Isotype control)}}{\text{MFI (DMSO control)} - \text{MFI (Isotype control)}}\right] \times 100 = \text{MFI as \% of DMSO control}$$

MFI – mean fluorescence intensity

Flow cytometry histograms were produced using the FlowJo software, and represent the fluorescence distribution of 5000 cell events.

6.2.4 Statistical analysis

To determine statistical significance of differences between DMSO-control and test compound-treated samples, one-way analysis of variance was used with Dunnett's post-hoc control-comparison test. A p-value < 0.05 was considered significant. Graphpad Prism 6.0 (Graphpad software, La Jolla, CA) was used for statistical analysis.

6.3 Results

6.3.1 Specificity of the cell surface staining to BCRP

Initially, the specificity of the cell surface staining protocol was assessed by staining parental MDCKII/P cells, and two BCRP-overexpressing cell lines, MDCKII/BCRP and BeWo choriocarcinoma cells, with the anti-BCRP 5D3 antibody. Non-BCRP specific staining was also determined using a host-species matched IgG2b isotype control. Both antibodies were biotin conjugated and detected with PE-conjugated streptavidin. Figure 6-1 shows greatly increased PE fluorescence with the 5D3 antibody in MDCKII/BCRP and BeWo cells (72- and 290-fold) compared to unstained samples; while only a 3-fold increase was observed in MDCKII/P cells. Staining with the isotype control also caused increased fluorescence in all three cell lines, but of a lesser magnitude than the 5D3 staining. With the fluorescence from isotype-stained samples as baseline, BCRP-specific staining was 12-fold and 25-fold over the background in MDCKII/BCRP and BeWo cells, and only 0.9-fold in MDCKII/P cells.

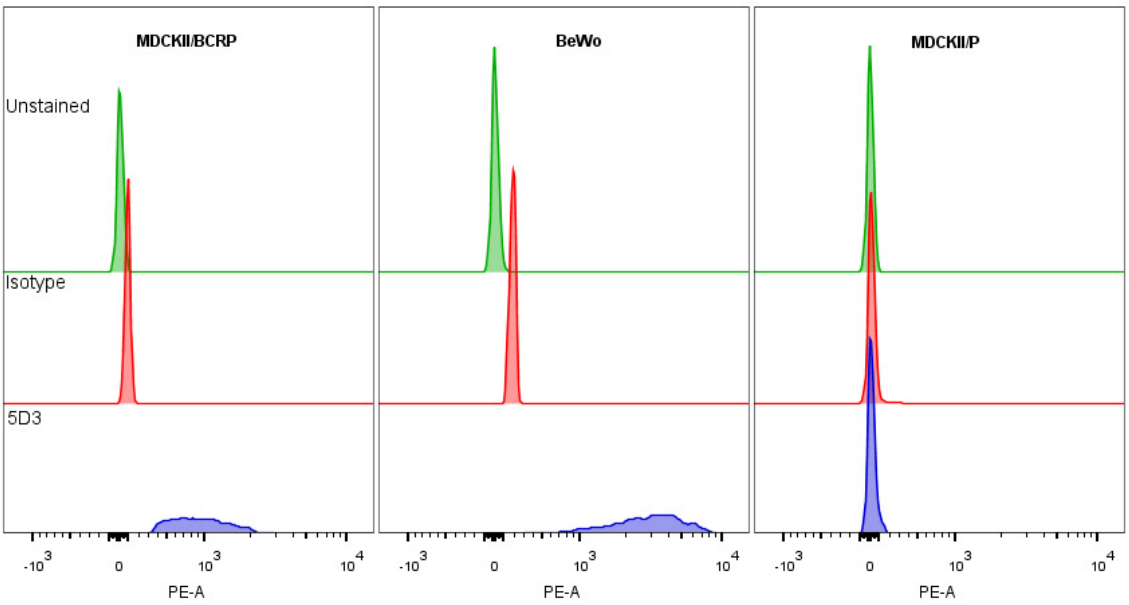

Figure 6-1. Flow cytometry histograms of cell surface staining using the anti-BCRP 5D3 antibody and an isotype control (IgG2b) on the parental MDCKII/P, BCRP-transfected MDCKII/BCRP and BeWo choriocarcinoma cell lines. The X – axis is fluorescence intensity in the PE (phycoerythrin) channel displayed in a biexponential (Log – linear) scale to better display values less than 0. Both 5D3 and isotype control were biotin labeled and detected using phycoerythrin-conjugated streptavidin. Y – axis represents the cell count. Histograms are representatives of n = 3 independent assays.

6.3.2 BCRP surface expression after incubation with low concentrations of curcumin and cyclohexanone analogues

To determine if curcumin, A12, A13, B11 and RL92 decreased the surface expression of BCRP in the resistance reversal assays, cell surface staining was conducted in the MDCKII/BCRP cells, treated under similar conditions. Figure 6-2 shows BCRP surface expression in MDCKII/BCRP cells as a % of DMSO-treated controls (see Equation 6-1), after incubation with non-cytotoxic test compound concentrations at three different incubation periods. In the 72 h treatment group (similar incubation time as the resistance reversal assay), neither curcumin, nor A12, significantly affected BCRP surface expression while A13 significantly increased expression by 20% ($p < 0.05$). Both B11 and RL92 decreased 5D3 staining, but this was not found to be significant. Similar results were observed after 24 h treatment, where only A13 significantly affected BCRP expression (seen as a 17% increase, $p < 0.01$). For the 2 h treatment group, a similar lack of effect was seen, with none of the analogues, nor curcumin, significantly affecting surface expression. In contrast, the positive control, wortmannin, consistently showed downregulation of BCRP surface expression at all three incubation periods. Another positive control, gefitinib, also significantly downregulated BCRP, but only after 24 and 72 h incubation. This was consistent with a previous report of a time-dependent effect on BCRP surface expression (Pick and Wiese, 2012). Both wortmannin and gefitinib were used at non-cytotoxic concentrations.

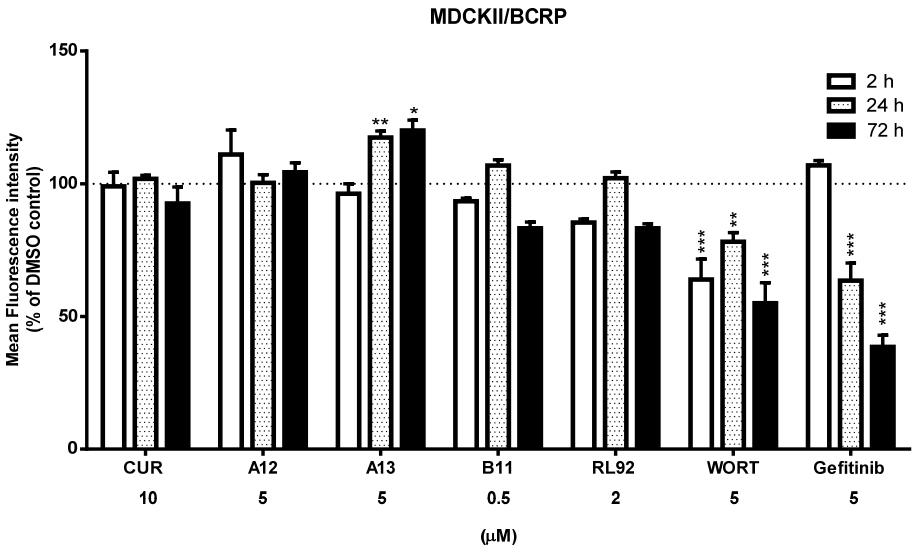

Figure 6-2. Cell surface expression of BCRP in MDCKII/BCRP cells treated with low concentrations of curcumin (CUR) or cyclohexanone analogues for 2, 24 and 72 h. Wortmannin (WORT) and gefitinib were included as positive controls for downregulation. The data is presented as a % of fluorescence in cells treated with DMSO only (see Equation 6-1). BCRP surface expression was detected with the biotin-conjugated 5D3 antibody and phycoerythrin-conjugated streptavidin, followed by flow cytometry to measure fluorescence intensity. Background fluorescence was substracted using the IgG2b isotype-control. Results are mean ± standard error of n = 3 experiments. *p < 0.05, **p < 0.01, ***p < 0.001 significantly different from DMSO-only control, calculated using one-way ANOVA and Dunnett's post-hoc test to compare all treatment groups with the DMSO control group.

6.3.3 BCRP surface expression after incubation with high concentrations of curcumin and cyclohexanone analogues

To determine if BCRP surface expression was affected in the flow cytometry assay, cell surface staining was conducted in MDCKII/BCRP cells after being treated under similar conditions as the mitoxantrone accumulation study. Figure 6-3A shows that after 2 h treatment with 20 μM of test compounds, significant downregulation was observed for curcumin (21% decrease, $p < 0.1$), A13 (36% decrease, $p < 0.01$) and RL92 (33% decrease, $p < 0.01$). Studies were also conducted in BeWo choriocarcinoma cells, which found that A13 treatment caused a greater downregulation of BCRP expression (45%, $p < 0.01$) than in MDCKII/BCRP cells. However, no significant effects were seen with curcumin or RL92 treatment. The analogues A12 and B11 did not cause any significant effects in either cell line while wortmannin significantly decreased expression ($p < 0.01$) in both cell lines. Treatment with gefitinib, which only downregulates surface BCRP at long-term incubations, did not cause significant effects on BCRP surface expression.

The BCRP downregulatory effects of A13, RL92 and wortmannin in MDCKII/BCRP and BeWo cells are presented as fluorescence histograms in Figure 6-3B. These show that staining with the 5D3 antibody caused significantly greater fluorescence than isotype controls in both cell lines and that A13 and wortmannin treatment decreased the mean PE fluorescence in these cells compared to the 5D3-DMSO control. For RL92, decreased fluorescence was clearly evident in MDCKII/BCRP cells, but not in BeWo cells, reflecting significant downregulation of BCRP surface expression in the former but not the latter.

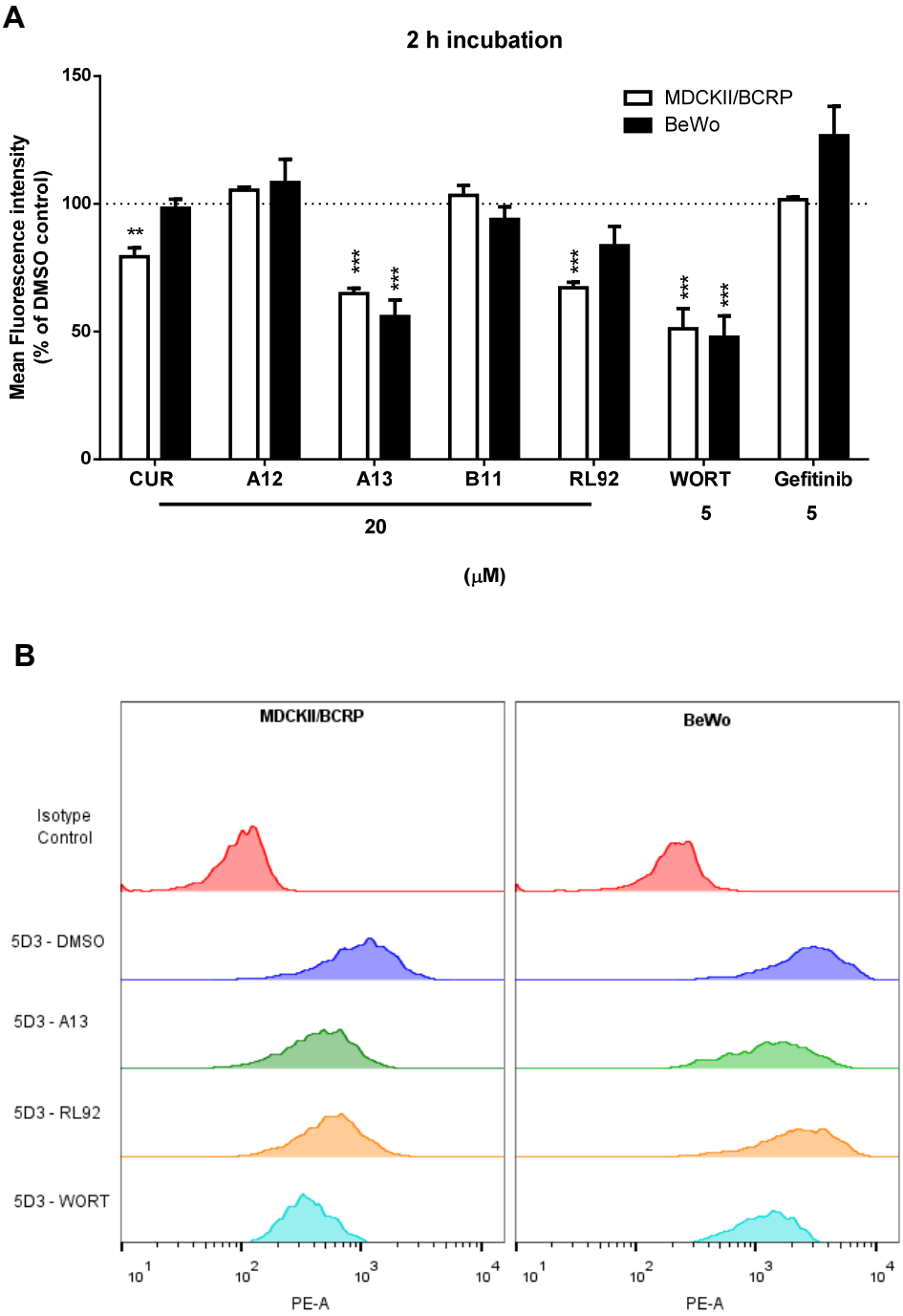

Figure 6-3. (A) Cell surface expression of BCRP in MDCKII/BCRP (□) and BeWo (■) cells after a 2 h incubation with 20 μM curcumin (CUR) or cyclohexanone analogues. Wortmannin (WORT) was included as positive control and gefitinib as negative control (downregulates only at long-term incubations). The data is presented as a % of the fluorescence in cells treated with DMSO only (see Equation 6-1). BCRP surface expression was detected with the biotin-conjugated 5D3 antibody and phycoerythrin-conjugated streptavidin. Background fluorescence was substracted using the IgG2b isotype-control. Results are mean ± standard error of n = 3 experiments. *p < 0.05, **p < 0.01, ***p < 0.001 significantly different from DMSO-only control, calculated using one-way ANOVA and Dunnett's post-hoc test to compare all treatment groups with DMSO control. **(B)** Representative flow cytometry histograms of selected compounds from (A). X – axis is the Log of fluorescence intensity measured using the phycoerythrin (PE) channel. Y – axis represents the cell count. The antibody used (isotype or anti-BCRP 5D3) and the treatment is indicated to the left of the histograms.

6.4 Discussion

The main aim of the surface staining studies was to determine if BCRP internalisation contributed to the reversal of mitoxantrone resistance by A12, A13, B11 and RL92 despite being used at concentrations that were lower than their IC_{50} values for BCRP inhibition (see Table 3-5). Internalisation was suspected because of the potent inhibitory effects by curcumin and other cyclohexanone analogues on the PI3K/AKT pathway, which is considered to be an important regulator of BCRP localisation to the plasma membrane (Mogi et al., 2003; Somers-Edgar et al., 2011; Takada et al., 2005; Yadav et al., 2012a, 2012b).

To investigate BCRP internalisation, a widely-used flow cytometry-based method of immunostaining surface BCRP was followed (Ozvegy-Laczka et al., 2008; Pick and Wiese, 2012; Vethanayagam et al., 2005). This involved the mouse monoclonal 5D3 antibody, targeted to an external epitope of BCRP, which has been used to detect BCRP surface downregulation by PI3K and EGFR inhibitors (e.g., LY294002 and gefitinib), and PPARγ agonists (e.g., telmisartan, rosiglitazone) (Pick and Wiese, 2012; To and Tomlinson, 2013). Prior to the immunostaining studies, preliminary experiments were carried out to ensure that the protocol specifically detected BCRP, and that non-specific binding of assay components were minimal. A BCRP-specific signal was only observed in BCRP-overexpressing BeWo and MDCKII/BCRP cells, with 5D3 staining in parental MDCKII/P cells being no different from the background signal (quantified using the isotype control). This confirmed that the assay specifically detected BCRP. Only a minimal increase in fluorescence was seen in isotype controls compared to unstained samples, suggesting that non-specific antibody binding or endogenous biotin were unlikely to have interfered with the results.

With the specificity of the immunostaining validated, studies were then conducted in MDCKII/BCRP cells treated with A12, A13, B11, RL92 and curcumin, under conditions corresponding to the 72 h mitoxantrone resistance reversal assay (see Section 2.3.2.2). Shorter time periods of 24 and 2 h were also included to detect any rapid internalisation of BCRP. None of the analogues were observed to decrease the surface expression of BCRP in any of the incubation periods (Figure 6-2). This was not due to MDCKII/BCRP being unresponsive to downregulation, as the PI3K inhibitor, wortmannin, decreased expression at all three time points (Takada et al., 2005). Furthermore, the time-dependent effect of gefitinib, observed by Pick and Wiese (2012) to induce

internalisation at 72 h but not 4 h in MDCKII/BCRP cells, was also correctly replicated by the assay. The negative result was therefore not an issue with the cell line or culture conditions. The results indicate that neither curcumin nor the analogues at the concentrations used can decrease the surface expression of BCRP. This suggests that BCRP internalisation was unlikely to have occurred in the resistance reversal assay, and therefore could not have contributed to the reversal of MDCKII/BCRP resistance to mitoxantrone. The lack of effect also supported the findings of the immunoblot assay (Chapter 5) that the tested analogues did not affect BCRP protein expression, as protein downregulation would have also decreased BCRP surface expression.

It was noted that curcumin at 10 μM did not decrease BCRP surface expression. As mentioned previously (Section 5.4), curcumin is not a very potent inhibitor of PI3K/AKT signaling (IC_{50} of AKT phosphorylation at ≥ 20 μM), and was not expected to cause significant suppression of this pathway in the current assay (Qiao et al., 2013; Yu et al., 2008). In addition, curcumin is rapidly conjugated and metabolised in MDCKII/BCRP cells, further decreasing its ability to suppress AKT phosphorylation in this cell line (Wortelboer et al., 2003).

The analogue A13 was observed to significantly increase 5D3 staining after 24 and 72 h incubation (Figure 6-2). This was not due to intrinsic fluorescence, as cells incubated with the analogues only were not fluorescent in the PE channel (see Appendix III). Also, the cells underwent multiple wash steps prior to analysis, reducing binding of the analogues to the cell surface. However, it has been previously shown that BCRP co-incubation with inhibitors, such as Ko143, can increase 5D3 staining by stabilising a high affinity conformation of BCRP (Ozvegy-Laczka et al., 2005). However, it was also observed that such an effect could not be induced in paraformaldehyde-fixed samples, since fixation already stabilises BCRP in a high affinity state (Ozvegy-Laczka et al., 2005). Thus, it appears that the increased 5D3 staining from A13 treatment was not caused by increased affinity to BCRP, but rather an increase in the plasma membrane localisation of the transporter. The mechanism by which A13 causes this effect is not known, but similar results have been observed from activation of the PI3K/AKT pathway, for example, by treatment with epidermal growth factor (Meyer zu Schwabedissen et al., 2006; Takada et al., 2005). Although the increased expression of surface BCRP may attenuate the inhibition of the transporter, the effect caused by A13 was limited, with 17% upregulation after 24 h, which

plateaued to 19% after 72 h. in addition, A13 fully reversed BCRP-mediated resistance in the resistance reversal assay (see Table 3-5), indicating that this upregulation did not compromise transport inhibition.

As BCRP internalisation may occur within 90 min, it remains a possibility that this may have occurred in the 2 h flow cytometry assay. The MDCKII/BCRP cells were also exposed to higher concentrations of the analogues (20 μM) compared to the mitoxantrone resistance reversal assay (Takada et al., 2005). This was investigated with MDCKII/BCRP and BeWo cells treated under similar conditions as the flow cytometry assay. In contrast to results from the previous section (Section 6.3.2), a significant decrease in 5D3 staining was observed after treatment of MDCKII/BCRP cells with 20 μM of curcumin, A13, RL92, or the positive control wortmannin (5 μM); while no effect was seen with gefitinib (negative control). The decreased staining was unlikely to have resulted from cytotoxicity since "live-gating" excluded apoptotic, necrotic and permeabilised cells (see Section 2.2.5.4). Also, cytotoxicity to MDCKII/BCRP cells (see Section 3.3.2) did not correlate with surface downregulation, since the most cytotoxic analogue (B11) had no effect on surface expression. Internalisation of the antibody-target complex or its capping and shedding to the media may also decrease staining, but these are energy-dependent processes that are unlikely to occur in dead paraformaldehyde-fixed samples (Radbruch, 2000; Smit et al., 1974).

It is also possible that decreased staining resulted from covalent modification of epitopes on BCRP, which prevents 5D3 binding to the transporter (Ozvegy-Laczka et al., 2008). To investigate this, immunostaining was conducted in cells that were fixed with paraformaldehyde first and then incubated with 20 μM A13 or RL92 for 2 h (the reverse of the usual protocol). BCRP internalisation will not be observed in these cells, but decreased fluorescence from covalent modification of the 5D3 binding site will be detected. However, no decreased fluorescence was observed in the samples that were fixed and then treated with either compound, indicating that they do not affect 5D3 binding to BCRP (Appendix IV). Lastly, the 5D3 antibody itself may have been covalently modified by the test compounds, decreasing its affinity to BCRP. However, samples were washed at least 6 times with PBS before incubation with 5D3 so that there should be little to no analogue present to bind to the antibody. Thus, it is clear that the decreased 5D3 staining after MDCKII/BCRP treatment with curcumin, A13 or RL92 was not an artifact of the assay, but was due

to internalisation of BCRP. It could therefore be concluded that in the flow cytometry studies, surface downregulation likely contributed to the inhibition of BCRP transport activity by curcumin, A13 and RL92. However, whether the 21% and 36% decrease in surface expression by curcumin and A13 respectively, also decreased BCRP-mediated mitoxantrone efflux to the same extent, cannot be concluded with certainty. To assess the impact of this downregulation, functional transport studies (e.g., mitoxantrone accumulation) would have to be conducted on treated cells.

Studies were also conducted in BeWo choriocarcinoma cells to confirm results observed in MDCKII/BCRP. It was found that A13 and wortmannin induced significant surface BCRP downregulation, but not curcumin or RL92. It is not known why curcumin and RL92 failed to show an effect in BeWo cells. It may be possible that their surface downregulatory effects are species-specific, as MDCKII cells are of canine origin, whereas BeWo are human. Further studies in human BCRP-expressing cell lines are therefore needed to clarify this issue. With A13, the results demonstrated that its effect is neither cell-line, nor species-specific, and might be observed in other BCRP-expressing cells.

Induction of BCRP internalisation was observed for curcumin, A13 and RL92, but the mechanism of action has not been determined. Given the important role of the PI3K/AKT signaling cascade on BCRP plasma membrane localisation, it is reasonable to assume that curcumin may have induced internalisation through its inhibitory effects on this pathway (Imai et al., 2012; Mogi et al., 2003; Nakanishi and Ross, 2012; Qiao et al., 2013). The IC_{50} of AKT phosphorylation for curcumin was previously found to be ~ 20 μM, matching the concentration used in Section 6.3.3 (Qiao et al., 2013; Yu et al., 2008). Whether A13 and RL92 decreased surface BCRP through a similar mechanism is not known, as neither analogue has been investigated for PI3K/AKT inhibition. Further studies should be conducted to ascertain the effects of the tested analogues (A12, A13, B11, RL92) on PI3K/AKT signaling, and determine if inhibition correlated with transporter internalisation. Characterising their effects on PI3K/AKT is important as inhibition of this pathway has been demonstrated to also decrease the expression of MRP1 and MRP5 (Duong et al., 2013; Gao et al., 2013; Tazzari et al., 2007). If A13, RL92 and curcumin were found to inhibit PI3K/AKT activation, this might also provide some explanation for their suppressive effects on MRP1 and MRP5 transport activity (Figure 2-16).

The PI3K/AKT signaling pathway is not the sole regulator of BCRP plasma membrane localisation (Meyer zu Schwabedissen et al., 2006; Nakanishi et al., 2006; Xie et al., 2008). This is supported by the partial decrease in BCRP surface expression despite treatment with wortmannin (5 μM), at a concentration expected to completely block AKT-phosphorylation (Figure 6-2 and Figure 6-3) (Arcaro and Wymann, 1993; Yano et al., 1993). Modulation of other pathways linked to BCRP localisation should therefore be investigated. This could include effects of the analogues on the serine/threonine-protein kinase pim-1 (Pim-1), which phosphorylates BCRP at threonine-362 (Xie et al., 2008). Inhibiting Pim-1 phosphorylation by mutating threonine-362 to alanine causes BCRP to localise in the cytoplasm rather than the plasma membrane (Xie et al., 2008).

Although internalisation of BCRP from the cell surface decreases the intracellular accumulation of fluorescent substrates, it may not translate to a reversal in BCRP-mediated drug resistance. Cytoplasmic BCRP has been shown to co-localise with lysosomal markers, suggesting that they may continue to resistance by sequestering drugs in sub-cellular compartments, such as lysosomes and endosomes (Rajagopal and Simon, 2003). This has been observed with P-gp by Yamagishi et al. (2013), which demonstrated that intracellular P-gp conferred doxorubicin resistance by pumping the basic drug into lysosomes, where it gets ionized and trapped due to the low intra-lysosomal pH. BCRP internalisation by A13 and RL92 should therefore be interpreted with caution as to their impact on drug resistance, especially for basic, ionisable drugs like mitoxantrone.

In summary, immunostaining of BCRP showed that A12, A13, B11, RL92 did not cause internalisation of the transporter under treatment conditions similar to the 72 h mitoxantrone resistance reversal assay. Hence, these analogues did not resensitise MDCKII/BCRP cells to mitoxantrone via this mechanism. In contrast, A13, RL92 and curcumin, significantly decreased BCRP surface expression under treatment conditions similar to the flow cytometry screening studies, suggesting that BCRP internalisation may have contributed to the increased intracellular accumulation of mitoxantrone in this assay. The discrepancy in the results between the two treatments could be possibly due to the higher concentrations of curcumin and the analogues (20 μM) used in the flow cytometry vs. the resistance reversal assays (10 μM curcumin, 5 μM A13 and 2 μM RL92). The mechanism of induction of BCRP internalisation by A13, RL92 and curcumin has

not been investigated but is suspected to be due to inhibition of the PI3K/AKT signaling cascade. As this mechanism has also been implicated in the expression of MRP1 and MRP5, investigating the effects of these three compounds on this pathway might also provide an explanation for their inhibition of MRP1 and MRP5-mediated transport.

7. General Discussion

7.1 Restatement of the aims

The main aim of this research was to determine whether 24 heterocyclic MACs retained the inhibitory effects of curcumin on the ABC transporter efflux pumps (P-gp, BCRP, MRP1 and MRP5), with the purpose of identifying more potent and stable alternatives to curcumin as ABC transporter inhibitors. As some of these analogues have potent anticancer activity, the possibility of identifying compounds with dual MDR-reversal and anticancer activity is an exciting prospect, and may lead to novel agents with superior anti-tumour efficacy.

7.2 Summary of results

In this study, 24 analogues plus curcumin were screened for inhibition of the three major ABC transporters (P-gp, BCRP and MRP1) reported to be involved in cancer MDR. In addition, inhibition of MRP5, a transporter implicated in pancreatic cancer resistance, was also investigated. Using flow cytometry, inhibitors were discovered for each of the four transporters examined. At a concentration of 20 μM, 2 compounds (C10 and RL92) completely inhibited P-gp mediated transport; 4 inhibited BCRP (A12, A13, B11 and RL92); and 2 inhibited MRP1 and MRP5 (A13, RL92). This is the first evidence of ABC transporter modulation by these analogues, and, to the knowledge of the author, the first evidence of BCRP and MRP1 inhibition by MACs. It was discovered that all analogues tested were either significantly more potent, or at least equipotent with curcumin at inhibiting these transporters. It was also found that certain analogues retained the broad inhibitory activity of the parent compound. These included RL92, which substantially decreased the transport of all four transporters at 20 μM, and A13, which completely inhibited BCRP, MRP1 and MRP5 transport at the same concentration.

After the most potent inhibitors were identified, they were tested for the ability to reverse ABC transporter-mediated resistance in various cell lines. It was found that the P-gp inhibitors C10 and RL92 could effectively reverse P-gp-mediated resistance to paclitaxel while the BCRP inhibitors A12, A13, B11 and RL92 significantly reversed BCRP-mediated resistance to mitoxantrone. For the two most potent BCRP inhibitors A12 and A13, it was demonstrated that these could also

sensitise MDCKII/BCRP cells to another BCRP substrate, topotecan, and could reverse mitoxantrone resistance in BeWo cells, showing that the action of both analogues was neither cell-line, nor substrate-specific. For the MRP1 and MRP5 inhibitors A13 and RL92, resistance reversal effects were not thoroughly assessed as their potent antiproliferative effects on the HEK293 cell line precluded the use of sufficiently high concentrations for transport inhibition. In addition to their resistance-reversal effects, it was also found that the analogues were unlikely to be substrates of the transporters that they inhibited, as transporter-expressing cell lines were as sensitive to the antiproliferative effects of the analogues as the parental cells.

It was evident from both the flow cytometry and cell proliferation assays that the analogues were most effective at inhibiting BCRP. Thus subsequent experiments focused on the BCRP inhibitors A12, A13, B11 and RL92 with the aim of better characterising their interaction with BCRP, and gaining some insight into the mechanism of transport inhibition. Using cell-free membrane vesicles, BCRP inhibition by these analogues was further confirmed, as well as their non-substrate specific inhibition of the transporter. It was also determined that the analogues could directly inhibit BCRP without requiring intracellular bioactivation to an active metabolite. As protein downregulation or BCRP internalisation may have been induced in the 72 h resistance-reversal assays, immunoblotting and cell surface immunostaining studies were conducted. It was found that none of the analogues affected BCRP protein levels, nor the localisation of BCRP after 72 h incubation with low concentrations. However, it was observed that A13, RL92 and curcumin could significantly decrease cell surface expression within 2 h, when used at a high concentration of 20 μM. Taking these results together, the major mechanism of BCRP inhibition by A12, A13, B11 and RL92 was considered to be direct inhibition of the transporter and not the modulation of transporter expression or plasma membrane localisation.

7.3 A13 and B11 as dual-role chemosensitisers

One of the main reasons for screening the cyclohexanone analogues for ABC transporter inhibitory activity was that some analogues have superior anticancer activity than curcumin. Hence, there was a possibility that dual-role chemosensitisers with both ABC transporter inhibitory effects and intrinsic antiproliferative activity might be identified.

In this study, five promising ABC transporter inhibitors, C10, A12, A13, B11 and RL92 were discovered. However, not all had intrinsic anticancer activity, as based on the cytotoxicity screening conducted by Yadav et al. (2010). Only A13 and B11 were found to have potent cytotoxic activity that was superior to curcumin. Thus, only these two analogues may be further considered as dual-role chemosensitisers.

7.3.1 The analogue A13 as dual-role chemosensitiser

A13 was a more potent inhibitor of BCRP, MRP1 and MRP5 than curcumin, although it lacked inhibitory effects on P-gp. As a BCRP inhibitor, it was not cell line, nor substrate-specific. It inhibited BCRP at sub-micromolar concentrations in the membrane vesicle assay and was a more effective downregulator of BCRP surface expression than curcumin. As an antiproliferative agent, A13 was more potent than curcumin against TNBC and other cell lines, such as pancreatic and colorectal cancer cells. A13 was found to be 3-fold more potent than curcumin at inhibiting the growth of the TNBC cell line, MDA-MB-231. Similarly it was reported to be 5-fold more potent at inhibiting pancreatic (Panc-1, IC_{50} = 4.43 μM) and colon cancer cells (HT-29, IC_{50} = 3.73 μM) (Liang et al., 2009; Wei et al., 2012; Yadav et al., 2010).

7.3.1.1 Triple-negative breast cancer

Both BCRP and MRP1 are upregulated in TNBC and may contribute to chemotherapy resistance (see Section 1.2.4.2) by effluxing anticancer drugs used in neoadjuvant therapy. Examples of anticancer drugs used to treat TNBC that are BCRP and MRP1 substrates include doxorubicin and epirubicin (MRP1), MTX (BCRP, MRP1), and 5-FU (BCRP) (Deeley and Cole, 2006; Isakoff, 2010; Litman et al., 1997; Volk and Schneider, 2003; de Wolf et al., 2008; Yuan et al., 2009; Zhang et al., 2014). As A13 inhibits both BCRP and MRP1, combining A13 with these compounds may block

the efflux of these drugs and reverse treatment resistance. Such combinations should therefore be further studied in *in vitro* models of TNBC.

TNBC has a high recurrence rate after neoadjuvant chemotherapy (André and Zielinski, 2012; Dent et al., 2007) which may result from the more frequent presence of side-population cells in TNBC than in less aggressive subtypes (Britton et al., 2012; Liu and Wicha, 2010). Side population cells are putative cancer stem cells, and are characterised by high BCRP expression (see Section 1.2.4.4) (Britton et al., 2011; Gangopadhyay et al., 2013; Patrawala et al., 2005). By inhibiting BCRP, A13 might sensitise the side population to BCRP substrates (e.g., MTX and 5-FU), helping to eradicate this resistant subpopulation. Aside from inhibiting BCRP, A13 itself may be cytotoxic against the cancer stem cell-like side population. A13 inhibits NF-κB, which has been linked with cancer stem cell survival (Prasad et al., 2010; Yadav et al., 2010). The specific inhibition of NF-κB activation by small molecule inhibitors such as parthenolide and pyrrolidinethiocarbamate, significantly decreased the side population in MCF-7 breast cancer cells (Prasad et al., 2010; Yadav et al., 2010; Zhou et al., 2008b).

7.3.1.2 Pancreatic cancer

In pancreatic cancer (see Section 1.2.4.4), A13 could be a promising alternative to curcumin as a dual-role chemosensitiser. It has superior anti-proliferative effects to curcumin against pancreatic cancer cells, and it inhibits NF-κB signaling which is linked to the high intrinsic resistance of pancreatic tumours to anticancer drugs (Arlt et al., 2003; Wang et al., 1999; Wei et al., 2012; Yadav et al., 2010). A13 is twice as potent as curcumin at inhibiting MRP5 which is considered an important target in reversing chemotherapy resistance due to its upregulation in pancreatic tumours and its ability to efflux the two main drugs used in pancreatic chemotherapy, gemcitabine and 5-FU (see Section 1.2.4.3). Inhibition of MRP5 has previously been demonstrated *in vitro* to reverse the resistance of pancreatic cancer and MRP5-transfected cells to gemcitabine and 5-FU (Hagmann et al., 2010b; Li et al., 2011; Nambaru et al., 2011). Curcumin in particular, reversed the resistance of Panc-1 and MiaPaca-2 cells to 5-FU, by inhibiting MRP5-mediated transport (Li et al., 2011). Given the superior activity of A13 over curcumin, improved resistance reversal might be observed with A13/gemcitabine or A13/5-FU combinations.

It should be noted that not only is A13 a more potent MRP5 inhibitor than curcumin but it also seems to be more potent than other MRP5 inhibitors reported in the literature (see Section 1.2.3.4). Although caution should be exercised in comparing IC_{50} values due to the differences in substrates and experimental conditions, it appears that A13 (IC_{50} = 12 μM) is more potent than MK-571 (16-17 μM), glyburide (15 μM), probenecid (34 – 70 μM), sildenafil (580 μM), trequinsin (218 – 580 μM) and zaprinast (20 – 32 μM) (Pratt et al., 2005, 2006; Reid et al., 2003). Two compounds, NPPB (IC_{50} = 2 μM) and hylin (5 μM), appear to be more potent than A13, but neither are known to have antiproliferative effects against pancreatic cancer cells (Pratt et al., 2005; Prehm, 2013). The potent inhibition by NPPB was also determined using membrane vesicles and not whole cells (Pratt et al., 2005, 2006). In Section 3.3.5.3, NPPB at a high concentration of 40 μM, only partially reversed resistance in HEK/MRP5 cells, suggesting that it is less potent in whole cells. Hence, A13 appears to be one of the best candidates as a dual-role chemosensitiser for resistant pancreatic cancer to date.

7.3.1.3 Colorectal cancer

The antiproliferative effects of A13 against colon cancer cells and its potent inhibition of BCRP also make it a possible candidate as a dual-role chemosensitiser in colorectal cancer. BCRP, but not P-gp or MRP1, has been implicated in the resistance of colorectal cancer to irinotecan, a widely used first-line drug (Lin et al., 2013; Mazard et al., 2013; Nakatomi et al., 2001; Yoshikawa et al., 2004). As BCRP inhibition has been demonstrated to reverse irinotecan resistance in *in vitro* and *in vivo* colorectal cancer models, combining A13 with irinotecan containing regimens, such as FOLFIRI (5-FU, leucovirin, irinotecan) might lead to improved treatment outcomes (Braun et al., 2005; Mazard et al., 2013; Yoshikawa et al., 2004). A recent study has also significantly linked high BCRP expression in colon cancer with poor response to FOLFOX (5-FU, leucovirin, oxaliplatin) (Lin et al., 2013). As 5-FU is a reported substrate of BCRP, A13/FOLFOX combinations could also be investigated in chemotherapy-resistant colon cancer models (de Wolf et al., 2008; Yuan et al., 2009).

7.3.2 B11 as dual-role chemosensitiser

The analogue B11 was a more potent BCRP inhibitor than curcumin. Studies into its BCRP inhibition indicate that it directly inhibits the transporter without requiring bioactivation. It was not

substrate-specific and was demonstrated to inhibit BCRP at sub-micromolar concentrations in membrane vesicle studies. As an anticancer agent, it was reported to be twice as effective at inhibiting MDA-MB-231 growth in cytotoxicity assays and has 4-fold greater antiproliferative activity against the colon cancer cell line (RKO) than curcumin (Gandhy et al., 2012; Yadav et al., 2010). Although B11 does not inhibit MRP1 and MRP5, it may be useful in TNBC when combined with BCRP substrates such as MTX and 5-FU (see Section 1.2.4.2). It might also sensitise BCRP-expressing side population cells to anticancer drugs, helping eradicate this tumourigenic subpopulation (see Section 7.3.1.1). Like A13, B11 inhibits NF-κB activation and may itself be cytotoxic against the side population (Yadav et al, 2010). B11 could also be investigated as a dual-role chemosensitiser in colorectal cancer, due to its inhibition of BCRP and intrinsic antiproliferative effects against colon cancer cells (Gandhy et al., 2012). Combinations of A13 with BCRP substrate drugs in colorectal cancer chemotherapy (e.g., MTX and 5-FU) should be further investigated in *in vitro* colon cancer models.

7.3.3 Future studies

7.3.3.1 *In vitro* and *in vivo* activity

The next step in investigating the potential of A13 and B11 as dual-role chemosensitisers is to assess their resistance-reversal effects in TNBC, pancreatic and colorectal cancer cell lines. This could include cell proliferation assays to investigate whether A13 or B11 increase the growth inhibitory effects of co-incubated drugs, and apoptosis assays (such as Annexin-V staining) to determine if they can enhance apoptosis induction. For TNBC, the triple-negative cell line, MDA-MB-231, could be used for such studies due to its similarities to TNBC tumour samples in its expression of BCRP and MRP1, and the presence of a resistant sub-population of cells (Hiraga et al., 2011; Da Silva et al., 2014). Possible combinations that might be investigated in TNBC could include A13 (or B11) with MTX or 5-FU, and A13 with doxorubicin or epirubicin (due to its inhibitory effects on MRP1). For pancreatic cancer, A13 combinations with gemcitabine or 5-FU could be tested in the pancreatic cancer cell lines, Panc-1 and MiaPaca-2, both of which overexpress MRP5 (Hagmann et al., 2010b; Li et al., 2011). Panc-1 is also positive for a BCRP-expressing side population, similar to that in patient tumour samples (Wang et al., 2009). For colorectal cancer, an A13 or B11 combination with irinotecan could be tested in the HT-29 cell line, which endogenously

expresses BCRP (Yanase et al., 2004). HT-29 has previously been used to demonstrate the reversal of irinotecan resistance by sunitinib and gefitinib via a BCRP-dependent mechanism (Mazard et al., 2013; Yanase et al., 2004). As many of the cell lines mentioned are positive for a side population of resistant cells, these could be isolated (e.g., by flow cytometry cell sorting) and the activity of A13 or B11 drug combinations evaluated against this intrinsically resistant, BCRP-expressing sub-population (Petriz, 2013). Cells could also be treated with anticancer drugs with or without the cyclohexanone analogues, and the proportion of the side population of cells after treatment could be monitored by flow cytometry and Hoechst 33342 staining. As BCRP expression is a marker for the side population, reduced accumulation of the BCRP substrate, Hoechst-33342, is the standard assay for detecting the side population fraction (Feuring-Buske and Hogge, 2001). Alternatively, CD44(+)/CD24(–) cells could be measured, as this immunostaining pattern is thought to represent the side population (Tanaka et al., 2009).

If promising chemosensitising activity is observed for A13 and B11 *in vitro*, studies could then be conducted in tumour xenograft models of TNBC, pancreatic and colorectal cancer. These could be established by the orthotopic implantation of MDA-MB-231, Panc-1 and HT-29 respectively into nude mice, a more clinically predictive model than subcutaneous tumour implantation (Bibby, 2004). In these studies, the *in vivo* chemosensitising effects of A13 and B11 in combination with anticancer drugs could be assessed together with their safety/toxicity and pharmacokinetics.

7.3.3.2 Inhibition of other ABC transporters

Aside from P-gp, BCRP, MRP1 and MRP5, other ABC transporters have also been implicated in cancer resistance. For example, MRP8 (ABCC11) has been found to be highly expressed in TNBC and its expression was significantly associated with a lower disease-free survival, as well as a decreased complete response rate to neoadjuvant therapy (Yamada et al., 2013). Although MRP8 was reported to efflux 5-FU, a decreased response to therapy was observed regardless if the treatment regimen contained 5-FU. It was hypothesised that MRP8 effluxes an endogenous substrate that affects drug resistance e.g., sphingosine-1-phosphate (Yamada et al., 2013). Nevertheless, inhibiting MRP8 efflux might help resensitise TNBC tumours to chemotherapy and both A13 and B11 should be screened for activity against this transporter. It should be noted that MRP8 shares a high sequence homology with MRP5 and both transporters export similar

substrates including cyclic nucleotides (e.g., cAMP and cGMP) and nucleoside-based drugs such as 9-(2-phosphonomethoxyethyl) adenine (PMEA) and 5-FU (Bera et al., 2001; Kruh et al., 2007). This suggests possible similarities between the substrate-binding sites of both transporters, and as A13 is an inhibitor of MRP5, it is likely that it may also inhibit MRP8.

Since both A13 and B11 have been proposed for use in combination with irinotecan in colon cancer, their inhibitory effects on MRP2 should also be assessed. The MRP2 transporter is thought to be responsible for the severe diarrhoea associated with irinotecan treatment (Middleton et al., 2013). This is caused by MRP2 efflux of the glucuronide conjugate of SN-38 (active metabolite of irinotecan) into the bile from where it is excreted into the intestines and subsequently cleaved by glucuronidases (Middleton et al., 2013; Swami et al., 2013). This releases the active SN-38 which causes the toxicity to the intestinal epithelium. If A13 or B11 inhibits MRP2, it is possible that these analogues could decrease this severe toxic side effect of irinotecan in the gut, in addition to reversing resistance of the tumour.

7.3.3.3 Nanomicelles and liposomal formulations

As both A13 and B11 are relatively hydrophobic, potential issues with solubility and pharmacokinetics may be encountered in future *in vivo* applications. For example, B10 (also known as RL71) was found by Yadav et al. (2012a) to be a potent inhibitor of TNBC cells *in vitro,* but was inactive *in vivo*. This was thought to be due to its hydrophobicity which limited its solubility and *in vivo* absorption. Taurin et al. (2013) encapsulated B10 in styrene-co-maleic acid (SMA) micelles which improved its solubility and stability, and increased its cytotoxic activity against a tumour spheroid model. Similar improvements in solubility, pharmacokinetic profile and activity have also been observed with liposomal formulations of curcumin (Anand et al., 2008; Li et al., 2005; Ranjan et al., 2013). Encapsulation of a drug in micelles and liposomes also has the advantage of improved targeting and accumulation in tumours due to the enhanced permeability and retention effect (Greish, 2010; Maeda, 2010). This may prevent off-target toxic side effects such as myelosuppression, neurotoxicity or nephrotoxicity which may arise from the inhibition of ABC transporters in tissues such as bone marrow, BBB or kidneys (Leonard et al., 2003; Palmeira et al., 2012a). As mentioned previously (see Section 0), increased toxicity due to ABC transporter

inhibition in normal tissue led to the failure of tariquidar in clinical trials. Hence, nanomicelle and liposomal formulations of A13 and B11 should be considered for future *in vitro* and *in vivo* studies.

7.3.3.4 PI3K/AKT inhibition

In cell surface staining studies, A13 significantly downregulated BCRP expression at the plasma membrane. This was thought to be due to possible inhibition of the PI3K/AKT pathway, a well-reported regulator of BCRP plasma membrane localisation (Huang et al., 2014; Mogi et al., 2003; Takada et al., 2005). A13 is known to decrease the activation of NF-κB, one of the downstream effectors of PI3K/AKT signaling (Yadav et al., 2010). Since it has not been demonstrated that A13 directly inhibits NF-κB, decreased activation may have been through modulation of PI3K/AKT signaling. Determining PI3K/AKT inhibition by A13 is important as this pathway has also been implicated in the expression of MRP1 and MRP5 (Duong et al., 2013; Gao et al., 2013; Tazzari et al., 2007). If it is demonstrated that A13 is a PI3K/AKT pathway inhibitor, it should be further investigated for surface and total protein downregulatory effects on MRP1 and MRP5.

7.3.3.5 MRP1 and MRP5 inhibition

So far, MRP1 and MRP5 inhibition by A13 has only been shown in flow cytometry screening, as the potent antiproliferative effects of the compound in HEK cells caused issues in the resistance reversal assays. To provide further evidence of inhibition, transport studies using membrane vesicles derived from MRP1 or MRP5 overexpressing cells could be conducted, as these cell-free systems are not susceptible to cytotoxic/cytostatic effects by the test compound. MRP1 membrane vesicles from transfected HeLa cells were used by Leslie et al. (2001) to show MRP1 inhibition by myricetin and quercetin, while Pratt et al. (2006) used MRP5 containing vesicles to show MRP5 inhibition by NPPB, probenecid and MK-571. In this study, it was observed that MDCKII cells were more resistant to A13's cytotoxic/cytostatic activity than HEK cells, indicating resistance-reversal assays should be conducted in MRP1 and MRP5 transfected MDCKII cells as these might allow higher concentrations of A13 to be used. Such cell lines were used by Luna-Tortos et al. (2010) to investigate MRP1 and MRP5 transport of antiepileptic drugs.

7.4 Future directions for C10, A12 and RL92

7.4.1 The analogue C10 as P-gp inhibitor

The C10 analogue did not have any cytotoxic activity against TNBC cell lines (Yadav et al., 2010). However, it was the most potent P-gp inhibitor of all the analogues investigated, and significantly reversed MDCKII/P-gp resistance to paclitaxel at a concentration as low as 0.5 μM. It has the potential to be a chemosensitiser in TNBC since P-gp expression was observed in a third of patients and important drugs used in neoadjuvant therapy are excellent P-gp substrates (Griffiths and Olin, 2012; Yamada et al., 2013). These include anthracyclines (e.g., doxorubicin and epirubicin) and taxels (e.g., paclitaxel and docetaxel), the latter being exclusive P-gp substrates (André and Zielinski, 2012; Griffiths and Olin, 2012; Isakoff, 2010). More importantly, P-gp inhibition by C10 suggests that it might also be useful to reverse the resistance of promising new drugs in TNBC. These include the P-gp substrate, ixabepilone, a newly approved first-in-class drug for the treatment of taxane-resistant cancer (Shen et al., 2011). The promising experimental drug, olaparib, has also been demonstrated as a P-gp substrate. Upregulation of the transporter caused resistance to olaparib in BRCA1/p53-deficient mice with triple-negative breast carcinomas (Jaspers et al., 2009). Hence, C10 may be able to reverse the resistance to olaparib treatment (Lawlor et al., 2014). Further studies for C10 should therefore investigate combinations with doxorubicin, epirubicin, paclitaxel, docetaxel, ixabepilone and olaparib in cytotoxicity or cell proliferation assays using TNBC cell lines (e.g., MDA-MB-231 or MDA-MB-468).

The involvement of P-gp in other diseases (e.g., HIV and epilepsy) suggests that C10 could have applications beyond cancer. In epilepsy, P-gp has been linked with resistance to treatment via the efflux of anti-epileptic drugs such as phenytoin, phenobarbital, carbamazepine and lamotrigine at the BBB (Hughes, 2008; Stępień et al., 2012; Zhang et al., 2012). P-gp inhibition by C10 could improve the brain penetration of these drugs to get to their site of action. P-gp efflux is also an issue in the treatment of HIV/AIDs as it limits the oral bioavailability of antiretrovirals and reduces their CNS access for the treatment of HIV brain infections (Cianfriglia et al., 2007; Weiss and Haefeli, 2006). Important antiretrovirals that are substrates of P-gp include saquinavir, ritonavir, indinavir and lopinavir (Weiss and Haefeli, 2006). To determine its potential effects on bioavailability, C10 could be investigated using Caco-2 cell monolayer transwell assays to see if it

can increase the apical-to-basolateral transport (representing absorption from the gut lumen) of the previously mentioned antiretrovirals. Similarly, C10's potential to increase the BBB penetration of such drugs could be determined in *in vitro* BBB models such as the transwell assays using glia and endothelial cell co-cultures. The addition of glial cells was found to increase the expression of ABC transporters, making it more representative of the BBB (Naik and Cucullo, 2012).

7.4.2 The analogue A12 as BCRP inhibitor

The analogue A12 was not active against TNBC cells but it was the most potent inhibitor of BCRP of the analogues investigated (Yadav et al., 2010). A12, with an IC_{50} of 1.1 – 1.6 μM (in both whole cells and membrane vesicles) was slightly less potent than other well-known BCRP inhibitors such as fumitremorgin C (IC_{50} = 0.5 μM) and elacridar (IC_{50} = 0.3 μM) but was more potent than cyclosporin A (K*i* = 6.7 μM) (Ahmed-Belkacem et al., 2005; Weiss et al., 2007; Xia et al., 2007b). The relatively high potency of A12 suggests that sufficient concentrations could be achieved in tumours to effectively block BCRP especially if A12 is co-encapsulated in liposomes or nanomicelles with BCRP substrate drugs, such as mitoxantrone, topotecan, irinotecan and 5-FU.

As with the other BCRP inhibitors, A13 and B11, A12 could also be investigated as a potential chemosensitiser in colorectal cancer due to the involvement of BCRP in the resistance to irinotecan and 5-FU (see Section 7.3.1.3). A12 could have an advantage over A13 and B11 due to its increased potency, although its lack of antiproliferative effects against colon cancer cells may also lead to inferior antitumour activity. Nevertheless, A12 combinations with irinotecan and 5-FU should be tested in cell proliferation or cytotoxicity assays using colon cancer cell lines e.g., HT-29 or HCT-116. It might also be worthwhile to investigate A12/5-FU combinations in breast cancer cells (e.g., MCF7, MDA-MB-231) based on a recent study significantly associating BCRP expression in clinical tissue samples with 5-FU resistance (Wang et al., 2013). A12 could also be used to sensitise cancer stem cell-like side population cells to BCRP substrates, although it might be less effective than A13 or B11 at suppressing this population, due to a lack of effect on NF-κB signaling (Yadav et al., 2010).

7.4.3 RL92 as an ABC transporter inhibitor

RL92 is the only compound that showed complete or near complete inhibition of P-gp, BCRP, MRP1 and MRP5 transport activity at ≤ 20 μM. In addition, with the exception of MRP1, it has superior or equal inhibitory potency to curcumin for these transporters. However, RL92 is not as potent as some of the other cyclohexanone analogues investigated. Its IC_{50} for the inhibition of ABC transporters ranged from 8.7 – 22.5 μM, and it is unclear if such concentrations are attainable in the tumour target tissue *in vivo*. RL92 might instead be used to enhance the oral bioavailability of therapeutic drugs whose absorption is limited by ABC transporters, as a higher concentration of RL92 is likely to be achieved in the intestinal lumen after oral administration (Oostendorp et al., 2009; Shukla et al., 2011). The induction of the rapid internalisation of cell surface BCRP may also occur in the enterocytes in the presence of 20 μM RL92.

7.4.3.1 Dual P-gp/BCRP inhibitor

The dual P-gp/BCRP inhibitory activity of RL92 makes it suitable for increasing the bioavailability of orally administered anticancer drugs, as many are dual substrates of P-gp and BCRP. These include topotecan and etoposide, and tyrosine kinase inhibitors, such as imatinib and dasatinib (Breedveld et al., 2006; Oostendorp et al., 2009; Shukla et al., 2011). The involvement of P-gp and BCRP in limiting the bioavailability of these drugs has been previously shown via pharmacological inhibition or single/double transporter KO mice studies (Breedveld et al., 2006; Oostendorp et al., 2009; Shukla et al., 2011). The potential impact of RL92 on oral bioavailability could be assessed using a Caco-2 cell monolayer assay in a transwell setup, and promising results could then be further investigated in animal studies (Sarmento et al., 2012).

7.4.3.2 MRP1 and MRP5 inhibitor

RL92 is a weak inhibitor of MRP1 but is equipotent with curcumin as an MRP5 inhibitor. As curcumin has been demonstrated to reverse the resistance of pancreatic cancer cell lines to MRP5 substrates (e.g., 5-FU), RL92 combinations with 5-FU and other drugs such as gemcitabine could be investigated in cytotoxicity or cell proliferation assays using pancreatic cancer cell lines, e.g., Panc-1, MiaPaca-2 or BxPC-3 (Griffin et al., 2007; Li et al., 2011). As discussed earlier in Section 7.3.3.2, due to high sequence homology, MRP5 inhibitors may also modulate MRP8 transporter

activity. Hence, RL92 should also be screened for inhibition against this emerging target in breast cancer, especially since very few compounds have been identified to be MRP8 inhibitors.

7.5 Structure-activity insights

7.5.1 β-diketone and transport inhibition

Removal of the β-diketone structure to produce MACs resulted in compounds with increased *in vitro* and *in vivo* stability compared to curcumin (Liang et al., 2009; Zhao et al., 2013). It was also demonstrated that the MACs had potent antiproliferative effects, indicating that the β-diketone was not essential for anticancer activity (Ishida et al., 2002; Mosley et al., 2007; Zhao et al., 2013). However, the impact of removing the β-diketone of curcumin on its broad ABC transporter inhibitory activity is less clear, as most studies on MACs have focused on their other biological effects (e.g., anticancer, antioxidant and antiinflammatory activity) (Mosley et al., 2007; Zhao et al., 2013). Dimmock et al. (2005) eventually demonstrated that the MACs could also inhibit P-gp, which was later confirmed by Um et al. (2008). Recently, Prehm et al. (2013) have reported MRP5 inhibition by hylin, which is the first report of MRP5 inhibition by a MAC. At present, inhibition of MRP1 and BCRP by MACs has not been reported. This study is therefore the first to demonstrate that MACs can also inhibit MRP1 and BCRP, indicating that the β-diketone group is not critical to curcumin's inhibitory effects on ABC transporters. This study is also the first to demonstrate that the MACs (e.g., A13 and RL92) can be broad inhibitors of ABC transporters, indicating that the β-diketone group is not critical to curcumin's inhibitory effects on the ABC transporters. These results have implications in the search for dual-role chemosensitisers as MACs with potent anticancer activity could also be screened for ABC transporter inhibitors.

7.5.2 The impact of structural features and physicochemical properties on transport inhibition and cytotoxicity

In addition to identifying new ABC transporter inhibitors, useful structure-activity relationship data was also gained from the screening studies. This could be compared with cytotoxicity screening data to determine the impact of specific structures or physicochemical properties on ABC transporter inhibition and anticancer activity (Yadav et al., 2010). This may help in the future design of second generation cyclohexanone analogues by incorporating structural features favourable for both cytotoxicity and ABC transporter inhibition, and avoiding groups that negatively impact on these properties.

For example, it was observed that the N-methylpiperidone (NMP) core of the B-series analogues was associated with increased cytotoxicity, and improved P-gp inhibition. This was apparent with B12 (structure in Figure 7-1) which had better cytotoxicity and P-gp inhibition compared to the cyclohexanone core-containing analogue, A12 (Table 7-1). The NMP core may improve P-gp inhibition due to the presence of a tertiary nitrogen, a common feature of potent P-gp inhibitors (Liu et al., 2013; Palmeira et al., 2012b). A nitrogen in the central ketone was also observed by Yadav et al. (2010) to be associated with increased cytotoxicity. The NMP core may therefore be considered as a base structure for synthesising second generation analogues. However, it should be noted that NMP has a lower lipophilicity than the cyclohexanone core which may lead to decreased BCRP inhibition, since it is significantly correlated with compound lipophilicity (Section 2.4) (Matsson et al., 2007).

The phenyl ring methoxy (PRM) groups were associated with enhanced P-gp inhibition, both in this study and that by Dimmock et al. (2005) (see Section 2.4). However, it was not always associated with potent cytotoxic activity since the trimethoxyphenyl-containing A10 and C10 were not cytotoxic (Table 7-1). However, the most cytotoxic analogue (B10) identified by Yadav et al. (2010) contained trimethoxylated phenyl rings (Figure 7-1) indicating that at least, PRM groups did not necessarily negatively impact cytotoxic activity. In addition, PRM groups, when combined with the NMP core, resulted in analogues with potent cytotoxic activity and significant P-gp and BCRP inhibitory activity, as seen with B10, B11 and B12 (Table 7-1). The NMP-PRM structure should therefore be further explored when synthesising additional novel analogues.

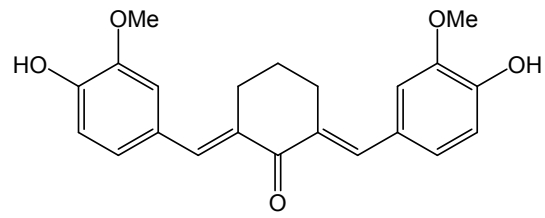

A13

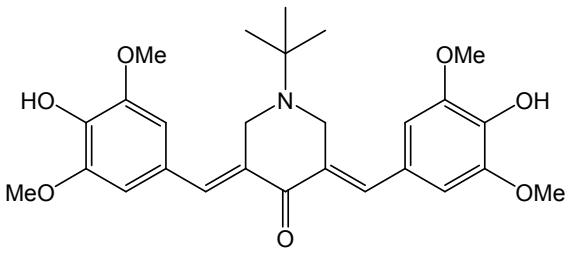

F14

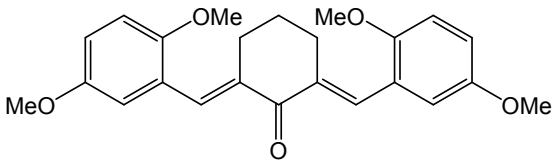

A12

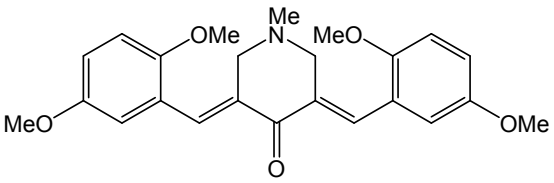

B12

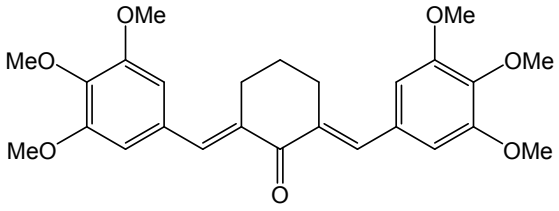

A10

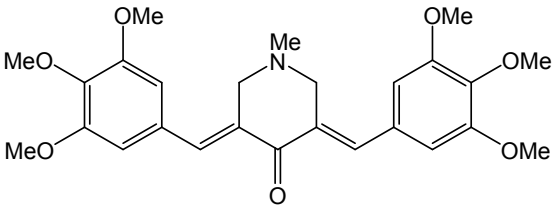

B10

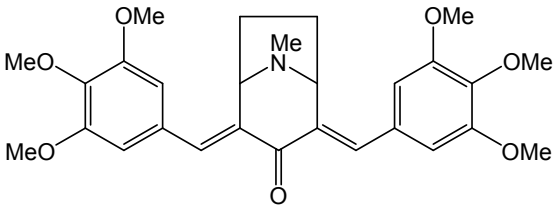

C10

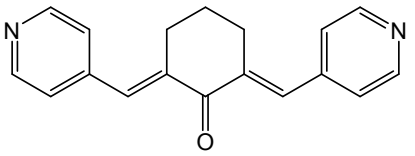

A1

Figure 7-1. Structures of selected cyclohexanone analogues.

Table 7-1. The cytotoxicity of cyclohexanone analogues against the TNBC cell line, MDA-MB-231, and their inhibition of ABC transporters.

	Cytotoxicity*	ABC transporter inhibition at 20 μM			
Compound	**MDA-MB-231 IC_{50} (μM)**	**P-gp**	**BCRP**	**MRP1**	**MRP5**
Curcumin	7.6	-	+	+++	+++
A1	1.1	-	-	-	-
A2	1.5	-	-	-	-
A3	3.3	-	-	-	-
A4	3.2	-	-	-	+
A5	>30	-	+	-	+
A6	>30	++	+	-	-
A7	>30	-	+	-	-
A8	1.9	-		-	-
A9	>10	-	++	-	-
A10	>30	not tested			
A12	>10	+	+++	-	-
A13	2.6	-	+++	+++	+++
B1	0.8	-	-	-	-
B2	2.1	-	-	-	-
B5	>30	-	+	-	-
B8	>30	-	-	-	-
B10	0.3	+	++	+	-
B11	3.8	++	+++	-	-
B12	1.1	++	+	-	-
C1	1.1	-	-	-	-
C2	12.9	-	-	-	-
C10	>30	+++	++	+	-
D2	8.6	-	-	-	-
E12	not tested	+	++	-	-
RL92	not tested	+++	+++	++	+++

* Cytotoxicity data adapted from (Yadav et al., 2010)
\+ 0 – 40% inhibition, ++ 40 – 80% inhibition, +++ > 80% inhibition
\- no significant inhibition

Lipophilicity alone significantly correlated with BCRP inhibition in this study (not shown), and was also critical for effective P-gp inhibition (Section 2.4). In contrast, for cytotoxicity, it was apparent that the antiproliferative effects of the analogues were independent of lipophilicity. Compounds with high (e.g., A13, cLogD $_{7.4}$ = 4.7) and low lipophilicity (e.g., B1, cLogD $_{7.4}$ = 1.8) were found to be potent cytotoxic agents (Table 7-1) (Appendix I). This suggests that the lipophilicity of the analogues may be increased to improve their P-gp and BCRP inhibitory activity without

compromising their cytotoxic activity. However, a caveat to this approach is that high lipophilicity might also cause issues with compound aqueous solubility (Taurin et al., 2013).

The para-substituted hydroxyl (PSH) group on the phenyl rings was associated with potent MRP1 and MRP5 inhibition (Section 2.4). This was observed with the complete inhibition of both MRP1 and MRP5 by curcumin and A13, which are the only compounds investigated with a PSH group. With regard to cytotoxicity, the impact of hydroxy substituents on the phenyl rings remains unclear, as only A13 contained a PSH group from the compounds investigated by Yadav et al. (2010). A13 was found to have potent cytotoxic activity which at least suggests that a PSH group does not negatively affect cytotoxicity (Yadav et al., 2010). Hence, the inclusion of a para-positioned hydroxyl in the phenyl rings may confer inhibitory affects against MRP1 and MRP5 without weakening cytotoxic activity.

Lastly, it should be noted that, although the nitrogen-containing pyridine aromatic groups were significantly associated with potent antiproliferative effects (e.g., analogues A1, A2, B1, B2, C1) (see Figure 7-1 for A1 structure), none of these analogues inhibited ABC transporters (Table 7-1). This was probably because the pyridine group is polar, which reduces compound lipophilicity and affects membrane partitioning (Seelig, 1998; Yadav et al., 2010). Thus, the inclusion of pyridine groups is unlikely to result in analogues with both good cytotoxicity and transporter inhibitory activity.

In summary, it is clear that there are structural motifs that are positively associated with both transporter inhibition and cytotoxicity (e.g., tertiary nitrogens in the core ketone) which could be incorporated to confer both transporter inhibition and cytotoxic effects on a second generation of analogues. It is also apparent that certain structural features and physicochemical properties (e.g., lipophilicity) associated with ABC transporter inhibition have no influence on compound cytotoxicity. This may make it possible to optimise transporter inhibitory effects without negatively affecting cytotoxic activity. Finally, some structural features (e.g., pyridine groups) were identified which increase cytotoxicity but are unfavourable for transporter inhibition. Such groups should be avoided in the future design of dual-role chemosensitisers.

7.5.3 F14, a novel cyclohexanone analogue

Applying the structure-activity knowledge as outlined previously, a new analogue (F14) is proposed (Figure 7-1) which may have better activity than A13, the best candidate identified in this study. Although A13 is a promising dual-role chemosensitiser, it cannot inhibit P-gp and is a less potent cytotoxic agent than some other cyclohexanones, such as A1, A2, B1, B2 and B10 (Table 7-1).

It is suggested that F14 will inhibit P-gp and have improved cytotoxicity due to a tertiary nitrogen-containing N-tertbutylpiperidone core (Figure 7-1). As discussed previously, the tertiary nitrogens were associated with P-gp inhibition; while the nitrogen-containing backbone improved cytotoxic activity. The tert-butyl group attached to the nitrogen increases the lipophilicity of the molecule, which is essential for both BCRP and P-gp inhibition (Liu et al., 2013; Matsson et al., 2007). The presence of an additional meta-positioned methoxy group compared to A13, might help further improve P-gp inhibition, while the 4'-hydroxy groups ensure that F14 also has MRP1 and MRP5 inhibitory activity (Section 2.4) (Prehm, 2013; Sreenivasan et al., 2013). As F14 has a piperidone core, it has a lower lipophilicity than A13 ($cLogD_{7.4}$ of 4.06 vs. 4.67 for A13, calculated using Marvin chemistry suite, ChemAxon, Cambridge, MA), but the presence of extra oxygen and nitrogen atoms increases its polarisability (52.0 vs. 39.9 for A13). Hence, the product of $cLogD_{7.4}$ and molecular polarisability for F14 (211.1) is greater than that for A13 (186.3). Given that this parameter was significantly correlated with BCRP inhibition (Section 2.4), it is possible that F14 may achieve equal or greater BCRP inhibition than A13 (Mattson et al., 2007).

Thus, the analogue F14 could potentially retain all of the desirable properties of A13 (such as the inhibition of BCRP, MRP1 and MRP5) and in addition, also inhibit P-gp and have improved cytotoxic activity. It might therefore address some of the limitations of A13 and be a more effective dual-role chemosensitiser.

7.6 Concluding remarks

The aim of this study was to determine the inhibitory effects of heterocyclic cyclohexanone MACs on the major ABC transporters involved in cancer MDR, and identify compounds with both intrinsic anticancer activity and ABC transporter inhibitory effects. Such 'dual-role' chemosensitisers are thought to be more effective MDR reversal agents than compounds that are only ABC transporter inhibitors. This study has shown that cyclohexanone analogues of curcumin can inhibit all four ABC transporters tested (P-gp, BCRP, MRP1 and MRP5), and provided the first evidence of BCRP and MRP1 inhibition by cyclohexanone analogues. The unstable β-diketone moiety was not essential for ABC transporter inhibition which will hopefully encourage the screening of other structurally similar MACs with potent anticancer activity for ABC transporter inhibitory effects. More potent inhibitors than curcumin have been identified for all the ABC transporters investigated, and these should be further assessed as cancer chemosensitisers and also as resistance-reversal agents in other diseases such as epilepsy and HIV. In particular, two compounds (A13, B11), both with potent antiproliferative effects and ABC transporter inhibitory activity, should be further investigated as dual-role chemosensitisers. These not only inhibit BCRP, which is protective of cancer stem-cell-like sub-population cells, but also suppress NF-κB activation, which is a contributor to cancer stem cell survival. Hence these analogues may not only sensitise the tumour bulk to anticancer drugs but may also cause a more effective suppression of the inherently resistant, highly tumourigenic 'side population' cells, thought to be responsible for residual disease and tumour recurrence. It is possible therefore that both compounds may be more effective MDR reversal agents than the non-cytotoxic ABC transporter modulators that have undergone clinical trials to date. Lastly, in the screening of the cyclohexanone analogues, this study has gained some structure-activity insights that may be considered together with cytotoxicity SAR studies to help synthesise the next generation of cyclohexanone analogues with improved anticancer and ABC transporter inhibitory activity. A new analogue, F14, has been proposed in this study based on SAR which will hopefully be an improvement over the current best candidate, A13.

Publications arising from this thesis

Papers submitted

1. Jezrael L Revalde, Yan Li, Lesley Larsen, Rhonda J Rosengren, and James W Paxton. Cyclohexanone analogues of curcumin inhibit the activity of ATP-binding cassette transporters. Submitted to *Biochemical Pharmacology*.

Conference abstracts

1. Revalde JL, Li Y, Rosengren R, Larsen L, Paxton JW. The Mechanism of Inhibition of Breast Cancer Resistance Protein Efflux Activity by Heterocyclic Cyclohexanone Analogues of Curcumin [abstract]. In: Proceedings of the 10th International ISSX Meeting; 2013 Sep 29 – Oct 3; Toronto, Canada. Abstract nr P467.
2. Revalde JL, Li Y, Rosengren R, Larsen L, Paxton JW. The Modulatory Effects of Novel Curcumin Analogues on Xenobiotic ABC Transporters [abstract]. In: Proceedings of the 19th MDO and 12th European Regional ISSX Meeting; 2012 Jun 17-21; Noordwijk Aan Zee, the Netherlands. Abstract nr P271.
3. Revalde JL, Li Y, Paxton JW. Thymoquinone Inhibition of Breast Cancer Resistance Protein Transport Activity [abstract]. In: Proceedings of the 4th Asian Pacific Regional ISSX Meeting; 2011 Apr 22-25; Tainan, Taiwan. Abstract nr 99.

References

Adams, B.K., Ferstl, E.M., Davis, M.C., Herold, M., Kurtkaya, S., Camalier, R.F., Hollingshead, M.G., Kaur, G., Sausville, E.A., Rickles, F.R., et al. (2004). Synthesis and biological evaluation of novel curcumin analogs as anti-cancer and anti-angiogenesis agents. Bioorg. Med. Chem. *12*, 3871–3883.

Adkison, K.K., Vaidya, S.S., Lee, D.Y., Koo, S.H., Li, L., Mehta, A.A., Gross, A.S., Polli, J.W., Humphreys, J.E., Lou, Y., et al. (2010). Oral sulfasalazine as a clinical BCRP probe substrate: pharmacokinetic effects of genetic variation (C421A) and pantoprazole coadministration. J. Pharm. Sci. *99*, 1046–1062.

Agarwal, S., Hartz, A.M.S., Elmquist, W.F. and Bauer, B. (2011). Breast cancer resistance protein and P-glycoprotein in brain cancer: two gatekeepers team up. Curr. Pharm. Des. *17*, 2793–2802.

Aguirre-Ghiso, J.A. (2007). Models, mechanisms and clinical evidence for cancer dormancy. Nat. Rev. Cancer *7*, 834–846.

Ahmed-Belkacem, A., Pozza, A., Muñoz-Martínez, F., Bates, S.E., Castanys, S., Gamarro, F., Di Pietro, A. and Pérez-Victoria, J.M. (2005). Flavonoid structure-activity studies identify 6-prenylchrysin and tectochrysin as potent and specific inhibitors of breast cancer resistance protein ABCG2. Cancer Res. *65*, 4852–4860.

Aldridge, G.M., Podrebarac, D.M., Greenough, W.T. and Weiler, I.J. (2008). The use of total protein stains as loading controls: an alternative to high-abundance single-protein controls in semi-quantitative immunoblotting. J. Neurosci. Methods *172*, 250–254.

Alison, M.R., Lin, W.-R., Lim, S.M.L. and Nicholson, L.J. (2012). Cancer stem cells: in the line of fire. Cancer Treat. Rev. *38*, 589–598.

Allen, J.D., van Loevezijn, A., Lakhai, J.M., van der Valk, M., van Tellingen, O., Reid, G., Schellens, J.H.M., Koomen, G.-J. and Schinkel, A.H. (2002). Potent and specific inhibition of the breast cancer resistance protein multidrug transporter in vitro and in mouse intestine by a novel analogue of fumitremorgin C. Mol. Cancer Ther. *1*, 417–425.

Aller, S.G., Yu, J., Ward, A., Weng, Y., Chittaboina, S., Zhuo, R., Harrell, P.M., Trinh, Y.T., Zhang, Q., Urbatsch, I.L., et al. (2009). Structure of P-glycoprotein reveals a molecular basis for poly-specific drug binding. Science *323*, 1718–1722.

Amiri-Kordestani, L., Basseville, A., Kurdziel, K., Fojo, A.T. and Bates, S.E. (2012). Targeting MDR in breast and lung cancer: discriminating its potential importance from the failure of drug resistance reversal studies. Drug Resist. Updat. *15*, 50–61.

Anand, P., Thomas, S.G., Kunnumakkara, A.B., Sundaram, C., Harikumar, K.B., Sung, B., Tharakan, S.T., Misra, K., Priyadarsini, I.K., Rajasekharan, K.N., et al. (2008). Biological activities of curcumin and its analogues (Congeners) made by man and Mother Nature. Biochem. Pharmacol. *76*, 1590–1611.

Anders, C.K., Zagar, T.M. and Carey, L.A. (2013). The management of early-stage and metastatic triple-negative breast cancer: a review. Hematol. Oncol. Clin. North Am. *27*, 737–749, viii.

André, F. and Zielinski, C.C. (2012). Optimal strategies for the treatment of metastatic triple-negative breast cancer with currently approved agents. Ann. Oncol. *23 Suppl 6*, vi46–51.

Arcaro, A. and Wymann, M.P. (1993). Wortmannin is a potent phosphatidylinositol 3-kinase inhibitor: the role of phosphatidylinositol 3,4,5-trisphosphate in neutrophil responses. Biochem. J. *296 (Pt 2)*, 297–301.

Arlt, A., Gehrz, A., Müerköster, S., Vorndamm, J., Kruse, M.-L., Fölsch, U.R. and Schäfer, H. (2003). Role of NF-kappaB and Akt/PI3K in the resistance of pancreatic carcinoma cell lines against gemcitabine-induced cell death. Oncogene *22*, 3243–3251.

Van Assema, D.M.E., Lubberink, M., Bauer, M., van der Flier, W.M., Schuit, R.C., Windhorst, A.D., Comans, E.F.I., Hoetjes, N.J., Tolboom, N., Langer, O., et al. (2012). Blood-brain barrier P-glycoprotein function in Alzheimer's disease. Brain *135*, 181–189.

Bachmeier, C.J., Trickler, W.J. and Miller, D.W. (2004). Drug efflux transport properties of 2',7'-bis(2-carboxyethyl)-5(6)-carboxyfluorescein acetoxymethyl ester (BCECF-AM) and its fluorescent free acid, BCECF. J. Pharm Sci. *93*, 932–942.

Baguley, B.C. (2010). Multiple drug resistance mechanisms in cancer. Mol. Biotechnol. *46*, 308–316.

Baines, P., Limaye, M., Hoy, T., Padua, R.A., Whittaker, J., al-Sabah, A. and Burnett, A. (1994). In vitro drug resistance in acute myeloid and chronic B-lymphocytic leukaemic blasts and in normal blood and marrow populations. Leuk. Res. *18*, 683–691.

Bakos, E. and Homolya, L. (2007). Portrait of multifaceted transporter, the multidrug resistance-associated protein 1 (MRP1/ABCC1). Pflugers Arch. *453*, 621–641.

Bakos, E., Evers, R., Szakács, G., Tusnády, G.E., Welker, E., Szabó, K., de Haas, M., van Deemter, L., Borst, P., Váradi, A., et al. (1998). Functional multidrug resistance protein (MRP1) lacking the N-terminal transmembrane domain. J. Biol. Chem. *273*, 32167–32175.

Bakos, E., Evers, R., Calenda, G., Tusnády, G.E., Szakács, G., Váradi, A. and Sarkadi, B. (2000). Characterization of the amino-terminal regions in the human multidrug resistance protein (MRP1). J. Cell. Sci. *113 Pt 24*, 4451–4461.

Ballatori, N., Krance, S.M., Marchan, R. and Hammond, C.L. (2009). Plasma membrane glutathione transporters and their roles in cell physiology and pathophysiology. Mol. Aspects Med. *30*, 13–28.

Batrakova, E.V., Li, S., Vinogradov, S.V., Alakhov, V.Y., Miller, D.W. and Kabanov, A.V. (2001). Mechanism of pluronic effect on P-glycoprotein efflux system in blood-brain barrier: contributions of energy depletion and membrane fluidization. J. Pharmacol. Exp. Ther. *299*, 483–493.

Beck, J., Bohnet, B., Brügger, D., Bader, P., Dietl, J., Scheper, R.J., Kandolf, R., Liu, C., Niethammer, D. and Gekeler, V. (1998). Multiple gene expression analysis reveals distinct differences between G2 and G3 stage breast cancers, and correlations of PKC eta with MDR1, MRP and LRP gene expression. Br. J. Cancer *77*, 87–91.

Becton, D., Dahl, G.V., Ravindranath, Y., Chang, M.N., Behm, F.G., Raimondi, S.C., Head, D.R., Stine, K.C., Lacayo, N.J., Sikic, B.I., et al. (2006). Randomized use of cyclosporin A (CsA) to modulate P-glycoprotein in children with AML in remission: Pediatric Oncology Group Study 9421. Blood *107*, 1315–1324.

Beedholm-Ebsen, R., van de Wetering, K., Hardlei, T., Nexø, E., Borst, P. and Moestrup, S.K. (2010). Identification of multidrug resistance protein 1 (MRP1/ABCC1) as a molecular gate for cellular export of cobalamin. Blood *115*, 1632–1639.

Bello-Reuss, E., Ernest, S., Holland, O.B. and Hellmich, M.R. (2000). Role of multidrug resistance P-glycoprotein in the secretion of aldosterone by human adrenal NCI-H295 cells. Am. J. Physiol., Cell Physiol. *278*, C1256–1265.

Belpomme, D., Gauthier, S., Pujade-Lauraine, E., Facchini, T., Goudier, M.J., Krakowski, I., Netter-Pinon, G., Frenay, M., Gousset, C., Marié, F.N., et al. (2000). Verapamil increases the survival of patients with anthracycline-resistant metastatic breast carcinoma. Ann. Oncol. *11*, 1471–1476.

Benderra, Z., Faussat, A.-M., Sayada, L., Perrot, J.-Y., Chaoui, D., Marie, J.-P. and Legrand, O. (2004). Breast cancer resistance protein and P-glycoprotein in 149 adult acute myeloid leukemias. Clin. Cancer Res. *10*, 7896–7902.

Benyahia, B., Huguet, S., Declèves, X., Mokhtari, K., Crinière, E., Bernaudin, J.F., Scherrmann, J.M. and Delattre, J.Y. (2004). Multidrug resistance-associated protein MRP1 expression in human gliomas: chemosensitization to vincristine and etoposide by indomethacin in human glioma cell lines overexpressing MRP1. J. Neurooncol. *66*, 65–70.

Bera, T.K., Lee, S., Salvatore, G., Lee, B. and Pastan, I. (2001). MRP8, a new member of ABC transporter superfamily, identified by EST database mining and gene prediction program, is highly expressed in breast cancer. Mol. Med. *7*, 509–516.

Bertho, A.L., Santiago, M.A. and Coutinho, S.G. (2000). Flow cytometry in the study of cell death. Mem. Inst. Oswaldo Cruz *95*, 429–433.

Bibby, M.C. (2004). Orthotopic models of cancer for preclinical drug evaluation: advantages and disadvantages. Eur. J. Cancer *40*, 852–857.

Biedler, J.L. and Riehm, H. (1970). Cellular resistance to actinomycin D in Chinese hamster cells in vitro: cross-resistance, radioautographic, and cytogenetic studies. Cancer Res. *30*, 1174–1184.

Biemans-Oldehinkel, E., Doeven, M.K. and Poolman, B. (2006). ABC transporter architecture and regulatory roles of accessory domains. FEBS Lett. *580*, 1023–1035.

Blancher, C. and Jones, A. (2001). SDS -PAGE and Western blotting techniques. Methods Mol. Med. *57*, 145–162.

Borst, P. (2012). Cancer drug pan-resistance: pumps, cancer stem cells, quiescence, epithelial to mesenchymal transition, blocked cell death pathways, persisters or what? Open Biol *2*, 120066.

Borst, P. and Elferink, R.O. (2002). Mammalian ABC transporters in health and disease. Annu. Rev. Biochem. *71*, 537–592.

Borst, P., Evers, R., Kool, M. and Wijnholds, J. (2000). A family of drug transporters: the multidrug resistance-associated proteins. J. Natl. Cancer Inst. *92*, 1295–1302.

Borst, P., Zelcer, N., van de Wetering, K. and Poolman, B. (2006). On the putative co-transport of drugs by multidrug resistance proteins. FEBS Lett. *580*, 1085–1093.

Borst, P., de Wolf, C. and van de Wetering, K. (2007). Multidrug resistance-associated proteins 3, 4, and 5. Pflugers Arch. *453*, 661–673.

Braun, A.H., Stark, K., Dirsch, O., Hilger, R.A., Seeber, S. and Vanhoefer, U. (2005). The epidermal growth factor receptor tyrosine kinase inhibitor gefitinib sensitizes colon cancer cells to irinotecan. Anticancer Drugs *16*, 1099–1108.

Breedveld, P., Beijnen, J.H. and Schellens, J.H.M. (2006). Use of P-glycoprotein and BCRP inhibitors to improve oral bioavailability and CNS penetration of anticancer drugs. Trends Pharmacol. Sci. *27*, 17–24.

Britton, K.M., Kirby, J.A., Lennard, T.W.J. and Meeson, A.P. (2011). Cancer stem cells and side population cells in breast cancer and metastasis. Cancers (Basel) *3*, 2106–2130.

Britton, K.M., Eyre, R., Harvey, I.J., Stemke-Hale, K., Browell, D., Lennard, T.W.J. and Meeson, A.P. (2012). Breast cancer, side population cells and ABCG2 expression. Cancer Lett. *323*, 97–105.

Brouwer, K.L.R., Keppler, D., Hoffmaster, K.A., Bow, D.A.J., Cheng, Y., Lai, Y., Palm, J.E., Stieger, B., Evers, R. and International Transporter Consortium (2013). In vitro methods to support transporter evaluation in drug discovery and development. Clin. Pharmacol. Ther. *94*, 95–112.

Burger, H., Foekens, J.A., Look, M.P., Meijer-van Gelder, M.E., Klijn, J.G.M., Wiemer, E.A.C., Stoter, G. and Nooter, K. (2003). RNA expression of breast cancer resistance protein, lung resistance-related protein, multidrug resistance-associated proteins 1 and 2, and multidrug resistance gene 1 in breast cancer: correlation with chemotherapeutic response. Clin. Cancer Res. *9*, 827–836.

Calcagno, A.M. and Ambudkar, S.V. (2010). Molecular mechanisms of drug resistance in single-step and multi-step drug-selected cancer cells. Methods Mol. Biol. *596*, 77–93.

Cascorbi, I. (2011). P-glycoprotein: tissue distribution, substrates, and functional consequences of genetic variations. Handb. Exp. Pharmacol. *201*, 261–283.

Ceckova, M., Libra, A., Pavek, P., Nachtigal, P., Brabec, M., Fuchs, R. and Staud, F. (2006). Expression and functional activity of breast cancer resistance protein (BCRP, ABCG2) transporter in the human choriocarcinoma cell line BeWo. Clin. Exp. Pharmacol. Physiol. *33*, 58–65.

Cetin, K., Ettinger, D.S., Hei, Y.-J. and O'Malley, C.D. (2011). Survival by histologic subtype in stage IV nonsmall cell lung cancer based on data from the Surveillance, Epidemiology and End Results Program. Clin. Epidemiol. *3*, 139–148.

Chan, H.S., DeBoer, G., Thiessen, J.J., Budning, A., Kingston, J.E., O'Brien, J.M., Koren, G., Giesbrecht, E., Haddad, G., Verjee, Z., et al. (1996). Combining cyclosporin with chemotherapy controls intraocular retinoblastoma without requiring radiation. Clin. Cancer Res. *2*, 1499–1508.

Chang, R.L., Yeh, C.-H. and Albitar, M. (2010). Quantification of intracellular proteins and monitoring therapy using flow cytometry. Curr. Drug Targets *11*, 994–999.

Chearwae, W., Anuchapreeda, S., Nandigama, K., Ambudkar, S.V. and Limtrakul, P. (2004). Biochemical mechanism of modulation of human P-glycoprotein (ABCB1) by curcumin I, II, and III purified from Turmeric powder. Biochem. Pharmacol. *68*, 2043–2052.

Chearwae, W., Shukla, S., Limtrakul, P. and Ambudkar, S.V. (2006a). Modulation of the function of the multidrug resistance-linked ATP-binding cassette transporter ABCG2 by the cancer chemopreventive agent curcumin. Mol. Cancer Ther. *5*, 1995–2006.

Chearwae, W., Wu, C.-P., Chu, H.-Y., Lee, T.R., Ambudkar, S.V. and Limtrakul, P. (2006b). Curcuminoids purified from turmeric powder modulate the function of human multidrug resistance protein 1 (ABCC1). Cancer Chemother. Pharmacol. *57*, 376–388.

Chen, C., Liu, X. and Smith, B.J. (2003). Utility of Mdr1-gene deficient mice in assessing the impact of P-glycoprotein on pharmacokinetics and pharmacodynamics in drug discovery and development. Curr. Drug Metab. *4*, 272–291.

Chen, L., Li, Y., Yu, H., Zhang, L. and Hou, T. (2012). Computational models for predicting substrates or inhibitors of P-glycoprotein. Drug Discov. Today *17*, 343–351.

Cheng, A.L., Hsu, C.H., Lin, J.K., Hsu, M.M., Ho, Y.F., Shen, T.S., Ko, J.Y., Lin, J.T., Lin, B.R., Ming-Shiang, W., et al. (2001). Phase I clinical trial of curcumin, a chemopreventive agent, in patients with high-risk or pre-malignant lesions. Anticancer Res. *21*, 2895–2900.

Cho, M.J., Thompson, D.P., Cramer, C.T., Vidmar, T.J. and Scieszka, J.F. (1989). The Madin Darby canine kidney (MDCK) epithelial cell monolayer as a model cellular transport barrier. Pharm. Res. *6*, 71–77.

Choi, B.H., Kim, C.G., Lim, Y., Shin, S.Y. and Lee, Y.H. (2008). Curcumin down-regulates the multidrug-resistance mdr1b gene by inhibiting the PI3K/Akt/NF kappa B pathway. Cancer Lett. *259*, 111–118.

Cianfriglia, M., Dupuis, M.L., Molinari, A., Verdoliva, A., Costi, R., Galluzzo, C.M., Andreotti, M., Cara, A., Di Santo, R. and Palmisano, L. (2007). HIV-1 integrase inhibitors are substrates for the multidrug transporter MDR1-P-glycoprotein. Retrovirology *4*, 17.

Clark, R., Kerr, I.D. and Callaghan, R. (2006). Multiple drugbinding sites on the R482G isoform of the ABCG2 transporter. Br. J. Pharmacol. *149*, 506–515.

Colabufo, N.A., Contino, M., Niso, M., Berardi, F., Leopoldo, M. and Perrone, R. (2011). EGFR tyrosine kinase inhibitors and multidrug resistance: perspectives. Front Biosci. (Landmark Ed) *16*, 1811–1823.

Cole, S.P. (2014). Targeting multidrug resistance protein 1 (MRP1, ABCC1): past, present, and future. Annu. Rev. Pharmacol. Toxicol. *54,* 95-117.

Coley, H.M. (2010). Overcoming multidrug resistance in cancer: clinical studies of p-glycoprotein inhibitors. Methods Mol. Biol. *596*, 341–358.

Cripe, L.D., Uno, H., Paietta, E.M., Litzow, M.R., Ketterling, R.P., Bennett, J.M., Rowe, J.M., Lazarus, H.M., Luger, S. and Tallman, M.S. (2010). Zosuquidar, a novel modulator of P-glycoprotein, does not improve the outcome of older patients with newly diagnosed acute myeloid leukemia: a randomized, placebo-controlled trial of the Eastern Cooperative Oncology Group 3999. Blood *116*, 4077–4085.

D'hautcourt, J.-L. (2002). Quantitative flow cytometric analysis of membrane antigen expression. Curr. Protoc. Cytom. *Chapter 6*, Unit 6.12.

Dallas, S., Schlichter, L. and Bendayan, R. (2004). Multidrug resistance protein (MRP) 4- and MRP 5-mediated efflux of 9-(2-phosphonylmethoxyethyl)adenine by microglia. J. Pharmacol. Exp. Ther. *309*, 1221–1229.

Dalton, W.S., Crowley, J.J., Salmon, S.S., Grogan, T.M., Laufman, L.R., Weiss, G.R. and Bonnet, J.D. (1995). A phase III randomized study of oral verapamil as a chemosensitizer to reverse drug resistance in patients with refractory myeloma. A Southwest Oncology Group study. Cancer *75*, 815–820.

Darby, R.A.J., Callaghan, R. and McMahon, R.M. (2011). P-glycoprotein inhibition: the past, the present and the future. Curr. Drug Metab. *12*, 722–731.

Dean, M. (2009). ABC transporters, drug resistance, and cancer stem cells. J. Mammary Gland Biol. Neoplasia *14*, 3–9.

Dean, M. and Annilo, T. (2005). Evolution of the ATP-binding cassette (ABC) transporter superfamily in vertebrates. Annu. Rev. Genomics Hum. Genet. *6*, 123–142.

Deeley, R.G. and Cole, S.P.C. (2006). Substrate recognition and transport by multidrug resistance protein 1 (ABCC1). FEBS Lett. *580*, 1103–1111.

Dent, R., Trudeau, M., Pritchard, K.I., Hanna, W.M., Kahn, H.K., Sawka, C.A., Lickley, L.A., Rawlinson, E., Sun, P. and Narod, S.A. (2007). Triple-negative breast cancer: clinical features and patterns of recurrence. Clin. Cancer Res. *13*, 4429–4434.

Diamandis, E.P. and Christopoulos, T.K. (1991). The biotin-(strept)avidin system: principles and applications in biotechnology. Clin. Chem. *37*, 625–636.

Dimmock, J.R., Das, U., Gul, H.I., Kawase, M., Sakagami, H., Baráth, Z., Ocsovsky, I. and Molnár, J. (2005). 3-Arylidene-1-(4-nitrophenylmethylene)-3,4-dihydro-1H-naphthalen-2-ones and related compounds displaying selective toxicity and reversal of multidrug resistance in neoplastic cells. Bioorg. Med. Chem. Lett. *15*, 1633–1636.

Dittmer, A. and Dittmer, J. (2006). Beta-actin is not a reliable loading control in Western blot analysis. Electrophoresis *27*, 2844–2845.

Doyle, L.A. and Ross, D.D. (2003). Multidrug resistance mediated by the breast cancer resistance protein BCRP (ABCG2). Oncogene *22*, 7340–7358.

Draper, M.P., Martell, R.L. and Levy, S.B. (1997). Indomethacin-mediated reversal of multidrug resistance and drug efflux in human and murine cell lines overexpressing MRP, but not P-glycoprotein. Br. J. Cancer *75*, 810–815.

Dreiseitel, A., Oosterhuis, B., Vukman, K.V., Schreier, P., Oehme, A., Locher, S., Hajak, G. and Sand, P.G. (2009). Berry anthocyanins and anthocyanidins exhibit distinct affinities for the efflux transporters BCRP and MDR1. Br. J. Pharmacol. *158*, 1942–1950.

Du, Z., Qin, R., Wei, C., Wang, M., Shi, C., Tian, R. and Peng, C. (2011). Pancreatic cancer cells resistant to chemoradiotherapy rich in “stem-cell-like” tumor cells. Dig. Dis. Sci. *56*, 741–750.

Duong, H.-Q., Yi, Y.W., Kang, H.J., Hong, Y.B., Tang, W., Wang, A., Seong, Y.-S. and Bae, I. (2014). Inhibition of NRF2 by PIK-75 augments sensitivity of pancreatic cancer cells to gemcitabine. Int. J. Oncol. *44*, 959–969.

Durand, R.E. and Olive, P.L. (1981). Flow cytometry studies of intracellular adriamycin in single cells in vitro. Cancer Res. *41*, 3489–3494.

Dyer, C.A. and Benjamins, J.A. (1988). Redistribution and internalization of antibodies to galactocerebroside by oligodendroglia. J. Neurosci. *8*, 883–891.

Ebert, B., Seidel, A. and Lampen, A. (2005). Identification of BCRP as transporter of benzo[a]pyrene conjugates metabolically formed in Caco-2 cells and its induction by Ah-receptor agonists. Carcinogenesis *26*, 1754–1763.

Ebert, B., Seidel, A. and Lampen, A. (2007). Phytochemicals induce breast cancer resistance protein in Caco-2 cells and enhance the transport of benzo[a]pyrene-3-sulfate. Toxicol. Sci. *96*, 227–236.

Ee, P.L.R., Kamalakaran, S., Tonetti, D., He, X., Ross, D.D. and Beck, W.T. (2004). Identification of a novel estrogen response element in the breast cancer resistance protein (ABCG2) gene. Cancer Res. *64*, 1247–1251.

Efferth, T., Löhrke, H. and Volm, M. (1989). Reciprocal correlation between expression of P-glycoprotein and accumulation of rhodamine 123 in human tumors. Anticancer Res. *9*, 1633–1637.

Efferth, T., Davey, M., Olbrich, A., Rücker, G., Gebhart, E. and Davey, R. (2002). Activity of drugs from traditional Chinese medicine toward sensitive and MDR1- or MRP1-overexpressing multidrug-resistant human CCRF-CEM leukemia cells. Blood Cells Mol. Dis. *28*, 160–168.

Ejendal, K.F.K. and Hrycyna, C.A. (2005). Differential sensitivities of the human ATP-binding cassette transporters ABCG2 and P-glycoprotein to cyclosporin A. Mol. Pharmacol. *67*, 902–911.

Evers, R., Kool, M., van Deemter, L., Janssen, H., Calafat, J., Oomen, L.C., Paulusma, C.C., Oude Elferink, R.P., Baas, F., Schinkel, A.H., et al. (1998). Drug export activity of the human canalicular multispecific organic anion transporter in polarized kidney MDCK cells expressing cMOAT (MRP2) cDNA. J. Clin. Invest. *101*, 1310–1319.

Falasca, M. and Linton, K.J. (2012). Investigational ABC transporter inhibitors. Expert Opin. Investig. Drugs *21*, 657–666.

Fallahian, F., Karami-Tehrani, F., Salami, S. and Aghaei, M. (2011). Cyclic GMP induced apoptosis via protein kinase G in oestrogen receptor-positive and -negative breast cancer cell lines. FEBS J. *278*, 3360–3369.

Farabegoli, F., Papi, A., Bartolini, G., Ostan, R. and Orlandi, M. (2010). (-)-Epigallocatechin-3-gallate downregulates Pg-P and BCRP in a tamoxifen resistant MCF-7 cell line. Phytomedicine *17*, 356–362.

Feller, N., Broxterman, H.J., Währer, D.C. and Pinedo, H.M. (1995). ATP-dependent efflux of calcein by the multidrug resistance protein (MRP): no inhibition by intracellular glutathione depletion. FEBS Lett. *368*, 385–388.

Ferguson, R.E., Carroll, H.P., Harris, A., Maher, E.R., Selby, P.J. and Banks, R.E. (2005). Housekeeping proteins: a preliminary study illustrating some limitations as useful references in protein expression studies. Proteomics *5*, 566–571.

Ferté, J. (2000). Analysis of the tangled relationships between P-glycoprotein-mediated multidrug resistance and the lipid phase of the cell membrane. Eur. J. Biochem. *267*, 277–294.

Feuring-Buske, M. and Hogge, D.E. (2001). Hoechst 33342 efflux identifies a subpopulation of cytogenetically normal CD34(+)CD38(-) progenitor cells from patients with acute myeloid leukemia. Blood *97*, 3882–3889.

Filipits, M., Pohl, G., Rudas, M., Dietze, O., Lax, S., Grill, R., Pirker, R., Zielinski, C.C., Hausmaninger, H., Kubista, E., et al. (2005). Clinical role of multidrug resistance protein 1 expression in chemotherapy resistance in early-stage breast cancer: the Austrian Breast and Colorectal Cancer Study Group. J. Clin. Oncol. *23*, 1161–1168.

Fletcher, J.I., Haber, M., Henderson, M.J. and Norris, M.D. (2010). ABC transporters in cancer: more than just drug efflux pumps. Nat. Rev. Cancer *10*, 147–156.

Fox, E. and Bates, S.E. (2007). Tariquidar (XR9576): a P-glycoprotein drug efflux pump inhibitor. Expert Rev. Anticancer Ther. *7*, 447–459.

Gandhi, Y.A. and Morris, M.E. (2009). Structure-activity relationships and quantitative structure-activity relationships for breast cancer resistance protein (ABCG2). AAPS J *11*, 541–552.

Gandhy, S.U., Kim, K., Larsen, L., Rosengren, R.J. and Safe, S. (2012a). Curcumin and synthetic analogs induce reactive oxygen species and decreases specificity protein (Sp) transcription factors by targeting microRNAs. BMC Cancer *12*, 564.

Gangopadhyay, S., Nandy, A., Hor, P. and Mukhopadhyay, A. (2013). Breast cancer stem cells: a novel therapeutic target. Clin. Breast Cancer *13*, 7–15.

Ganta, S. and Amiji, M. (2009). Coadministration of Paclitaxel and curcumin in nanoemulsion formulations to overcome multidrug resistance in tumor cells. Mol. Pharm. *6*, 928–939.

Ganta, S., Devalapally, H. and Amiji, M. (2010). Curcumin enhances oral bioavailability and anti-tumor therapeutic efficacy of paclitaxel upon administration in nanoemulsion formulation. J. Pharm. Sci. *99*, 4630–4641.

Gao, A.-M., Ke, Z.-P., Shi, F., Sun, G.-C. and Chen, H. (2013). Chrysin enhances sensitivity of BEL-7402/ADM cells to doxorubicin by suppressing PI3K/Akt/Nrf2 and ERK/Nrf2 pathway. Chem. Biol. Interact. *206*, 100–108.

Gekeler, V., Ise, W., Sanders, K.H., Ulrich, W.R. and Beck, J. (1995). The leukotriene LTD4 receptor antagonist MK571 specifically modulates MRP associated multidrug resistance. Biochem. Biophys. Res. Commun. *208*, 345–352.

Gennari, A., D'amico, M. and Corradengo, D. (2011). Extending the duration of first-line chemotherapy in metastatic breast cancer: a perspective review. Ther. Adv. Med. Oncol. *3*, 229–232.

Giacomini, K.M., Balimane, P.V., Cho, S.K., Eadon, M., Edeki, T., Hillgren, K.M., Huang, S.-M., Sugiyama, Y., Weitz, D., Wen, Y., et al. (2013). International Transporter Consortium commentary on clinically important transporter polymorphisms. Clin. Pharmacol. Ther. *94*, 23–26.

Gilda, J.E. and Gomes, A.V. (2013). Stain-Free total protein staining is a superior loading control to β-actin for Western blots. Anal. Biochem. *440*, 186–188.

Gillet, J.-P. and Gottesman, M.M. (2010). Mechanisms of multidrug resistance in cancer. Methods Mol. Biol. *596*, 47–76.

Gillet, J.-P., Efferth, T. and Remacle, J. (2007). Chemotherapy-induced resistance by ATP-binding cassette transporter genes. Biochim. Biophys. Acta *1775*, 237–262.

Girardin, F. (2006). Membrane transporter proteins: a challenge for CNS drug development. Dialogues Clin. Neurosci. *8*, 311–321.

Giri, N., Agarwal, S., Shaik, N., Pan, G., Chen, Y. and Elmquist, W.F. (2009). Substrate-dependent breast cancer resistance protein (Bcrp1/Abcg2)-mediated interactions: consideration of multiple binding sites in in vitro assay design. Drug Metab. Dispos. *37*, 560–570.

Glaeser, H. (2011). Importance of P-glycoprotein for drug-drug interactions. Handb. Exp. Pharmacol. 285–297.

Glavinas, H., Kis, E., Pál, A., Kovács, R., Jani, M., Vági, E., Molnár, E., Bánsághi, S., Kele, Z., Janáky, T., et al. (2007). ABCG2 (breast cancer resistance protein/mitoxantrone resistance-associated protein) ATPase assay: a useful tool to detect drug-transporter interactions. Drug Metab. Dispos. *35*, 1533–1542.

Glavinas, H., Méhn, D., Jani, M., Oosterhuis, B., Herédi-Szabó, K. and Krajcsi, P. (2008). Utilization of membrane vesicle preparations to study drug-ABC transporter interactions. Expert Opin. Drug Metab. Toxicol. *4*, 721–732.

Goel, A. and Aggarwal, B.B. (2010). Curcumin, the golden spice from Indian saffron, is a chemosensitizer and radiosensitizer for tumors and chemoprotector and radioprotector for normal organs. Nutr. Cancer *62*, 919–930.

Goler-Baron, V., Sladkevich, I. and Assaraf, Y.G. (2012). Inhibition of the PI3K-Akt signaling pathway disrupts ABCG2-rich extracellular vesicles and overcomes multidrug resistance in breast cancer cells. Biochem. Pharmacol. *83*, 1340–1348.

Gordon, O.N. and Schneider, C. (2012). Vanillin and ferulic acid: not the major degradation products of curcumin. Trends Mol. Med. *18*, 361–363; author reply 363–364.

Gottesman, M.M., Fojo, T. and Bates, S.E. (2002). Multidrug resistance in cancer: role of ATP-dependent transporters. Nat. Rev. Cancer *2*, 48–58.

Greish, K. (2010). Enhanced permeability and retention (EPR) effect for anticancer nanomedicine drug targeting. Methods Mol. Biol. *624*, 25–37.

Griesser, M., Pistis, V., Suzuki, T., Tejera, N., Pratt, D.A. and Schneider, C. (2011). Autoxidative and cyclooxygenase-2 catalyzed transformation of the dietary chemopreventive agent curcumin. J. Biol. Chem. *286*, 1114–1124.

Griffin, C.A., Morsberger, L., Hawkins, A.L., Haddadin, M., Patel, A., Ried, T., Schrock, E., Perlman, E.J. and Jaffee, E. (2007). Molecular cytogenetic characterization of pancreas cancer cell lines reveals high complexity chromosomal alterations. Cytogenet. Genome Res. *118*, 148–156.

Griffiths, C.L. and Olin, J.L. (2012). Triple negative breast cancer: a brief review of its characteristics and treatment options. J. Pharm. Pract. *25*, 319–323.

Grynkiewicz, G. and Ślifirski, P. (2012). Curcumin and curcuminoids in quest for medicinal status. Acta Biochim. Pol. *59*, 201–212.

Gupta, A., Dai, Y., Vethanayagam, R.R., Hebert, M.F., Thummel, K.E., Unadkat, J.D., Ross, D.D. and Mao, Q. (2006). Cyclosporin A, tacrolimus and sirolimus are potent inhibitors of the human breast cancer resistance protein (ABCG2) and reverse resistance to mitoxantrone and topotecan. Cancer Chemother. Pharmacol. *58*, 374–383.

Gupta, P.B., Chaffer, C.L. and Weinberg, R.A. (2009). Cancer stem cells: mirage or reality? Nat. Med. *15*, 1010–1012.

Gupta, S.C., Prasad, S., Kim, J.H., Patchva, S., Webb, L.J., Priyadarsini, I.K. and Aggarwal, B.B. (2011). Multitargeting by curcumin as revealed by molecular interaction studies. Nat. Prod. Rep. *28*, 1937–1955.

Gupta, S.C., Patchva, S., Koh, W. and Aggarwal, B.B. (2012). Discovery of curcumin, a component of golden spice, and its miraculous biological activities. Clin. Exp. Pharmacol. Physiol. *39*, 283–299.

Gupta, S.C., Kismali, G. and Aggarwal, B.B. (2013a). Curcumin, a component of turmeric: from farm to pharmacy. Biofactors *39*, 2–13.

Gupta, S.C., Patchva, S. and Aggarwal, B.B. (2013b). Therapeutic roles of curcumin: lessons learned from clinical trials. AAPS J *15*, 195–218.

Hagmann, W., Jesnowski, R., Faissner, R., Guo, C. and Löhr, J.M. (2009). ATP-binding cassette C transporters in human pancreatic carcinoma cell lines. Upregulation in 5-fluorouracil-resistant cells. Pancreatology *9*, 136–144.

Hagmann, W., Faissner, R., Schnölzer, M., Löhr, M. and Jesnowski, R. (2010a). Membrane drug transporters and chemoresistance in human pancreatic carcinoma. Cancers (Basel) *3*, 106–125.

Hagmann, W., Jesnowski, R. and Löhr, J.M. (2010b). Interdependence of gemcitabine treatment, transporter expression, and resistance in human pancreatic carcinoma cells. Neoplasia *12*, 740–747.

Al-Hajj, M., Wicha, M.S., Benito-Hernandez, A., Morrison, S.J. and Clarke, M.F. (2003). Prospective identification of tumorigenic breast cancer cells. Proc. Natl. Acad. Sci. U.S.A. *100*, 3983–3988.

Hammond, C.L., Marchan, R., Krance, S.M. and Ballatori, N. (2007). Glutathione export during apoptosis requires functional multidrug resistance-associated proteins. J. Biol. Chem. *282*, 14337–14347.

Hartz, A.M.S. and Bauer, B. (2010). Regulation of ABC transporters at the blood-brain barrier: new targets for CNS therapy. Mol. Interv. *10*, 293–304.

Hazai, E., Hazai, I., Ragueneau-Majlessi, I., Chung, S.P., Bikadi, Z. and Mao, Q. (2013). Predicting substrates of the human breast cancer resistance protein using a support vector machine method. BMC Bioinformatics *14*, 130.

He, S.-M., Li, R., Kanwar, J.R. and Zhou, S.-F. (2011). Structural and functional properties of human multidrug resistance protein 1 (MRP1/ABCC1). Curr. Med. Chem. *18*, 439–481.

He, X., Mo, L., Li, Z.-Y., Tan, Z.-R., Chen, Y. and Ouyang, D.-S. (2012). Effects of curcumin on the pharmacokinetics of talinolol in human with ABCB1 polymorphism. Xenobiotica *42*, 1248–1254.

Hegedus, C., Szakács, G., Homolya, L., Orbán, T.I., Telbisz, A., Jani, M. and Sarkadi, B. (2009). Ins and outs of the ABCG2 multidrug transporter: an update on in vitro functional assays. Adv. Drug Deliv. Rev. *61*, 47–56.

Hendrick, A.M., Harris, A.L. and Cantwell, B.M. (1991). Verapamil with mitoxantrone for advanced ovarian cancer: a negative phase II trial. Ann. Oncol. *2*, 71–72.

Van Herwaarden, A.E., Wagenaar, E., Karnekamp, B., Merino, G., Jonker, J.W. and Schinkel, A.H. (2006). Breast cancer resistance protein (Bcrp1/Abcg2) reduces systemic exposure of the dietary carcinogens aflatoxin B1, IQ and Trp-P-1 but also mediates their secretion into breast milk. Carcinogenesis *27*, 123–130.

Van Herwaarden, A.E., Wagenaar, E., Merino, G., Jonker, J.W., Rosing, H., Beijnen, J.H. and Schinkel, A.H. (2007). Multidrug transporter ABCG2/breast cancer resistance protein secretes riboflavin (vitamin B2) into milk. Mol. Cell. Biol. *27*, 1247–1253.

Higgins, C.F. and Linton, K.J. (2004). The ATP switch model for ABC transporters. Nat. Struct. Mol. Biol. *11*, 918–926.

Hiraga, T., Ito, S. and Nakamura, H. (2011). Side population in MDA-MB-231 human breast cancer cells exhibits cancer stem cell-like properties without higher bone-metastatic potential. Oncol. Rep. *25*, 289–296.

Hirata, S., Izumi, S., Furukubo, T., Ota, M., Fujita, M., Yamakawa, T., Hasegawa, I., Ohtani, H. and Sawada, Y. (2005). Interactions between clarithromycin and digoxin in patients with end-stage renal disease. Int. J. Clin. Pharmacol. Ther. *43*, 30–36.

Hirschmann-Jax, C., Foster, A.E., Wulf, G.G., Nuchtern, J.G., Jax, T.W., Gobel, U., Goodell, M.A. and Brenner, M.K. (2004). A distinct “side population” of cells with high drug efflux capacity in human tumor cells. Proc. Natl. Acad. Sci. U.S.A. *101*, 14228–14233.

Holder, G.M., Plummer, J.L. and Ryan, A.J. (1978). The metabolism and excretion of curcumin (1,7-bis-(4-hydroxy-3-methoxyphenyl)-1,6-heptadiene-3,5-dione) in the rat. Xenobiotica *8*, 761–768.

Hoque, M.T., Robillard, K.R. and Bendayan, R. (2012). Regulation of breast cancer resistant protein by peroxisome proliferator-activated receptor α in human brain microvessel endothelial cells. Mol. Pharmacol. *81*, 598–609.

Hosomi, A., Nakanishi, T., Fujita, T. and Tamai, I. (2012). Extra-renal elimination of uric acid via intestinal efflux transporter BCRP/ABCG2. PloS One 7, e30456.

Hou, X.-L., Takahashi, K., Tanaka, K., Tougou, K., Qiu, F., Komatsu, K., Takahashi, K. and Azuma, J. (2008). Curcuma drugs and curcumin regulate the expression and function of P-gp in Caco-2 cells in completely opposite ways. Int. J. Pharm. *358*, 224–229.

Howlander, N., Noone, A., Krapcho, M. and Garshell, J. (2013). SEER Cancer Statistics Review (CSR) 1975-2010.

Huang, F.-F., Zhang, L., Wu, D.-S., Yuan, X.-Y., Chen, F.-P., Zeng, H., Yu, Y.-H. and Zhao, X.-L. (2014). PTEN regulates BCRP/ABCG2 and the side population through the PI3K/Akt Pathway in chronic myeloid leukemia. PLoS ONE *9*, e88298.

Huang, J., Zhang, T., Ma, K., Fan, P., Liu, Y., Weng, C., Fan, G., Duan, Q. and Zhu, X. (2013). Clinical evaluation of targeted arterial perfusion of verapamil and chemotherapeutic drugs in interventional therapy of advanced lung cancer. Cancer Chemother. Pharmacol. *72*, 889–896.

Huang, S.-M., Zhang, L. and Giacomini, K.M. (2010). The International Transporter Consortium: a collaborative group of scientists from academia, industry, and the FDA. Clin. Pharmacol. Ther. *87*, 32–36.

Hughes, J.R. (2008). One of the hottest topics in epileptology: ABC proteins. Their inhibition may be the future for patients with intractable seizures. Neurol. Res. *30*, 920–925.

Huls, M., Russel, F.G.M. and Masereeuw, R. (2009). The role of ATP binding cassette transporters in tissue defense and organ regeneration. J. Pharmacol. Exp. Ther. *328*, 3–9.

Hutson, J.R., Koren, G. and Matthews, S.G. (2010). Placental P-glycoprotein and breast cancer resistance protein: influence of polymorphisms on fetal drug exposure and physiology. Placenta *31*, 351–357.

Imai, Y., Ishikawa, E., Asada, S. and Sugimoto, Y. (2005). Estrogen-mediated post transcriptional down-regulation of breast cancer resistance protein/ABCG2. Cancer Res. *65*, 596–604.

Imai, Y., Yamagishi, H., Ono, Y. and Ueda, Y. (2012). Versatile inhibitory effects of the flavonoid-derived PI3K/Akt inhibitor, LY294002, on ATP-binding cassette transporters that characterize stem cells. Clin. Transl. Med. *1*, 24.

Isakoff, S.J. (2010). Triple-negative breast cancer: role of specific chemotherapy agents. Cancer J. *16*, 53–61.

Ishida, J., Ohtsu, H., Tachibana, Y., Nakanishi, Y., Bastow, K.F., Nagai, M., Wang, H.-K., Itokawa, H. and Lee, K.-H. (2002). Antitumor agents. Part 214: synthesis and evaluation of curcumin analogues as cytotoxic agents. Bioorg. Med. Chem. *10*, 3481–3487.

Ishikawa, T., Sakurai, A., Kanamori, Y., Nagakura, M., Hirano, H., Takarada, Y., Yamada, K., Fukushima, K. and Kitajima, M. (2005). High-speed screening of human ATP-binding cassette transporter function and genetic polymorphisms: new strategies in pharmacogenomics. Meth. Enzymol. *400*, 485–510.

Jamur, M.C. and Oliver, C. (2010). Permeabilization of cell membranes. Methods Mol. Biol. *588*, 63–66.

Jang, S.H., Wientjes, M.G. and Au, J.L. (2001). Kinetics of P-glycoprotein-mediated efflux of paclitaxel. J. Pharmacol. Exp. Ther. *298*, 1236–1242.

Jaspers, J.E., Rottenberg, S. and Jonkers, J. (2009). Therapeutic options for triple-negative breast cancers with defective homologous recombination. Biochim. Biophys. Acta *1796*, 266–280.

Jedlitschky, G. and Keppler, D. (2002). Transport of leukotriene C4 and structurally related conjugates. Vitam. Horm. *64*, 153–184.

Jedlitschky, G., Burchell, B. and Keppler, D. (2000). The multidrug resistance protein 5 functions as an ATP-dependent export pump for cyclic nucleotides. J. Biol. Chem. *275*, 30069–30074.

Jensen, U.B., Owens, D.M., Pedersen, S. and Christensen, R. (2010). Zinc fixation preserves flow cytometry scatter and fluorescence parameters and allows simultaneous analysis of DNA content and synthesis, and intracellular and surface epitopes. Cytometry A *77*, 798–804.

Jin, Y. and Penning, T.M. (2007). Aldo-keto reductases and bioactivation/detoxication. Annu. Rev. Pharmacol. Toxicol. *47*, 263–292.

Jin, M.S., Oldham, M.L., Zhang, Q. and Chen, J. (2012). Crystal structure of the multidrug transporter P-glycoprotein from *C. elegans*. Nature *490*, 566–569.

Jonker, J.W., Smit, J.W., Brinkhuis, R.F., Maliepaard, M., Beijnen, J.H., Schellens, J.H. and Schinkel, A.H. (2000). Role of breast cancer resistance protein in the bioavailability and fetal penetration of topotecan. J. Natl. Cancer Inst. *92*, 1651–1656.

Jonker, J.W., Buitelaar, M., Wagenaar, E., Van Der Valk, M.A., Scheffer, G.L., Scheper, R.J., Plosch, T., Kuipers, F., Elferink, R.P.J.O., Rosing, H., et al. (2002). The breast cancer resistance protein protects against a major chlorophyll-derived dietary phototoxin and protoporphyria. Proc. Natl. Acad. Sci. U.S.A. *99*, 15649–15654.

Juliano, R.L. and Ling, V. (1976). A surface glycoprotein modulating drug permeability in Chinese hamster ovary cell mutants. Biochim. Biophys. Acta *455*, 152–162.

Kakarala, M., Brenner, D.E., Khorkaya, H., Cheng, C., Tazi, K., Ginestier, C., Liu, S., Dontu, G. and Wicha, M.S. (2010). Targeting breast stem cells with the cancer preventive compounds curcumin and piperine. Breast Cancer Res. Treat. *122*, 777–785.

Karla, P.K., Quinn, T.L., Herndon, B.L., Thomas, P., Pal, D. and Mitra, A. (2009). Expression of multidrug resistance associated protein 5 (MRP5) on cornea and its role in drug efflux. J. Ocul. Pharmacol. Ther. *25*, 121–132.

Katayama, R., Koike, S., Sato, S., Sugimoto, Y., Tsuruo, T. and Fujita, N. (2009). Dofequidar fumarate sensitizes cancer stem-like side population cells to chemotherapeutic drugs by inhibiting ABCG2/BCRP-mediated drug export. Cancer Sci. *100*, 2060–2068.

Kawano, S., Inohana, Y., Hashi, Y. and Lin, J.-M. (2013). Analysis of keto-enol tautomers of curcumin by liquid chromatography/mass spectrometry. Chin.Chem. Lett. *24*, 685–687.

Kelly, R.J., Draper, D., Chen, C.C., Robey, R.W., Figg, W.D., Piekarz, R.L., Chen, X., Gardner, E.R., Balis, F.M., Venkatesan, A.M., et al. (2011). A pharmacodynamic study of docetaxel in combination with the P-glycoprotein antagonist tariquidar (XR9576) in patients with lung, ovarian, and cervical cancer. Clin. Cancer Res. *17*, 569–580.

Keppler, D. (2011). Multidrug resistance proteins (MRPs, ABCCs): importance for pathophysiology and drug therapy. Handb. Exp. Pharmacol. 299–323.

Keppler, D. and Konig, J. (1997). Hepatic canalicular membrane 5: Expression and localization of the conjugate export pump encoded by the MRP2 (cMRP/cMOAT) gene in liver. FASEB J. *11*, 509–516.

Knauer, M.J., Urquhart, B.L., Meyer zu Schwabedissen, H.E., Schwarz, U.I., Lemke, C.J., Leake, B.F., Kim, R.B. and Tirona, R.G. (2010). Human skeletal muscle drug transporters determine local exposure and toxicity of statins. Circ. Res. *106*, 297–306.

Kolev, T.M., Velcheva, E.A., Stamboliyska, B.A. and Spiteller, M. (2005). DFT and experimental studies of the structure and vibrational spectra of curcumin. Int. J. Quant. Chem. *102*, 1069–1079.

König, J., Hartel, M., Nies, A.T., Martignoni, M.E., Guo, J., Büchler, M.W., Friess, H. and Keppler, D. (2005). Expression and localization of human multidrug resistance protein (ABCC) family members in pancreatic carcinoma. Int. J. Cancer *115*, 359–367.

Kovalev, A.A., Tsvetaeva, D.A. and Grudinskaja, T.V. (2013). Role of ABC-cassette transporters (MDR1, MRP1, BCRP) in the development of primary and acquired multiple drug resistance in patients with early and metastatic breast cancer. Exp. Oncol. *35*, 287–290.

Krishan, A. and Hamelik, R.M. (2005). Flow cytometric monitoring of fluorescent drug retention and efflux. Methods Mol. Med. *111*, 149–166.

Krishan, A., Fitz, C.M. and Andritsch, I. (1997a). Drug retention, efflux, and resistance in tumor cells. Cytometry *29*, 279–285.

Krishan, A., Sauerteig, A., Andritsch, I. and Wellham, L. (1997b). Flow cytometric analysis of the multiple drug resistance phenotype. Leukemia *11*, 1138–1146.

Krishnamurthy, P., Ross, D.D., Nakanishi, T., Bailey-Dell, K., Zhou, S., Mercer, K.E., Sarkadi, B., Sorrentino, B.P. and Schuetz, J.D. (2004). The stem cell marker Bcrp/ABCG2 enhances hypoxic cell survival through interactions with heme. J. Biol. Chem. *279*, 24218–24225.

Kruh, G.D., Guo, Y., Hopper-Borge, E., Belinsky, M.G. and Chen, Z.-S. (2007). ABCC10, ABCC11, and ABCC12. Pflugers Arch. *453*, 675–684.

Kunnumakkara, A.B., Anand, P. and Aggarwal, B.B. (2008). Curcumin inhibits proliferation, invasion, angiogenesis and metastasis of different cancers through interaction with multiple cell signaling proteins. Cancer Lett. *269*, 199–225.

Kurita, T. and Makino, Y. (2013). Novel curcumin oral delivery systems. Anticancer Res. *33*, 2807–2821.

Kusuhara, H., Furuie, H., Inano, A., Sunagawa, A., Yamada, S., Wu, C., Fukizawa, S., Morimoto, N., Ieiri, I., Morishita, M., et al. (2012). Pharmacokinetic interaction study of sulphasalazine in healthy subjects and the impact of curcumin as an in vivo inhibitor of BCRP. Br. J. Pharmacol. *166*, 1793–1803.

Kuteykin-Teplyakov, K., Luna-Tortós, C., Ambroziak, K. and Löscher, W. (2010). Differences in the expression of endogenous efflux transporters in MDR1-transfected versus wildtype cell lines affect P-glycoprotein mediated drug transport. Br. J. Pharmacol. *160*, 1453–1463.

Lage, H. (2008). An overview of cancer multidrug resistance: a still unsolved problem. Cell. Mol. Life Sci. *65*, 3145–3167.

Lai, Y., Sampson, K.E. and Stevens, J.C. (2010). Evaluation of drug transporter interactions in drug discovery and development. Comb. Chem. High Throughput Screen. *13*, 112–134.

Lawlor, D., Martin, P., Busschots, S., Thery, J., O'Leary, J.J., Hennessy, B.T. and Stordal, B. (2014). PARP inhibitors as P-glyoprotein substrates. J. Pharm. Sci. *103*, 1913–1920.

Lee, S.H., Kim, H., Hwang, J.-H., Lee, H.S., Cho, J.Y., Yoon, Y.-S. and Han, H.-S. (2012). Breast cancer resistance protein expression is associated with early recurrence and decreased survival in resectable pancreatic cancer patients. Pathol. Int. *62*, 167–175.

Leggate, J., Allain, R., Isaac, L. and Blais, B.W. (2006). Microplate fluorescence assay for the quantification of double stranded DNA using SYBR Green I dye. Biotechnol. Lett. *28*, 1587–1594.

Legrand, O., Simonin, G., Beauchamp-Nicoud, A., Zittoun, R. and Marie, J.P. (1999). Simultaneous activity of MRP1 and Pgp is correlated with in vitro resistance to daunorubicin and with in vivo resistance in adult acute myeloid leukemia. Blood *94*, 1046–1056.

Leonard, G.D., Fojo, T. and Bates, S.E. (2003). The role of ABC transporters in clinical practice. Oncologist *8*, 411–424.

Leslie, E.M., Mao, Q., Oleschuk, C.J., Deeley, R.G. and Cole, S.P. (2001). Modulation of multidrug resistance protein 1 (MRP1/ABCC1) transport and ATPase activities by interaction with dietary flavonoids. Mol. Pharmacol. *59*, 1171–1180.

Leslie, E.M., Deeley, R.G. and Cole, S.P.C. (2005). Multidrug resistance proteins: role of P-glycoprotein, MRP1, MRP2, and BCRP (ABCG2) in tissue defense. Toxicol. Appl. Pharmacol. *204*, 216–237.

Li, Y. and Paxton, J.W. (2013). The effects of flavonoids on the ABC transporters: consequences for the pharmacokinetics of substrate drugs. Expert Opin. Drug. Metab. Toxicol. *9*, 267–285.

Li, G.-Y., Liu, J.-Z., Zhang, B., Wang, L.-X., Wang, C.-B. and Chen, S.-G. (2009). Cyclosporine diminishes multidrug resistance in K562/ADM cells and improves complete remission in patients with acute myeloid leukemia. Biomed. Pharmacother. *63*, 566–570.

Li, J., Jaimes, K.F. and Aller, S.G. (2014). Refined structures of mouse P-glycoprotein. Protein Sci. *23*, 34-46.

Li, L., Braiteh, F.S. and Kurzrock, R. (2005). Liposome-encapsulated curcumin: in vitro and in vivo effects on proliferation, apoptosis, signaling, and angiogenesis. Cancer *104*, 1322–1331.

Li, Y., Yuan, H., Yang, K., Xu, W., Tang, W. and Li, X. (2010a). The structure and functions of P-glycoprotein. Curr. Med. Chem. *17*, 786–800.

Li, Y., Revalde, J.L., Reid, G. and Paxton, J.W. (2010b). Interactions of dietary phytochemicals with ABC transporters: possible implications for drug disposition and multidrug resistance in cancer. Drug Metab. Rev. *42*, 590–611.

Li, Y., Revalde, J.L., Reid, G. and Paxton, J.W. (2011). Modulatory effects of curcumin on multi-drug resistance-associated protein 5 in pancreatic cancer cells. Cancer Chemother. Pharmacol. *68*, 603–610.

Liang, G., Shao, L., Wang, Y., Zhao, C., Chu, Y., Xiao, J., Zhao, Y., Li, X. and Yang, S. (2009). Exploration and synthesis of curcumin analogues with improved structural stability both in vitro and in vivo as cytotoxic agents. Bioorg. Med. Chem. *17*, 2623–2631.

Libby, E. and Hromas, R. (2010). Dismounting the MDR horse. Blood *116*, 4037–4038.

Limtrakul, P. (2007). Curcumin as chemosensitizer. Adv. Exp. Med. Biol. *595*, 269–300.

Limtrakul, P., Chearwae, W., Shukla, S., Phisalphong, C. and Ambudkar, S.V. (2007). Modulation of function of three ABC drug transporters, P-glycoprotein (ABCB1), mitoxantrone resistance protein (ABCG2) and multidrug resistance protein 1 (ABCC1) by tetrahydrocurcumin, a major metabolite of curcumin. Mol. Cell. Biochem. *296*, 85–95.

Lin, P.-C., Lin, H.-H., Lin, J.-K., Lin, C.-C., Yang, S.-H., Li, A.F.-Y., Chen, W.-S. and Chang, S.-C. (2013). Expression of ABCG2 associated with tumor response in metastatic colorectal cancer patients receiving first-line FOLFOX therapy--preliminary evidence. Int. J. Biol. Markers *28*, 182–186.

Linton, K.J. (2007). Structure and function of ABC transporters. Physiology (Bethesda) *22*, 122–130.

List, A.F., Kopecky, K.J., Willman, C.L., Head, D.R., Persons, D.L., Slovak, M.L., Dorr, R., Karanes, C., Hynes, H.E., Doroshow, J.H., et al. (2001). Benefit of cyclosporine modulation of drug resistance in patients with poor-risk acute myeloid leukemia: a Southwest Oncology Group study. Blood *98*, 3212–3220.

Litman, T., Zeuthen, T., Skovsgaard, T. and Stein, W.D. (1997). Competitive, non-competitive and cooperative interactions between substrates of P-glycoprotein as measured by its ATPase activity. Biochim. Biophys. Acta *1361*, 169–176.

Liu, R.H. (2013). Dietary bioactive compounds and their health implications. J. Food Sci. *78 Suppl 1*, A18–25.

Liu, S. and Wicha, M.S. (2010). Targeting breast cancer stem cells. J. Clin. Oncol. *28*, 4006–4012.

Liu, H., Ma, Z. and Wu, B. (2013). Structure-activity relationships and in silico models of P-glycoprotein (ABCB1) inhibitors. Xenobiotica *43*, 1018–1026.

Loe, D.W., Deeley, R.G. and Cole, S.P. (2000). Verapamil stimulates glutathione transport by the 190-kDa multidrug resistance protein 1 (MRP1). J. Pharmacol. Exp. Ther. *293*, 530–538.

Loebinger, M.R., Giangreco, A., Groot, K.R., Prichard, L., Allen, K., Simpson, C., Bazley, L., Navani, N., Tibrewal, S., Davies, D., et al. (2008). Squamous cell cancers contain a side population of stem-like cells that are made chemosensitive by ABC transporter blockade. Br. J. Cancer *98*, 380–387.

Lopez, M.F., Berggren, K., Chernokalskaya, E., Lazarev, A., Robinson, M. and Patton, W.F. (2000). A comparison of silver stain and SYPRO Ruby Protein Gel Stain with respect to protein detection in two-dimensional gels and identification by peptide mass profiling. Electrophoresis *21*, 3673–3683.

LoTempio, M.M., Veena, M.S., Steele, H.L., Ramamurthy, B., Ramalingam, T.S., Cohen, A.N., Chakrabarti, R., Srivatsan, E.S. and Wang, M.B. (2005). Curcumin suppresses growth of head and neck squamous cell carcinoma. Clin. Cancer Res. *11*, 6994–7002.

Luna-Tortós, C., Fedrowitz, M. and Löscher, W. (2010). Evaluation of transport of common antiepileptic drugs by human multidrug resistance-associated proteins (MRP1, 2 and 5) that are overexpressed in pharmacoresistant epilepsy. Neuropharmacology *58*, 1019–1032.

Lundholt, B.K., Scudder, K.M. and Pagliaro, L. (2003). A simple technique for reducing edge effect in cell-based assays. J. Biomol. Screen *8*, 566–570.

Madamanchi, N.R. and Runge, M.S. (2001). Western blotting. Methods Mol. Med. *51*, 245–256.

Maeda, H. (2010). Tumor-selective delivery of macromolecular drugs via the EPR effect: background and future prospects. Bioconjug. Chem. *21*, 797–802.

Maeno, K., Nakajima, A., Conseil, G., Rothnie, A., Deeley, R.G. and Cole, S.P.C. (2009). Molecular basis for reduced estrone sulfate transport and altered modulator sensitivity of transmembrane helix (TM) 6 and TM17 mutants of multidrug resistance protein 1 (ABCC1). Drug Metab. Dispos. *37*, 1411–1420.

Mahringer, A. and Fricker, G. (2010). BCRP at the blood-brain barrier: genomic regulation by 17β-estradiol. Mol. Pharm. *7*, 1835–1847.

Maki, N., Hafkemeyer, P. and Dey, S. (2003). Allosteric modulation of human P-glycoprotein. Inhibition of transport by preventing substrate translocation and dissociation. J. Biol. Chem. *278*, 18132–18139.

Maliepaard, M., Scheffer, G.L., Faneyte, I.F., van Gastelen, M.A., Pijnenborg, A.C., Schinkel, A.H., van De Vijver, M.J., Scheper, R.J. and Schellens, J.H. (2001). Subcellular localization and distribution of the breast cancer resistance protein transporter in normal human tissues. Cancer Res. *61*, 3458–3464.

Mao, Q. (2008). BCRP/ABCG2 in the placenta: expression, function and regulation. Pharm. Res. *25*, 1244–1255.

Mao, Q. and Unadkat, J.D. (2005). Role of the breast cancer resistance protein (ABCG2) in drug transport. AAPS J *7*, E118–133.

Margulis, M., Sorota, S., Chu, I., Soares, A., Priestley, T. and Nomeir, A.A. (2010). Protein binding-dependent decreases in hERG channel blocker potency assessed by whole-cell voltage clamp in serum. J. Cardiovasc. Pharmacol. *55*, 368–376.

Marie, J.P., Zittoun, R. and Sikic, B.I. (1991). Multidrug resistance (mdr1) gene expression in adult acute leukemias: correlations with treatment outcome and in vitro drug sensitivity. Blood *78*, 586–592.

Martelli, A.M., Evangelisti, C., Follo, M.Y., Ramazzotti, G., Fini, M., Giardino, R., Manzoli, L., McCubrey, J.A. and Cocco, L. (2011). Targeting the phosphatidylinositol 3-kinase/Akt/mammalian target of rapamycin signaling network in cancer stem cells. Curr. Med. Chem. *18*, 2715–2726.

Martin, C., Berridge, G., Higgins, C.F. and Callaghan, R. (1997). The multi-drug resistance reversal agent SR33557 and modulation of vinca alkaloid binding to P-glycoprotein by an allosteric interaction. Br. J. Pharmacol. *122*, 765–771.

Martin, C., Berridge, G., Higgins, C.F., Mistry, P., Charlton, P. and Callaghan, R. (2000). Communication between multiple drug binding sites on P-glycoprotein. Mol. Pharmacol. *58*, 624–632.

Matsson, P., Englund, G., Ahlin, G., Bergström, C.A.S., Norinder, U. and Artursson, P. (2007). A global drug inhibition pattern for the human ATP-binding cassette transporter breast cancer resistance protein (ABCG2). J. Pharmacol. Exp. Ther. *323*, 19–30.

Matsuo, H., Takada, T., Ichida, K., Nakamura, T., Nakayama, A., Suzuki, H., Hosoya, T. and Shinomiya, N. (2011). ABCG2/BCRP dysfunction as a major cause of gout. Nucleosides Nucleotides Nucleic Acids *30*, 1117–1128.

Mazard, T., Causse, A., Simony, J., Leconet, W., Vezzio-Vie, N., Torro, A., Jarlier, M., Evrard, A., Del Rio, M., Assenat, E., et al. (2013). Sorafenib overcomes irinotecan resistance in colorectal cancer by inhibiting the ABCG2 drug-efflux pump. Mol. Cancer Ther. *12*, 2121–2134.

McAleer, M.A., Breen, M.A., White, N.L. and Matthews, N. (1999). pABC11 (also known as MOAT-C and MRP5), a member of the ABC family of proteins, has anion transporter activity but does not confer multidrug resistance when overexpressed in human embryonic kidney 293 cells. J. Biol. Chem. *274*, 23541–23548.

McGowan, E.M., Alling, N., Jackson, E.A., Yagoub, D., Haass, N.K., Allen, J.D. and Martinello-Wilks, R. (2011). Evaluation of cell cycle arrest in estrogen responsive MCF-7 breast cancer cells: pitfalls of the MTS assay. PLoS ONE *6*, e20623.

Mennone, A., Soroka, C.J., Harry, K.M. and Boyer, J.L. (2010). Role of breast cancer resistance protein in the adaptive response to cholestasis. Drug Metab. Dispos. *38*, 1673–1678.

Mertz, D., Battegay, M., Marzolini, C. and Mayr, M. (2009). Drug-drug interaction in a kidney transplant recipient receiving HIV salvage therapy and tacrolimus. Am. J. Kidney Dis. *54*, e1–4.

Metzler, M., Pfeiffer, E., Schulz, S.I. and Dempe, J.S. (2013). Curcumin uptake and metabolism. Biofactors *39*, 14–20.

Meyer zu Schwabedissen, H.E. and Kroemer, H.K. (2011). In vitro and in vivo evidence for the importance of breast cancer resistance protein transporters (BCRP/MXR/ABCP/ABCG2). Handb. Exp. Pharmacol. 325–371.

Meyer zu Schwabedissen, H.E., Grube, M., Dreisbach, A., Jedlitschky, G., Meissner, K., Linnemann, K., Fusch, C., Ritter, C.A., Völker, U. and Kroemer, H.K. (2006). Epidermal growth factor-mediated activation of the map kinase cascade results in altered expression and function of ABCG2 (BCRP). Drug Metab. Dispos. *34*, 524–533.

Middleton, G., Brown, S., Lowe, C., Maughan, T., Gwyther, S., Oliver, A., Richman, S., Blake, D., Napp, V., Marshall, H., et al. (2013). A randomised phase III trial of the pharmacokinetic biomodulation of irinotecan using oral ciclosporin in advanced colorectal cancer: results of the Panitumumab, Irinotecan & Ciclosporin in COLOrectal cancer therapy trial (PICCOLO). Eur. J. Cancer *49*, 3507–3516.

Milroy, R. (1993). A randomised clinical study of verapamil in addition to combination chemotherapy in small cell lung cancer. West of Scotland Lung Cancer Research Group, and the Aberdeen Oncology Group. Br. J. Cancer *68*, 813–818.

Minchinton, A.I. and Tannock, I.F. (2006). Drug penetration in solid tumours. Nat. Rev. Cancer *6*, 583–592.

Minderman, H., Suvannasankha, A., O'Loughlin, K.L., Scheffer, G.L., Scheper, R.J., Robey, R.W. and Baer, M.R. (2002). Flow cytometric analysis of breast cancer resistance protein expression and function. Cytometry *48*, 59–65.

Mistry, P., Stewart, A.J., Dangerfield, W., Okiji, S., Liddle, C., Bootle, D., Plumb, J.A., Templeton, D. and Charlton, P. (2001). In vitro and in vivo reversal of P-glycoprotein-mediated multidrug resistance by a novel potent modulator, XR9576. Cancer Res. *61*, 749–758.

Mizutani, T., Masuda, M., Nakai, E., Furumiya, K., Togawa, H., Nakamura, Y., Kawai, Y., Nakahira, K., Shinkai, S. and Takahashi, K. (2008). Genuine functions of P-glycoprotein (ABCB1). Curr. Drug Metab. *9*, 167–174.

Mo, W. and Zhang, J.-T. (2009). Oligomerization of human ATP-binding cassette transporters and its potential significance in human disease. Expert Opin. Drug Metab. Toxicol. *5*, 1049–1063.

Mogi, M., Yang, J., Lambert, J.-F., Colvin, G.A., Shiojima, I., Skurk, C., Summer, R., Fine, A., Quesenberry, P.J. and Walsh, K. (2003). Akt signaling regulates side population cell phenotype via Bcrp1 translocation. J. Biol. Chem. *278*, 39068–39075.

Mohelnikova-Duchonova, B., Brynychova, V., Oliverius, M., Honsova, E., Kala, Z., Muckova, K., and Soucek, P. (2013). Differences in transcript levels of ABC transporters between pancreatic adenocarcinoma and nonneoplastic tissues. Pancreas *42*, 707–716.

Mohrmann, K., van Eijndhoven, M.A.J., Schinkel, A.H. and Schellens, J.H.M. (2005). Absence of N-linked glycosylation does not affect plasma membrane localization of breast cancer resistance protein (BCRP/ABCG2). Cancer Chemother. Pharmacol. *56*, 344–350.

Moitra, K., Lou, H. and Dean, M. (2011). Multidrug efflux pumps and cancer stem cells: insights into multidrug resistance and therapeutic development. Clin. Pharmacol. Ther. *89*, 491–502.

Molnár, J., Engi, H., Hohmann, J., Molnár, P., Deli, J., Wesolowska, O., Michalak, K. and Wang, Q. (2010). Reversal of multidrug resitance by natural substances from plants. Curr. Top. Med. Chem. *10*, 1757–1768.

Morris, M.E. and Zhang, S. (2006). Flavonoid-drug interactions: effects of flavonoids on ABC transporters. Life Sci. *78*, 2116–2130.

Morrow, C.S., Smitherman, P.K., Diah, S.K., Schneider, E. and Townsend, A.J. (1998). Coordinated action of glutathione S-transferases (GSTs) and multidrug resistance protein 1 (MRP1) in antineoplastic drug detoxification. Mechanism of GST A1-1- and MRP1-associated resistance to chlorambucil in MCF7 breast carcinoma cells. J. Biol. Chem. *273*, 20114–20120.

Morrow, C.S., Peklak-Scott, C., Bishwokarma, B., Kute, T.E., Smitherman, P.K. and Townsend, A.J. (2006). Multidrug resistance protein 1 (MRP1, ABCC1) mediates resistance to mitoxantrone via glutathione-dependent drug efflux. Mol. Pharmacol. *69*, 1499–1505.

Mosley, C.A., Liotta, D.C. and Snyder, J.P. (2007). Highly active anticancer curcumin analogues. Adv. Exp. Med. Biol. *595*, 77–103.

Motomura, S., Motoji, T., Takanashi, M., Wang, Y.H., Shiozaki, H., Sugawara, I., Aikawa, E., Tomida, A., Tsuruo, T., Kanda, N., et al. (1998). Inhibition of P-glycoprotein and recovery of drug sensitivity of human acute leukemic blast cells by multidrug resistance gene (mdr1) antisense oligonucleotides. Blood *91*, 3163–3171.

Munić, V., Kelnerić, Z., Mikac, L. and Eraković Haber, V. (2010). Differences in assessment of macrolide interaction with human MDR1 (ABCB1, P-gp) using rhodamine-123 efflux, ATPase activity and cellular accumulation assays. Eur. J. Pharm. Sci. *41*, 86–95.

Myers, M.A. (1998). Direct measurement of cell numbers in microtitre plate cultures using the fluorescent dye SYBR green I. J. Immunol. Methods *212*, 99–103.

Nabekura, T. (2010). Overcoming multidrug resistance in human cancer cells by natural compounds. Toxins (Basel) *2*, 1207–1224.

Nabekura, T., Kamiyama, S. and Kitagawa, S. (2005). Effects of dietary chemopreventive phytochemicals on P-glycoprotein function. Biochem. Biophys. Res. Commun. *327*, 866–870.

Naik, P. and Cucullo, L. (2012). In vitro blood-brain barrier models: current and perspective technologies. J. Pharm. Sci. *101*, 1337–1354.

Nakanishi, T. and Ross, D.D. (2012). Breast cancer resistance protein (BCRP/ABCG2): its role in multidrug resistance and regulation of its gene expression. Chin. J. Cancer *31*, 73–99.

Nakanishi, T., Doyle, L.A., Hassel, B., Wei, Y., Bauer, K.S., Wu, S., Pumplin, D.W., Fang, H.-B. and Ross, D.D. (2003). Functional characterization of human breast cancer resistance protein (BCRP, ABCG2) expressed in the oocytes of *Xenopus laevis*. Mol. Pharmacol. *64*, 1452–1462.

Nakanishi, T., Shiozawa, K., Hassel, B.A. and Ross, D.D. (2006). Complex interaction of BCRP/ABCG2 and imatinib in BCR-ABL-expressing cells: BCRP-mediated resistance to imatinib is attenuated by imatinib-induced reduction of BCRP expression. Blood *108*, 678–684.

Nakanishi, T., Chumsri, S., Khakpour, N., Brodie, A.H., Leyland-Jones, B., Hamburger, A.W., Ross, D.D. and Burger, A.M. (2010). Side-population cells in luminal-type breast cancer have tumour-initiating cell properties, and are regulated by HER2 expression and signalling. Br. J. Cancer *102*, 815–826.

Nakatomi, K., Yoshikawa, M., Oka, M., Ikegami, Y., Hayasaka, S., Sano, K., Shiozawa, K., Kawabata, S., Soda, H., Ishikawa, T., et al. (2001). Transport of 7-ethyl-10-hydroxycamptothecin (SN-38) by breast cancer resistance protein ABCG2 in human lung cancer cells. Biochem. Biophys. Res. Commun. *288*, 827–832.

Nambaru, P.K., Hübner, T., Köck, K., Mews, S., Grube, M., Payen, L., Guitton, J., Sendler, M., Jedlitschky, G., Rimmbach, C., et al. (2011). Drug efflux transporter multidrug resistance-associated protein 5 affects sensitivity of pancreatic cancer cell lines to the nucleoside anticancer drug 5-fluorouracil. Drug Metab. Dispos. *39*, 132–139.

Natarajan, K., Xie, Y., Baer, M.R. and Ross, D.D. (2012). Role of breast cancer resistance protein (BCRP/ABCG2) in cancer drug resistance. Biochem. Pharmacol. *83*, 1084–1103.

Nautiyal, J., Kanwar, S.S., Yu, Y. and Majumdar, A.P. (2011). Combination of dasatinib and curcumin eliminates chemo-resistant colon cancer cells. J. Mol. Signal. *6*, 7.

Nervi, P., Li-Blatter, X., Aänismaa, P. and Seelig, A. (2010). P-glycoprotein substrate transport assessed by comparing cellular and vesicular ATPase activity. Biochim. Biophys. Acta *1798*, 515–525.

Neyfakh, A.A. (1988). Use of fluorescent dyes as molecular probes for the study of multidrug resistance. Exp. Cell Res. *174*, 168–176.

Ni, Z., Bikadi, Z., Rosenberg, M.F. and Mao, Q. (2010a). Structure and function of the human breast cancer resistance protein (BCRP/ABCG2). Curr. Drug Metab. *11*, 603–617.

Ni, Z., Bikadi, Z., Cai, X., Rosenberg, M.F. and Mao, Q. (2010b). Transmembrane helices 1 and 6 of the human breast cancer resistance protein (BCRP/ABCG2): identification of polar residues important for drug transport. Am. J. Physiol., Cell Physiol. *299*, C1100–1109.

Nicolazzo, J.A. and Katneni, K. (2009). Drug transport across the blood-brain barrier and the impact of breast cancer resistance protein (ABCG2). Curr. Top Med. Chem. *9*, 130–147.

Niles, A.L., Moravec, R.A. and Riss, T.L. (2008). Update on in vitro cytotoxicity assays for drug development. Expert Opin. Drug Discov. *3*, 655–669.

Norman, B.H., Lander, P.A., Gruber, J.M., Kroin, J.S., Cohen, J.D., Jungheim, L.N., Starling, J.J., Law, K.L., Self, T.D., Tabas, L.B., et al. (2005). Cyclohexyl-linked tricyclic isoxazoles are potent and selective modulators of the multidrug resistance protein (MRP1). Bioorg. Med. Chem. Lett. *15*, 5526–5530.

O'Driscoll, L., Walsh, N., Larkin, A., Ballot, J., Ooi, W.S., Gullo, G., O'Connor, R., Clynes, M., Crown, J. and Kennedy, S. (2007). MDR1/P-glycoprotein and MRP-1 drug efflux pumps in pancreatic carcinoma. Anticancer Res. *27*, 2115–2120.

Ohnuma, K., Yomo, T., Asashima, M. and Kaneko, K. (2006). Sorting of cells of the same size, shape, and cell cycle stage for a single cell level assay without staining. BMC Cell Biol. *7*, 25.

Ohtsuki, S., Ito, S. and Terasaki, T. (2010). Is P-glycoprotein involved in amyloid-β elimination across the blood-brain barrier in Alzheimer's disease? Clin. Pharmacol. Ther. *88*, 443–445.

Oi, V.T., Glazer, A.N. and Stryer, L. (1982). Fluorescent phycobiliprotein conjugates for analyses of cells and molecules. J. Cell Biol. *93*, 981–986.

Olson, D.P., Taylor, B.J. and Ivy, S.P. (2001). Detection of MRP functional activity: calcein AM but not BCECF AM as a Multidrug Resistance-related Protein (MRP1) substrate. Cytometry *46*, 105–113.

Oostendorp, R.L., Beijnen, J.H. and Schellens, J.H.M. (2009). The biological and clinical role of drug transporters at the intestinal barrier. Cancer Treat. Rev. *35*, 137–147.

Ozols, R.F., Cunnion, R.E., Klecker, R.W., Hamilton, T.C., Ostchega, Y., Parrillo, J.E. and Young, R.C. (1987). Verapamil and adriamycin in the treatment of drug-resistant ovarian cancer patients. J. Clin. Oncol *5*, 641–647.

Ozvegy-Laczka, C., Várady, G., Köblös, G., Ujhelly, O., Cervenak, J., Schuetz, J.D., Sorrentino, B.P., Koomen, G.-J., Váradi, A., Német, K., et al. (2005). Function-dependent conformational changes of the ABCG2 multidrug transporter modify its interaction with a monoclonal antibody on the cell surface. J. Biol. Chem. *280*, 4219–4227.

Ozvegy-Laczka, C., Laczkó, R., Hegedus, C., Litman, T., Várady, G., Goda, K., Hegedus, T., Dokholyan, N.V., Sorrentino, B.P., Váradi, A., et al. (2008). Interaction with the 5D3 monoclonal antibody is regulated by intramolecular rearrangements but not by covalent dimer formation of the human ABCG2 multidrug transporter. J. Biol. Chem. *283*, 26059–26070.

Pajeva, I.K., Globisch, C. and Wiese, M. (2009). Combined pharmacophore modeling, docking, and 3D QSAR studies of ABCB1 and ABCC1 transporter inhibitors. ChemMedChem. *4*, 1883–1896.

Pajic, M., Iyer, J.K., Kersbergen, A., van der Burg, E., Nygren, A.O.H., Jonkers, J., Borst, P. and Rottenberg, S. (2009). Moderate increase in Mdr1a/1b expression causes in vivo resistance to doxorubicin in a mouse model for hereditary breast cancer. Cancer Res. *69*, 6396–6404.

Palmeira, A., Sousa, E., Vasconcelos, M.H. and Pinto, M.M. (2012a). Three decades of P-gp inhibitors: skimming through several generations and scaffolds. Curr. Med. Chem. *19*, 1946–2025.

Palmeira, A., Sousa, E., Vasconcelos, M.H., Pinto, M.M. and Fernandes, M.X. (2012b). Structure and ligand-based design of P-glycoprotein inhibitors: a historical perspective. Curr. Pharm. Des. *18*, 4197–4214.

Pan, G., Giri, N. and Elmquist, W.F. (2007). Abcg2/Bcrp1 mediates the polarized transport of antiretroviral nucleosides abacavir and zidovudine. Drug Metab. Dispos. *35*, 1165–1173.

Patel, B.B., Gupta, D., Elliott, A.A., Sengupta, V., Yu, Y. and Majumdar, A.P.N. (2010). Curcumin targets FOLFOX-surviving colon cancer cells via inhibition of EGFRs and IGF-1R. Anticancer Res. *30*, 319–325.

Patil, Y., Sadhukha, T., Ma, L. and Panyam, J. (2009). Nanoparticle-mediated simultaneous and targeted delivery of paclitaxel and tariquidar overcomes tumor drug resistance. J. Control Release *136*, 21–29.

Patrawala, L., Calhoun, T., Schneider-Broussard, R., Zhou, J., Claypool, K. and Tang, D.G. (2005). Side population is enriched in tumorigenic, stem-like cancer cells, whereas ABCG2+ and ABCG2- cancer cells are similarly tumorigenic. Cancer Res. *65*, 6207–6219.

Pavek, P., Merino, G., Wagenaar, E., Bolscher, E., Novotna, M., Jonker, J.W. and Schinkel, A.H. (2005). Human breast cancer resistance protein: interactions with steroid drugs, hormones, the dietary carcinogen 2-amino-1-methyl-6-phenylimidazo(4,5-b)pyridine, and transport of cimetidine. J. Pharmacol. Exp. Ther. *312*, 144–152.

Payton, F., Sandusky, P. and Alworth, W.L. (2007). NMR study of the solution structure of curcumin. J. Nat. Prod. *70*, 143–146.

Perek, N., Koumanov, F., Denoyer, D., Boudard, D. and Dubois, F. (2002). Modulation of the multidrug resistance of glioma by glutathione levels depletion--interaction with Tc-99M-Sestamibi and Tc-99M-Tetrofosmin. Cancer Biother. Radiopharm. *17*, 291–302.

Petriz, J. (2013). Flow cytometry of the side population (SP). Curr. Protoc. Cytom. *Chapter 9*, Unit 9.23.

Pick, A., Klinkhammer, W. and Wiese, M. (2010). Specific inhibitors of the breast cancer resistance protein (BCRP). ChemMedChem. *5*, 1498–1505.

Pick A., Müller H., Mayer R., Haenisch B., Pajeva I.K., Weigt M., Bönisch H., Müller C.E. and Wiese M. (2011). Structure-activity relationships of flavonoids as inhibitors of breast cancer resistance protein (BCRP). Bioorg. Med. Chem. *19*, 2090-2102.

Pick, A. and Wiese, M. (2012). Tyrosine kinase inhibitors influence ABCG2 expression in EGFR-positive MDCK BCRP cells via the PI3K/Akt signaling pathway. ChemMedChem. *7*, 650–662.

Pirker, R., Wallner, J., Geissler, K., Linkesch, W., Haas, O.A., Bettelheim, P., Hopfner, M., Scherrer, R., Valent, P. and Havelec, L. (1991). MDR1 gene expression and treatment outcome in acute myeloid leukemia. J. Natl. Cancer Inst. *83*, 708–712.

Pratt, S., Shepard, R.L., Kandasamy, R.A., Johnston, P.A., Perry, W., 3rd and Dantzig, A.H. (2005). The multidrug resistance protein 5 (ABCC5) confers resistance to 5-fluorouracil and transports its monophosphorylated metabolites. Mol. Cancer Ther. *4*, 855–863.

Pratt, S., Chen, V., Perry, W.I., 3rd, Starling, J.J. and Dantzig, A.H. (2006). Kinetic validation of the use of carboxydichlorofluorescein as a drug surrogate for MRP5-mediated transport. Eur. J. Pharm. Sci. *27*, 524–532.

Prehm, P. (2013). Curcumin analogue identified as hyaluronan export inhibitor by virtual docking to the ABC transporter MRP5. Food Chem. Toxicol. *62*, 76–81.

Prinz, H. (2010). Hill coefficients, dose-response curves and allosteric mechanisms. J. Chem. Biol. *3*, 37–44.

Priyadarsini, K.I. (2013). Chemical and structural features influencing the biological activity of curcumin. Curr. Pharm. Des. *19*, 2093–2100.

Qiao, Q., Jiang, Y. and Li, G. (2013). Inhibition of the PI3K/AKT-NF-κB pathway with curcumin enhanced radiation-induced apoptosis in human Burkitt's lymphoma. J. Pharmacol. Sci. *121*, 247–256.

Radbruch, A. (2000). Immunofluorescence: Basic Considerations. In Flow Cytometry and Cell Sorting, P.D.A. Radbruch, ed. (Springer Berlin Heidelberg), pp. 38–52.

Rajagopal, A. and Simon, S.M. (2003). Subcellular localization and activity of multidrug resistance proteins. Mol. Biol. Cell *14*, 3389–3399.

Ranjan, A.P., Mukerjee, A., Helson, L., Gupta, R. and Vishwanatha, J.K. (2013). Efficacy of liposomal curcumin in a human pancreatic tumor xenograft model: inhibition of tumor growth and angiogenesis. Anticancer Res. *33*, 3603–3609.

Ravindran, J., Prasad, S. and Aggarwal, B.B. (2009). Curcumin and cancer cells: how many ways can curry kill tumor cells selectively? AAPS J *11*, 495–510.

Ravna, A.W., Sylte, I. and Sager, G. (2008). A molecular model of a putative substrate releasing conformation of multidrug resistance protein 5 (MRP5). Eur. J. Med. Chem. *43*, 2557–2567.

Reid, G., Wielinga, P., Zelcer, N., De Haas, M., Van Deemter, L., Wijnholds, J., Balzarini, J. and Borst, P. (2003). Characterization of the transport of nucleoside analog drugs by the human multidrug resistance proteins MRP4 and MRP5. Mol. Pharmacol. *63*, 1094–1103.

Reid, G., Wallant, N.C., Patel, R., Antonic, A., Saxon-Aliifaalogo, F., Cao, H., Webster, G. and Watson, J.D. (2009). Potent subunit-specific effects on cell growth and drug sensitivity from optimised siRNA-mediated silencing of ribonucleotide reductase. J RNAi Gene Silencing *5*, 321–330.

Ries, F. and Dicato, M. (1991). Treatment of advanced and refractory breast cancer with doxorubicin, vincristine and continuous infusion of verapamil. A phase I-II clinical trial. Med. Oncol. Tumor Pharmacother. *8*, 39–43.

Ringman, J.M., Frautschy, S.A., Teng, E., Begum, A.N., Bardens, J., Beigi, M., Gylys, K.H., Badmaev, V., Heath, D.D., Apostolova, L.G., et al. (2012). Oral curcumin for Alzheimer's disease: tolerability and efficacy in a 24-week randomized, double blind, placebo-controlled study. Alzheimers Res. Ther. *4*, 43.

Robbins, A.K. and Horlick, R.A. (1998). Macrophage scavenger receptor confers an adherent phenotype to cells in culture. BioTechniques *25*, 240–244.

Robey, R.W., Honjo, Y., van de Laar, A., Miyake, K., Regis, J.T., Litman, T. and Bates, S.E. (2001). A functional assay for detection of the mitoxantrone resistance protein, MXR (ABCG2). Biochim. Biophys. Acta *1512*, 171–182.

Robey, R.W., Steadman, K., Polgar, O., Morisaki, K., Blayney, M., Mistry, P. and Bates, S.E. (2004). Pheophorbide a is a specific probe for ABCG2 function and inhibition. Cancer Res. *64*, 1242–1246.

Robey, R.W., To, K.K.K., Polgar, O., Dohse, M., Fetsch, P., Dean, M. and Bates, S.E. (2009). ABCG2: a perspective. Adv. Drug Deliv. Rev. *61*, 3–13.

Robey, R.W., Massey, P.R., Amiri-Kordestani, L. and Bates, S.E. (2010). ABC transporters: unvalidated therapeutic targets in cancer and the CNS. Anticancer Agents Med. Chem. *10*, 625–633.

Robey, R.W., Ierano, C., Zhan, Z. and Bates, S.E. (2011). The challenge of exploiting ABCG2 in the clinic. Curr. Pharm. Biotechnol. *12*, 595–608.

Romero-Calvo, I., Ocón, B., Martínez-Moya, P., Suárez, M.D., Zarzuelo, A., Martínez-Augustin, O. and de Medina, F.S. (2010). Reversible Ponceau staining as a loading control alternative to actin in Western blots. Anal. Biochem. *401*, 318–320.

Rothnie, A., Conseil, G., Lau, A.Y.T., Deeley, R.G. and Cole, S.P.C. (2008). Mechanistic differences between GSH transport by multidrug resistance protein 1 (MRP1/ABCC1) and GSH modulation of MRP1-mediated transport. Mol. Pharmacol. *74*, 1630–1640.

Ruan, W. and Lai, M. (2007). Actin, a reliable marker of internal control? Clin. Chim. Acta *385*, 1–5.

Al-Rubeai, M., Welzenbach, K., Lloyd, D.R. and Emery, A.N. (1997). A rapid method for evaluation of cell number and viability by flow cytometry. Cytotechnology *24*, 161–168.

Rybalkin, S.D., Yan, C., Bornfeldt, K.E. and Beavo, J.A. (2003). Cyclic GMP phosphodiesterases and regulation of smooth muscle function. Circ. Res. *93*, 280–291.

Sager, G., Ørvoll, E.Ø., Lysaa, R.A., Kufareva, I., Abagyan, R. and Ravna, A.W. (2012). Novel cGMP efflux inhibitors identified by virtual ligand screening (VLS) and confirmed by experimental studies. J. Med. Chem. *55*, 3049–3057.

Saha, S., Adhikary, A., Bhattacharyya, P., DAS, T. and Sa, G. (2012). Death by design: where curcumin sensitizes drug-resistant tumours. Anticancer Res. *32*, 2567–2584.

Saito, H., Hirano, H., Nakagawa, H., Fukami, T., Oosumi, K., Murakami, K., Kimura, H., Kouchi, T., Konomi, M., Tao, E., et al. (2006). A new strategy of high-speed screening and quantitative structure-activity relationship analysis to evaluate human ATP-binding cassette transporter ABCG2-drug interactions. J. Pharmacol. Exp. Ther. *317*, 1114–1124.

Santucci, R., Levêque, D., Kemmel, V., Lutz, P., Gérout, A.-C., N'guyen, A., Lescoute, A., Schneider, F., Bergerat, J.-P. and Herbrecht, R. (2010). Severe intoxication with methotrexate possibly associated with concomitant use of proton pump inhibitors. Anticancer Res. *30*, 963–965.

Sarkadi, B., Price, E.M., Boucher, R.C., Germann, U.A. and Scarborough, G.A. (1992). Expression of the human multidrug resistance cDNA in insect cells generates a high activity drug-stimulated membrane ATPase. J. Biol. Chem. *267*, 4854–4858.

Sarkadi, B., Homolya, L., Szakács, G. and Váradi, A. (2006). Human multidrug resistance ABCB and ABCG transporters: participation in a chemoimmunity defense system. Physiol. Rev. *86*, 1179–1236.

Sarmento, B., Andrade, F., da Silva, S.B., Rodrigues, F., das Neves, J. and Ferreira, D. (2012). Cell-based in vitro models for predicting drug permeability. Expert Opin. Drug Metab. Toxicol. *8*, 607–621.

Schaich, M., Soucek, S., Thiede, C., Ehninger, G., Illmer, T. and SHG AML96 Study Group (2005). MDR1 and MRP1 gene expression are independent predictors for treatment outcome in adult acute myeloid leukaemia. Br. J. Haematol. *128*, 324–332.

Schinkel, A.H., Smit, J.J., van Tellingen, O., Beijnen, J.H., Wagenaar, E., van Deemter, L., Mol, C.A., van der Valk, M.A., Robanus-Maandag, E.C. and te Riele, H.P. (1994). Disruption of the mouse mdr1a P-glycoprotein gene leads to a deficiency in the blood-brain barrier and to increased sensitivity to drugs. Cell *77*, 491–502.

Schinkel, A.H., Mayer, U., Wagenaar, E., Mol, C.A., van Deemter, L., Smit, J.J., van der Valk, M.A., Voordouw, A.C., Spits, H., van Tellingen, O., et al. (1997). Normal viability and altered pharmacokinetics in mice lacking mdr1-type (drug-transporting) P-glycoproteins. Proc. Natl. Acad. Sci. U.S.A. *94*, 4028–4033.

Schnepf, R. and Zolk, O. (2013). Effect of the ATP-binding cassette transporter ABCG2 on pharmacokinetics: experimental findings and clinical implications. Expert Opin. Drug Metab. Toxicol. *9*, 287–306.

Schulz, T., Schumacher, U. and Prehm, P. (2007). Hyaluronan export by the ABC transporter MRP5 and its modulation by intracellular cGMP. J. Biol. Chem. *282*, 20999–21004.

Schulz, T., Schumacher, U., Prante, C., Sextro, W. and Prehm, P. (2010). Cystic fibrosis transmembrane conductance regulator can export hyaluronan. Pathobiology *77*, 200–209.

Seelig, A. (1998). A general pattern for substrate recognition by P-glycoprotein. Eur. J. Biochem. *251*, 252–261.

Seelig, A. and Gatlik-Landwojtowicz, E. (2005). Inhibitors of multidrug efflux transporters: their membrane and protein interactions. Mini Rev. Med. Chem. *5*, 135–151.

Shaffer, B.C., Gillet, J.-P., Patel, C., Baer, M.R., Bates, S.E. and Gottesman, M.M. (2012). Drug resistance: still a daunting challenge to the successful treatment of AML. Drug Resist. Updat. *15*, 62–69.

Shapiro, H.M. (2005a). Learning Flow Cytometry. In Practical Flow Cytometry, (John Wiley & Sons, Inc.), pp. 61–72.

Shapiro, H.M. (2005b). Parameters and Probes. In Practical Flow Cytometry, (John Wiley & Sons, Inc.), pp. 273–410.

Shapiro, A.B. and Ling, V. (1997). Positively cooperative sites for drug transport by P-glycoprotein with distinct drug specificities. Eur. J. Biochem. *250*, 130–137.

Shapiro, A.B., Fox, K., Lam, P. and Ling, V. (1999). Stimulation of P-glycoprotein-mediated drug transport by prazosin and progesterone. Evidence for a third drug-binding site. Eur. J. Biochem. *259*, 841–850.

Sharom, F.J. (2008). ABC multidrug transporters: structure, function and role in chemoresistance. Pharmacogenomics *9*, 105–127.

Sharom, F.J. (2011). The P-glycoprotein multidrug transporter. Essays Biochem. *50*, 161–178.

Shehzad, A., Lee, J. and Lee, Y.S. (2013). Curcumin in various cancers. Biofactors *39*, 56–68.

Shen, H., Lee, F.Y. and Gan, J. (2011). Ixabepilone, a novel microtubule-targeting agent for breast cancer, is a substrate for P-glycoprotein (P-gp/MDR1/ABCB1) but not breast cancer resistance protein (BCRP/ABCG2). J. Pharmacol. Exp. Ther. *337*, 423–432.

Sherley, J.L., Stadler, P.B. and Stadler, J.S. (1995). A quantitative method for the analysis of mammalian cell proliferation in culture in terms of dividing and non-dividing cells. Cell Prolif. *28*, 137–144.

Shukla, S., Sauna, Z.E. and Ambudkar, S.V. (2008). Evidence for the interaction of imatinib at the transport-substrate site(s) of the multidrug-resistance-linked ABC drug transporters ABCB1 (P-glycoprotein) and ABCG2. Leukemia *22*, 445–447.

Shukla, S., Zaher, H., Hartz, A., Bauer, B., Ware, J.A. and Ambudkar, S.V. (2009). Curcumin inhibits the activity of ABCG2/BCRP1, a multidrug resistance-linked ABC drug transporter in mice. Pharm. Res. *26*, 480–487.

Shukla, S., Ohnuma, S. and Ambudkar, S.V. (2011). Improving cancer chemotherapy with modulators of ABC drug transporters. Curr. Drug Targets *12*, 621–630.

Shukla, S., Chen, Z.-S. and Ambudkar, S.V. (2012). Tyrosine kinase inhibitors as modulators of ABC transporter-mediated drug resistance. Drug Resist. Updat. *15*, 70–80.

DA Silva, V.A., DA Silva, K.A.E.P., Delou, J.M.A., DA Fonseca, L.M., Lopes, A.G. and Capella, M.A.M. (2014). Modulation of ABCC1 and ABCG2 proteins by ouabain in human breast cancer cells. Anticancer Res. *34*, 1441–1448.

Simmonds, P.C. (2000). Palliative chemotherapy for advanced colorectal cancer: systematic review and meta-analysis. Colorectal Cancer Collaborative Group. BMJ *321*, 531–535.

Singh, A., Wu, H., Zhang, P., Happel, C., Ma, J. and Biswal, S. (2010). Expression of ABCG2 (BCRP) is regulated by Nrf2 in cancer cells that confers side population and chemoresistance phenotype. Mol. Cancer Ther. *9*, 2365–2376.

Slot, A.J., Molinski, S.V. and Cole, S.P.C. (2011). Mammalian multidrug-resistance proteins (MRPs). Essays Biochem. *50*, 179–207.

Smit, J.W., Meijer, C.J., Decary, F. and Feltkamp-Vroom, T.M. (1974). Paraformaldehyde fixation in immunofluorescence and immunoelectron microscopy. Preservation of tissue and cell surface membrane antigens. J. Immunol. Methods *6*, 93–98.

Somers-Edgar, T.J., Taurin, S., Larsen, L., Chandramouli, A., Nelson, M.A. and Rosengren, R.J. (2011). Mechanisms for the activity of heterocyclic cyclohexanone curcumin derivatives in estrogen receptor negative human breast cancer cell lines. Invest. New Drugs *29*, 87–97.

Sonneveld, P., Suciu, S., Weijermans, P., Beksac, M., Neuwirtova, R., Solbu, G., Lokhorst, H., van der Lelie, J., Dohner, H., Gerhartz, H., et al. (2001). Cyclosporin A combined with vincristine, doxorubicin and dexamethasone (VAD) compared with VAD alone in patients with advanced refractory multiple myeloma: an EORTC-HOVON randomized phase III study (06914). Br. J. Haematol. *115*, 895–902.

Spoelstra, E.C., Westerhoff, H.V., Pinedo, H.M., Dekker, H. and Lankelma, J. (1994). The multidrug-resistance-reverser verapamil interferes with cellular P-glycoprotein-mediated pumping of daunorubicin as a non-competing substrate. Eur. J. Biochem. *221*, 363–373.

Sreenivasan, S., Ravichandran, S., Vetrivel, U. and Krishnakumar, S. (2013). Modulation of multidrug resistance 1 expression and function in retinoblastoma cells by curcumin. J. Pharmacol. Pharmacother. *4*, 103–109.

Steinbach, D. and Legrand, O. (2007). ABC transporters and drug resistance in leukemia: was P-gp nothing but the first head of the Hydra? Leukemia *21*, 1172–1176.

Stępień, K.M., Tomaszewski, M., Tomaszewska, J. and Czuczwar, S.J. (2012). The multidrug transporter P-glycoprotein in pharmacoresistance to antiepileptic drugs. Pharmacol. Rep. *64*, 1011–1019.

Straganz, G.D., Glieder, A., Brecker, L., Ribbons, D.W. and Steiner, W. (2003). Acetylacetone-cleaving enzyme Dke1: a novel C-C-bond-cleaving enzyme from *Acinetobacter johnsonii*. Biochem. J. *369*, 573–581.

Sun, A., Lu, Y.J., Hu, H., Shoji, M., Liotta, D.C. and Snyder, J.P. (2009). Curcumin analog cytotoxicity against breast cancer cells: exploitation of a redox-dependent mechanism. Bioorg. Med. Chem. Lett. *19*, 6627–6631.

Sun, Z.-J., Chen, G., Hu, X., Zhang, W., Liu, Y., Zhu, L.-X., Zhou, Q. and Zhao, Y.-F. (2010). Activation of PI3K/Akt/IKK-alpha/NF-kappaB signaling pathway is required for the apoptosis-evasion in human salivary adenoid cystic carcinoma: its inhibition by quercetin. Apoptosis *15*, 850–863.

Surowiak, P., Materna, V., Matkowski, R., Szczuraszek, K., Kornafel, J., Wojnar, A., Pudelko, M., Dietel, M., Denkert, C., Zabel, M., et al. (2005). Relationship between the expression of cyclooxygenase 2 and MDR1/P-glycoprotein in invasive breast cancers and their prognostic significance. Breast Cancer Res. *7*, R862–870.

Suvannasankha, A., Minderman, H., O'Loughlin, K.L., Nakanishi, T., Greco, W.R., Ross, D.D. and Baer, M.R. (2004). Breast cancer resistance protein (BCRP/MXR/ABCG2) in acute myeloid leukemia: discordance between expression and function. Leukemia *18*, 1252–1257.

Suzuki, H. and Sugiyama, Y. (1998). Excretion of GSSG and glutathione conjugates mediated by MRP1 and cMOAT/MRP2. Semin. Liver Dis. *18*, 359–376.

Suzuki, M., Suzuki, H., Sugimoto, Y. and Sugiyama, Y. ABCG2 transports sulfated conjugates of steroids and xenobiotics. J. Biol. Chem. *25,* 22644-9.

Swami, U., Goel, S. and Mani, S. (2013). Therapeutic targeting of CPT-11 induced diarrhea: a case for prophylaxis. Curr. Drug Targets *14*, 777–797.

Szakács, G., Paterson, J.K., Ludwig, J.A., Booth-Genthe, C. and Gottesman, M.M. (2006). Targeting multidrug resistance in cancer. Nat. Rev. Drug Discov. *5*, 219–234.

Szakács, G., Váradi, A., Ozvegy-Laczka, C. and Sarkadi, B. (2008a). The role of ABC transporters in drug absorption, distribution, metabolism, excretion and toxicity (ADME-Tox). Drug Discov. Today *13*, 379–393.

Szakács, G., Homolya, L., Sarkadi, B. and Váradi, A. (2008b). MDR-ABC Transporters. In Encyclopedia of Molecular Pharmacology, D.S. Offermanns, and D.W. Rosenthal, eds. (Springer Berlin Heidelberg), pp. 748–752.

Tahara, H., Kusuhara, H., Maeda, K., Koepsell, H., Fuse, E. and Sugiyama, Y. (2006). Inhibition of oat3-mediated renal uptake as a mechanism for drug-drug interaction between fexofenadine and probenecid. Drug Metab. Dispos. *34*, 743–747.

Takada, T., Suzuki, H., Gotoh, Y. and Sugiyama, Y. (2005). Regulation of the cell surface expression of human BCRP/ABCG2 by the phosphorylation state of Akt in polarized cells. Drug Metab. Dispos. *33*, 905–909.

Takeshita, A., Shinjo, K., Ohnishi, K. and Ohno, R. (1996). Expression of multidrug resistance P-glycoprotein in myeloid progenitor cells of different phenotype: comparison between normal bone marrow cells and leukaemia cells. Br. J. Haematol. *93*, 18–21.

Takigawa, N., Takeyama, M., Kozuki, T., Shibayama, T., Hisamoto, A., Kiura, K., Tada, A., Hotta, K., Umemura, S., Ohashi, K., et al. (2007). Combination of SN-38 with gefitinib or imatinib overcomes SN-38-resistant small-cell lung cancer cells. Oncol. Rep. *17*, 983–987.

Tan, K.W., Li, Y., Paxton, J.W., Birch, N.P. and Scheepens, A. (2013a). Identification of novel dietary phytochemicals inhibiting the efflux transporter breast cancer resistance protein (BCRP/ABCG2). Food Chem. *138*, 2267–2274.

Tan, K.W., Killeen, D.P., Li, Y., Paxton, J.W., Birch, N.P. and Scheepens, A. (2013b). Dietary polyacetylenes of the falcarinol type are inhibitors of breast cancer resistance protein (BCRP/ABCG2). Eur. J. Pharmacol. *723*, 346–352.

Tanaka, H., Nakamura, M., Kameda, C., Kubo, M., Sato, N., Kuroki, S., Tanaka, M. and Katano, M. (2009). The Hedgehog signaling pathway plays an essential role in maintaining the CD44+CD24-/low subpopulation and the side population of breast cancer cells. Anticancer Res. *29*, 2147–2157.

Tanaka, M., Okazaki, T., Suzuki, H., Abbruzzese, J.L. and Li, D. (2011). Association of multi-drug resistance gene polymorphisms with pancreatic cancer outcome. Cancer *117*, 744–751.

Tang, X., Bi, H., Feng, J. and Cao, J. (2005). Effect of curcumin on multidrug resistance in resistant human gastric carcinoma cell line SGC7901/VCR. Acta Pharmacol. Sin. *26*, 1009–1016.

Taurin, S., Nehoff, H., Diong, J., Larsen, L., Rosengren, R.J. and Greish, K. (2013). Curcumin-derivative nanomicelles for the treatment of triple negative breast cancer. J. Drug Target. *21*, 675–683.

Tazzari, P.L., Cappellini, A., Ricci, F., Evangelisti, C., Papa, V., Grafone, T., Martinelli, G., Conte, R., Cocco, L., McCubrey, J.A., et al. (2007). Multidrug resistance-associated protein 1 expression is under the control of the phosphoinositide 3 kinase/Akt signal transduction network in human acute myelogenous leukemia blasts. Leukemia *21*, 427–438.

Timcheva, C.V. and Todorov, D.K. (1996). Does verapamil help overcome multidrug resistance in tumor cell lines and cancer patients? J. Chemother. *8*, 295–299.

Tiwari, A.K., Sodani, K., Dai, C.-L., Ashby, C.R., Jr and Chen, Z.-S. (2011). Revisiting the ABCs of multidrug resistance in cancer chemotherapy. Curr. Pharm. Biotechnol. *12*, 570–594.

To, K.K.W., and Tomlinson, B. (2013). Targeting the ABCG2-overexpressing multidrug resistant (MDR) cancer cells by PPARγ agonists. Br. J. Pharmacol. *170*, 1137–1151.

Tokh, M., Bathini, V. and Saif, M.W. (2012). First-line treatment of metastatic pancreatic cancer. JOP *13*, 159–162.

Tomiyasu, H., Watanabe, M., Sugita, K., Goto-Koshino, Y., Fujino, Y., Ohno, K., Sugano, S. and Tsujimoto, H. (2013). Regulations of ABCB1 and ABCG2 expression through MAPK pathways in acute lymphoblastic leukemia cell lines. Anticancer Res. *33*, 5317–5323.

Trédan, O., Galmarini, C.M., Patel, K. and Tannock, I.F. (2007). Drug resistance and the solid tumor microenvironment. J. Natl. Cancer Inst. *99*, 1441–1454.

Trock, B.J., Leonessa, F. and Clarke, R. (1997). Multidrug resistance in breast cancer: a meta-analysis of MDR1/gp170 expression and its possible functional significance. J. Natl. Cancer Inst. *89*, 917–931.

Tröger, U., Stötzel, B., Martens-Lobenhoffer, J., Gollnick, H. and Meyer, F.P. (2002). Drug points: Severe myalgia from an interaction between treatments with pantoprazole and methotrexate. BMJ *324*, 1497.

Tsuruo, T., Iida, H., Tsukagoshi, S. and Sakurai, Y. (1981). Overcoming of vincristine resistance in P388 leukemia in vivo and in vitro through enhanced cytotoxicity of vincristine and vinblastine by verapamil. Cancer Res. *41*, 1967–1972.

Tung, J.W., Heydari, K., Tirouvanziam, R., Sahaf, B., Parks, D.R., Herzenberg, L.A. and Herzenberg, L.A. (2007). Modern flow cytometry: a practical approach. Clin. Lab. Med. *27*, 453–468, v.

Uchiyama-Kokubu, N., Naito, M., Nakajima, M. and Tsuruo, T. (2004). Transport of somatostatin and substance P by human P-glycoprotein. FEBS Lett. *574*, 55–61.

Um, Y., Cho, S., Woo, H.B., Kim, Y.K., Kim, H., Ham, J., Kim, S.-N., Ahn, C.M. and Lee, S. (2008). Synthesis of curcumin mimics with multidrug resistance reversal activities. Bioorg. Med. Chem. *16*, 3608–3615.

Vareed, S.K., Kakarala, M., Ruffin, M.T., Crowell, J.A., Normolle, D.P., Djuric, Z. and Brenner, D.E. (2008). Pharmacokinetics of curcumin conjugate metabolites in healthy human subjects. Cancer Epidemiol. Biomarkers Prev. *17*, 1411–1417.

Varma, M.V.S., Ashokraj, Y., Dey, C.S. and Panchagnula, R. (2003). P-glycoprotein inhibitors and their screening: a perspective from bioavailability enhancement. Pharmacol. Res. *48*, 347–359.

Vasiliou, V., Vasiliou, K. and Nebert, D.W. (2009). Human ATP-binding cassette (ABC) transporter family. Hum. Genomics *3*, 281–290.

Vergote, J., Moretti, J.L., Kouyoumdjian, J.C. and Garnier-Suillerot, A. (2002). MRP1 modulation by PAK-104P: detection with technetium-99m-MIBI in cultured lung tumor cells. Anticancer Res. *22*, 251–256.

Vethanayagam, R.R., Wang, H., Gupta, A., Zhang, Y., Lewis, F., Unadkat, J.D. and Mao, Q. (2005). Functional analysis of the human variants of breast cancer resistance protein: I206L, N590Y, and D620N. Drug Metab. Dispos. *33*, 697–705.

Vinod, B.S., Maliekal, T.T. and Anto, R.J. (2013). Phytochemicals as chemosensitizers: from molecular mechanism to clinical significance. Antioxid. Redox Signal. *18*, 1307–1348.

Da Violante, G., Zerrouk, N., Richard, I., Provot, G., Chaumeil, J.C. and Arnaud, P. (2002). Evaluation of the cytotoxicity effect of dimethyl sulfoxide (DMSO) on Caco2/TC7 colon tumor cell cultures. Biol. Pharm. Bull. *25*, 1600–1603.

Vishnukumar, S., Umamaheswaran, G., Anichavezhi, D., Indumathy, S., Adithan, C., Srinivasan, K. and Kadambari, D. (2013). P-glycoprotein expression as a predictor of response to neoadjuvant chemotherapy in breast cancer. Indian J. Cancer *50*, 195–199.

Vistica, D.T., Skehan, P., Scudiero, D., Monks, A., Pittman, A. and Boyd, M.R. (1991). Tetrazolium-based assays for cellular viability: a critical examination of selected parameters affecting formazan production. Cancer Res. *51*, 2515–2520.

Visvader, J.E. and Lindeman, G.J. (2008). Cancer stem cells in solid tumours: accumulating evidence and unresolved questions. Nat. Rev. Cancer *8*, 755–768.

Vlaming, M.L.H., Lagas, J.S. and Schinkel, A.H. (2009). Physiological and pharmacological roles of ABCG2 (BCRP): recent findings in Abcg2 knockout mice. Adv. Drug Deliv. Rev. *61*, 14–25.

Volk, E.L. and Schneider, E. (2003). Wild-type breast cancer resistance protein (BCRP/ABCG2) is a methotrexate polyglutamate transporter. Cancer Res. *63*, 5538–5543.

Volk, E.L., Farley, K.M., Wu, Y., Li, F., Robey, R.W. and Schneider, E. (2002). Overexpression of wild-type breast cancer resistance protein mediates methotrexate resistance. Cancer Res. *62*, 5035–5040.

Vyas, A., Dandawate, P., Padhye, S., Ahmad, A. and Sarkar, F. (2013). Perspectives on new synthetic curcumin analogs and their potential anticancer properties. Curr. Pharm. Des. *19*, 2047–2069.

Wanek, T., Kuntner, C., Bankstahl, J.P., Mairinger, S., Bankstahl, M., Stanek, J., Sauberer, M., Filip, T., Erker, T., Müller, M., et al. (2012). A novel PET protocol for visualization of breast cancer resistance protein function at the blood-brain barrier. J. Cereb. Blood Flow Metab. *32*, 2002–2011.

Wang, E.J., Casciano, C.N., Clement, R.P. and Johnson, W.W. (2000a). In vitro flow cytometry method to quantitatively assess inhibitors of P-glycoprotein. Drug Metab. Dispos. *28*, 522–528.

Wang, E.J., Casciano, C.N., Clement, R.P. and Johnson, W.W. (2000b). Cooperativity in the inhibition of P-glycoprotein-mediated daunorubicin transport: evidence for half-of-the-sites reactivity. Arch. Biochem. Biophys. *383*, 91–98.

Wang, H., Zhou, L., Gupta, A., Vethanayagam, R.R., Zhang, Y., Unadkat, J.D. and Mao, Q. (2006). Regulation of BCRP/ABCG2 expression by progesterone and 17β-estradiol in human placental BeWo cells. Am. J. Physiol. Endocrinol. Metab. *290*, E798–807.

Wang, H., Lee, E.-W., Zhou, L., Leung, P.C.K., Ross, D.D., Unadkat, J.D. and Mao, Q. (2008). Progesterone receptor (PR) isoforms PRA and PRB differentially regulate expression of the breast cancer resistance protein in human placental choriocarcinoma BeWo cells. Mol. Pharmacol. *73*, 845–854.

Wang, H., Khor, T.O., Shu, L., Su, Z.-Y., Fuentes, F., Lee, J.-H. and Kong, A.-N.T. (2012). Plants vs. cancer: a review on natural phytochemicals in preventing and treating cancers and their druggability. Anticancer Agents Med. Chem. *12*, 1281–1305.

Wang, M., Wang, X., Yuan, J. and Guo, L. (2013). Expression of the breast cancer resistance protein and 5-fluorouracil resistance in clinical breast cancer tissue specimens. Mol. Clin. Oncol. *1*, 853–857.

Wang, P., Henning, S.M. and Heber, D. (2010a). Limitations of MTT and MTS-based assays for measurement of antiproliferative activity of green tea polyphenols. PLoS ONE *5*, e10202.

Wang, R.B., Kuo, C.L., Lien, L.L. and Lien, E.J. (2003). Structure-activity relationship: analyses of p-glycoprotein substrates and inhibitors. J. Clin. Pharm. Ther. *28*, 203–228.

Wang, W., Abbruzzese, J.L., Evans, D.B., Larry, L., Cleary, K.R. and Chiao, P.J. (1999). The nuclear factor-kappa B RelA transcription factor is constitutively activated in human pancreatic adenocarcinoma cells. Clin. Cancer Res. *5*, 119–127.

Wang, X., Wu, X., Wang, C., Zhang, W., Ouyang, Y., Yu, Y. and He, Z. (2010b). Transcriptional suppression of breast cancer resistance protein (BCRP) by wild-type p53 through the NF-kappaB pathway in MCF-7 cells. FEBS Lett. *584*, 3392–3397.

Wang, Y.H., Li, F., Luo, B., Wang, X.H., Sun, H.C., Liu, S., Cui, Y.Q. and Xu, X.X. (2009). A side population of cells from a human pancreatic carcinoma cell line harbors cancer stem cell characteristics. Neoplasma *56*, 371–378.

Wang, Y.J., Pan, M.H., Cheng, A.L., Lin, L.I., Ho, Y.S., Hsieh, C.Y. and Lin, J.K. (1997). Stability of curcumin in buffer solutions and characterization of its degradation products. J. Pharm. Biomed. Anal. *15*, 1867–1876.

Ward, A.B., Szewczyk, P., Grimard, V., Lee, C.-W., Martinez, L., Doshi, R., Caya, A., Villaluz, M., Pardon, E., Cregger, C., et al. (2013). Structures of P-glycoprotein reveal its conformational flexibility and an epitope on the nucleotide-binding domain. Proc. Natl. Acad. Sci. U.S.A. *110*, 13386–13391.

Warner, E., Tobe, S.W., Andrulis, I.L., Pei, Y., Trachtenberg, J. and Skorecki, K.L. (1995). Phase I-II study of vinblastine and oral cyclosporin A in metastatic renal cell carcinoma. Am. J. Clin. Oncol. *18*, 251–256.

Weber, D., Dimopoulos, M., Sinicrope, F. and Alexanian, R. (1995). VAD-cyclosporine therapy for VAD-resistant multiple myeloma. Leuk. Lymphoma *19*, 159–163.

Wei, X., Du, Z.-Y., Zheng, X., Cui, X.-X., Conney, A.H. and Zhang, K. (2012). Synthesis and evaluation of curcumin-related compounds for anticancer activity. Eur. J. Med. Chem. *53*, 235–245.

Weiss, J. and Haefeli, W.E. (2006). Evaluation of inhibitory potencies for compounds inhibiting P-glycoprotein but without maximum effects: f2 values. Drug Metab. Dispos. *34*, 203–207.

Weiss, J., Rose, J., Storch, C.H., Ketabi-Kiyanvash, N., Sauer, A., Haefeli, W.E. and Efferth, T. (2007). Modulation of human BCRP (ABCG2) activity by anti-HIV drugs. J. Antimicrob. Chemother. *59*, 238–245.

Wersto, R.P., Chrest, F.J., Leary, J.F., Morris, C., Stetler-Stevenson, M.A. and Gabrielson, E. (2001). Doublet discrimination in DNA cell-cycle analysis. Cytometry *46*, 296–306.

West, C.L. and Mealey, K.L. (2007). Assessment of antiepileptic drugs as substrates for canine P-glycoprotein. Am. J. Vet. Res. *68*, 1106–1110.

Wielinga, P., Hooijberg, J.H., Gunnarsdottir, S., Kathmann, I., Reid, G., Zelcer, N., van der Born, K., de Haas, M., van der Heijden, I., Kaspers, G., et al. (2005). The human multidrug resistance protein MRP5 transports folates and can mediate cellular resistance against antifolates. Cancer Res. *65*, 4425–4430.

Wijnholds, J., Evers, R., van Leusden, M.R., Mol, C.A., Zaman, G.J., Mayer, U., Beijnen, J.H., van der Valk, M., Krimpenfort, P. and Borst, P. (1997). Increased sensitivity to anticancer drugs and decreased inflammatory response in mice lacking the multidrug resistance-associated protein. Nat. Med. *3*, 1275–1279.

Wijnholds, J., Scheffer, G.L., van der Valk, M., van der Valk, P., Beijnen, J.H., Scheper, R.J. and Borst, P. (1998). Multidrug resistance protein 1 protects the oropharyngeal mucosal layer and the testicular tubules against drug-induced damage. J. Exp. Med. *188*, 797–808.

Wijnholds, J., deLange, E.C., Scheffer, G.L., van den Berg, D.J., Mol, C.A., van der Valk, M., Schinkel, A.H., Scheper, R.J., Breimer, D.D. and Borst, P. (2000a). Multidrug resistance protein 1 protects the choroid plexus epithelium and contributes to the blood-cerebrospinal fluid barrier. J. Clin. Invest. *105*, 279–285.

Wijnholds, J., Mol, C.A., van Deemter, L., de Haas, M., Scheffer, G.L., Baas, F., Beijnen, J.H., Scheper, R.J., Hatse, S., De Clercq, E., et al. (2000b). Multidrug-resistance protein 5 is a multispecific organic anion transporter able to transport nucleotide analogs. Proc. Natl. Acad. Sci. U.S.A. *97*, 7476–7481.

Wind, N.S. and Holen, I. (2011). Multidrug resistance in breast cancer: from in vitro models to clinical studies. Int. J. Breast Cancer *2011*, 967419.

De Wolf, C., Jansen, R., Yamaguchi, H., de Haas, M., van de Wetering, K., Wijnholds, J., Beijnen, J. and Borst, P. (2008). Contribution of the drug transporter ABCG2 (breast cancer resistance protein) to resistance against anticancer nucleosides. Mol. Cancer Ther. *7*, 3092–3102.

Woodward, O.M., Köttgen, A. and Köttgen, M. (2011). ABCG transporters and disease. FEBS J. *278*, 3215–3225.

Wortelboer, H.M., Usta, M., van der Velde, A.E., Boersma, M.G., Spenkelink, B., van Zanden, J.J., Rietjens, I.M.C.M., van Bladeren, P.J. and Cnubben, N.H.P. (2003). Interplay between MRP

inhibition and metabolism of MRP inhibitors: the case of curcumin. Chem. Res. Toxicol. *16*, 1642–1651.

Wortelboer, H.M., Usta, M., van Zanden, J.J., van Bladeren, P.J., Rietjens, I.M.C.M. and Cnubben, N.H.P. (2005). Inhibition of multidrug resistance proteins MRP1 and MRP2 by a series of α,β-unsaturated carbonyl compounds. Biochem. Pharmacol. *69*, 1879–1890.

Wu, C.-P., Calcagno, A.M., Hladky, S.B., Ambudkar, S.V. and Barrand, M.A. (2005). Modulatory effects of plant phenols on human multidrug-resistance proteins 1, 4 and 5 (ABCC1, 4 and 5). FEBS J. *272*, 4725–4740.

Wu, X., Zhang, X., Zhang, H., Su, P., Li, W., Li, L., Wang, Y., Liu, W., Gao, P. and Zhou, G. (2012). Progesterone receptor downregulates breast cancer resistance protein expression via binding to the progesterone response element in breast cancer. Cancer Sci. *103*, 959–967.

Xia, C.Q. and Smith, P.G. (2012). Drug efflux transporters and multidrug resistance in acute leukemia: therapeutic impact and novel approaches to mediation. Mol. Pharmacol. *82*, 1008–1021.

Xia, C.Q., Liu, N., Yang, D., Miwa, G. and Gan, L.-S. (2005). Expression, localization, and functional characteristics of breast cancer resistance protein in Caco-2 cells. Drug Metab. Dispos. *33*, 637–643.

Xia, C.Q., Milton, M.N. and Gan, L.-S. (2007a). Evaluation of drug-transporter interactions using in vitro and in vivo models. Curr. Drug Metab. *8*, 341–363.

Xia, C.Q., Liu, N., Miwa, G.T. and Gan, L.-S. (2007b). Interactions of cyclosporin a with breast cancer resistance protein. Drug Metab. Dispos. *35*, 576–582.

Xie, Y., Xu, K., Linn, D.E., Yang, X., Guo, Z., Shimelis, H., Nakanishi, T., Ross, D.D., Chen, H., Fazli, L., et al. (2008). The 44-kDa Pim-1 kinase phosphorylates BCRP/ABCG2 and thereby promotes its multimerization and drug-resistant activity in human prostate cancer cells. J. Biol. Chem. *283*, 3349–3356.

Xu, J., Liu, Y., Yang, Y., Bates, S. and Zhang, J.-T. (2004). Characterization of oligomeric human half-ABC transporter ATP-binding cassette G2. J. Biol. Chem. *279*, 19781–19789.

Yadav, B., Taurin, S., Rosengren, R.J., Schumacher, M., Diederich, M., Somers-Edgar, T.J. and Larsen, L. (2010). Synthesis and cytotoxic potential of heterocyclic cyclohexanone analogues of curcumin. Bioorg. Med. Chem. *18*, 6701–6707.

Yadav, B., Taurin, S., Larsen, L. and Rosengren, R.J. (2012a). RL71, a second-generation curcumin analog, induces apoptosis and downregulates Akt in ER-negative breast cancer cells. Int. J. Oncol. *41*, 1119–1127.

Yadav, B., Taurin, S., Larsen, L. and Rosengren, R.J. (2012b). RL66 a second-generation curcumin analog has potent in vivo and in vitro anticancer activity in ER negative breast cancer models. Int. J. Oncol. *41*, 1723–1732.

Yahanda, A.M., Alder, K.M., Fisher, G.A., Brophy, N.A., Halsey, J., Hardy, R.I., Gosland, M.P., Lum, B.L. and Sikic, B.I. (1992). Phase I trial of etoposide with cyclosporine as a modulator of multidrug resistance. J. Clin. Oncol. *10*, 1624–1634.

Yallapu, M.M., Maher, D.M., Sundram, V., Bell, M.C., Jaggi, M. and Chauhan, S.C. (2010). Curcumin induces chemo/radio-sensitization in ovarian cancer cells and curcumin nanoparticles inhibit ovarian cancer cell growth. J. Ovarian Res. *3*, 11.

Yamada, A., Ishikawa, T., Ota, I., Kimura, M., Shimizu, D., Tanabe, M., Chishima, T., Sasaki, T., Ichikawa, Y., Morita, S., et al. (2013). High expression of ATP-binding cassette transporter ABCC11 in breast tumors is associated with aggressive subtypes and low disease-free survival. Breast Cancer Res. Treat. *137*, 773–782.

Yamagishi, T., Sahni, S., Sharp, D.M., Arvind, A., Jansson, P.J. and Richardson, D.R. (2013). P-glycoprotein mediates drug resistance via a novel mechanism involving lysosomal sequestration. J. Biol. Chem. *288*, 31761–31771.

Yanase, K., Tsukahara, S., Asada, S., Ishikawa, E., Imai, Y. and Sugimoto, Y. (2004). Gefitinib reverses breast cancer resistance protein-mediated drug resistance. Mol. Cancer Ther. *3*, 1119–1125.

Yang, K.-Y., Lin, L.-C., Tseng, T.-Y., Wang, S.-C. and Tsai, T.-H. (2007). Oral bioavailability of curcumin in rat and the herbal analysis from *Curcuma longa* by LC-MS/MS. J. Chromatogr. B Analyt. Technol. Biomed. Life Sci. *853*, 183–189.

Yano, H., Nakanishi, S., Kimura, K., Hanai, N., Saitoh, Y., Fukui, Y., Nonomura, Y. and Matsuda, Y. (1993). Inhibition of histamine secretion by wortmannin through the blockade of phosphatidylinositol 3-kinase in RBL-2H3 cells. J. Biol. Chem. *268*, 25846–25856.

Liu Yin, J.A., Wheatley, K., Rees, J.K., Burnett, A.K. and UK MRC Adult Leukemia Working Party (2001). Comparison of “sequential” versus “standard” chemotherapy as re-induction treatment, with or without cyclosporine, in refractory/relapsed acute myeloid leukaemia (AML): results of the UK Medical Research Council AML-R trial. Br. J. Haematol. *113*, 713–726.

Yoshikawa, M., Ikegami, Y., Sano, K., Yoshida, H., Mitomo, H., Sawada, S. and Ishikawa, T. (2004). Transport of SN-38 by the wild type of human ABC transporter ABCG2 and its inhibition by quercetin, a natural flavonoid. J. Exp. Ther. Oncol. *4*, 25–35.

Yu, M., Ocana, A. and Tannock, I.F. (2013). Reversal of ATP-binding cassette drug transporter activity to modulate chemoresistance: why has it failed to provide clinical benefit? Cancer Metastasis Rev. *32*, 211–227.

Yu, S., Shen, G., Khor, T.O., Kim, J.-H. and Kong, A.-N.T. (2008). Curcumin inhibits Akt/mammalian target of rapamycin signaling through protein phosphatase-dependent mechanism. Mol. Cancer Ther. *7*, 2609–2620.

Yuan, J., Lv, H., Peng, B., Wang, C., Yu, Y. and He, Z. (2009). Role of BCRP as a biomarker for predicting resistance to 5-fluorouracil in breast cancer. Cancer Chemother. Pharmacol. *63*, 1103–1110.

Yumoto, R., Murakami, T., Nakamoto, Y., Hasegawa, R., Nagai, J. and Takano, M. (1999). Transport of rhodamine 123, a P-glycoprotein substrate, across rat intestine and Caco-2 cell monolayers in the presence of cytochrome P-450 3A-related compounds. J. Pharmacol. Exp. Ther. *289*, 149–155.

Zander, S.A.L., Kersbergen, A., van der Burg, E., de Water, N., van Tellingen, O., Gunnarsdottir, S., Jaspers, J.E., Pajic, M., Nygren, A.O.H., Jonkers, J., et al. (2010). Sensitivity and acquired resistance of BRCA1;p53-deficient mouse mammary tumors to the topoisomerase I inhibitor topotecan. Cancer Res. *70*, 1700–1710.

Zhang, S., Yang, X., Coburn, R.A. and Morris, M.E. (2005). Structure activity relationships and quantitative structure activity relationships for the flavonoid-mediated inhibition of breast cancer resistance protein. Biochem. Pharmacol. *70*, 627–639.

Zhang, W. and Lim, L.-Y. (2008). Effects of spice constituents on P-glycoprotein-mediated transport and CYP3A4-mediated metabolism in vitro. Drug Metab. Dispos. *36*, 1283–1290.

Zhang, C., Kwan, P., Zuo, Z. and Baum, L. (2012). The transport of antiepileptic drugs by P-glycoprotein. Adv. Drug Deliv. Rev. *64*, 930–942.

Zhang, H., Yu, T., Wen, L., Wang, H., Fei, D. and Jin, C. (2013). Curcumin enhances the effectiveness of cisplatin by suppressing CD133(+) cancer stem cells in laryngeal carcinoma treatment. Exp. Ther. Med. *6*, 1317–1321.

Zhang, J., Sun, T., Liang, L., Wu, T. and Wang, Q. (2014). Drug promiscuity of P-glycoprotein and its mechanism of interaction with paclitaxel and doxorubicin. Soft Matter *10*, 438–445.

Zhang, W., Tan, T.M.C. and Lim, L.-Y. (2007). Impact of curcumin-induced changes in P-glycoprotein and CYP3A expression on the pharmacokinetics of peroral celiprolol and midazolam in rats. Drug Metab. Dispos. *35*, 110–115.

Zhang, W., Ding, W., Chen, Y., Feng, M., Ouyang, Y., Yu, Y. and He, Z. (2011). Up-regulation of breast cancer resistance protein plays a role in HER2-mediated chemoresistance through PI3K/Akt and nuclear factor-kappa B signaling pathways in MCF7 breast cancer cells. Acta Biochim. Biophys. Sin. (Shanghai) *43*, 647–653.

Zhao, C., Liu, Z. and Liang, G. (2013). Promising curcumin-based drug design: mono-carbonyl analogues of curcumin (MACs). Curr. Pharm. Des. *19*, 2114–2135.

Zhao, J., Yu, B.-Y., Wang, D.-Y. and Yang, J.-E. (2010). Promoter polymorphism of MRP1 associated with reduced survival in hepatocellular carcinoma. World J. Gastroenterol. *16*, 6104–6110.

Zhou, S.F. (2008a). Role of multidrug resistance associated proteins in drug development. Drug Discov. Ther. *2*, 305–332.

Zhou, S.-F. (2008b). Structure, function and regulation of P-glycoprotein and its clinical relevance in drug disposition. Xenobiotica *38*, 802–832.

Zhou, J., Wang, C.-Y., Liu, T., Wu, B., Zhou, F., Xiong, J.-X., Wu, H.-S., Tao, J., Zhao, G., Yang, M., et al. (2008). Persistence of side population cells with high drug efflux capacity in pancreatic cancer. World J. Gastroenterol. *14*, 925–930.

Zhou, S., Schuetz, J.D., Bunting, K.D., Colapietro, A.M., Sampath, J., Morris, J.J., Lagutina, I., Grosveld, G.C., Osawa, M., Nakauchi, H., et al. (2001). The ABC transporter Bcrp1/ABCG2 is expressed in a wide variety of stem cells and is a molecular determinant of the side-population phenotype. Nat. Med. *7*, 1028–1034.

Appendix

Appendix I. BCRP structure-activity data

Table A-1. Calculated lipophilicity and polarisability of the analogues with values for BCRP inhibition.

Analogue	$cLogD_{7.4}$	cPolarisability	[LogD * polarisability]	Rank[a]	BCRP inhibition[b]	Rank
A1	3.16	31.88	100.74	16	0.65	18
A2	3.16	31.89	100.77	15	-0.79	21
A3	4.24	31.2	132.29	13	1.12	16
A4	4.24	31.21	132.33	12	4.36	15
A5	5.42	30.96	167.80	7	31.91	11
A6	4.04	32.62	131.78	14	27.69	13
A7	1.56	30.81	48.06	23	36.47	10
A8	2.2	30.82	67.80	20	19.63	14
A9	6.24	47.79	298.21	1	45.31	7
A12	4.97	43.73	217.34	3	89.86	1
A13	4.67	39.9	186.33	5	86.50	3
B1	1.84	33.41	61.47	21	-3.86	23
B2	1.84	33.41	61.47	22	0.78	17
B5	4.11	32.49	133.53	11	29.85	12
B8	0.89	32.34	28.78	24	-0.29	19
B10	3.33	50.31	167.53	8	48.14	6
B11	3.94	44.63	175.84	6	88.14	2
B12	3.65	45.26	165.20	9	38.08	8
C1	2.28	36.36	82.90	18	-15.04	24
C2	2.3	36.36	83.63	17	-0.99	22
C10	3.78	53.26	201.32	4	68.00	4
D2	2.72	30.04	81.71	19	-0.52	20
E12	4.55	53.01	241.20	2	65.59	5
CUR	3.65	39.71	144.94	10	36.91	9

[a] – Values were ranked highest to lowest 1-23. [b] – % of Ko143 inhibition. $cLogD_{7.4}$ and molecular polarisability were calculated using Marvin chemistry suite (ChemAxon, Cambridge, MA).

Appendix II. Flow cytometry fluorescence histograms

A

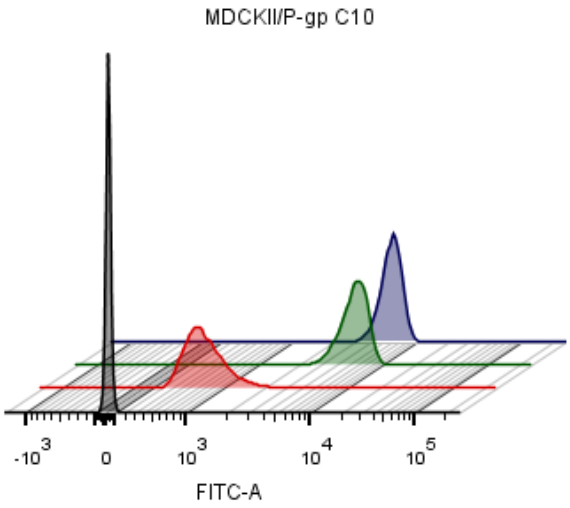

	TUBE NAME	Geometric Mean : FITC-A
	P-gp unstained	16.0
	P-gp Control	803
	P-gp C10 20 uM	6034
	P-gp verapamil 25 uM	6300

B

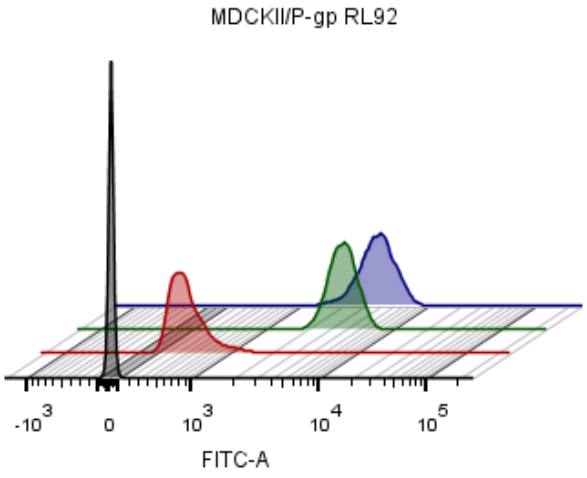

	TUBE NAME	Geometric Mean : FITC-A
	P-gp unstained	11.7
	P-gp Control	488
	P-gp RL92 20 uM	4120
	P-gp verapamil 25	3883

C

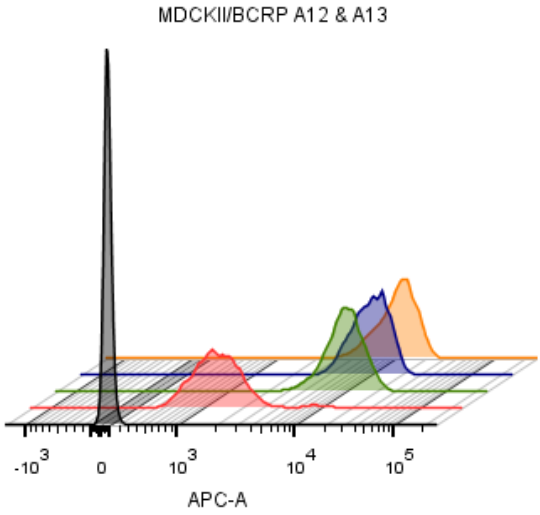

	TUBE NAME	Geometric Mean : APC-A
	BCRP unstained	68.1
	BCRP control	1504
	BCRP A12 20 uM	10266
	BCRP A13 20 uM	10488
	BCRP Ko143 5 uM	10750

D

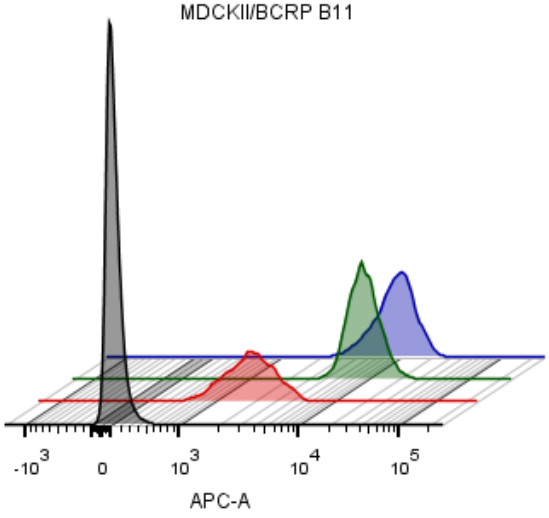

	TUBE NAME	Geometric Mean : APC-A
	BCRP unstained	128
	BCRP control	2077
	BCRP B11 20 uM	9852
	BCRP Ko143 5 uM	9186

E

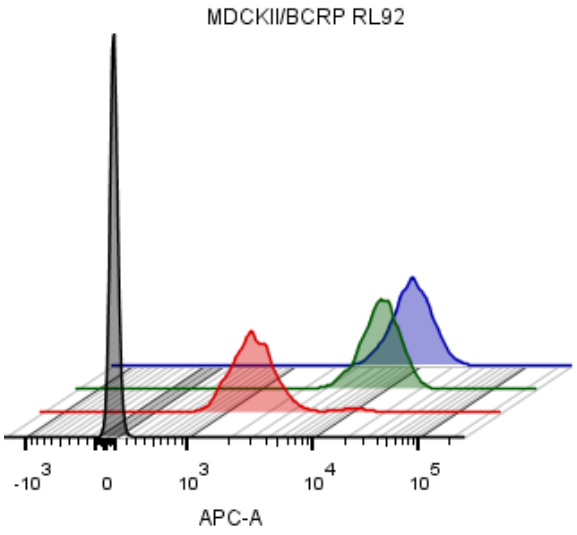

	TUBE NAME	Geometric Mean : APC-A
	BCRP unstained	71.9
	BCRP control	1915
	BCRP RL92 20 uM	9590
	BCRP Ko143 5 uM	8878

F

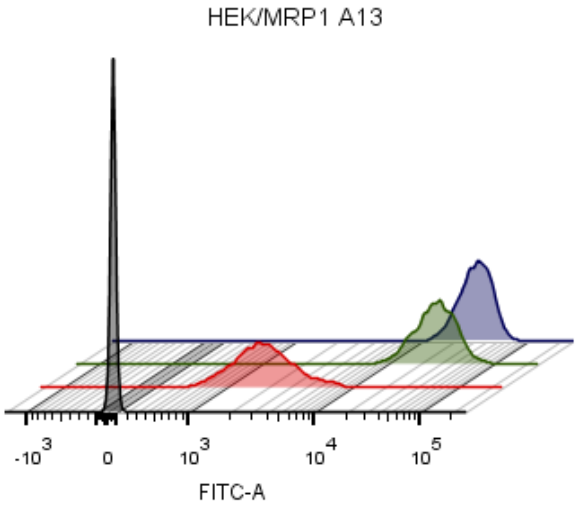

	TUBE NAME	Geometric Mean : FITC-A
	MRP1 unstained	53.0
	MRP1 control	2093
	MRP1 A13 20 uM	29332
	MRP1 MK-571 60 uM	31894

G

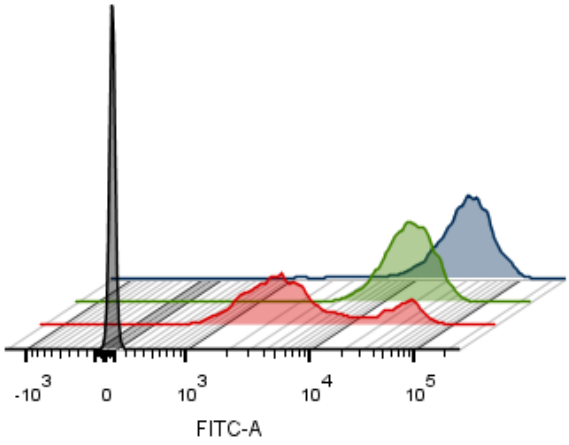

	TUBE NAME	Geometric Mean : FITC-A
	MRP1 unstained	58.9
	MRP1 control	4653
	MRP1 RL92 20 uM	18506
	MRP1 MK-571 60 uM	25780

H

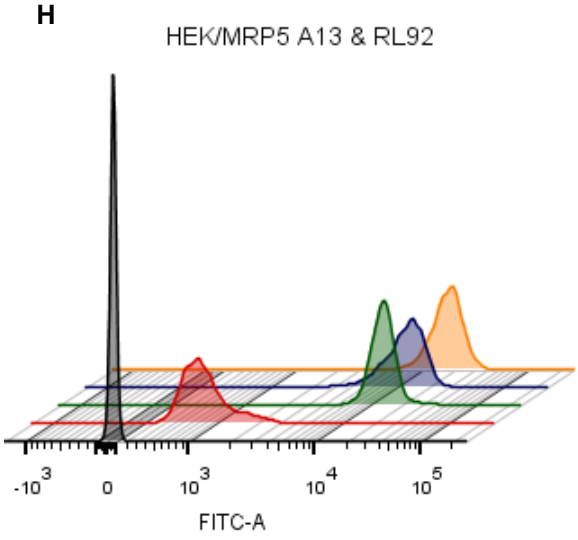

	TUBE NAME	Geometric Mean : FITC-A
	MRP5 unstained	56.7
	MRP5 control	897
	MRP5 A13 20 uM	14299
	MRP5 RL92 20 uM	12162
	MRP5 MK-571 60 uM	17199

Figure A-1. Representative fluorescence histograms of flow cytometry accumulation experiments done in MDCKII/P-gp (**A & B**), MDCKII/BCRP (**C, D & E**), HEK/MRP1 (**F & G**), and HEK/MRP5 (**H**) cells. Experiments include unstained controls (no fluorescent probe), probe-only controls and positive inhibition controls, in addition to the selected analogues. Fluorescent probes used were rhodamine-123 (MDCKII/P-gp), mitoxantrone (MDCKII/BCRP), calcein-AM (HEK/MRP1) and BCECF-AM (HEK/MRP5). The x – axis for each histogram represents mean fluorescence intensity for each cell population. Mean fluorescence values for each sample are also indicated in a table below the figures.

Appendix III. Intrinsic fluorescence in the phycoerythrin channel

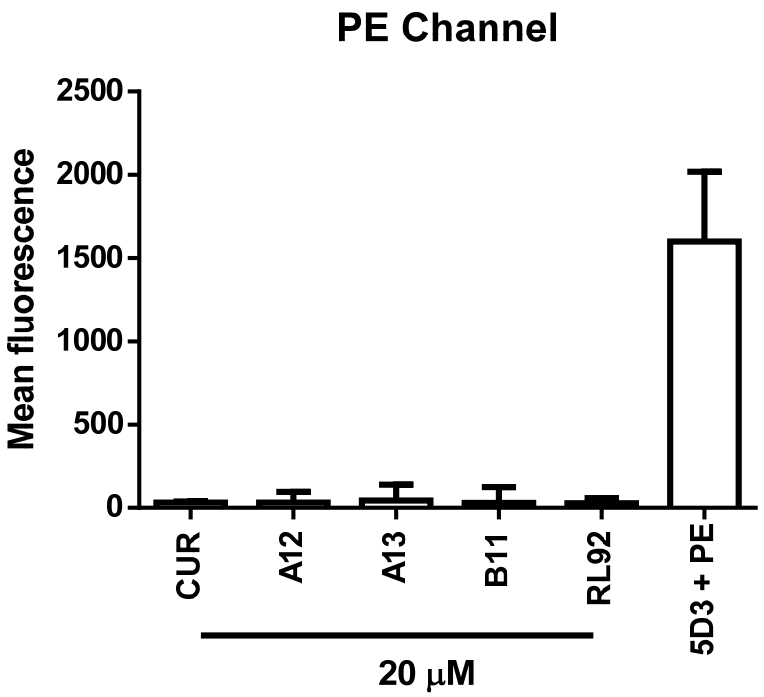

Figure A-2. Intrinsic fluorescence of MDCKII/BCRP cells treated with 20 μM of curcumin (CUR) and selected analogues for 2 h (see Section 2.2.5.4 for methods) in the PE channel (excitation 488 nm/emission 562 – 588 nm). MDCKII/BCRP cells stained with 5D3 and streptavidin-PE were included as positive control. Results are mean ± standard error of n = 2 experiments.

Appendix IV. Effects of A13 and RL92 on 5D3 binding to BCRP

To test if A13 and RL92 covalently modified surface residues in BCRP and prevented the binding of 5D3 to its epitope; the protocol outlined in Section 6.2.2.2 was modified so that cells were fixed before, rather than after analogue treatment. This prevents BCRP internalisation and allows the monitoring of any effects A13 and RL92 treatment has on the binding of 5D3 to BCRP. Results of this experiment are shown in Figure A-3.

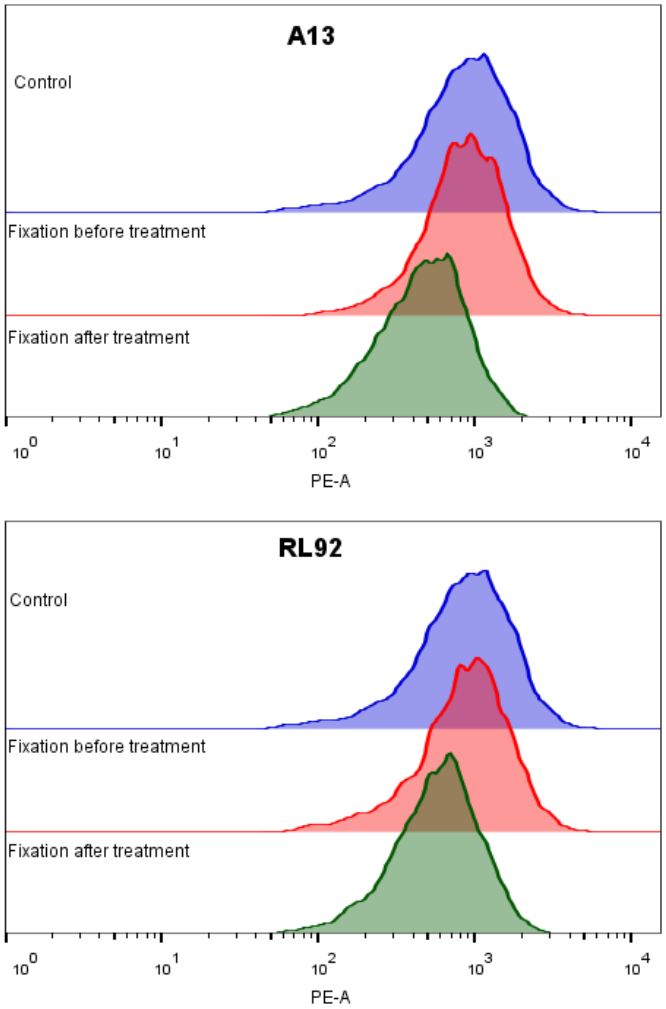

Figure A-3. Flow cytometry histograms of MDCKII/BCRP cells that have been paraformaldehyde-fixed before or after treatment with 20 μM A13 or RL92 for 2 h (see Section 6.2.2.2 for methods). Control are cells treated for 2 h with DMSO prior to fixation. Y – axis is the number of cellular events and X – axis is Log fluorescence in the PE channel.

Appendix V. Permissions for figures/tables

Figure/Table in thesis	Source	License number	Content publisher
Figure 1-1	(Szakács et al., 2008b)	3396850257272	Springer
Figure 1-3	(Linton, 2007)	Permission not required for reuse in thesis	The American Physiological Society
Figure 1-4 Figure 1-6 Figure 1-7	(Metzler et al., 2013)	3396390990005	John Wiley and Sons